

# **Identification of centrally active drugs and herbal constituents as substrates of OATP2B1 and OATP1A2 applying the method of competitive counterflow**

**Inauguraldissertation**

zur

Erlangung der Würde eines Doktors der Philosophie

vorgelegt der

Philosophisch-Naturwissenschaftlichen Fakultät

der Universität Basel

von

**Anima Schäfer**

2021

Originaldokument gespeichert auf dem Dokumentenserver der Universität Basel  
edoc.unibas.ch

Genehmigt von der Philosophisch-Naturwissenschaftlichen Fakultät

auf Antrag von

Henriette Meyer zu Schwabedissen, Stephan Krähenbühl und Veronika Butterweck

Basel, den 30.03.2021

**Prof. Dr. Marcel Mayor**

(Dekan)





Für meine Familie







*«Überzeugungen sind Gefängnisse»*

Friedrich Nietzsche

1844 - 1900







## Acknowledgements

First of all, I would like to express my deepest gratitude to my excellent supervisor **Henriette Meyer zu Schwabedissen**. Thank you so much for giving me the opportunity to do my PhD studies in your group - I felt and continue to feel honored for being a member of your team. From the first day on you gave me inspiring, encouraging and greatly supportive guidance, you forced me to look closer, and your advices and feedbacks were invaluable.

I am profoundly honored for having **Stephan Krähenbühl** as co-supervisor, **Veronika Butterweck** as external examiner and **Kurt Hersberger** chairing my defense.

I owe debts of gratitude to my current and former colleagues of the Biopharmacy group (I chose the alphabetical order to not to give the appearance of a preference). **Anja Fuchs, Célio Ferreira, Isabell Seibert, Janine Hussner, and Karin Brecht** thank you so much for your advice on matters large and small, all the motivating words and for sharing your scientific and hands-on expertise which allowed me to grow scientifically and personally.

I highly appreciate your precious help, **Petra Rohrwild**, and your guidance through the jungle of all administration and office issues.

My deepest thanks to my PhD student fellows of the Biopharmacy group **Daniel Ehram, Jonny Kinzi, and Vanessa Malagnino** for all the scientific (and less scientific) discussions, for your support in chemical questions, as well as for sharing the ups and downs of our PhD time.

Thank you so much **Rommel Tirona**, for supervising my master thesis exactly the way you did it and for reading over my PhD thesis. You awakened my enthusiasm for science, and I will always remember the long and cold winter in London, Ontario as one of my best.

Many thanks to **Markus Grube** and **Olivier Potterat** for the great and fruitful collaborations and a special thanks to Olivier for reading over the passage about the herbal remedies. Furthermore, I want to thank **Andrea Treyer**, **Orlando Fertig** and all the members of the Pharmaceutical Biology group for always welcoming me and my questions.

I would also like to appreciate the work of **Andrea Brodbeck**, **Clara Spirgi**, **Flavia Trüb**, **Julia Schädeli**, **Michelle Fehr**, **Pierrine Gilgen**, and **Vanessa Müller**. Your help in the lab was fantastic and so were your challenging questions and inspiring discussions.

To my mom **Wilma Schäfer**, my dad **Walter Schäfer** and my sister **Sina Schäfer**, my deepest gratitude for your endless support throughout my life, your love and for always being there for me. Without you, I would not be where I am today.

To **Thomas Balke**, thank you for taking me as I am, for inspiring me, for encouraging me in times of frustration, for just being the way you are. Thank you for the exciting years that are behind us and I'm so much looking forward to what lays ahead of us.

To my best friends, **Alexandra Höfler** and **Nicole Heinig**, for almost 20 years filled with wonderful and funny moments. Thank you for everything you did for me and I'm looking forward to the next 20 years.

Last but not least I want to thank Haribo and the brilliant film score composer Hans Zimmer - you helped me through many writing sessions.

# Table of Contents

---

1 **Abbreviations**

---

3 **Summary**

---

5 **Introduction**

7 Efflux transporters

8 Uptake transporters

10 *Current understanding of OATP1A2/SLCO1A2*

14 *Current understanding of OATP2B1/SLCO2B1*

17 Competitive Counterflow

21 Herbal remedies

21 *Hypericum perforatum*

22 *Passiflora incarnata*

---

25 **Aims of the thesis**

---

27 **Results**

29 **Chapter 1**

Establishment and Validation of Competitive Counterflow as a Method to Detect Substrates of the Organic Anion Transporting Polypeptide 2B1

45 **Chapter 2**

OATP1A2 and OATP2B1 Are Interacting with Dopamine-Receptor Agonists and Antagonists

57 **Chapter 3**

Constituents of *Passiflora incarnata*, but not of *Valeriana officinalis*, interact with the Organic Anion Transporting Polypeptides (OATP)2B1 and OATP1A2

71 **Chapter 4**

Hyperforin-Induced Activation of the Pregnane X Receptor Is Influenced by the Organic Anion Transporting Polypeptide 2B1

---

85 **Conclusion and Outlook**

---

93 **Supporting Information** for Molecular Pharmaceutics

99 **Supporting Information** for Planta Medica

105 **Supporting Information** for Molecular Pharmacology

---

113 **Appendix**

---

117 **Bibliography**

---

125 **Curriculum Vitae**



## Abbreviations

### By appearance

FDA, Food and Drug Administration; ADME, absorption distribution metabolism elimination; ATP, adenosine triphosphate; BBB, blood-brain barrier; ABC, ATP binding cassette; SLC, solute carriers; OATP, organic anion transporting polypeptides; E<sub>1</sub>S, estrone 3-sulfate; DHEAS, dehydroepiandrosterone sulfate; AUC, area under the curve; C<sub>max</sub>, maximal plasma concentration; PregS, pregnenolone sulfate; V<sub>max</sub>, maximal transport rate; K<sub>m</sub>, Michaelis constant; PXR, pregnane X receptor; GABA, gamma-aminobutyric acid; CCF, competitive counterflow

### Alphabetical

ABC, ATP binding cassette; ADME, absorption distribution metabolism elimination; ATP, adenosine triphosphate; AUC, area under the curve; BBB, blood-brain barrier; CCF, competitive counterflow; C<sub>max</sub>, maximal plasma concentration; DHEAS, dehydroepiandrosterone sulfate; E<sub>1</sub>S, estrone 3-sulfate; FDA, Food and Drug Administration; GABA, gamma-aminobutyric acid; K<sub>m</sub>, Michaelis constant; OATP, organic anion transporting polypeptides; PregS, pregnenolone sulfate; PXR, pregnane X receptor; SLC, solute carriers; V<sub>max</sub>, maximal transport rate



## Summary

For a large number of compounds in clinical use we know that membrane transporter proteins modulate their pharmacokinetic properties. The family of organic anion transporting polypeptides (OATP) facilitates the cellular entry of such compounds. In my thesis I will focus on two members of this phylogenetically conserved protein family, namely OATP2B1 and OATP1A2. While OATP2B1 is relatively unique in its ubiquitous expression throughout the body, particularly in key organs contributing to drug absorption, metabolism and elimination, the tissue localization of OATP1A2 is more restricted to few organs such as the brain. Currently, various exogenous substrates of OATP2B1 and OATP1A2 have been identified, many of which are shared among other members of the OATP family. Important tools to better understand the physiological and pharmacological functions of each OATP are the use of transporter-specific substrates. Consequently, experimental approaches for fast and easy transporter substrate identification are desired. The competitive counterflow technique is one such method enabling the screening of compounds with reasonable throughput and cost. In this work, I demonstrated that the method could be successfully applied to identify substrates of OATP2B1 and OATP1A2. Competitive counterflow experiments were performed with both transporters to test centrally active drugs belonging to the class of dopamine receptor agonists and antagonists. Bromocriptine, cabergoline, and domperidone were identified as novel substrates of OATP2B1 while OATP1A2 was additionally identified to transport metoclopramide. Confirmation of the transporter expression in cellular structures of the brain suggests their involvement in the uptake of the drugs from the blood-stream into the central nervous system. Beside synthetic drugs, there are also herbal remedies with therapeutic indications to manage diseases of the central nervous system. In this regard, constituents of *Passiflora incarnata* and *Valeriana officinalis* were investigated for interaction with OATP2B1 and OATP1A2. Whereas no transporter interactions were shown for constituents of *Valeriana officinalis*, the flavonoids orientin and vitexin present in *Passiflora incarnata* were identified

as substrates of OATP2B1. Vitexin was also identified as a substrate of OATP1A2 as well as the aglycon apigenin. Mass spectrometric analysis of *Passiflora incarnata* formulations identified vitexin and orientin, but not apigenin. Consequently, these two constituents could be involved in possible interactions between the formulations and the transporters. Importantly, there is still limited knowledge about systemic availability of flavonoids and to what extent they reach the central nervous system. However, OATP2B1 is widely considered to be important in intestinal drug absorption, and it follows that constituents of herbal remedies may interact with co-administered oral drugs which are OATP2B1 substrates. Another herbal constituent that we found to interact with OATP2B1 is the St. John's wort constituent hyperforin. It is a potent inhibitor of OATP2B1 function with an  $IC_{50}$  of 0.32  $\mu$ M and indeed, competitive counterflow experiments identified it as an OATP2B1 substrate. This phloroglucinol is known for drug-herb interactions involving induction of enzymes which mediate drug metabolism. Our finding of OATP2B1 playing a role in cellular uptake of hyperforin suggests that the transporter is a determinant influencing the intracellular effect of the herbal constituent. Furthermore, the identification of hyperforin as an OATP2B1 substrate would imply by extension the plant's interaction potential with OATP2B1 substrates.

## Introduction

Progress in medicine would be unimaginable without the continued development of therapeutics. Starting with mixtures of herbal and animal origin, the chemical understanding and finally the possibility to synthesize drugs, the treatment of diseases has rapidly evolved in the last 100 years. Today, synthetic molecules dominate the drug market; however, herbal compounds remain popular in the society. Altogether, there are approximately 15 000 molecules that have been approved by the US Food and Drug Administration (FDA) that are widely and often used. According to the definition provided by the FDA, a drug is a compound used to diagnose, treat, cure, mitigate, or prevent disease or other abnormal conditions<sup>1</sup>. As reported in the 2017 World Drug Report, around a quarter of a billion people across the world used drugs at least once in the year 2015, which represents around 5 percent of the global adult population<sup>2</sup>. Although medications have been optimized for their indication through studies involving populations of patients, there is a need to consider the phenomenon of interindividual differences in the response to the xenobiotic when prescribing for individuals. Among the reasons for these differences is the variable handling and processing of the substance by the organism, which is termed pharmacokinetics. The parameters that are used to characterize drug disposition are the magnitude of achieved plasma concentrations and their duration over time. With this assessment, it may be possible to infer the most important mechanisms influencing the plasma concentration. Here, one usually refers to the different processes of drug disposition with the acronym ADME. This means, compounds have to be **A**bsorbed to enter the system after administration, they have to be **D**istributed in order to exert their pharmacological effect and they have to be **M**etabolized and **E**xcreted from the organism in order to avoid toxicity. One molecular mechanism which influences each ADME process and which determines interindividual differences in drug response is the transmembrane transfer.

---

<sup>1</sup> <https://www.fda.gov/drugs/drug-approvals-and-databases/drugsfda-glossary-terms>, last access on February 18, 2021

<sup>2</sup> [https://www.unodc.org/wdr2017/field/Booklet\\_1\\_EXSUM.pdf](https://www.unodc.org/wdr2017/field/Booklet_1_EXSUM.pdf); last access on February 18, 2021

Each cell is surrounded by a highly dynamic, semipermeable lipid bilayer consisting of phospholipids whose tails form a hydrophobic core. This is covered by a hydrophilic layer consisting of the hydrophilic head groups. It is widely accepted that the plasma membrane, due to its composition and function, impacts the crossing of a substance depending on its physicochemical properties. Permeation of biological membranes can occur either passively, actively, or via vesicle transport. Passive transport occurs without the need of energy and can be further divided into simple diffusion, facilitated diffusion, and osmosis. Osmosis describes the movement of water, whereas simple diffusion is defined as the random movement of a solute along a concentration gradient. The rates of solute movement from regions of high to a low concentration occur without reaching a saturation limit. In the process of facilitated diffusion, solute permeation requires membrane proteins that are located within the lipid bilayer. In general, these processes are saturable, compound selective and sometimes stereo-specific. Finally, there is active transport defined by the need of direct energy in the form of adenosine triphosphate (ATP) which allows the transport of the substrate against a concentration gradient via an integral membrane protein. It is widely accepted that both proteins enabling facilitated diffusion or active transport are key determinants of ADME and hence the overall pharmacokinetics of a molecule.

## **Efflux transporters**

One important and highly studied group of active membrane transporters comprise the efflux transporters of the ATP-binding cassette (ABC) superfamily. ABCB1 (Permeability glycoprotein (P-gp), multidrug resistance protein 1 (MDR1)) was first identified in 1976 by Ling *et al.* as a mechanism contributing to the multidrug resistance in cancer cells. Since then the field has enormously evolved [1]. Today we know that ABCB1 is not only expressed in cancer cells, but also contributes to intestinal, hepatic and renal excretion of its substrate drugs. Furthermore, ABCB1 is of major relevance in tissue barriers to drugs such as the brain (blood-brain barrier, BBB) and the placenta [2]. Importantly, it is not only the understanding of function and relevance of ABCB1 that has evolved; it is also the number of other efflux transporters that have become known to contribute to the handling of drugs in the human organism. Indeed, today we know that the phylogenetically conserved family of ABC-transporters consists of 48 members, of which several have been shown to be involved in the handling of drugs in the human organism [3]. I want to highlight the members of the ABCC-subfamily, namely ABCC2 and ABCC3 and the transporter ABCG2 (breast cancer resistance protein, BCRP), which have been intensively investigated for their role in pharmacokinetics. Briefly, ABCC2 and ABCC3 are highly expressed in the liver, where they are assumed to transport products of the Phase II-drug metabolism, namely sulfated and glucuronidated metabolites produced through the actions of sulfotransferases (SULTs) and UDP-glucuronosyltransferases (UGTs). Importantly, while ABCC2 is expressed in the canalicular membrane of hepatocytes, extruding its substrates into bile [4], ABCC3 is expressed in the sinusoidal membrane transporting molecules from hepatocytes back into the systemic circulation [5]. Although highly expressed in the liver, both transporters have also been observed in other tissues including intestine, kidney, and placenta [5-8]. For ABCG2 it should be mentioned that it has a similar tissue distribution as ABCB1, and this transporter is known

to be of relevance for the limitation of intestinal absorption, dia-placental transfer and brain entry of drugs as well as for the promotion of renal and hepatic drug elimination [9].

In summary, members of the ABC-family are efflux transporters that actively extrude compounds, thereby reducing the intracellular amount of their substrates. These ABC transporters have broad substrate specificity that contributes to limiting drug exposure in the tissues and promoting drug elimination, which in a broader sense, act with a xenoprotection function to the human organism. However, when considering the mechanisms of directed transport or transcellular transfer, it seems evident that if there is a mechanism mediating extrusion there should also be a mechanism facilitating cellular entry or uptake.

### **Uptake transporters**

One example of membrane proteins facilitating the cellular uptake of their substrates is the superfamily of solute carriers (SLC). They form the second largest family of membrane proteins and consist of 52 gene families. The SLCO (former SLC21) or organic anion transporting polypeptides (OATP) represent one type of SLC transporters, which are divided into 6 families with 13 subfamilies. An overview of the OATP transporters is shown in Figure 1.

In general, OATPs are assumed to be integral membrane proteins of 652-848 amino acids in length with 12 transmembrane domains, where both the N- and C-terminus are located in the cytosol. Among the OATPs, there are members showing a wide distribution in human tissues, while others appear to be only expressed in specific organs. Although the exact mechanism of transport remains to be fully elucidated, the OATPs are generally involved in the sodium-independent transport of a broad range of rather large (>350 Da) amphipathic organic anions [10], including compounds of endogenous and exogenous origin. However, there are also neutral or even positively charged substrates of OATPs. Generally, the transport via an OATP is considered to facilitate cellular uptake in exchange for intracellular anions such as reduced glutathione [11, 12], or bicarbonate [13, 14].

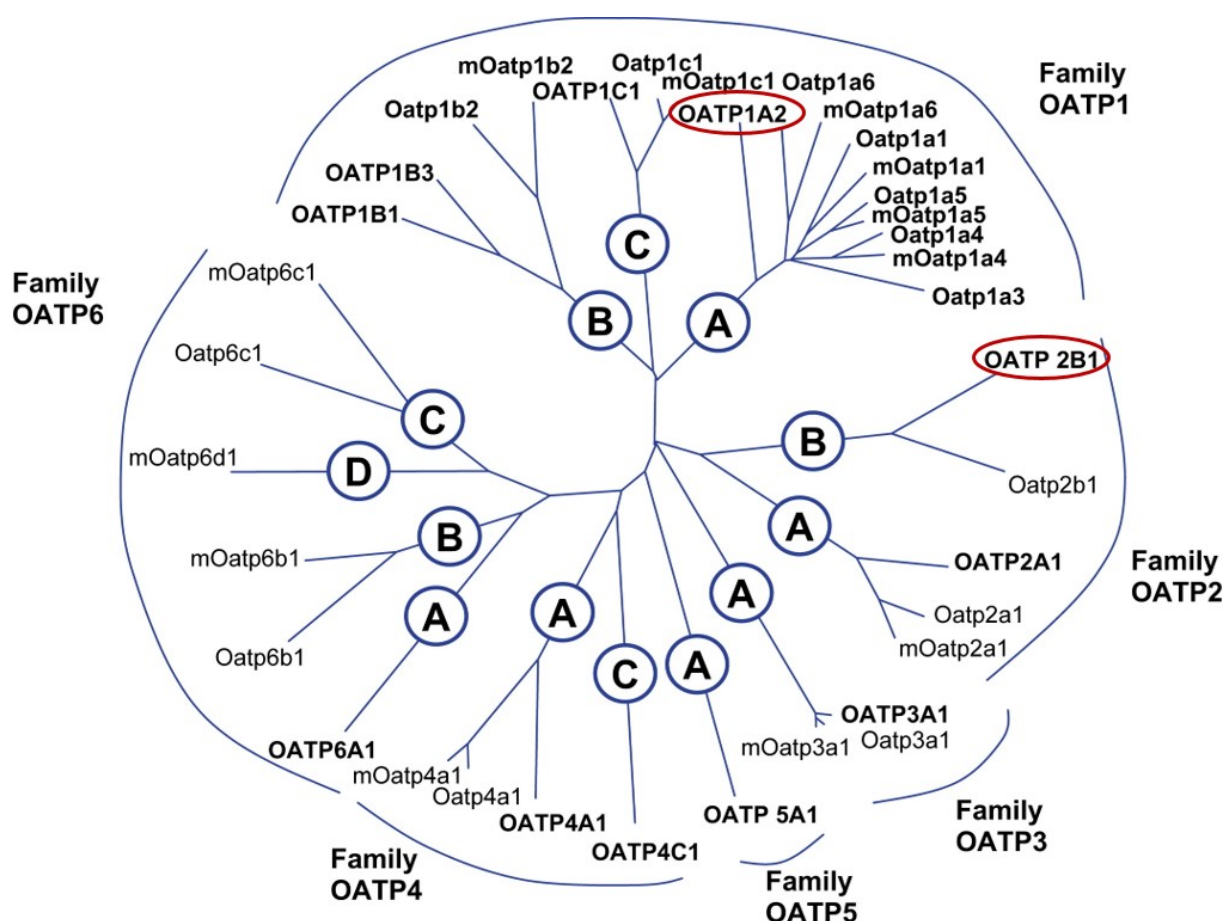


**Figure 1. Phylogenetic tree of the families and subfamilies of OATP transporters.** With more than 40% amino acid sequence identity, transporters are categorized in the same family (OATP1-OATP6). The sub-families are defined by a sequence identity with more than 60% (OATP1A-OATP1D). Human OATPs are written with capital letters, animal with small letters. b, bovine; c, chicken; m, mouse; r, rat; s, skate; red circles indicate the transporters of interest in this work. Adapted from Hagenbuch [15].

Since their first identification in 1995, the rapidly growing family of OATPs have become increasingly relevant, especially concerning their contribution to the handling of drugs in the organism. In terms of pharmacokinetics, the liver specific OATP1B1 and OATP1B3 are best investigated for their role in hepatic handling of their substrate drugs. Briefly, both OATP1B transporters are highly expressed in the sinusoidal membrane of hepatocytes, and are shown to recognize a broad range of substrates [16-18]. With the identification of naturally occurring genetic variants of OATP1B1 with altered expression and/or transport activity, there were additional implications of this particular transporter in the variable pharmacokinetics of drugs [19]. Beside the impacts of pharmacogenetics, OATP1B transporters are considered important determinants of drug-drug interactions (summarized by Shitara [20]). Today, it is recommended

that new molecular entities be tested for interaction with the OATP1B transporters during drug discovery and development by the FDA and the European Medicines Agency.<sup>3</sup> Importantly, a great overlap in substrates and/ or inhibitors has been recognized among other OATPs such as OATP2B1 and OATP1A2. Their relevance in the organism has not been clarified so far and will be addressed, investigated and discussed in the present work.

#### Current understanding of OATP1A2/SLCO1A2

OATP1A2 (also known as OATP, OATP1 or OATP-A) belongs to the OATP1 family and was the first human OATP studied [21]. In this first report, OATP1A2 was cloned from the human liver and its transport function was assessed. Moreover, expression was shown in liver, brain, lung, kidney, and testis [21]. Since then, expression of OATP1A2 has been studied by multiple groups, suggesting the highest expression of OATP1A2 in endothelial cells of the blood-brain barrier [22, 23] and in the neuronal membrane [24], as indicated in Figure 2. Here, OATP1A2 is assumed to participate in the brain entry and in neuronal processes, respectively. In liver, OATP1A2 has been reported to be located within cholangiocytes [25], where it is thought to be involved in maintaining the homeostasis of bile acids [21]. The transport protein was also reported to be expressed in the distal tubule of the nephron, where it may play a role in the tubular reabsorption [25, 26]. Furthermore, OATP1A2 expression was found in different cell types of the placenta including villous cytotrophoblasts, syncytiotrophoblasts, and extravillous trophoblasts [27]. In the syncytiotrophoblasts expression was found in the apical membrane suggesting that the transporter is involved in the transfer from the mother to the fetus [28]. Notably, an early report by Glaeser *et al.* revealed OATP1A2 in the intestine [29]. However, recent findings of studies testing the abundance of transporters by LC-MS/MS analytics were

---

<sup>3</sup> US Food and Drug Administration. Guidance for industry: drug interaction studies—study design, data analysis, implications for dosing, and labeling recommendations. 2012; European Medicines Agency. Guideline on the Investigation of Drug Interactions, 2012; last access on February 18, 2021

not able to confirm the presence of the transporter in this particular tissue [30]. In accordance, the intestinal presence and function of OATP1A2 is no longer considered by many.

Taken together, OATP1A2 has been reported to be expressed in multiple organs of the human organism, however its role and relevance in the handling of molecules is still poorly understood. Clinical studies to investigate a transporter's function can be either drug-drug interaction studies, with concomitant administration of drugs functioning as victim and perpetrator or they can be pharmacogenetic studies where genetic variants are granting a loss of function. The design of either type of study includes the selection of a substrate. Here, OATP1A2 has been reported to transport molecules of exogenous and endogenous origin. The latter include the common OATP substrate estrone-3 sulfate ( $E_1S$ ), but also dehydroepiandrosterone sulfate (DHEAS) [31], and thyroid hormones [32]. In terms of xenobiotics, OATP1A2 substrates are within the class of antihistamines (e.g., fexofenadine [33]), beta-blockers (e.g., nadolol [34]), statins (e.g., rosuvastatin [35]), central active drugs such as serotonin-receptor agonists (e.g., triptanes [36, 37]), or  $\delta$ -opioid peptides (e.g., deltorphin II [22]) and anti-cancer drugs (e.g., imatinib [38]). Additionally, OATP1A2 is assumed to interact with food constituents as reported for naringin, a constituent of grapefruit juice, or honey flavonoids and catechins of green tea [39-41].

Some of the above mentioned substrates have been used in clinical studies, where the investigators intended to study the role of OATP1A2 in pharmacokinetics. Briefly, pharmacokinetic parameters were determined in patients receiving a known OATP1A2 substrate and a competitor, which was previously shown to inhibit the transporter's function. Naringin, often found in fruit juices, or catechins which are constituents of green tea are examples of the studied OATP1A2 competitors. In this regard, patients received fexofenadine or nadolol as known OATP1A2 substrates [34, 42] co-administered with fruit juices or green tea which contained the inhibiting constituents (an overview of the study designs and their

outcomes can be found in the Appendix, Table 1). Interestingly, a decrease of the AUC and  $C_{\max}$  were observed in most studies. Since OATP1A2 was previously assumed to be localized in the apical membrane of enterocytes, the phenomenon was attributed to a change in intestinal absorption via OATP1A2. Today, we venture to contend that this might not be the case and observations must be ascribed to mechanisms aside from OATP1A2 inhibition. Similarly, there are studies trying to elucidate the relevance of OATP1A2 in brain drug entry. In this context, Li *et al.* investigated the BBB penetration of the small-molecule AZD1775 (adavosertib), a WEE1 kinase inhibitor under investigation for the treatment of glioblastoma. Briefly, with a combination of *in vivo*, *in vitro* and physiologically based pharmacokinetic (PBPK) modeling the authors provide evidence that the penetration of this molecule into the tumor tissue is most likely mediated by OATP1A2. The authors base this assumption on the acidic tumor environment which decreases the efflux of AZD1775 via ABCB1 and ABCG2, while OATP1A2 is not affected [43]. Consequently, OATP1A2 is assumed to facilitate the brain entry of AZD1775, at least under pathological conditions as shown for glioblastoma.

In addition to drug-drug interaction studies, there are examples, where genetic variants were of great value for the investigation of a transporter's function in the human organisms [44]. As summarized in the Appendix, Table 2, there are various genetic variants for OATP1A2 reported of which rs11568563 (c.516A>C, p.172E>D) was shown to exhibit reduced capacity for uptake of E<sub>1</sub>S, the delta-opioid receptor agonists deltorphin II, [D-penicillamine(2,5)]-enkephalin (DPDPE), and methotrexate in *in vitro* experiments [25, 26]. On the contrary, rs10841795 (c.38T>C, p.13I>T) was shown to induce uptake of E<sub>1</sub>S and methotrexate [26]. Beside *in vitro* investigations there are also clinical studies investigating the impact of genetic variations on the pharmacokinetics of substrate drugs. Briefly, the rs3764043 (intronic c.-423G>A aka c.-361G>A) was investigated for its influence on imatinib clearance in patients with chronic myeloid leukemia. Individuals homozygous for the reference G allele had a significantly lower clearance than carriers of the GA or AA genotype, however, no influence on clinical response

was observed [45]. For darunavir, the change of T to C in position 38 (rs10841795 (c.38T>C, p.13I>T)) was linked to a slightly higher cerebrospinal fluid concentration compared to that observed in individuals carrying the reference variant [46]. Finally, the variants rs4762699 and rs2857468 were shown to be highly associated with the risk of life-threatening febrile neutropenia in breast cancer patients treated with docetaxel and doxorubicin [47]. The neuromuscular blocker rocuronium which is mainly eliminated by excretion into the bile was identified as OATP1A2 substrate and the genotypes -A or AA for SLCO1A2 -189\_-188InsA showed a reduced total clearance assuming involvement of the transporter in the elimination pathway of this drug [48].

In summary, with the hitherto available data on OATP1A2, it is reasonable to conclude that this transporter has an impact on the handling of its substrate drugs. Although OATP1A2 may not be involved in the absorption of compounds in the intestine, there is clinical data suggesting a role in elimination and brain entry of selected compounds. Whether this is of clinical relevance, warrants further studies. Notably, OATP1A2 transports E<sub>1</sub>S and DHEAS and is highly expressed at the blood brain barrier, where it may be involved in neurosteroid homeostasis [31]. Clearly, there is a need to further investigate the transporter's role in the handling of molecules. However, an important prerequisite to future studies is the identification of more specific substrates and innovative experimental approaches which could better expose the physiological and pharmacological roles of OATP1A2.

### Current understanding of OATP2B1/SLCO2B1

In 2000 Tamai *et al.* were the first to report on OATP2B1 (also known as OATP-B) as an uptake transporter and its broad expression profile in human tissues [49]. Hitherto, expression was confirmed in various tissues including the coronary artery [50], heart [51], lung [52], mammary gland [53], pancreas [54], placenta [55], platelets [56], skeletal muscle [57], and skin [58] (compare Figure 2). Moreover, OATP2B1 was shown to be expressed in endothelial cells of the blood-brain barrier [24]. Importantly, OATP2B1 expression was found in tissue contributing to the absorption, metabolism and elimination of drugs, namely the intestine, the liver, and the kidney. In the liver, OATP2B1 was shown to be located within the sinusoidal membrane of hepatocytes, where the transporter is assumed to facilitate the hepatocellular entry of its substrates [59]. In the kidney, OATP2B1 was found in the apical membrane of proximal tubular cells. However, in distal tubules the transporter sorts to the basal membrane [60]. For the localization in enterocytes, there are contradictory findings.

Specifically, Kobayashi *et al.* detected the transporter on the luminal surface of enterocytes performing immunohistochemical analysis of human intestinal tissue slices [61]. In a more recent publication, Keiser *et al.* argued against these findings, proposing a basolateral localization of OATP2B1 [62]. Here, the authors enriched the basal and apical membrane fraction of enterocytes prior to mass spectrometric analysis revealing the protein in the basolateral fraction. Notably however, the authors rated their immunofluorescent staining as ambiguous. Their proteomic finding was supported by *in vitro* studies testing the vectorial transport of known OATP2B1 substrates using the Ussing Chamber with human jejunal mucosa as well as the Caco2-Transwell system. They found a dominating flux of known OATP2B1 from the basolateral to the apical compartment and concluded that this disqualifies the transporter's involvement in intestinal drug absorption [62].

Despite the debate on its localization in the intestine, various groups have conducted clinical studies in order to elucidate the relevance of OATP2B1 in pharmacokinetics of its substrates. In these studies, the following compounds aliskiren [63], celiprolol [64], fexofenadine [65], glibenclamide [66], montelukast [67], rosuvastatin [66, 68, 69], sulfasalazine [66], sumatriptan [66], and voriconazole [70] were used. Most of the studies were designed to test for the influence of coadministered substrates and/or genetic variants on the oral absorption of the test compound. The potential relevance of OATP2B1 on drug disposition was determined by comparing systemic exposure (AUC), level of the maximal plasma concentration ( $C_{\max}$ ) and time to  $C_{\max}$  ( $t_{\max}$ ). One example is voriconazole where systemic exposure of patients carrying the genetic variant rs3781727 (c.\*396T>C) was compared to carriers of the reference allele. Notably, the carriers of the genetic variant exhibited a lower systemic exposure ( $AUC_{0-4}$ ), and a reduced  $C_{\max}$  of voriconazole than carriers of the wild type variant [70]. Furthermore, pronounced reduction in systemic exposure was observed, when selected OATP2B1 substrates were coadministered with fruit juices [63-66]. Importantly, there is *in vitro* data showing inhibition of OATP2B1 with constituents of fruit juices including nobiletin, naringin or hesperidin [71, 72]. Nobiletin is a polymethoxy-flavone and naringin and hesperidin are flavanone glycosides belonging to the class of flavonoids, a large group of polyphenolic secondary metabolites which are often found in plants. Accordingly, in the clinical studies which observed reduced exposure of selected substrates is currently interpreted as reduced intestinal absorption due to inhibition of OATP2B1 [63, 65, 67]. The assumption that intestinal OATP2B1 is prone to drug-food interaction is further supported by findings in *Slco2b1*<sup>-/-</sup> mice. Here, the authors not only observed reduced fexofenadine maximal plasma concentrations and AUC after oral application compared to wildtype (wt) mice, they also found that grapefruit juice reduced the  $C_{\max}$  and AUC in wt mice. No such effect was observed in animals lacking the transporter [73]. Although fruit juices and their constituents including naringin or hesperidin are most extensively studied for their influence on OATP2B1 and oral drug absorption, there

are several other flavonoids reported to interact with the transporter. In this regard, Mandery *et al.* identified apigenin, kaempferol, and quercetin to inhibit the transporter-mediated cellular uptake of atorvastatin and fexofenadine [74]. They conclude that co-administration of a drug and a herbal remedy might result in drug-herb interactions because of competition for cellular entry via OATP2B1. Whether these findings are of clinical relevance warrants further testing.

Beside drugs, OATP2B1 is also shown to transport endogenous compounds including the thyroid hormones thyroxine ( $T_4$ ) and triiodothyronine ( $T_3$ ) and coproporphyrin (CP) III [75, 76]. The isomers CPI and CPIII are byproducts of the heme biosynthesis and due to their interaction with hepatic OATPs, they are currently under investigation as biomarkers to monitor the function of hepatic OATP-transporters [77, 78]. Moreover, OATP2B1 was shown to transport the steroid hormones DHEAS,  $E_1S$  and pregnenolone-sulfate (PregS) [79]. In addition to DHEAS,  $E_1S$  is a highly abundant steroid hormone in the human organism that exhibits poor binding activity to the estrogen receptor. Indeed, its physiological function is rather the provision of a precursor reservoir that intracellular steroid sulfatases convert to unconjugated, active estrone and estradiol when needed. Due to the hydrophilic sulfate moiety, sulfated steroids depend on a transporter-mediated mechanism for the transmembrane transfer. It is generally assumed that OATPs are involved in the handling of conjugated steroids. OATP2B1 is presumed to play a role due to its ubiquitous expression and abundance in organs targeted by steroid hormones such as the placenta, the mammary gland or the gonads. One organ, where OATP2B1 may be of relevance for the transmembrane transfer of sulfated steroids is the brain. Here, the transporter is assumed to be localized in the luminal membrane of endothelial cells of the blood brain barrier (BBB). In this regard, there is particular interest in DHEAS and PregS since there are reports showing these endogenous compounds affect neuronal excitability and have been considered in the treatment of brain disorders [80-83]. Both DHEAS and PregS can either be synthesized directly in the brain or they are taken up from the bloodstream [82, 83]. It remains to be tested whether OATP2B1 is of relevance in this process.

To summarize, OATP2B1 has a broad expression pattern including high abundance in organs of pharmacokinetic relevance, and possesses an affinity towards many endogenous and exogenous compounds. Further studies are warranted to better understand its apical and basolateral sorting, especially in the intestine since there continues the debate whether OATP2B1 is involved in the intestinal absorption of its substrate drugs. Nevertheless, the available data demonstrate beyond doubt that OATP2B1 is involved in cellular substrate entry. However, due to the significant and complicating substrate overlap between OATP2B1 and other OATPs, the pharmacological understanding of OATP2B1 is still in its infancy. Consequently, the identification of a specific OATP2B1 substrate would provide a necessary chemical tool to investigate specific physiological functions and to test clinical hypotheses.

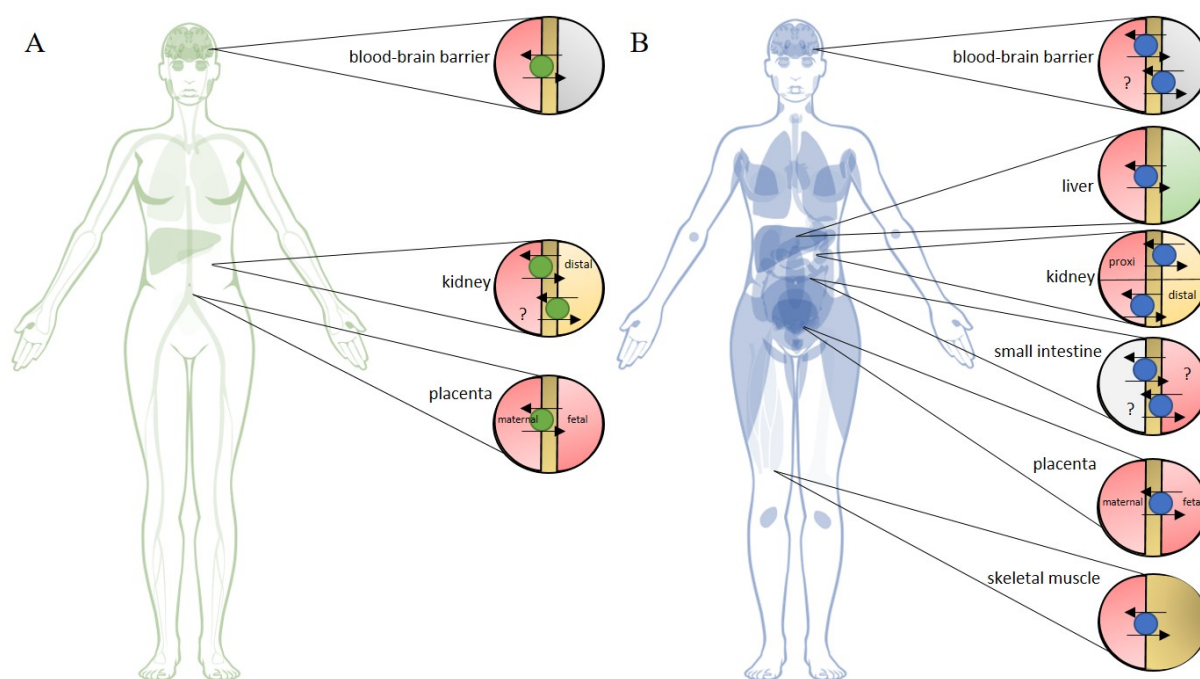


**Figure 2. Summary of tissue expression and membrane sorting of (A) OATP1A2 and (B) OATP2B1.** Green circles, OATP1A2; blue circles, OATP2B1; Color-coding of the semi-circles: red, blood; grey, brain; yellow, urine; green, bile; white, intestinal lumen, ochre, cells of the respective tissue, question mark indicates that there is inconsistent data. Adapted from the Human Protein Atlas (<https://www.proteinatlas.org/>; last access on February 18, 2021) and Hagenbuch and Stieger [84].

### Competitive Counterflow

The pharmacokinetics of a drug highly depend on its permeability or in other word its ability to cross cellular membranes. It is assumed that various molecules due to their favorable

physicochemical properties readily diffuse across lipid bilayers. Important physicochemical properties to promote diffusion of a drug include good lipophilicity (often defined as the partition coefficient between octanol and water), smaller molecular size, low numbers of hydrogen bond acceptors and donors and neutral charge state. Conversely, molecules that do not conform to these physicochemical properties have limited transmembrane transfer by passive diffusion. Consequently, the permeability of molecules that are hydrophilic and charged is assumed to rely on facilitating mechanisms such as uptake transporters. As an essential property conveying a drug's pharmacokinetics, it is a prerequisite to understand how a drug is penetrating through membranes. New molecular entities are commonly tested for their permeability. The Caco-2 transwell system is an *in vitro* intestinal transport model where the vectorial transport of drugs is measured by their fluxes across cell monolayers in the apical to basolateral direction and vice versa. The observation of asymmetric drug fluxes across the transwell system indicates that there are active components involved in the transcellular transport. However, one limitation is that Caco-2 cells vary in their transporter expression across and within laboratories making it difficult to reliably identify interaction with specific transporters. In order to test for interaction with selected drug transporters, there are experimental recommendations by the International Transporter Consortium [85]. Hitherto, every approach is based on cell models in which the transporter of interest can either be transiently or stably overexpressed. These cell models are used to quantify the transported amount of the test compound. There are different approaches to make the compound "measurable" of which the labeling with a radioactive isotope is one possibility. Additionally, in case the test compound is fluorescent it can be quantified by detection of its spectral emission at a certain excitation. Commonly, the highly sensitive liquid chromatography-mass spectrometry approach is used to quantify the intracellular amount of the test compound [85]. In the case where a 2-fold or higher intracellular increase of the test compound is measured

compared to control cells, the compound is considered a substrate according to the guidance<sup>4</sup>. The above described methods provide the opportunity to calculate the kinetic parameters conforming to the Michaelis-Menten equation (Figure 3) based on the observations. The Michaelis-Menten equation is originally based on the description of an enzymatic reaction - the existence of an enzyme and its substrate, the forming of a complex, and the resulting product leading to the preserved enzyme. Translating this concept to an uptake transporter and its substrate in a simple way would mean the binding of the substrate to the transporter on the cellular surface, its transport through the membrane and its intracellular release. As shown in Figure 3 Michaelis-Menten kinetics are described by two parameters: the maximal velocity or maximal transport rate of substrate ( $V_{\max}$ ) and the Michaelis constant  $k_m$ .  $V_{\max}$  describes the maximal amount of substrate that can be transported in the system in a certain time. Reaching  $V_{\max}$  means that the transporting system reaches the maximal capacity and increasing the amount of substrate (concentration) would not change the turnover rate. The Michaelis constant  $k_m$  describes the affinity of the substrate to the transporter and it corresponds to the concentration at half-maximal velocity ( $\frac{1}{2} V_{\max}$ ). A small value for  $k_m$  indicates a high affinity of the substrate to the transporter. Certainly, the meaning of these parameters obtained in *in vitro* experiments is challenging to extrapolate to a complex system such as the human organism. However, advancements in mathematical modeling provide somewhat reliable *in vitro* to *in vivo* prediction of drug-drug interaction potential in the case of coadministration of two substrates.

The above-mentioned methods provide important information on the interaction of a molecule with a transporter, however, they are expensive in both time and costs. Interestingly, in 1956 Rosenberg and Wilbrandt introduced a method called competitive counterflow based on their observation for glucose transport in human red blood cells [86]. In detail, Rosenberg and

---

<sup>4</sup> US Food and Drug Administration. Guidance for industry: drug interaction studies—study design, data analysis, implications for dosing, and labeling recommendations. 2012; last access on February 18, 2021

Wilbrandt treated human red blood cells with glucose until a steady state was reached. Subsequently, they found that addition of substrates, but not of inhibitors of the glucose transporter significantly changed this equilibrium [86]. Later, the method was described by William Stein who defined it as a phenomenon of competitive exchange in a system where a transport mechanism is at or close to saturation on both sides of the membrane [87]. Importantly, this implies bidirectional transport of the system which controls the substrate equilibrium. As soon as a second substrate is added, the net-flux of the primary substrate becomes unidirectional – in our case an outward direction. This results in a decreased intracellular amount of the primary substrate. However, if the test compound is an inhibitor it will block transport turnover, the first substrate is “caught” inside the cell and the equilibrium remains unaffected. Since it is only possible to measure the changed accumulation of the primary substrate, competitive counterflow is defined as an indirect method. So far, it was successfully applied to identify substrates of the organic cation transporter 2 and the organic anion transporters 2 and 3 [88, 89]. Currently, it is unknown whether this method can be applied to identify substrates of OATPs.

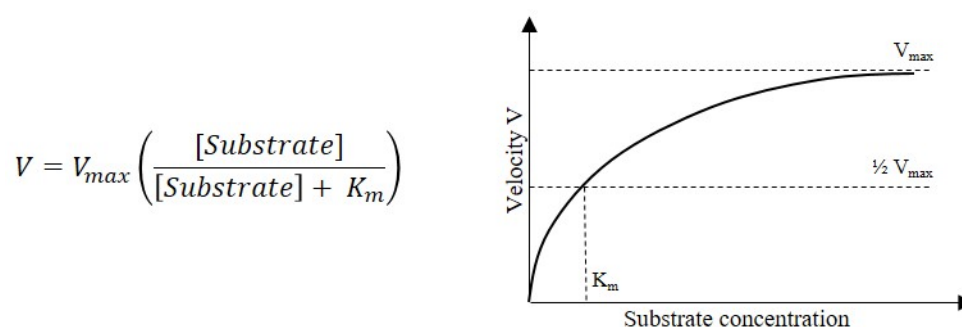


**Figure 3. Michaelis-Menten equation and Michaelis-Menten saturation curve.** V, velocity; V<sub>max</sub>, maximal velocity; [Substrate], concentration of the substrate; K<sub>m</sub>, Michaelis-Menten constant.

## Herbal remedies

### *Hypericum perforatum*

The use of St. John's wort (*Hypericum perforatum*) as medication enjoys a long history. The first description of the plant and its use to heal burns dates back to the year 50 AD. In the Middle Ages it was recognized as psychotherapeutic agent to treat melancholy [90]. Finally, since 1985, the plant has been used to treat mild to moderate depressive symptoms and is still an important medication in this field. Its activity has been confirmed in several clinical studies [91-93]. Numerous compounds belonging to various substance classes have been identified in extracts of St John's wort [94]. The major classes of compounds are naphthodianthrones (e.g. hypericin), phloroglucinol derivatives (e.g. hyperforin), and flavonoids (e.g. quercetin, hyperoside, rutoside). The amounts of the respective constituent in the extracts strongly depend on the method applied for extraction. This is in particular the case for hyperforin. With the extraction method originally used, hyperforin, which is chemically unstable, was degraded rapidly. However, around 1990 a new extraction method was developed resulting in higher hyperforin contents. This was seen as an improvement since hyperforin was thought to be one of the determinants of the extract's pharmacological activity [95]. Today we know that the antidepressant effect cannot be reduced to one single constituent but is the result of a synergistic effect of multiple components, and is potentially independent of the hyperforin content. Importantly, there are formulations on the market containing a very little amount of hyperforin for which an antidepressant effect was clinically confirmed, when compared to synthetic antidepressants [91, 93]. The exact mechanism of action is indeed still not fully understood. There are studies reporting an interaction with monoamine-receptors, neurotransmitter reuptake or catechol-o-methyltransferase which could contribute to the observed antidepressant effect [96]. Recently, the effect of St. John's wort was also linked to a modulation of the membrane fluidity [97]. Beside its antidepressant effect, St. John's wort has also been the subject of negative headlines due to severe adverse events observed after coadministration with drugs.

These mainly occurred after the extraction method had been changed resulting in a higher content of hyperforin. There were in particular reports showing reduced exposure of the protease inhibitor indinavir and heart transplant rejection because of an elevated metabolism of the immunosuppressant cyclosporine [98, 99]. Enhancements of first pass-metabolism and clearance of the co-administered drugs are responsible for the observed events. Moreover, it was demonstrated that hyperforin binds and activates the nuclear receptor Pregnane X Receptor (PXR) thereby upregulating the expression and activity of its target genes. Target genes of PXR include the important metabolising enzyme CYP3A4 and the efflux transporters ABCB1, and ABCC3 [100-102]. Indinavir and cyclosporin are substrates of both CYP3A4 and ABCB1, thereby explaining the reduction in exposure due to limited bioavailability and enhanced clearance. The elevated expression of PXR target genes was shown in enterocytes and hepatocytes thereby suggesting cellular entry of hyperforin. It is currently unknown whether there are transporters involved in facilitating the transmembrane transport of hyperforin.

#### *Passiflora incarnata*

The extract of *Passiflora incarnata* has been medicinally used since the 16th century [103]. *P. incarnata* is one of about 500 different species, which belong to the genus of *Passiflora*. Often used in combination with other plants such as *Petasites hybridus* or *Valeriana officinalis*, *Passiflora* is believed to exert an anxiolytic and sedative effect. This indication is supported by findings in rodents, where *Passiflora* treatment affected the outcomes of behavioral tests including the elevated plus maze test, the water maze test or the light/dark box choice situation test [104-106]. Furthermore, in a double blind randomized trial of patients with generalized anxiety disorder that received either a *Passiflora incarnata* extract or oxazepam no significant difference in efficacy between interventions was observed. Moreover, in the group treated with the *Passiflora* extract, lower incidences of impairment of job performance were reported [107]. The observed anxiolytic effect might be mediated by interaction of the extract with the gamma-aminobutyric acid (GABA)<sub>A</sub>/ benzodiazepine receptor and the GABA<sub>B</sub> receptor as shown in *in*

*vitro* experiments [104, 108]. However, the identification of specific constituents that are major active ingredients have not yet been determined. Nevertheless, flavonoids are known to be a major group of constituents, and include vitexin, isovitexin, orientin, isoorientin, and apigenin [109]. In comparative analysis of 34 *Passiflora* species, the C-glycosylflavones orientin and vitexin were reported to be the most abundant flavonoids [109]. Data from *in vitro* experiments suggest that orientin exerts a neuroprotective effect possibly mediated by activation of the phosphatidylinositol-3 kinase (PI3K)/AKT signaling pathway [110]. As to vitexin, Abbasi *et al.* showed an anticonvulsant effect in the rat brain after intracerebroventricular administration of the compound [111]. In addition, Gozalo *et al.* compared the *per os* treatment with a *Passiflora* extract and apigenin alone, thereby observing a comparable sedative response in mice for both treatments. After pretreatment with the benzodiazepine antagonist flumazenil, the effect of apigenin was no longer observed suggesting the binding of the compound to the GABA<sub>A</sub> receptor [112]. In contrast, Zanoli *et al.* compared intraperitoneally administered apigenin and chrysin, another flavonoid found in *Passiflora* extracts showing an anxiolytic effect after treatment with chrysin. This effect could not be observed after treatment with apigenin. Notably, the anxiolytic effect of chrysin was blocked by flumazenil, indicating its binding to the GABA<sub>A</sub> receptor [113].

Although there are indicators suggesting that constituents of *Passiflora* have to enter the brain in order to exert their pharmacological effects, it is currently unknown whether and to what extent the flavonoids are systemically available after oral administration. Indeed, flavonoids are known to be extensively metabolized by the gut microbiome [114, 115]. However, the catechin epigallocatechin gallate, a tea polyphenol, was radioactively labeled and a broad tissue distribution of the radionuclide was observed in mice [116]. For major flavonoids of *Passiflora* species, such experiments have not been conducted so far nor are there any studies investigating their interaction with OATPs which may influence their pharmacokinetics.



## **Aims of the thesis**

1. To test the applicability and validity of the competitive counterflow approach for the identification of OATP2B1 or OATP1A2 substrates
2. To test the applicability of the competitive counterflow method for the investigation of the influence of herbal extracts on the transporters function
3. To further investigate the role of OATP2B1 in the handling of the identified substrate hyperforin, a component of St. John's wort



## Results

The doctoral thesis is based on four peer-reviewed publications:

### Chapter 1

Establishment and Validation of Competitive Counterflow as a Method To Detect Substrates of the Organic Anion Transporting Polypeptide 2B1

Schäfer AM, Bock T, Meyer zu Schwabedissen HE

### Chapter 2

OATP1A2 and OATP2B1 Are Interacting with Dopamine-Receptor Agonists and Antagonists.

Schäfer AM, Meyer zu Schwabedissen HE, Bien-Möller S, Hubeny A, Vogelgesang S, Oswald S, Grube M

### Chapter 3

Constituents of *Passiflora incarnata*, but Not of *Valeriana officinalis*, Interact with the Organic Anion Transporting Polypeptides (OATP)2B1 and OATP1A2

Schäfer AM, Gilgen PM, Spirgi C, Potterat O, Meyer zu Schwabedissen HE

### Chapter 4

Hyperforin-Induced Activation of the Pregnane X Receptor Is Influenced by the Organic Anion-Transporting Polypeptide 2B1

Schäfer AM, Potterat O, Seibert I, Fertig O, Meyer zu Schwabedissen HE



## Chapter 1

### **Establishment and Validation of Competitive Counterflow as a Method To Detect Substrates of the Organic Anion Transporting Polypeptide 2B1**

Schäfer AM<sup>1</sup>, Bock T<sup>2</sup>, Meyer zu Schwabedissen HE<sup>1</sup>

#### *Laboratories of Origin:*

<sup>1</sup>Biopharmacy, Department of Pharmaceutical Sciences, University of Basel, 4056 Basel, Switzerland

<sup>2</sup>Proteomics Core Facility, Biozentrum, University of Basel, 4056 Basel, Switzerland

#### *Contribution of Anima Schäfer:*

Study design, acquisition, analysis and interpretation of data, drafting of manuscript

#### *Journal:*

Molecular Pharmaceutics (2018), 15, 5501-5513





OATP2B1 contributing to the apical uptake in enterocytes and, therefore, intestinal drug absorption. One compound assessed in this perspective is fexofenadine. Several groups reported *in vitro* findings on fexofenadine being a substrate of OATP2B1,<sup>14,15</sup> even if others were not able to show an interaction with this transporter.<sup>16</sup> Utilizing the inhibition of the OATP2B1 function by grapefruit juice (GFJ),<sup>17</sup> Dresser et al. were able to show that concomitant ingestion of GFJ significantly reduces the AUC and  $C_{\max}$  of the antihistaminic in healthy volunteers, measured over an 8 h period, whereby suggesting reduction of fexofenadine bioavailability by inhibition of transporter-mediated uptake.<sup>18</sup> This is further supported by recent findings showing that GFJ interacts with intestinal absorption of the OATP2B1-substrates rosuvastatin, glibenclamide, celirololol, and sumatriptan.<sup>19</sup> Multiple constituents of GFJ are assumed to inhibit OATP2B1, including the flavonoid naringin.<sup>20,21</sup> However, it seems noteworthy, that OATP2B1 has been shown to exhibit two distinct substrate binding sites, and naringin only inhibits one of them. The binding site interacting with naringin (site A) was shown to bind the known OATP2B1 substrate estrone 3-sulfate ( $E_1S$ )<sup>8</sup> at low concentrations, while binding site B mostly drives  $E_1S$  uptake at higher concentrations. Additionally, site B interacts with testosterone, which is assumed to be a specific substrate of this binding site of OATP2B1.<sup>22</sup> Notably, the presence of multiple binding sites and the variable experimental set up of *in vitro* studies may be reasons for controversial findings on substrates and inhibitors as described above for fexofenadine.

The International Transporter Consortium recommended different approaches to test the interaction of new molecular entities (NME) with transport proteins.<sup>23</sup> In detail, they suggest the use of transient or stable cellular models overexpressing the transporter of interest and various methods to quantify substrate accumulation. The recommended techniques to detect the NME are radiolabeled or fluorescent tracers or the employment of highly sensitive liquid chromatography–mass spectrometry.<sup>23</sup> These detection methods imply direct uptake studies of the compound of interest, which will provide a reliable result, but can be extremely consuming either in time, money, or both. Interestingly, in 1956, Rosenberg and Wilbrandt introduced the method of competitive counterflow (CCF) and applied it to verify transporter-mediated handling of glucose in human red blood cells. Performing experiments after reaching the steady state, they were able to show that addition of a substrate, but not of an inhibitor, of the transporter significantly changed the observed equilibrium of the test compound.<sup>24</sup> Recently this method was used to successfully identify substrates of the organic cation transporter 2 (OCT2).<sup>25</sup>

It was the aim of this study to test whether CCF experiments can also be applied to identify substrates of the organic anion transporting polypeptide OATP2B1.

## ■ EXPERIMENTAL SECTION

**Substances.** Radiolabeled compounds [<sup>3</sup>H]-estrone 3-sulfate ( $E_1S$ ) and [<sup>3</sup>H]-domperidone were purchased from Hartmann Analytic (Braunschweig, Germany), while [<sup>3</sup>H]-astemizole was commercially obtained from PerkinElmer (Waltham, USA). Compounds applied in this study, except for fexofenadine (Lubio Science, Luzern, Switzerland), ketoconazole and troglitazone (TOCRIS, Bio-Techne AG, Zug, Switzerland), and paclitaxel (Lucerna-Chem AG, Luzern, Switzerland), were from Sigma-Aldrich (Buchs, Switzerland).

**Cell Culture.** The cell lines MDCKII (ATCC No. CRL-2936), HeLa (ATCC No. CCL-2), and HepG2 (ATCC No. HB-8065) were originally obtained from the American Type Culture Collection (ATCC, Wesel, Germany) and were cultured in Dulbecco's modified Eagle medium (DMEM, Sigma-Aldrich) supplemented with 10% fetal calf serum (FCS, Sigma-Aldrich) and 1% stable glutamine (BioConcept, Basel, Switzerland). MDCKII-OATP2B1 cells have previously been established<sup>2</sup> and were kept under continuous selection by addition of 0.75 mg/mL hygromycin B (Carl Roth, Karlsruhe, Germany). Cells were maintained at 37 °C in a humidified atmosphere with 5% CO<sub>2</sub>.

**Western Blot Analysis.** MDCKII-OATP2B1 and MDCKII cells were seeded at a density of  $1.8 \times 10^6$  cells/10 cm cell culture dish (Eppendorf, Hamburg, Germany). One day after seeding, cells were treated with sodium butyrate (2 mM) for 24 h and then harvested in 5 mM-Tris HCl (pH 7.4) supplemented with the protease inhibitor cocktail (Sigma-Aldrich). After three cycles of freezing and thawing, the cell homogenate was centrifuged for 45 min at 100 000g and 4 °C for membrane fraction enrichment. The resulting pellet was suspended in 5 mM-Tris HCl, and the amount of protein was quantified by BCA assay (Thermo Fisher Scientific, Reinach, Switzerland). HeLa cells were seeded to the same amount, and 24 h later they were infected with the recombinant attenuated vaccinia virus vTF-7 (ATCC No. VR-2153; 100 pfu/well).<sup>26</sup> After 30 min of incubation with the virus, jetPRIME (2  $\mu$ L/  $\mu$ g DNA) (Polyplus distributed by Chemie Brunschwig, Basel, Switzerland) was used to transfect 800 ng/well of OATP2B1-pEF6 or pEF6-control (pEF6-V5/HIS, Thermo Fisher Scientific). After 24 h of incubation, the cells were harvested as described above. For the adenoviral expression system, HeLa cells were infected with 200 pfu/cell Ad-OATP2B1<sup>9</sup> or Ad-LacZ as the control 1 day after seeding. Adenoviral titer was determined using the Adeno-X Rapid Titer Kit (Clontech, Saint-Germain-en-Laye, France). Cells were harvested 48 h after infection. Proteins were separated by 10% SDS-PAGE using the Mini-PROTEAN System, followed by transfer onto a nitrocellulose membrane using the Mini Trans-blot Cell (Bio-Rad Laboratories AG, Cressier, Switzerland). After protein transfer, the membranes were incubated in blocking buffer (5% FCS- Tris-buffered saline with 0.04% Tween 20 (TBST)) for 1 h, followed by incubation with the primary antibody at 4 °C overnight. For the detection of OATP2B1, the previously reported antiserum was used (diluted 1:5000).<sup>27</sup> The Na<sup>+</sup>/K<sup>+</sup>-ATPase served as a loading control (ab76020, abcam, Lucerna Chem AG). Immobilization of the primary antibody was detected with HRP-labeled secondary antibodies and the ECL Western blotting substrate (Pierce distributed by Thermo Fisher Scientific). Chemiluminescence was visualized and digitalized using the Chemidoc XRS system (Bio-Rad Laboratories AG). Finally, the Image Lab 4.1 software (Bio-Rad Laboratories AG) was used for densitometrical analysis of the protein content normalizing the observed amount of OATP2B1 to that of Na<sup>+</sup>/K<sup>+</sup>-ATPase in the same sample.

**Immunofluorescent Staining.** For immunofluorescent staining, cells were seeded on coverslips at a density of 75 000 cells/well in 12-well plates (Eppendorf). One day after seeding, MDCKII-OATP2B1 or HeLa cells were treated as described in detail above. Cells were fixed with ice-cold methanol:acetone (1:2) for 15 min, permeabilized with 0.2% Tween 20 phosphate buffer saline (PBS), and then incubated with 5%-FCS-1% bovine serum albumin (BSA)-PBS before exposure to

the anti-OATP2B1-anti-serum (1:100).<sup>27</sup> The anti-rabbit Alexa Fluor 488 antibody was used as the secondary antibody (Life Technologies distributed by Thermo Fisher Scientific). After mounting the cells with Roti-Mount FluorCare containing 4',6-diamidino-2-phenylindole (DAPI) for nuclei staining, expression and localization was detected using the Leica DMi8Microscope and the LASX software (Leica Microsystems, Heerbrugg, Switzerland).

**LC-MS/MS Sample Preparation.** Cells infected or transfected as described above were the basis for the mass spectrometric analysis. In detail, cells were harvested and homogenized in 10 mM Tris-0.5 mM MgCl<sub>2</sub> (pH 7.5) using the Potter S homogenizer (Sartorius, Göttingen, Germany). Then the cell homogenate was centrifuged for 5 min at 600g followed by a 5 min centrifugation of the supernatant at 15 000g and 4 °C. Finally, the resulting supernatant was centrifuged for 1 h at 100 000g and 4 °C. The resulting pellet was dissolved in 100  $\mu$ L 2% sodium-deoxycholate in 100 mM ammonium bicarbonate. After the addition of 10 mM tris(2-carboxyethyl)phosphine (TCEP, Sigma-Aldrich) and ultrasonication with a vial Tweeter Ultrasonicator (Hielscher, Teltow, Germany), samples were heated at 95 °C and 300 rpm (Micro Centrifuge Tube Thermomixer; Eppendorf) for 10 min before protein concentration was determined with the Microplate BCA Protein Assay Kit (Thermo Fisher Scientific). Then, 15 mM chloroacetamide (Sigma-Aldrich) was added for carbamidomethylation of cysteins at 37 °C and 500 rpm for 30 min. Of each sample, a total of 50  $\mu$ g was digested for 12 h at 37 °C with porcine trypsin (Promega, Madison, USA) at a final enzyme/protein-ratio of 1:50. The reaction was stopped with 50  $\mu$ L of 5% trifluoroacetic acid (TFA) in water. Peptides were desalted by solid phase extraction using iST cartridges (PreOmics, Planegg/Martinsried, Germany) and dried using an acid resistant CentriVap concentrator (Labcono, Kansas City, USA). Before MS analysis, dried peptides were resuspended in 0.15% formic acid (Sigma-Aldrich) and 2% acetonitrile (Thermo Fisher Scientific).

**Mass Spectrometry.** Mass spectrometric analysis of peptide samples was performed on a Q-Exactive HF mass spectrometer equipped with a nanoelectrospray ion source (both Thermo Fisher Scientific). Data were acquired in the data dependent acquisition (DDA) mode. The  $\mu$ RPLC-MS system was set up as described previously.<sup>28</sup> The chromatographic separation of peptides was performed by an EASY nano-LC 1000 system (Thermo Fisher Scientific) equipped with a heated RP-HPLC column (75  $\mu$ m  $\times$  37 cm) packed in-house with 1.9  $\mu$ m C18 resin (Reprosil-AQ Pur, Dr. Maisch). Peptides were separated using a linear gradient ranging from 95% solvent A (0.1% formic acid) and 5% solvent B (80% acetonitrile, 20% water, 0.1% formic acid) to 45% solvent B over 60 min at a flow rate of 200 nL/min. For DDA acquisition, each MS1 scan was followed by high-collision-dissociation (HCD) of the 20 most abundant precursor ions with an active dynamic exclusion setting of 30 s. The total cycle time was approximately 1 s. For MS1,  $3 \times 10^6$  ions were accumulated in the Orbitrap cell over a maximum time of 100 ms and scanned at a resolution of 120 000 fwhm (at 200  $m/z$ ). MS2 scans were acquired at a target setting of  $1 \times 10^5$  ions, an accumulation time of 50 ms, and a resolution of 15 000 fwhm (at 200  $m/z$ ). Singly charged ions and ions with an unassigned charge state were excluded from the triggering of MS2 events. The normalized collision energy was set to 28%, the mass isolation window was set to 1.4  $m/z$ .

**Mass Spectrometry Data Analysis.** The acquired DDA-based raw-files were converted to a MASCOT generic file format using the msconvert tool (part of ProteoWizard, version 3.0.4624 (2013-6-3)). Converted files were searched using a target decoy strategy by MASCOT (Matrix Sciences) against the UniProt databases of *Homo sapiens* (May 2016, HeLa cell data) and *Canis familiaris* (Feb 2018, MDCK cell data) containing commonly observed contaminant proteins. Additionally, the human OATP2B1 (UniProt ID O94956) was added to the *Canis familiaris* database. The precursor ion tolerance was set to 10 ppm, and fragment ion tolerance was set to 0.02 Da. For database search, strict trypsin specificity allowing for three missed cleavages was used. Carbamidomethylation of cysteins (+57 Da) was set as a fixed modification, and oxidation of methionine (+16 Da) or protein N-terminal acetylation (+42 Da) was set as a variable peptide modification. Scaffold (version 4.8.4 Proteome Software Inc.) was used to validate MS/MS-based peptide and protein identifications. The protein false discovery rate (FDR) was set to 1%, and protein identifications were accepted if they contained at least 2 identified peptides. Protein probabilities were assigned by the Protein Prophet algorithm.<sup>29</sup> Proteins that contained similar peptides and could not be differentiated based on MS/MS analysis alone were grouped to satisfy the principles of parsimony. The normalized spectral abundance factor (NSAF) method was used to calculate OATP2B1 protein intensity.

**OATP2B1 Transport Inhibition Study.** For transport experiments, MDCKII-OATP2B1 or MDCKII cells were seeded at a density of 50 000 cells/well in 24-well plates. One day after seeding, the cells were treated with 2 mM sodium butyrate for another day. After preincubation with Hank's balanced salt solution (HANKs) (Sigma-Aldrich), the cells were exposed to HANKs containing [<sup>3</sup>H]-E<sub>1</sub>S (100 000 dpm/well, 6 nM) and the respective test compound. After 5 min of incubation, cells were washed twice with ice-cold PBS and lysed in 200  $\mu$ L of lysis buffer (10% SDS-5 mM EDTA, pH 7.4). Protein quantification was determined using the Pierce BCA Protein Assay Kit (Thermo Fisher Scientific) and the microplate reader Infinite M200 Pro (Tecan, Männedorf, Switzerland). The residual of the cell homogenate was used to measure the amount of radiolabeled substrate using 2 mL of scintillation fluid (Rotiszint eco Plus, Carl Roth) and the liquid scintillation counter Tri-Carb 2900TR (TopLab, Basel, Switzerland).

**CCF Experiments.** MDCKII-OATP2B1 or MDCKII cells were seeded and stimulated as described above. On the day of experiment, cells were preincubated with HANKs buffer containing 100 000 dpm/well (6 nM) [<sup>3</sup>H]-E<sub>1</sub>S for 30 min to reach steady state. Then, the supernatant was removed, and HANKs buffer (pH 5.5 or pH 7.4) was added containing 100 000 dpm/well (6 nM) [<sup>3</sup>H]-E<sub>1</sub>S and the respective test compounds. The cells were exposed for 90 s to reach the equilibrium of the CCF. The concentration of the test compounds was 10 $\times$  the estimated IC<sub>50</sub>; this concentration had been recommended to be applied in CCF experiments.<sup>25</sup> Protein quantification and intracellular radioactivity were measured as described above. Data were analyzed relating [<sup>3</sup>H]-E<sub>1</sub>S uptake in the presence of the tested compound to the percent of the respective solvent control.

**Determination of OATP2B1-Mediated Uptake of Astemizole and Domperidone.** MDCKII as a control and MDCKII-OATP2B1, seeded and stimulated as described

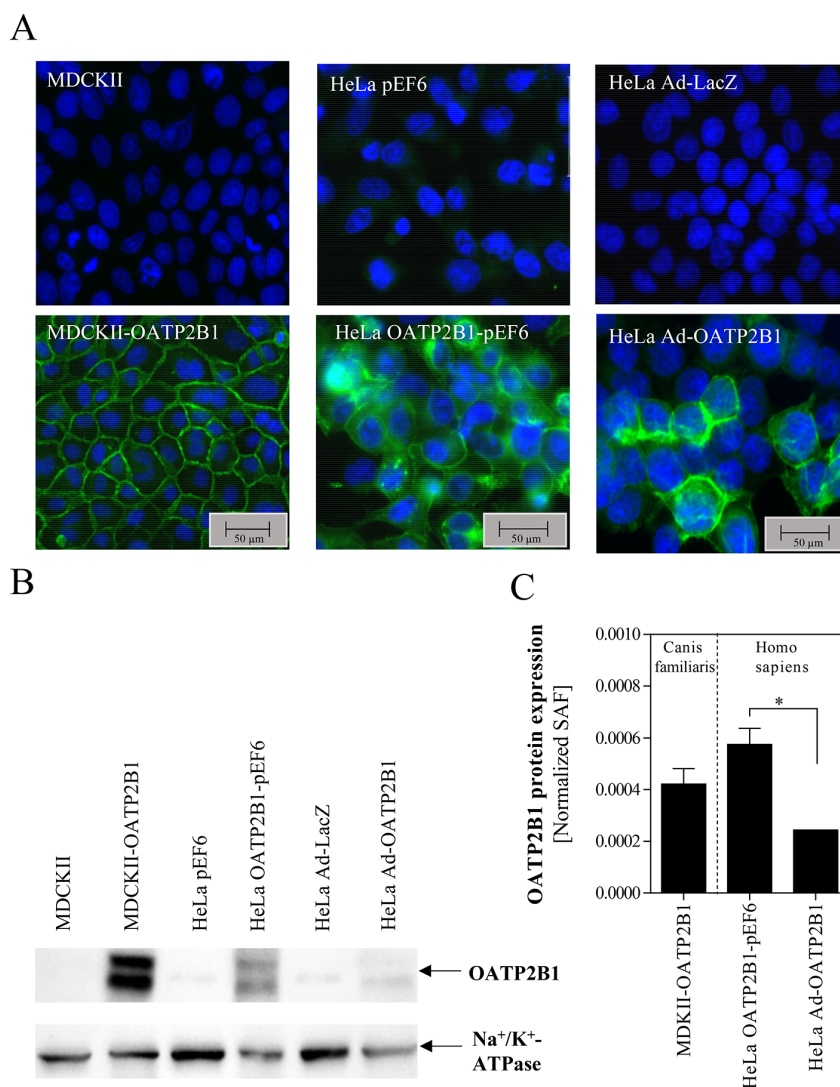


**Figure 1.** OATP2B1 protein expression comparing different methods of cellular delivery. Expression and localization of the transporter were assessed by immunofluorescent staining (A). In detail, MDCKII-OATP2B1 and HeLa cells either infected with vTF-7 and transfected with OATP2B1-pEF6 or infected with Ad-OATP2B1 were fixed and then stained. Antibody binding and nucleic counterstaining with DAPI was visualized by fluorescence microscopy. Amount of OATP2B1 was determined by Western blot analysis of the enriched membrane fraction. Na<sup>+</sup>/K<sup>+</sup>-ATPase served as the control (B). Amount of OATP2B1 was determined by LC-MS/MS in each cellular expression system. Data are shown as the NSAF presenting protein intensity in the respective cellular system (C). Data are presented as mean  $\pm$  SD,  $n = 3$ ,  $*p \leq 0.05$ , one-way ANOVA with Student's *t*-test.

above, were exposed to 0.1  $\mu$ M astemizole or 0.1  $\mu$ M domperidone supplemented with 50 000 dpm/well of the respective radiolabeled tracer [<sup>3</sup>H]-astemizole (2 nM) or [<sup>3</sup>H]-domperidone (4.3 nM) for 5 min. Cellular accumulation of the radiolabel was quantified as described above. For inhibition studies, MDCKII-OATP2B1 cells were treated with the same amount of astemizole or domperidone plus 100  $\mu$ M BSP. Data were analyzed as fmol/ $\mu$ g of protein/min and compared to the solvent control.

**Cell-Based Reporter Gene Assay.** MDCKII-OATP2B1 cells were seeded at a density of 40 000 cells/well in 24-well plates. One day after seeding, the cells were transfected with hPXR-pEF6 or pEF6-control (250 ng/well). The previously reported CYP3A4-XREM-pGL3basic<sup>30</sup> (250 ng/well) was used as the reporter gene construct, while pRL-TK (25 ng/

well) encoding for *Renilla* luciferase served as the transfection control. One day after transfection with jetPRIME using 2  $\mu$ L/ $\mu$ g of DNA, the cells were exposed to hyperforin (0.1  $\mu$ M) and/or bromosulfophthalein (BSP, 10  $\mu$ M) or solvent control for 24 h. Luciferase activity was determined using the Dual-Luciferase Assay System (Promega, Dübendorf, Switzerland) and the plate reader Infinite M200 Pro as recommended by the manufacturer. The luminescence detected for the *Firefly* luciferase was normalized to that observed for the *Renilla* in each sample. Data are presented as the fold of solvent control.

**Determination of Cellular Viability.** MDCKII and MDCKII-OATP2B1 cells were seeded at a density of 10 000 cells/well in 96-well plates (Eppendorf) and stimulated as described above. After 6 h of incubation with etoposide or teniposide, the medium was changed. The treatment with

**Table 1.** Influence of Compounds on the OATP2B1-Mediated Uptake Accounting for the Previously Reported Binding Site A (Low Concentration of E<sub>1</sub>S) or Binding Site B (High Concentration of E<sub>1</sub>S)<sup>a,b</sup>

compound	binding site A		binding site B		previously reported IC <sub>50</sub> (μM)	ref	previously reported k <sub>m</sub> (μM)	ref
	estimated IC <sub>50</sub> (μM)	95% confidence interval	estimated IC <sub>50</sub> (μM)	95% confidence interval				
astemizole	20.71	13.98–30.66	170.20	104.30–277.60	n.r.	38	n.d.	
atorvastatin	0.26	0.18–0.37	4.32	3.29–5.66	0.7	2	0.2	2
							2.84	38
BSP	1.91	0.93–3.92	23.76	14.18–39.81	2.0	67	0.7	10
cerivastatin	5.40	2.17–13.43	43.41	22.03–85.56	66.2	2	n.r.	32
cyclosporin A	61.14	29.35–127.4			0.07	36	n.d.	
					37	38		
					20	42		
domperidone	6.31	3.27–12.17	70.57	36.40–136.80	n.d.		n.d.	
dronedarone	96.36	55.00–168.80	342.60	203.20–577.70	n.d.		n.d.	
enalapril					n.i.	38	n.d.	
erythromycin					>1100	39	n.d.	
etoposide	71.23	54.93–92.37			n.i.	38	n.d.	
fenofibrate	118.20	47.70–292.90	42.88	18.70–98.29	n.i.	38	n.d.	
fexofenadine	524.50	418.3–657.50			n.d.		0.14	17
fluoxetine					n.i.	38	n.d.	
FTC					n.d.		n.d.	
gemfibrozil	388.30	264.0–571.1			8.0	36	n.d.	
glibenclamide	0.57	0.26–1.27			2.0	68	6.3	34
hyperforin	0.55	0.29–1.06	12.89	4.73–35.10	n.d.		n.d.	
indomethacin	22.14	11.06–44.30	239.30	73.31–781.20	n.i.	38	n.d.	
irbesartan	6.92	3.70–12.93	445.40	172.3–1151	n.d.		n.d.	
itraconazole	79.49	30.97–204.0	174.40	73.88–411.90	n.r.	38	n.d.	
ketoconazole	5.25	3.36–8.23	23.61	8.26–67.55	n.i.	38	n.d.	
lorglumide	0.89	0.36–2.23			n.d.		n.d.	
loxiglumide	7.33	4.89–10.97			n.d.		n.d.	
metoprolol					n.d.		n.d.	
naringin	12.62	7.70–20.66			36.4	20	n.d.	
					4.63	21		
paclitaxel					25	42	n.s.	42
					n.i.	38		
penicillin G					n.r.	22	n.s.	42
					n.i.	38		
probenecid					n.i.	38		
proglumide					n.d.		n.d.	
sunitinib	88.34	49.01–159.20			88	40	n.d.	
talinolol	407.40	297.0–558.8			n.r.	22	629	33
teniposide	14.24	9.68–20.94			n.r.	37		
tolbutamide					n.i.	38		
T <sub>4</sub>	7.68	3.83–15.38	41.67	13.27–130.90	2.43	41	0.77	35
T <sub>3</sub>	2.10	1.35–3.12	19.65	8.77–44.02	0.51	41		
trogliatzone	8.87	3.88–20.30	51.26	22.06–119.10	n.d.		n.d.	
valproate					n.r.	38		
valsartan					n.i.	38		
venlafaxin					n.d.		n.d.	
verapamil					n.i.	38	n.d.	

<sup>a</sup>Inhibitory potency was estimated calculating the respective IC<sub>50</sub> using data obtained in transport experiments using MDCKII-OATP2B1 cells. In addition, previously reported IC<sub>50</sub> and k<sub>m</sub> (Michaelis Menten constant) values are listed. <sup>b</sup>n = 3–5 experiments; BSP, bromosulphothalein; FTC, funitremorin C; T<sub>4</sub>, thyroxine; T<sub>3</sub>, triiodothyronine; n.r., not reported; n.d., not determined; n.i., no inhibition; and n.s., no substrate.

paclitaxel was performed for 24 h. Cell viability was assessed 24 h after the treatment started using the Resazurin Fluorometric Cell Viability Kit (PromoCell GmbH, Heidelberg, Germany) according to the manufacturers' instruction. Fluorescence was detected using the Infinite M200 Pro plate reader (Ex = 530 nm, Em = 590 nm). Viability was calculated as the percent of

solvent control after subtracting the fluorescence of the medium control, as follows:

$$\% \text{ of solvent control} = \frac{\text{sample} - \text{control medium}}{\text{control} - \text{control medium}} \times 100$$

**Statistical Analysis.** Analysis of data was performed using the GraphPad Prism software 6.0 (GraphPad Software) and

Microsoft Excel (Microsoft, Redmond, USA). In the context of data presentation, the respective statistical test is indicated. A *p*-value below 0.05 was considered statistically significant.

## RESULTS

**Comparison of Cellular OATP2B1 Content in Different Heterologous Expression Systems.** OATP2B1 expression was assessed after applying three methods for the delivery of the information encoding for the transporter. These systems were stably transfected MDCKII-OATP2B1 cells, a vTF-7-based expression system (HeLa OATP2B1-pEF6), and an adenoviral expression system (HeLa Ad-OATP2B1). At first, expression and localization of OATP2B1 was compared by immunofluorescent staining. As shown in Figure 1A, all cellular expression systems resulted in a positive fluorescent signal. Especially in MDCKII-OATP2B1, we observed a well-defined signal at the basolateral membrane of these polarized cells. In HeLa cells either transfected with OATP2B1-pEF6 or infected with Ad-OATP2B1, we observed some membrane enrichment even if the fluorescent signal was much less defined. No staining was observed in MDCKII, HeLa pEF6, or HeLa Ad-LacZ cells, which served as controls. As shown in Figure 1B by a representative image, Western blot analysis detecting the uptake transporter in the enriched membrane fraction revealed the highest level of the transporter in the stable expression system, while the lowest amount was found after adenoviral delivery (mean OATP2B1 expression normalized to  $\text{Na}^+/\text{K}^+\text{-ATPase} \pm \text{SD}$ ; MDCKII-OATP2B1 vs HeLa OATP2B1-pEF6 vs HeLa Ad-OATP2B1;  $1.67 \pm 0.32$  vs  $0.73 \pm 0.75$  ( $p > 0.05$ ) vs  $0.07 \pm 0.01$  ( $p < 0.05$ ),  $n = 3$ , one-way ANOVA corrected for multiple comparisons). Verification of OATP2B1 protein expression was successfully performed by mass spectrometry in the MDCKII-based and in the HeLa-based expression systems. Similar to the results above, we observed a significantly higher amount of OATP2B1 in transiently transfected HeLa OATP2B1-pEF6 vs HeLa Ad-OATP2B1 cells and a robust expression of OATP2B1 in the MDCKII-OATP2B1 cell line by quantitative mass spectrometry (Figure 1C).

**Screening of a Compound Library for Interaction with OATP2B1.** A list of 40 compounds was prepared, summarizing known substrates,<sup>2,10,14,17,31–35</sup> known inhibitors,<sup>18,21,22,36–41</sup> and substances without impact on OATP2B1.<sup>37,38,42</sup> In addition, 11 molecules were added to the library where interaction with OATP2B1 was unknown. All compounds were tested for inhibition of OATP2B1-mediated uptake of  $\text{E}_1\text{S}$  in MDCKII-OATP2B1 cells. In order to account for the previously reported binding sites,<sup>22</sup> we tested inhibition of OATP2B1 using a low ( $0.005 \mu\text{M}$ ) and a high ( $50 \mu\text{M}$ ) concentration of  $\text{E}_1\text{S}$  referred to as binding site A and B, respectively. Three concentrations of each compound were used for an estimation of inhibitory potency ( $\text{IC}_{50}$ ). Selection of the concentrations applied in the inhibition study was either based on  $\text{IC}_{50}$  values reported in the literature (compare Table 1) or, if no  $\text{IC}_{50}$  was available, the experiment was performed with 1, 10,  $100 \mu\text{M}$  of the respective test compound. As summarized in Table 1, inhibition of both binding sites was observed for the previously reported substrates atorvastatin, bromosulphophthalein, cerivastatin, and thyroxine ( $\text{T}_4$ ), while fexofenadine, glibenclamide, and talinolol were binding site A inhibitors. Furthermore, the previously reported inhibitors astemizole, itraconazole, and triiodothyronine ( $\text{T}_3$ ) were verified. Cyclosporine A, gemfibrozil, naringin, sunitinib, and

teniposide were specifically inhibiting binding site A. However, even if no interaction with OATP2B1 was shown by others,<sup>37,38,40</sup> we observed potent inhibition by etoposide, fenofibrate, indomethacin, and ketoconazole. For the compounds where interaction with OATP2B1 was unknown, we observed potent inhibition of binding site A in the presence of lorglumide and loxiglumide and for both binding sites in the presence of domperidone, dronedarone, hyperforin, irbesartan, and troglitazone. Finally, no inhibition was observed for enalapril, erythromycin, fluoxetine, funitremorgin C (FTC), metoprolol, paclitaxel, penicillin G, probenecid, proglumide, tolbutamid, valproate, valsartan, venlafaxine, and verapamil.

**CCF Experiments.** CCF experiments are conducted after reaching the steady state, whereby defining the time of preincubation in the experimental set up. Accordingly, this time of preincubation was determined performing time-dependent uptake studies using tritium-labeled  $\text{E}_1\text{S}$  at a concentration of 6 nM. Independent of the cellular expression system, the steady state was reached after at least 30 min (Figure S1). This time of preincubation was the basis for the following experiments, where the time of reaching equilibration in the CCF was assessed, exchanging the supernatant used for preincubation with transport buffer containing the same amount of  $\text{E}_1\text{S}$  (6 nM) and a very high amount ( $50 \mu\text{M}$ ) of  $\text{E}_1\text{S}$ . In MDCKII-OATP2B1 cells and in the vTF-7-based expression system, the equilibrium was reached after 90 s of incubation. However, we were not able to determine the equilibrium in the adenoviral system (Figure S1). We interpreted this by the much lower transport rate, which might be explained by the much lower amount of OATP2B1 detected in these cells (Figure 1). The time of reaching equilibration in the CCF was validated in MDCKII-OATP2B1 cells using the known substrates BSP and atorvastatin, both applied at a concentration of  $50 \mu\text{M}$  (Figure S2).

**Application of CCF with a Compound Library.** Subsequently, we applied the established CCF protocol to our compound library using MDCKII-OATP2B1 cells. As recommended by Harper et al.,<sup>25</sup> concentrations used in the CCF experiment were 10-fold higher than the estimated  $\text{IC}_{50}$  value (Table 1), if applicable. In the case of solubility issues, we used a concentration of  $250 \mu\text{M}$  of the respective compound.

As shown in Figure 2 and summarized in Table S1, we observed a significantly reduced amount of  $\text{E}_1\text{S}$  in the CCF for all previously validated substrates of OATP2B1 (atorvastatin, BSP, cerivastatin, fexofenadine, glibenclamide, talinolol, and thyroxine ( $\text{T}_4$ ), compared to Table 1). All but fexofenadine, glibenclamide, and talinolol were identified above as inhibitors of both binding sites. Furthermore, among the compounds we observed to inhibit binding site A and B, we identified astemizole, domperidone, hyperforin, irbesartan, itraconazole, ketoconazole, and triiodothyronine ( $\text{T}_3$ ) as substrates of OATP2B1, while troglitazone, indomethacin, fenofibrate, and dronedarone did not significantly influence the steady state of  $\text{E}_1\text{S}$ . However, for fenofibrate and dronedarone, we did not reach the recommended 10-fold of  $\text{IC}_{50}$ .

Among the compounds, which we observed to only inhibit binding site A, cyclosporine A, etoposide, lorglumide, loxiglumide, naringin, sunitinib, and teniposide significantly reduced the amount of  $\text{E}_1\text{S}$ , suggesting that these compounds are substrates of the transporter. For cyclosporine A, gemfibrozil, and sunitinib, the used concentration ( $250 \mu\text{M}$ ) did not reach the recommended 10-fold of  $\text{IC}_{50}$ . Accordingly, the lack of interaction observed for gemfibrozil does not

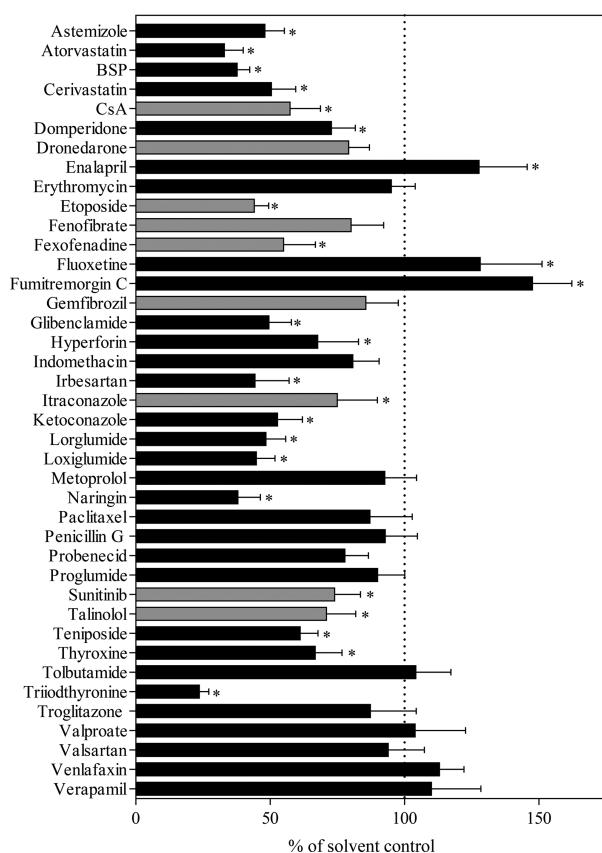


**Figure 2.** CCF experiments in MDCKII-OATP2B1 cells testing a compound library. CCF experiments were conducted in MDCKII cells expressing OATP2B1. The amount of  $E_1S$  was determined 90 s after exchanging the supernatant in the steady state. The experiment was conducted using each inhibitor at 10-fold  $IC_{50}$ . For some inhibitors, this concentration was not reached due to solubility issues (indicated in gray). These and all noninhibitors were tested at 250  $\mu M$ . Data are shown as mean  $\pm$  SD,  $n = 3$  independent experiments each performed in biological triplicates. \* $p \leq 0.05$ , one-way ANOVA with Dunnett's multiple comparisons test. BSP, bromosulphthalein; CsA, cyclosporine A.

necessarily mean that this compound is not a substrate of OATP2B1. The same applies to the above-mentioned dronedarone and fenofibrate.

Analyzing the amount of  $E_1S$  in MDCKII-OATP2B1 cells revealed no significant reduction in the presence of molecules identified to be noninhibitors of OATP2B1 (enalapril, erythromycin, fluoxetine, fumitremorgin C, metoprolol, paclitaxel, penicillin G, probenecid, proglumide, valproate, valsartan, venlafaxine, and verapamil). Interestingly, for enalapril, fluoxetine, and fumitremorgin C, we even observed significantly increased amounts compared to the solvent control. In order to determine whether these compounds influence the cellular amount of  $E_1S$  in native MDCKII cells direct inhibition or CCF, experiments were conducted. As shown in Figure S4A, none of the tested compounds influenced cellular  $E_1S$  accumulation at 5 min of exposure or the steady-state equilibrium (Figure S4B) ( $p > 0.05$ , one-way ANOVA with Dunnett's test). The molecules tested were identified inhibitors and substrates (astemizole, atorvastatin, and hyperforin), compounds that did not interact with

OATP2B1 in CCF experiments but were identified as inhibitors (dronedarone, fenofibrate, gemfibrozil, indomethacin, and troglitazone), or the above-mentioned fluoxetine and fumitremorgin C, where we observed significantly increased  $E_1S$  accumulation in the steady state equilibrium but no direct interaction with OATP2B1-mediated transport.

#### Validation of Identified Substrates of OATP2B1.

Applying CCF, we identified the epipodophyllotoxins, etoposide, and teniposide, but not the taxane paclitaxel, as substrates of OATP2B1. In order to verify this observation, we tested the influence of OATP2B1 expression on the cytotoxic effect of these molecules. In detail, in the presence of OATP2B1, etoposide exhibited a significantly enhanced cytotoxicity, as determined by estimating the inhibitory potency ( $IC_{50}$ ; MDCKII vs MDCKII-OATP2B1; 1559  $\mu M$ , CI 63.46 to 38323  $\mu M$  vs 101.3  $\mu M$ , CI 73.30 to 140.1  $\mu M$ ; Figure 3A). Similar results were obtained for teniposide (362.8  $\mu M$ , CI 224.1 to 587.3  $\mu M$  vs 7.848  $\mu M$ , CI 5.141 to 11.98  $\mu M$ ; Figure 3B) but not for paclitaxel (234.9  $\mu M$ , CI 119.5 to 461.7  $\mu M$  vs 385.3  $\mu M$ , CI 148.1 to 1003  $\mu M$ ; Figure 3C). These results supported the notion that etoposide and teniposide are substrates of the uptake transporter.

Another compound herein identified as a substrate was hyperforin. This constituent of St John's wort is a known activating ligand of the pregnane X receptor (PXR), whereby enhancing expression of CYP3A4.<sup>43</sup> Assuming that cellular accumulation and thereby the cellular activity of hyperforin is influenced by the function of OATP2B1, we tested whether concomitant administration of BSP, a known competitive inhibitor of OATP2B1, influences hyperforin-induced transactivation of CYP3A4 in cell-based reporter gene assays. As shown in Figure 3D we observed significantly reduced transactivation when exposing the cells to hyperforin (0.1  $\mu M$ ) and BSP (10  $\mu M$ ) compared to hyperforin alone, no such effect was observed in MDCKII cells. Importantly BSP does not function as a ligand of PXR.

Finally, the CCF experiments suggested that the antihistamine astemizole and the dopamine  $D_2$  receptor antagonist domperidone are substrates of OATP2B1. In order to validate those findings, direct uptake experiments were performed using [ $^3H$ ]-astemizole and [ $^3H$ ]-domperidone. As shown in Figure 4, MDCKII-OATP2B1 exhibited significant [ $^3H$ ]-astemizole uptake (mean uptake  $\pm$  SEM 2.3  $\pm$  0.31 pmol/ $\mu g$  of protein/min, Figure 4A) and [ $^3H$ ]-domperidone uptake (mean uptake  $\pm$  SEM 2.2  $\pm$  0.2 pmol/ $\mu g$  of protein/min, Figure 4B) compared to MDCKII. Testing the influence of concomitant administration of BSP on the cellular accumulation revealed significantly reduced uptake of [ $^3H$ ]-astemizole (Figure 4C) or [ $^3H$ ]-domperidone (Figure 4D) compared to the solvent control.

**Influence of the pH on CCF Experiments with OATP2B1.** It has been reported that OATP2B1 function is sensitive to pH, especially for  $E_1S$ . Nozawa et al. reported increased uptake with decreasing pH.<sup>14</sup> In accordance with their findings, we observed an almost 2-fold increase in cellular accumulation in the presence of pH 5.5 compared to experiments conducted at physiological pH assessing the time-dependent uptake of  $E_1S$  (Figure 5A). To test, whether pH affects the results from CCF, we performed the experiment at pH 5.5 (Figure 5B) using a selection of the tested compounds, namely, atorvastatin, BSP, and naringin, which we identified as substrates in the CCF conducted at physiological pH (Figure 5C). Penicillin G was chosen as a negative control

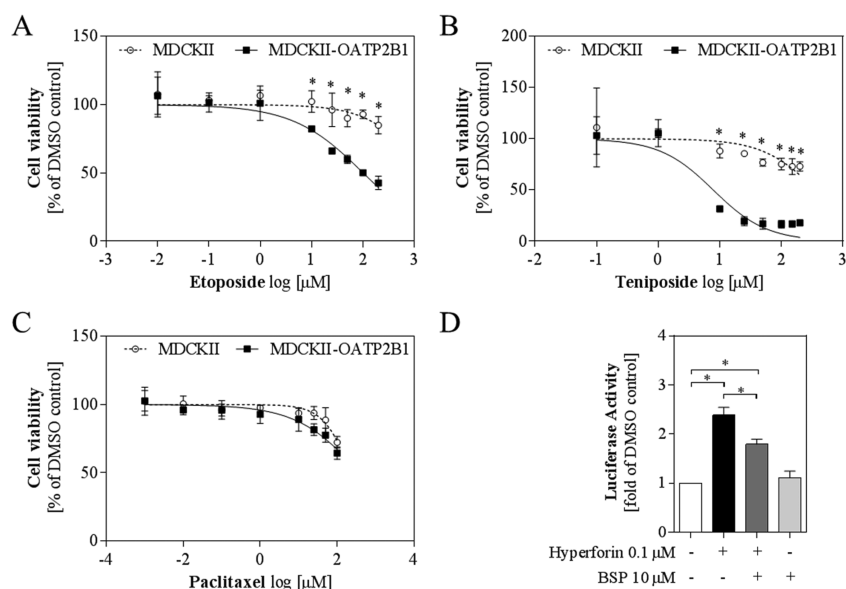


**Figure 3.** Verification of newly identified substrates of OATP2B1 by indirect methods. MDCKII or MDCKII-OATP2B1 cells were treated with increasing concentrations of etoposide (A), teniposide (B), or paclitaxel (C), followed by determination of cell viability. The dose response curves were fitted to estimate the  $IC_{50}$  value in the presence or absence of OATP2B1. Data are presented as mean  $\pm$  SD,  $n = 3$  experiments,  $*p \leq 0.05$ , and two-way ANOVA with Sidak's multiple comparisons test. MDCKII-OATP2B1 cells were transfected with the synthetic CYP3A4-XREM-pGL3-basic reporter construct and tested for PXR-mediated transactivation by hyperforin in the presence or absence of the OATP2B1-inhibitor BSP (D). Data are presented as mean  $\pm$  SD,  $n = 3$  independent experiments each conducted in biological triplicates.  $*p \leq 0.05$ , one-way ANOVA with Dunnett's multiple comparisons test.

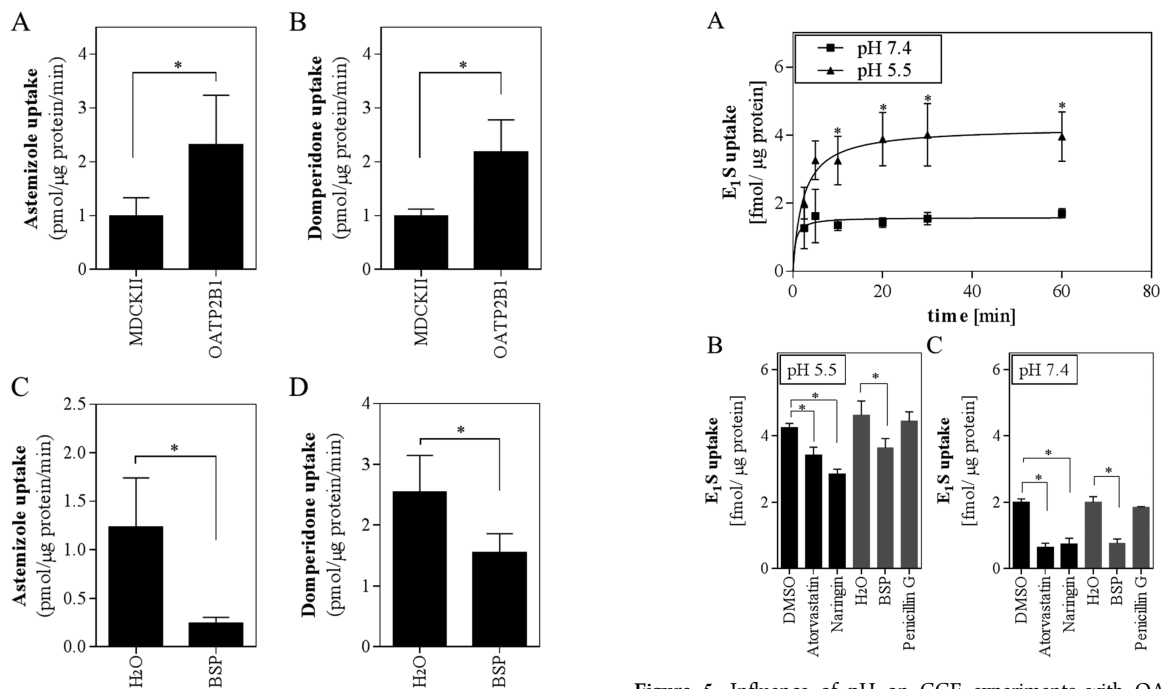


**Figure 4.** Transport of astemizole and domperidone by OATP2B1. Cellular uptake of astemizole (A) and domperidone (B) was assessed in MDCKII and MDCKII-OATP2B1 cells. Inhibition studies were conducted in MDCKII-OATP2B1 cells comparing uptake of astemizole (C) and domperidone (D) in the presence of 100  $\mu$ M BSP compared to the solvent control. Data are presented as mean  $\pm$  SD,  $n = 3$  independent experiments each conducted in biological triplicates.  $*p \leq 0.05$ , Student's *t*-test.

**Figure 5.** Influence of pH on CCF experiments with OATP2B1. Time-dependent uptake of  $E_1S$  at pH 5.5 and pH 7.4 was determined in MDCKII-OATP2B1 cells (A). Data are presented as mean  $\pm$  SD,  $n = 3$  in biological triplicates,  $*p \leq 0.05$ , two-way ANOVA with Sidak's multiple comparisons test. CCF experiments were conducted at pH 5.5 (B) and pH 7.4 (C). Data are presented as mean  $\pm$  SD of  $n = 3$  independent experiments performed in biological triplicates.  $*p \leq 0.05$ , one-way ANOVA with Dunnett's multiple comparisons test.

since it did not influence the equilibrium, and as it was previously reported to not be substrate of OATP2B1.<sup>42</sup> For atorvastatin, BSP, and naringin, we observed significantly decreased cellular E<sub>1</sub>S accumulation at pH 5.5, while penicillin G did not affect the equilibrium.

## DISCUSSION

In this article we report, that the method of CCF is applicable for OATP2B1 substrate identification. According to the FDA guidelines, an attempt to identify potential drug transporter interactions has to be made if available clinical data suggest that renal, biliary, or gut secretion contributes significantly to drug elimination observed in available clinical data.<sup>44</sup> With the CCF, the portfolio of approaches to screen for transporter interaction is broadened by an additional method. Kim Brouwer and colleagues, on behalf of the International Transporter Consortium, summarized the procedures that could be used to test transport of new molecular entities.<sup>45</sup> All of the methods described apply direct quantification of the compound of interest using cellular systems overexpressing the transporter of interest. Most of the approaches described by Brouwer et al. are based on the quantification of unidirectional flow, which would be, in the case of a transporter facilitating uptake, the determination of the cellular accumulation. In contrast, the CCF finds its basis in considerations on net fluxes in a cellular system, where the facilitating mechanism would certainly contribute. Another method considering fluxes, which is often applied in the preclinical assessment of new molecular entities, are transcellular flux experiments. Most common are transwell studies with Caco-2 cells, where the transcellular net flux in the apical to basal (A → B) and basal to apical (B → A) direction is applied to determine whether there is an active uptake component and to predict oral bioavailability of a compound.<sup>46</sup> As previously and excellently summarized by the Nobel prize winner William Stein,<sup>47</sup> the CCF is based on an early observation made for the accumulation of glucose in erythrocytes by Rosenberg and Wilbrandt.<sup>24</sup> According to Stein, the phenomenon of competitive exchange will be found in any situation where a facilitated diffusion system is at or close to saturation at both faces of the membrane and a second substrate sharing the same facilitating system is added. In this situation, the original low net flux, which is observed in the steady state, will be converted into a high unidirectional transport, as the second substrate is competing for substrate binding.<sup>47</sup> Inhibitors not being substrates of the facilitating system do not significantly influence the amount of the driven substrate (in our case E<sub>1</sub>S). According to Harper et al., who provided the first evidence that CCF could be applied to differentiate inhibitors and competing substrates of the drug transporter organic cation transporter 2 (OCT2, SLC22A2), a ligand or substrate competes with the driven substrate for recognition but allows transporter turnover, whereby contributing to the observed reduction in cellular accumulation. In contrast, an inhibitor would block the turnover of the transporter, whereby reducing the so-called “up-hill” transport, the equilibrium stays unchanged. This allows for the differentiation between inhibitors and substrates.<sup>25</sup> With the herein reported method, we extend the application to organic anions.

We think the observation that the presence of a competing substrate reduces the cellular amount of the driven substrate (in our case E<sub>1</sub>S) does not necessarily have to be translated into an equimolar bidirectional function of the investigated

transporter. Especially, considering that endogenously expressed ABC-transporters significantly contribute to the steady state equilibrium, and that these efflux transporters are sharing multiple substrates with uptake transporters. This may not be as important for the previously reported CCF application on OCTs as there is less overlap between ABC-transporters and OCTs. The driven substrate in our experiments was E<sub>1</sub>S. It has previously been reported that E<sub>1</sub>S is a substrate of human ABCG2.<sup>48</sup> When we determined the amount of E<sub>1</sub>S in the presence of fumitremorgin C, a potent and specific ABCG2 inhibitor,<sup>49</sup> we observed significantly enhanced cellular amounts of E<sub>1</sub>S, whereby supporting the idea that ABCG2 at least participates at the steady state. Furthermore, enalapril has been reported as a substrate of the efflux transporter ABCC2,<sup>50</sup> and flouxetine has been reported as an inhibitor of P-glycoprotein (ABCB1);<sup>51</sup> both compounds significantly enhanced the cellular amount in our experimental set up, even if not interacting with the investigated transporter. Consequently, it may be speculated that if a molecule is a potent inhibitor of efflux transporters, it may not be identified as a substrate of OATP2B1 when applying CCF experiments. However, some of the herein identified substrates are known to interact with ABC-transporters, including atorvastatin,<sup>52</sup> bromosulphthalein,<sup>53</sup> etoposide,<sup>54</sup> fexofenadine,<sup>55</sup> and hyperforin,<sup>56</sup> suggesting that this limitation does not necessarily apply. Importantly, when we tested a selection of compounds for their influence on cellular accumulation in native MDCKII cells, we observed no impact on the cellular amount neither after short-term exposure nor in the steady state equilibrium, suggesting that the efflux component can only be seen, when the cellular amount is increased by an uptake mechanism.

We tested multiple compounds for interaction with OATP2B1 and were able to differentiate inhibitors and substrates of OATP2B1. However, some of the herein identified inhibitors have previously been qualified as non-inhibitors of OATP2B1. Indeed, Karlgren et al. tested a library of 225 substances for interaction with the hepatically expressed OATPs, namely, OATP1B1, OATP1B3, and OATP2B1. In their analysis, a compound was considered an inhibitor when reducing cellular accumulation of E<sub>1</sub>S by at least 50% in the presence of 20 μM of the test compound. Applying these identifiers, they qualified several inhibitors of our library as noninhibitors.<sup>38</sup> However, testing a wider range of concentrations, we observed statistically significant concentration-dependent inhibition of binding site A of OATP2B1 for etoposide (IC<sub>50</sub> 71 μM) and gemfibrozil (IC<sub>50</sub> 388 μM). Indomethacin (IC<sub>50</sub> A, 22 μM; B, 44 μM), fenofibrate (IC<sub>50</sub> A, 118 μM; B, 43 μM), and ketoconazole (IC<sub>50</sub> A, 5 μM; B, 23 μM), which are also reported to be noninhibitors, interacted with both sites, binding site A and binding site B. Considering the observed inhibitory potency in our study, the classification as noninhibitor or inhibitor was similar. Our findings on paclitaxel not being an inhibitor and finally not a substrate of OATP2B1 are in accordance with those by Karlgren et al., while others observed an IC<sub>50</sub> of 25 μM.<sup>42</sup>

Applying the CCF, none of the noninhibitors as determined in our inhibition study significantly reduced the amount of E<sub>1</sub>S in equilibrium. Importantly, all known OATP2B1 substrates were identified. Furthermore, we were able to report novel substrates of OATP2B1. One of these is the antihistaminic astemizole, where transport was validated by direct uptake studies. Known for its QT interval prolongation,<sup>57</sup> astemizole was withdrawn from the market in most countries. Never-

theless, it has been tested as a novel approach in breast cancer therapy.<sup>58</sup> Consequently, it seems to still be a medication where knowledge about the uptake mechanism is of interest. Another antihistamine drug, which we identified applying CCF as a substrate of OATP2B1, is fexofenadine. Although this compound has been reported as being a substrate of OATP1A2,<sup>16</sup> our findings are in accordance with those by Shirasaka et al.<sup>17</sup> Furthermore, there are multiple lines of evidence supporting a role of OATP2B1 in fexofenadine pharmacokinetics, as recently summarized by Akamine and Miura, including the influence of genetic variants of OATP2B1 and the shown influence of fruit juices on fexofenadine disposition (AUC and  $C_{max}$ ) in vivo.<sup>59</sup> Multiple components of fruit juices efficiently inhibit OATP2B1 function.<sup>21</sup> One major constituent of GFJ is naringin, which we also identified as a substrate of OATP2B1 when performing CCF experiments.

There are various approaches to verify transporter mediated uptake of a compound. One possibility is to test the influence of a transporter on the pharmacological effect if this is depending on cellular accumulation. In this study, we applied cell-based reporter gene assays and cytotoxicity assays to verify interaction with OATP2B1. Using MDCKII and MDCKII-OATP2B1 cells, we were able to show that the cytotoxic effect of teniposide is significantly enhanced by OATP2B1, whereby supporting the idea that teniposide is a substrate of OATP2B1, as we have previously shown by overexpressing OATP2B1 in human coronary artery smooth muscle cells.<sup>37</sup> Etoposide is another topoisomerase II inhibitor used as a chemotherapeutic medication. Even if this compound does not interact with OATP2B1 at low concentrations,<sup>37,38</sup> we were able to show inhibition and to identify it as a substrate. The notion of etoposide being a substrate of OATP2B1 was validated by comparing its cytotoxic effect in OATP2B1-expressing and wild-type cells. Etoposide was significantly more efficient in cells overexpressing OATP2B1. Interestingly, Reif et al. were able to show significantly reduced oral bioavailability of etoposide when drinking GFJ before intake of the medication.<sup>60</sup> Considering the above-mentioned beverage-drug interactions, these data support our finding of etoposide being a substrate of the uptake transporter. The chemotherapeutic paclitaxel served as the control in our indirect validation experiment, as it was not identified as a substrate of OATP2B1.

Finally, we validated hyperforin as a substrate of OATP2B1. This constituent of St. John's wort is not only assumed to be of pharmacological relevance in terms of antidepressant activity,<sup>61</sup> but it is also a key component for the drug-drug interaction potential of this commonly used herbal extract.<sup>62</sup> Indeed, hyperforin is a ligand and potent activator of PXR, which after activation induces the transcription of multiple genes involved in drug metabolism.<sup>63</sup> The enhanced transcription and expression of drug metabolizing enzymes (e.g., CYP3A4) and drug transporters (e.g., P-glycoprotein/ABCB1) is the basis of current considerations on drug interactions.<sup>64</sup> Our findings, showing that inhibition of OATP2B1 by BSP influences transactivation by hyperforin, not only support that hyperforin is indeed a substrate of OATP2B1 but also broadened the spectrum of possibilities one has to consider when evaluating the consequences of concomitant drug use. However, it is beyond the scope of this study to speculate on the consequences of the concomitant use of OATP2B1 inhibitors and hyperforin.

When establishing CCF conditions, three different OATP2B1 overexpressing cellular systems were examined. Interestingly, when comparing the amount of OATP2B1 expression, Western blot analysis reflected functional data, while the LC-MS/MS data did not. Notably, our LC-MS/MS data suggest that membrane enrichment is influenced by the cellular background, which is in agreement with previous findings by Wegler et al.<sup>65</sup> who compared LC-MS/MS data from different laboratories by applying different methods of cellular fractionation. Even if we used HeLa cells for both viral driven expression systems, the difference in the viruses (adenovirus and vaccinia virus) may certainly have influenced the enrichment of the cellular fractions, especially considering that the vTF-7 virus is lytic in HeLa cells.<sup>66</sup>

Taken together, the herein established experimental set up for CCF experiments can be implemented to identify substrates of OATP2B1. Performance is independent whether substrates are interacting with binding site A and B or only with binding site A. Factors limiting the applicability of the experimental procedure are the inhibitory potency (as solubility might become an issue) and the amount of transporter expressed in the cellular system.

## ■ ASSOCIATED CONTENT

### 📄 Supporting Information

The Supporting Information is available free of charge on the ACS Publications website at DOI: 10.1021/acs.molpharmaceut.8b00631.

Data about the establishment of experimental conditions for CCF, the time dependent uptake of estrone 3-sulfate at pH 5.5 and pH 7.4, a summary of the data underlying Figure 2, and transport experiments performed in native MDCKII cells (PDF)

## ■ AUTHOR INFORMATION

### Corresponding Author

\*E-mail: [h.meyerauschwabedissen@unibas.ch](mailto:h.meyerauschwabedissen@unibas.ch); Phone: 0041-61 207 1495.

### ORCID <sup>®</sup>

Henriette E. Meyer zu Schwabedissen: 0000-0003-0458-4579

### Notes

The authors declare no competing financial interest.

## ■ ACKNOWLEDGMENTS

This work was fully funded by the Biopharmacy of the University of Basel. The authors thank Dr. Celio Ferreira for his support at the initiation of the project.

## ■ ABBREVIATIONS

BSA, bovine serum albumin; BSP, bromosulphophthalein; CCF, competitive counterflow; CsA, cyclosporine A; DAPI, 4',6-diamidino-2-phenylindole; DDA, data dependent acquisition; DHEAS, dehydroepiandrosterone-sulfate; DMEM, Dulbecco's modified Eagle medium; E<sub>1</sub>S, estrone 3-sulfate; FCS, fetal calf serum; FDA, Food and Drug Administration; GFJ, grapefruit juice; HANKS, Hank's balanced salt solution; HCD, high collision dissociation; NME, new molecular entity; OATP, organic anion transporting polypeptide; OCT, organic cation transporter; PBS, phosphate buffered saline; PXR, pregnane X receptor; SDS, sodium dodecyl sulfate; SLC, solute carrier transporter; T<sub>4</sub>, thyroxine; T<sub>3</sub>, triiodothyronine; TBST, tris-

buffered saline with Tween 20; TCEP, tris(2-carboxyethyl)-phosphine; TFA, trifluoroacetic acid

## REFERENCES

- Hagenbuch, B.; Meier, P. J. Organic anion transporting polypeptides of the OATP/ SLC21 family: phylogenetic classification as OATP/ SLCO superfamily, new nomenclature and molecular/ functional properties. *Pflugers Arch.* **2004**, *447* (5), 653–65.
- Grube, M.; Kock, K.; Oswald, S.; Draber, K.; Meissner, K.; Eckel, L.; Bohm, M.; Felix, S. B.; Vogelgesang, S.; Jedlitschky, G. Organic anion transporting polypeptide 2B1 is a high-affinity transporter for atorvastatin and is expressed in the human heart. *Clin. Pharmacol. Ther.* **2006**, *80* (6), 607–620.
- St-Pierre, M. V.; Hagenbuch, B.; Ugele, B.; Meier, P. J.; Stallmach, T. Characterization of an organic anion-transporting polypeptide (OATP-B) in human placenta. *J. Clin. Endocrinol. Metab.* **2002**, *87* (4), 1856–63.
- Bronger, H.; Konig, J.; Kopplow, K.; Steiner, H. H.; Ahmadi, R.; Herold-Mende, C.; Keppler, D.; Nies, A. T. ABC drug efflux pumps and organic anion uptake transporters in human gliomas and the blood-tumor barrier. *Cancer Res.* **2005**, *65* (24), 11419–28.
- Schiffer, R.; Neis, M.; Holler, D.; Rodriguez, F.; Geier, A.; Gartung, C.; Lammert, F.; Dreuw, A.; Zwadlo-Klarwasser, G.; Merk, H.; Jugert, F.; Baron, J. M. Active influx transport is mediated by members of the organic anion transporting polypeptide family in human epidermal keratinocytes. *J. Invest. Dermatol.* **2003**, *120* (2), 285–91.
- Niessen, J.; Jedlitschky, G.; Grube, M.; Bien, S.; Schwertz, H.; Ohtsuki, S.; Kawakami, H.; Kamiie, J.; Oswald, S.; Starke, K.; Strobel, U.; Siegmund, W.; Roskopf, D.; Greinacher, A.; Terasaki, T.; Kroemer, H. K. Human platelets express organic anion-transporting peptide 2B1, an uptake transporter for atorvastatin. *Drug Metab. Dispos.* **2009**, *37* (5), 1129–37.
- Sakamoto, A.; Matsumaru, T.; Yamamura, N.; Uchida, Y.; Tachikawa, M.; Ohtsuki, S.; Terasaki, T. Quantitative expression of human drug transporter proteins in lung tissues: analysis of regional, gender, and interindividual differences by liquid chromatography-tandem mass spectrometry. *J. Pharm. Sci.* **2013**, *102* (9), 3395–406.
- Pizzagalli, F.; Varga, Z.; Huber, R. D.; Folkers, G.; Meier, P. J.; St-Pierre, M. V. Identification of steroid sulfate transport processes in the human mammary gland. *J. Clin. Endocrinol. Metab.* **2003**, *88* (8), 3902–12.
- Knauer, M. J.; Urquhart, B. L.; Meyer zu Schwabedissen, H. E.; Schwarz, U. L.; Lemke, C. J.; Leake, B. F.; Kim, R. B.; Tirona, R. G. Human skeletal muscle drug transporters determine local exposure and toxicity of statins. *Circ. Res.* **2010**, *106* (2), 297–306.
- Kullak-Ublick, G. A.; Ismail, M. G.; Stieger, B.; Landmann, L.; Huber, R.; Pizzagalli, F.; Fattinger, K.; Meier, P. J.; Hagenbuch, B. Organic anion-transporting polypeptide B (OATP-B) and its functional comparison with three other OATPs of human liver. *Gastroenterology* **2001**, *120* (2), 525–33.
- Kobayashi, D.; Nozawa, T.; Imai, K.; Nezu, J.; Tsuji, A.; Tamai, I. Involvement of human organic anion transporting polypeptide OATP-B (SLC21A9) in pH-dependent transport across intestinal apical membrane. *J. Pharmacol. Exp. Ther.* **2003**, *306* (2), 703–708.
- Tamai, I. Oral drug delivery utilizing intestinal OATP transporters. *Adv. Drug Delivery Rev.* **2012**, *64* (6), 508–14.
- Keiser, M.; Kaltheuner, L.; Wildberg, C.; Muller, J.; Grube, M.; Partecke, L. I.; Heidecke, C. D.; Oswald, S. The Organic Anion-Transporting Peptide 2B1 Is Localized in the Basolateral Membrane of the Human Jejunum and Caco-2 Monolayers. *J. Pharm. Sci.* **2017**, *106* (9), 2657–2663.
- Nozawa, T.; Imai, K.; Nezu, J.; Tsuji, A.; Tamai, I. Functional characterization of pH-sensitive organic anion transporting polypeptide OATP-B in human. *J. Pharmacol. Exp. Ther.* **2003**, *308* (2), 438–445.
- Ming, X.; Knight, B. M.; Thakker, D. R. Vectorial transport of fexofenadine across Caco-2 cells: involvement of apical uptake and basolateral efflux transporters. *Mol. Pharmaceutics* **2011**, *8* (5), 1677–86.
- Glaeser, H.; Bailey, D. G.; Dresser, G. K.; Gregor, J. C.; Schwarz, U. L.; McGrath, J. S.; Jolicoeur, E.; Lee, W.; Leake, B. F.; Tirona, R. G.; Kim, R. B. Intestinal drug transporter expression and the impact of grapefruit juice in humans. *Clin. Pharmacol. Ther.* **2007**, *81* (3), 362–70.
- Shirasaka, Y.; Mori, T.; Murata, Y.; Nakanishi, T.; Tamai, I. Substrate- and dose-dependent drug interactions with grapefruit juice caused by multiple binding sites on OATP2B1. *Pharm. Res.* **2014**, *31* (8), 2035–43.
- Dresser, G. K.; Bailey, D. G.; Leake, B. F.; Schwarz, U. L.; Dawson, P. A.; Freeman, D. J.; Kim, R. B. Fruit juices inhibit organic anion transporting polypeptide-mediated drug uptake to decrease the oral availability of fexofenadine. *Clin. Pharmacol. Ther.* **2002**, *71* (1), 11–20.
- Kashihara, Y.; Ieiri, I.; Yoshikado, T.; Maeda, K.; Fukae, M.; Kimura, M.; Hirota, T.; Matsuki, S.; Irie, S.; Izumi, N.; Kusahara, H.; Sugiyama, Y. Small-Dosing Clinical Study: Pharmacokinetic, Pharmacogenomic (SLCO2B1 and ABCG2), and Interaction (Atorvastatin and Grapefruit Juice) Profiles of 5 Probes for OATP2B1 and BCRP. *J. Pharm. Sci.* **2017**, *106* (9), 2688–2694.
- Johnson, E. J.; Won, C. S.; Kock, K.; Paine, M. F. Prioritizing pharmacokinetic drug interaction precipitants in natural products: application to OATP inhibitors in grapefruit juice. *Biopharm. Drug Dispos.* **2017**, *38* (3), 251–259.
- Shirasaka, Y.; Shichiri, M.; Mori, T.; Nakanishi, T.; Tamai, I. Major active components in grapefruit, orange, and apple juices responsible for OATP2B1-mediated drug interactions. *J. Pharm. Sci.* **2013**, *102* (9), 3418–26.
- Shirasaka, Y.; Mori, T.; Shichiri, M.; Nakanishi, T.; Tamai, I. Functional pleiotropy of organic anion transporting polypeptide OATP2B1 due to multiple binding sites. *Drug Metab. Pharmacokinet.* **2012**, *27* (3), 360–4.
- International Transporter, C.; Giacomini, K. M.; Huang, S. M.; Tweedie, D. J.; Benet, L. Z.; Brouwer, K. L.; Chu, X.; Dahlin, A.; Evers, R.; Fischer, V.; Hillgren, K. M.; Hoffmaster, K. A.; Ishikawa, T.; Keppler, D.; Kim, R. B.; Lee, C. A.; Niemi, M.; Polli, J. W.; Sugiyama, Y.; Swaan, P. W.; Ware, J. A.; Wright, S. H.; Yee, S. W.; Zamek-Gliszczynski, M. J.; Zhang, L. Membrane transporters in drug development. *Nat. Rev. Drug Discov* **2010**, *9* (3), 215–236.
- Rosenberg, T.; Wilbrandt, W. Uphill transport induced by counterflow. *J. Gen. Physiol.* **1957**, *41* (2), 289–296.
- Harper, J. N.; Wright, S. H. Multiple mechanisms of ligand interaction with the human organic cation transporter, OCT2. *Am. J. Physiol. Renal Physiol* **2013**, *304* (1), F56–67.
- Fuerst, T. R.; Earl, P. L.; Moss, B. Use of a hybrid vaccinia virus-T7 RNA polymerase system for expression of target genes. *Mol. Cell. Biol.* **1987**, *7* (7), 2538–44.
- Grube, M.; Meyer zu Schwabedissen, H.; Draber, K.; Prager, D.; Moritz, K. U.; Linnemann, K.; Fusch, C.; Jedlitschky, G.; Kroemer, H. K. Expression, localization, and function of the carnitine transporter octn2 (slc22a5) in human placenta. *Drug Metab. Dispos.* **2005**, *33* (1), 31–37.
- Ahrne, E.; Glatter, T.; Vigano, C.; Schubert, C.; Nigg, E. A.; Schmidt, A. Evaluation and Improvement of Quantification Accuracy in Isobaric Mass Tag-Based Protein Quantification Experiments. *J. Proteome Res.* **2016**, *15* (8), 2537–47.
- Nesvizhskii, A. I.; Keller, A.; Kolker, E.; Aebersold, R. A statistical model for identifying proteins by tandem mass spectrometry. *Anal. Chem.* **2003**, *75* (17), 4646–58.
- Tirona, R. G.; Lee, W.; Leake, B. F.; Lan, L. B.; Cline, C. B.; Lamba, V.; Parviz, F.; Duncan, S. A.; Inoue, Y.; Gonzalez, F. J.; Schuetz, E. G.; Kim, R. B. The orphan nuclear receptor HNF4alpha determines PXR- and CAR-mediated xenobiotic induction of CYP3A4. *Nat. Med.* **2003**, *9* (2), 220–4.
- Tirona, R. G.; Kim, R. B. Organic Anion-Transporting Polypeptides. *Wiley Ser. Drug Disc* **2014**, 43–66.

- (32) Varma, M. V.; Rotter, C. J.; Chupka, J.; Whalen, K. M.; Duignan, D. B.; Feng, B.; Litchfield, J.; Goosen, T. C.; El-Kattan, A. F. pH-sensitive interaction of HMG-CoA reductase inhibitors (statins) with organic anion transporting polypeptide 2B1. *Mol. Pharmaceutics* **2011**, *8* (4), 1303–13.
- (33) Shirasaka, Y.; Kuraoka, E.; Spahn-Langguth, H.; Nakanishi, T.; Langguth, P.; Tamai, I. Species difference in the effect of grapefruit juice on intestinal absorption of talinolol between human and rat. *J. Pharmacol. Exp. Ther.* **2010**, *332* (1), 181–9.
- (34) Satoh, H.; Yamashita, F.; Tsujimoto, M.; Murakami, H.; Koyabu, N.; Ohtani, H.; Sawada, Y. Citrus juices inhibit the function of human organic anion-transporting polypeptide OATP-B. *Drug Metab. Dispos.* **2005**, *33* (4), 518–523.
- (35) Leuthold, S.; Hagenbuch, B.; Mohebbi, N.; Wagner, C. A.; Meier, P. J.; Stieger, B. Mechanisms of pH-gradient driven transport mediated by organic anion polypeptide transporters. *Am. J. Physiol. Cell Physiol.* **2009**, *296* (3), C570–82.
- (36) Ho, R. H.; Tirona, R. G.; Leake, B. F.; Glaeser, H.; Lee, W.; Lemke, C. J.; Wang, Y.; Kim, R. B. Drug and bile acid transporters in rosuvastatin hepatic uptake: function, expression, and pharmacogenetics. *Gastroenterology* **2006**, *130* (6), 1793–806.
- (37) Hussner, J.; Begunk, R.; Boettcher, K.; Gliesche, D. G.; Prestin, K.; Meyer Zu Schwabedissen, H. E. Expression of OATP2B1 as determinant of drug effects in the microcompartment of the coronary artery. *Vasc. Pharmacol.* **2015**, *72*, 25–34.
- (38) Karlgren, M.; Vildhede, A.; Norinder, U.; Wisniewski, J. R.; Kimoto, E.; Lai, Y.; Haglund, U.; Artursson, P. Classification of inhibitors of hepatic organic anion transporting polypeptides (OATPs): influence of protein expression on drug-drug interactions. *J. Med. Chem.* **2012**, *55* (10), 4740–63.
- (39) Lan, T.; Rao, A.; Haywood, J.; Davis, C. B.; Han, C.; Garver, E.; Dawson, P. A. Interaction of macrolide antibiotics with intestinally expressed human and rat organic anion-transporting polypeptides. *Drug Metab. Dispos.* **2009**, *37* (12), 2375–82.
- (40) Johnston, R. A.; Rawling, T.; Chan, T.; Zhou, F.; Murray, M. Selective inhibition of human solute carrier transporters by multi-kinase inhibitors. *Drug Metab. Dispos.* **2014**, *42* (11), 1851–7.
- (41) Meyer zu Schwabedissen, H. E.; Ferreira, C.; Schaefer, A. M.; Oufir, M.; Seibert, I.; Hamburger, M.; Tirona, R. G. Thyroid hormones are transport substrates and transcriptional regulators of Organic Anion Transporting Polypeptide 2B1. *Mol. Pharmacol.* **2018**, *94* (1), 700.
- (42) Letschert, K.; Faulstich, H.; Keller, D.; Keppler, D. Molecular characterization and inhibition of amanitin uptake into human hepatocytes. *Toxicol. Sci.* **2006**, *91* (1), 140–9.
- (43) Moore, L. B.; Goodwin, B.; Jones, S. A.; Wisely, G. B.; Serabjit-Singh, C. J.; Willson, T. M.; Collins, J. L.; Kliewer, S. A. St. John's wort induces hepatic drug metabolism through activation of the pregnane X receptor. *Proc. Natl. Acad. Sci. U. S. A.* **2000**, *97* (13), 7500–2.
- (44) Food and Drug Administration, <https://www.fda.gov/downloads/Drugs/GuidanceComplianceRegulatoryInformation/Guidances/UCMS81965.pdf>, 2017.
- (45) Brouwer, K. L.; Keppler, D.; Hoffmaster, K. A.; Bow, D. A.; Cheng, Y.; Lai, Y.; Palm, J. E.; Stieger, B.; Evers, R. In vitro methods to support transporter evaluation in drug discovery and development. *Clin. Pharmacol. Ther.* **2013**, *94* (1), 95–112.
- (46) Hubatsch, I.; Ragnarsson, E. G.; Artursson, P. Determination of drug permeability and prediction of drug absorption in Caco-2 monolayers. *Nat. Protoc.* **2007**, *2* (9), 2111–9.
- (47) Stein, W. H. *The movement of molecules across cell membranes*; Academic Press: New York, 1967.
- (48) Suzuki, M.; Suzuki, H.; Sugimoto, Y.; Sugiyama, Y. ABCG2 transports sulfated conjugates of steroids and xenobiotics. *J. Biol. Chem.* **2003**, *278* (25), 22644–9.
- (49) Allen, J. D.; van Loevezijn, A.; Lakhai, J. M.; Valk, M.; van Tellingen, O.; Reid, G.; Schellens, J. H.; Koomen, G. J.; Schinkel, A. H. Potent and specific inhibition of the breast cancer resistance protein multidrug transporter in vitro and in mouse intestine by a novel analogue of fumitremorgin C. *Mol. Cancer Ther.* **2002**, *1* (6), 417–425.
- (50) Liu, L.; Cui, Y.; Chung, A. Y.; Shitara, Y.; Sugiyama, Y.; Keppler, D.; Pang, K. S. Vectorial transport of enalapril by Oatp1a1/Mrp2 and OATP1B1 and OATP1B3/MRP2 in rat and human livers. *J. Pharmacol. Exp. Ther.* **2006**, *318* (1), 395–402.
- (51) Hellum, B. H.; Tosse, A.; Hoybakk, K.; Thomsen, M.; Rohloff, J.; Georg Nilsen, O. Potent in vitro inhibition of CYP3A4 and P-glycoprotein by *Rhodiola rosea*. *Planta Med.* **2010**, *76* (4), 331–8.
- (52) Boyd, R. A.; Stern, R. H.; Stewart, B. H.; Wu, X.; Reyner, E. L.; Zegarac, E. A.; Randinitis, E. J.; Whitfield, L. Atorvastatin coadministration may increase digoxin concentrations by inhibition of intestinal P-glycoprotein-mediated secretion. *J. Clin. Pharmacol.* **2000**, *40* (1), 91–8.
- (53) Horikawa, M.; Kato, Y.; Tyson, C. A.; Sugiyama, Y. The potential for an interaction between MRP2 (ABCC2) and various therapeutic agents: probenecid as a candidate inhibitor of the biliary excretion of irinotecan metabolites. *Drug Metab. Pharmacokinet.* **2002**, *17* (1), 23–33.
- (54) Guo, A.; Marinario, W.; Hu, P.; Sinko, P. J. Delineating the contribution of secretory transporters in the efflux of etoposide using Madin-Darby canine kidney (MDCK) cells overexpressing P-glycoprotein (Pgp), multidrug resistance-associated protein (MRP1), and canalicular multispecific organic anion transporter (cMOAT). *Drug Metab. Dispos.* **2002**, *30* (4), 457–463.
- (55) Cvetkovic, M.; Leake, B.; Fromm, M. F.; Wilkinson, G. R.; Kim, R. B. OATP and P-glycoprotein transporters mediate the cellular uptake and excretion of fexofenadine. *Drug Metab. Dispos.* **1999**, *27* (8), 866–871.
- (56) Quiney, C.; Billard, C.; Faussat, A. M.; Salanoubat, C.; Kolb, J. P. Hyperforin inhibits P-gp and BCRP activities in chronic lymphocytic leukaemia cells and myeloid cells. *Leuk. Lymphoma* **2007**, *48* (8), 1587–99.
- (57) Zhou, Z.; Vorperian, V. R.; Gong, Q.; Zhang, S.; January, C. T. Block of HERG potassium channels by the antihistamine astemizole and its metabolites desmethylastemizole and norastemizole. *J. Cardiovasc. Electrophysiol.* **1999**, *10* (6), 836–43.
- (58) Garcia-Quiroz, J.; Garcia-Becerra, R.; Barrera, D.; Santos, N.; Avila, E.; Ordaz-Rosado, D.; Rivas-Suarez, M.; Halhali, A.; Rodriguez, P.; Gamboa-Dominguez, A.; Medina-Franco, H.; Camacho, J.; Larrea, F.; Diaz, L. Astemizole synergizes calcitriol antiproliferative activity by inhibiting CYP24A1 and upregulating VDR: a novel approach for breast cancer therapy. *PLoS One* **2012**, *7* (9), e45063.
- (59) Akamine, Y.; Miura, M. An update on the clinical pharmacokinetics of fexofenadine enantiomers. *Expert Opin. Drug Metab. Toxicol.* **2018**, *14* (4), 429–434.
- (60) Reif, S.; Nicolson, M. C.; Bisset, D.; Reid, M.; Kloft, C.; Jaehde, U.; McLeod, H. L. Effect of grapefruit juice intake on etoposide bioavailability. *Eur. J. Clin. Pharmacol.* **2002**, *58* (7), 491–4.
- (61) Chatterjee, S. S.; Bhattacharya, S. K.; Wonnemann, M.; Singer, A.; Muller, W. E. Hyperforin as a possible antidepressant component of hypericum extracts. *Life Sci.* **1998**, *63* (6), 499–510.
- (62) Chrubasik-Hausmann, S.; Vlachojannis, J.; McLachlan, A. J. Understanding drug interactions with St John's wort (*Hypericum perforatum* L.): impact of hyperforin content. *J. Pharm. Pharmacol.* **2018**, *7*, 1.
- (63) Aleksunes, L. M.; Klaassen, C. D. Coordinated regulation of hepatic phase I and II drug-metabolizing genes and transporters using AhR-, CAR-, PXR-, PPARalpha-, and Nrf2-null mice. *Drug Metab. Dispos.* **2012**, *40* (7), 1366–79.
- (64) Thummel, K. E.; Wilkinson, G. R. In vitro and in vivo drug interactions involving human CYP3A. *Annu. Rev. Pharmacol. Toxicol.* **1998**, *38*, 389–430.
- (65) Wegler, C.; Gaugaz, F. Z.; Andersson, T. B.; Wisniewski, J. R.; Busch, D.; Groer, C.; Oswald, S.; Noren, A.; Weiss, F.; Hammer, H. S.; Joos, T. O.; Poetz, O.; Achour, B.; Rostami-Hodjegan, A.; van de Steeg, E.; Wortelboer, H. M.; Artursson, P. Variability in Mass Spectrometry-based Quantification of Clinically Relevant Drug

Transporters and Drug Metabolizing Enzymes. *Mol. Pharmaceutics* **2017**, *14* (9), 3142–3151.

(66) Ausubel, F. M.; Brent, R.; Kingston, R. E.; Moore, D. D.; Seidman, J. G.; Smith, J. A.; Struhl, K. *Current Protocols in Molecular Biology*; John Wiley & Sons Inc., 2003.

(67) Annaert, P.; Ye, Z. W.; Stieger, B.; Augustijns, P. Interaction of HIV protease inhibitors with OATP1B1, 1B3, and 2B1. *Xenobiotica* **2010**, *40* (3), 163–76.

(68) Klatt, S.; Fromm, M. F.; König, J. The influence of oral antidiabetic drugs on cellular drug uptake mediated by hepatic OATP family members. *Basic Clin. Pharmacol. Toxicol.* **2013**, *112* (4), 244–50.



## Chapter 2

### **OATP1A2 and OATP2B1 Are Interacting with Dopamine-Receptor Agonists and Antagonists**

Schäfer AM<sup>1</sup>, Meyer zu Schwabedissen HE<sup>1</sup>, Bien-Möller S<sup>2</sup>, Hubeny A<sup>2</sup>, Vogelgesang S<sup>3</sup>, Oswald S<sup>2,4</sup>, Grube M<sup>2</sup>

#### *Laboratories of Origin:*

<sup>1</sup>Biopharmacy, Department of Pharmaceutical Sciences, University of Basel, 4056 Basel, Switzerland

<sup>2</sup>Center of Drug Absorption and Transport (C\_DAT), Department of Pharmacology and Clinical Pharmacology, University Medicine Greifswald, 17487 Greifswald, Germany

<sup>3</sup>Department of Pathology, University Medicine Greifswald, 17487 Greifswald, Germany

<sup>4</sup>Institute of Pharmacology and Toxicology, Rostock, University Medical Center, 18057 Rostock, Germany

#### *Contribution of Anima Schäfer:*

Study design, acquisition, analysis and interpretation of data, drafting of manuscript

#### *Journal:*

Molecular Pharmaceutics (2020) 17, 1987-1995

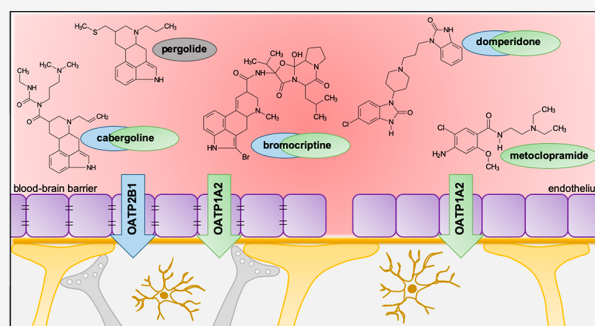


## OATP1A2 and OATP2B1 Are Interacting with Dopamine-Receptor Agonists and Antagonists

Anima M. Schäfer, Henriette E. Meyer zu Schwabedissen, Sandra Bien-Möller, Andrea Hubeny, Silke Vogelgesang, Stefan Oswald, and Markus Grube\*

**ABSTRACT:** Interaction with the dopaminergic system in the central nervous system is either therapeutically intended or it is a side effect. In both cases, dopamine-receptor agonists (DRA) like the ergoline derivative bromocriptine and dopamine-receptor antagonists (DRAn) like metoclopramide have to cross the blood–brain barrier (BBB). The organic anion transporting polypeptides (OATP) 1A2 and 2B1 are cellular uptake carriers for a variety of endogenous and xenobiotic compounds. As both transporters are expressed in endothelial cells of the BBB, the aim of the present study was to determine whether the DRA bromocriptine, cabergoline, and pergolide and the DRAn metoclopramide and domperidone are interacting with OATP1A2 and 2B1 and could therefore be candidate genes modifying wanted and unwanted effects of these drugs. Localization of both transporters in the brain was confirmed using LC–MS/MS and immunofluorescence stainings. For the functional studies, MDCKII cells stably expressing OATP1A2 or 2B1 were used. Initial interaction studies with the well-characterized transporter substrate estrone 3-sulfate revealed that all tested compounds except pergolide inhibit the transport function of both proteins with the most potent effect for bromocriptine ( $IC_{50} = 2.2 \mu\text{M}$  (OATP1A2) and  $IC_{50} = 2.5 \mu\text{M}$  (OATP2B1)). Further studies using the indirect competitive counterflow method identified bromocriptine, cabergoline, and domperidone as substrates of both transporters, whereas metoclopramide was only transported by OATP1A2. These findings were verified for domperidone by direct measurements using its tritium-labeled form as a tracer. Moreover, the transporter-mediated uptake of this compound was sensitive to the OATP1A2 and OATP2B1 inhibitor naringin. In conclusion, this study suggests that OATP1A2 and 2B1 may play a role in the uptake of DR agonists and antagonists into the brain.

**KEYWORDS:** dopamine receptor, OATP1A2, OATP2B1, bromocriptine, domperidone, substrate, competitive counterflow



### INTRODUCTION

The dopaminergic system is an important pharmacological target structure. For example, dopamine-receptor agonists (DRA) like ergoline derivatives are very successfully used in the treatment of Parkinson's disease (PD) and are important therapeutic options in the treatment of acromegaly and suppression of prolactin secretion by activating dopamine D2 receptors in the anterior pituitary gland.<sup>1–3</sup> In addition, important indications for dopamine-receptor antagonists (DRAn) are the therapy of depression and the treatment of nausea and vomiting.<sup>4</sup> Regardless of their indication, both DRA and DRAn have in common that for most of their pharmacological effects (and side effects), they have to cross the blood–brain barrier (BBB).

The BBB is a dynamic barrier of cerebral microvessels located in the brain parenchyma, which is essential to protect the brain from toxins circulating in the blood. As summarized by Abbott et al., there are different transport pathways across

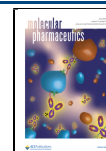
the brain endothelial cells.<sup>5</sup> One pathway is the active transport mediated by transport proteins involved in uptake and efflux mechanisms. The centrally active group of DRA includes ergolines such as bromocriptine, pergolide, cabergoline, or lisuride and nonergolines including pramipexole, ropinirole, or piripiedil. Some members of the DRA (bromocriptine, cabergoline, pergolide, and pramipexole) have been shown to interact with P-glycoprotein (P-gp, ABCB1, MDR1), an efflux pump localized at the luminal membrane of capillary endothelial cells at the BBB.<sup>6–9</sup> DRAn like domperidone and metoclopramide are acting on dopamine receptors localized in

**Received:** February 13, 2020

**Revised:** April 22, 2020

**Accepted:** April 28, 2020

**Published:** April 28, 2020



the central and peripheral nervous system. Compared to metoclopramide, the CNS penetration of domperidone across the BBB is poor, which could be explained by its high affinity to P-gp shown by Schinkel et al.<sup>10</sup> However, both domperidone as well as metoclopramide showed increased pituitary prolactin secretion.<sup>11</sup> Of note, the anterior pituitary gland is localized outside the brain with respect to the BBB.

To maintain the integrity of the BBB efflux transporters including P-gp are of particular importance, however, besides passive diffusion, the selective uptake of substances across the membrane via transport mechanisms is needed. Potential candidates are members of the organic anion transporting polypeptide family (OATP);<sup>12,13</sup> particularly, OATP1A2 and OATP2B1 were described to be localized in the brain.<sup>14</sup> Initially, OATP1A2 was found in human brain microvessels and capillaries,<sup>15,16</sup> but the transporter is also localized in the neuronal membranes.<sup>14</sup> OATP1A2 is discussed to play a crucial role in the neuroactive steroid transport across the BBB,<sup>17</sup> and indeed, a cellular uptake of sulfated steroids including dehydroepiandrosterone sulfate has been demonstrated for this transporter.<sup>17</sup> Furthermore, OATP1A2 is involved in the uptake of several central active drugs like serotonin receptor agonists (triptans),<sup>18,19</sup> and Gao et al. identified  $\delta$ -opioid peptides, which have to cross the BBB to fulfill their therapeutic action, including deltorphin II as OATP1A2 substrates.<sup>15</sup> Besides the brain, the transporter is expressed in the other cell types like the cholangiocytes of the liver, the cells of the distal convoluted tubule of the nephron, or the retinal pigment epithelium.<sup>14,20,21</sup>

OATP2B1 is ubiquitously expressed in the human body. Localization was confirmed in the heart, intestine, kidney, lung, mammary gland, pancreas, placenta, platelets, skeletal muscle, and skin.<sup>22–32</sup> Importantly, the transporter was also shown to be expressed in the BBB.<sup>14,16</sup> In contrast to OATP1A2, its localization seems to be limited to endothelial cells of brain capillaries, assuming a preferential function in substance penetration across the BBB rather than in maintaining neurosteroid homeostasis.<sup>14</sup> OATP2B1 is involved in the uptake of endogenous substances including sulfated steroids<sup>17</sup> and thyroid hormones<sup>33</sup> as well as of exogenous compounds including statins,<sup>22</sup> antihistamines,<sup>34,35</sup> or antidiabetics.<sup>36</sup>

In summary, little is known about the impact of uptake transporters for the transmembrane transport of dopamine-receptor agonists and antagonists into the brain. Since OATP1A2 and OATP2B1 are interesting candidates in this context, the aim of the present study was to evaluate whether DRA and DRAn are transported by OATP1A2 and OATP2B1. Therefore, we verified the expression and localization of the transporters in the brain and performed interaction studies between the transporters and clinical important DRA and DRAn. In addition, we established the competitive counterflow method (CCF), which was recently applied by us to OATP2B1,<sup>35</sup> for identification of OATP1A2 transporter substrates.

## EXPERIMENTAL SECTION

**Materials.** Tritium-labeled tracer compounds [<sup>3</sup>H]-estrone 3-sulfate (E<sub>1</sub>S, specific activity 50 Ci/mmol) and [<sup>3</sup>H]-domperidone (specific activity 34 Ci/mmol) were obtained from Hartmann Analytic (Braunschweig, Germany). All other substances were obtained from Sigma-Aldrich (St. Louis, MO, USA) if not otherwise stated. Brain tissue specimens for immunofluorescence staining and protein measurements using

LC–MS/MS were provided by the Department of Pathology from routine autopsies after the local ethics committee approval (registration number BB 92/13). Human pituitary paraffin sections were obtained from Zyagen (San Diego, California, USA).

**Cell Culture.** MDCKII cells (ATCC no. CRL-2936) stably transfected with human OATP1A2 or OATP2B1, respectively, were grown in 75 cm<sup>2</sup> cell culture flasks in Dulbecco's modified Eagle's medium (DMEM, Sigma-Aldrich, Buchs, Switzerland) supplemented with 2 mmol/L L-glutamine (BioConcept, Basel, Switzerland) and 10% fetal calf serum (FCS, Sigma-Aldrich), at 37 °C in a humidified atmosphere containing 5% CO<sub>2</sub>. Except for the experiments, the transfected cell lines were maintained in a medium containing 500  $\mu$ g/mL Geneticin (OATP1A2; Carl Roth, Karlsruhe, Germany) or 350  $\mu$ g/mL hygromycin B (OATP2B1; Carl Roth). MDCKII-OATP1A2 and MDCKII-OATP2B1 cells were generated as described before.<sup>37</sup>

**Immunofluorescent Staining.** Localization of OATP transporters in transfected MDCKII cells was performed on ethanol fixed cells. Primary antibodies were detected using Alexa-Fluor-488-labeled secondary antibodies (Life Technologies, Darmstadt, Germany). For nuclear costaining, fluorescence mounting medium was supplemented with DAPI (Life Technologies, Darmstadt, Germany). Localization of OATP1A2 and OATP2B1 as well as P-gp and glial fibrillary acidic protein (GFAP) in human brain was characterized by immunofluorescence staining using paraffin-embedded tissue slides. After deparaffinization and rehydration, sections were boiled in target retrieval solution using citrate buffer (pH 6.0) for OATP2B1 and P-gp staining or the DAKO target retrieval buffer pH 9.0 (Dako, Hamburg, Germany) for OATP1A2 and GFAP. After blocking with 5% FCS in phosphate buffered saline (PBS), samples were probed with the respective antibodies (OATP1A2: ab105124, Abcam, Cambridge, UK, 1:50; OATP2B1:<sup>22</sup> 1:100; P-gp: C219, Calbiochem/Merck Millipore, Billerica, MA, USA, 1:20; GFAP: Cell Signaling Technology, Boston, MA, USA, 1:100) overnight at 4 °C. After additional washing steps using PBS, samples were incubated with anti-rabbit Alexa-Fluor-488- or anti-mouse Alexa-Fluor-568-labeled secondary antibodies (Life Technologies, Darmstadt, Germany) at room temperature for 1 h. After removal of unbound secondary antibodies by further washing steps (PBS, 3 $\times$ ), the samples were embedded using fluorescence mounting medium supplemented with DAPI (Life Technologies) for nuclear costaining. Immunofluorescence microscopy analysis was performed using the laser scanning confocal microscopy system LSM780 (Carl Zeiss MicroImaging, Jena, Germany).

**Protein Quantification by LC–MS/MS.** Protein quantification of P-gp, OATP1A2, and OATP2B1 was done by mass-spectrometry-based targeted proteomics on a 5500 QTRAP triple quadrupole mass spectrometer (AB Sciex, Darmstadt, Germany) coupled to an Agilent Technologies 1260 Infinity system (Agilent Technologies) using a validated LC–MS/MS method as recently described.<sup>38</sup> The following proteospecific peptides were used for quantification: P-gp, AGAVAEVLA-AIR; OATP1A2, EGLETNADIIK; and OATP2B1, SSPAV-EQQLLVSGPGK while IATEAIENFR (P-gp), YIYLG-LPAALR (OATP1A2), and YYNNDLLR (OATP2B1) were used as qualifier peptides. In each case, three mass transitions were analyzed, and corresponding stable-isotope-labeled peptides were used as internal standards (ThermoFisher

Scientific). Sample preparation of human brain tissue was done using the ProteoExtract Native Membrane Protein Extraction Kit (Merck, Darmstadt, Germany) as described elsewhere.<sup>39</sup> Accuracy (error) and precision (CV) of the assay during sample analysis were below  $\pm 15\%$ . Final protein expression data (pmol/mg) were calculated by normalization to total protein content of the isolated membrane fraction as determined by the BCA method (Thermo Scientific, Waltham, MA, USA).

**Inhibition Assays.** For transport studies, cells were seeded on 24-well plates. The next day, cells were incubated with 2.5 mmol/L sodium butyrate for an additional 24 h to stimulate transporter expression. For transport experiments, the cell culture medium was removed, cells were washed once with PBS (37 °C) and incubated with transport buffer (142 mmol/L NaCl, 5 mmol/L KCl, 1 mmol/L  $\text{KH}_2\text{PO}_4$ , 1.5 mmol/L  $\text{CaCl}_2$ , 5 mmol/L glucose, 1.2 mmol/L  $\text{MgSO}_4$ , and 12.5 mmol/L HEPES; pH 7.3) containing the OATP1A2/OATP2B1 substrate [ $^3\text{H}$ ]-estrone 3-sulfate ( $\text{E}_1\text{S}$ , 0.25  $\mu\text{Ci}/\text{ml}$ , 1  $\mu\text{mol}/\text{L}$ ). After 5 min of incubation at 37 °C, substrate uptake was stopped by aspiration of transport buffer and twice washing with ice-cold PBS. Subsequently, cells were lysed in 0.2% SDS containing 5 mmol/L EDTA. An aliquot of 200  $\mu\text{L}$  was dissolved in a 2 mL scintillation cocktail (Rotiszint eco plus, Carl Roth, Karlsruhe, Germany), and the radioactivity was measured using a scintillation  $\beta$ -counter (LKB-Wallac/PerkinElmer, Freiburg, Germany). For normalization, protein concentration of the whole cell lysate was determined using the bicinchoninic acid (BCA) assay (Thermo Fisher Scientific).

**Competitive Counterflow.** For competitive counterflow (CCF) experiments, MDCKII-control and MDCKII-OATP1A2 cells were seeded and stimulated as described above. On the day of experiment, cells were washed once with prewarmed PBS and incubated with Hanks' balanced salt solution (Hanks') buffer for 10 min. Since CCF experiments are conducted in the steady state, this time point was determined by treating MDCKII-control and MDCKII-OATP1A2 cells with [ $^3\text{H}$ ]- $\text{E}_1\text{S}$  (0.25  $\mu\text{Ci}/\text{ml}$ ) for 2.5, 5, 10, 20, 30, 40, 50, and 60 min. The time point of reaching the steady state was the starting point for the next step. In a new experiment, MDCKII-control and MDCKII-OATP1A2 cells were treated until the steady state was reached before the supernatant was exchanged to [ $^3\text{H}$ ]- $\text{E}_1\text{S}$  (0.25  $\mu\text{Ci}/\text{ml}$ ) either alone (control) or supplemented with 50  $\mu\text{M}$  or 30  $\mu\text{M}$   $\text{E}_1\text{S}$  or bromosulphophthalein (BSP), respectively. Both  $\text{E}_1\text{S}$  and BSP are known substrates of OATP1A2, resulting in a decrease of intracellular [ $^3\text{H}$ ]- $\text{E}_1\text{S}$  due to the change in equilibration state. In order to determine the new equilibrium, MDCKII-control and MDCKII-OATP1A2 were treated for 0.5, 1, 1.5, 2, 5, 10, 15, and 20 min. After treatment for the respective time, cells were washed twice with ice-cold PBS and lysed before protein content and intracellular radioactivity were determined as described above. CCF experiments with DRA and DRAn were performed using a concentration of  $10 \times \text{IC}_{50}$  as described by Harper and Wright.<sup>40</sup> Due to solubility issues, the highest concentration was 250  $\mu\text{M}$ . CCF experiments with MDCKII-OATP2B1 cells were conducted as previously established by our group.<sup>35</sup>

**Domperidone Uptake Assays.** Cells were seeded as described above. For the domperidone uptake assay, cells were washed once with PBS (37 °C) and incubated with Hanks' balanced salt solution (Sigma-Aldrich) for 10 min. Cells were preincubated with 0.1  $\mu\text{mol}/\text{L}$  domperidone for 30 s before

the supernatant was replaced by 0.1  $\mu\text{mol}/\text{L}$  domperidone supplemented with [ $^3\text{H}$ ]-domperidone (0.15  $\mu\text{Ci}/\text{ml}$ ). For inhibition of the uptake, 100  $\mu\text{M}$  naringin was added. Substrate uptake was stopped after 5 min by aspiration of transport buffer and washing with ice-cold PBS before lysing as described above. An aliquot of 200  $\mu\text{L}$  was dissolved in a 2 mL scintillation cocktail, and the radioactivity and protein concentration were measured as described above.

**Statistical Method.** All data are presented as arithmetic means and standard deviations (SDs). Effects were tested for statistical significance as indicated in the respective figure legends. A *p*-value below 0.05 was considered as statistically significant. The half-maximal inhibitory concentration ( $\text{IC}_{50}$ ) was determined by nonlinear regression analysis using GraphPad Prism (GraphPad, San Diego, USA) with a bottom constrained to be  $>0$  and a top constant equal to 100. Curve fitting of time-dependent uptake studies was accomplished using Savitzky–Golay smoothing.

## RESULTS

**Expression of OATP1A2 and OATP2B1 in Human Brain and Anterior Pituitary Gland.** The expression of OATP2B1 and OATP1A2 in human brain was determined by immunofluorescence and LC–MS/MS-based targeted proteomics detection. We confirmed the expression of OATP2B1 in the vascular endothelium of the BBB as shown by colocalization with P-gp. In contrast, OATP1A2 was detected in endothelial cells and, additionally, in glia cells as shown by colocalization with the glial fibrillary acidic protein (GFAP). Furthermore, OATP1A2 was present in the anterior pituitary gland, most likely in vascular structures. Protein abundance in general was studied in whole human brain homogenates by LC–MS/MS demonstrating OATP1A2 as the most abundant transporter compared to OATP2B1 and P-gp ( $\text{OATP1A2} \gg \text{P-gp}$  and  $\text{OATP2B1}$ ) (Figure 1).

**Interaction Study of DRA and DRAn in MDCKII-OATP1A2 and MDCKII-OATP2B1 Cells.** To study the interaction of the DRA bromocriptine, cabergoline, and pergolide as well as the DRAn domperidone and metoclopramide (Figure 2) with OATPs, transporter-overexpressing MDCKII cells were used. Immunofluorescence staining indicated a strong OATP2B1 signal in the basolateral membrane, while OATP1A2 was strongly expressed in the apical membrane (Figure 3, left panel). As shown in Figure 3, functional activity of the respective cells was verified by testing the uptake of the well-established transporter substrate  $\text{E}_1\text{S}$ <sup>20,27</sup> in transporter-overexpressing cells compared to wild type cells. The interaction between the substrate uptake and the above-mentioned DRA and DRAn (100  $\mu\text{mol}/\text{L}$  each) was tested for both transporters. The DRA cabergoline and especially bromocriptine strongly inhibited both OATPs ( $p < 0.05$ ). For pergolide, no significant inhibition was observed. The DRAn domperidone inhibited the OATP1A2- and OATP2B1-mediated  $\text{E}_1\text{S}$  uptake ( $p < 0.05$ ), whereas metoclopramide only inhibited OATP1A2 function. Subsequently, the half-maximal inhibitory concentrations ( $\text{IC}_{50}$  values) were determined. As shown in Figure 4 and summarized in Table 1, bromocriptine and domperidone were potent inhibitors of OATP1A2 and OATP2B1. On the contrary, cabergoline and metoclopramide inhibited OATP1A2-mediated transport but only moderately affected OATP2B1-mediated  $\text{E}_1\text{S}$  accumulation.

**Competitive Counterflow Experiments with DRA and DRAn.** Besides the interaction between DRA/DRAn and

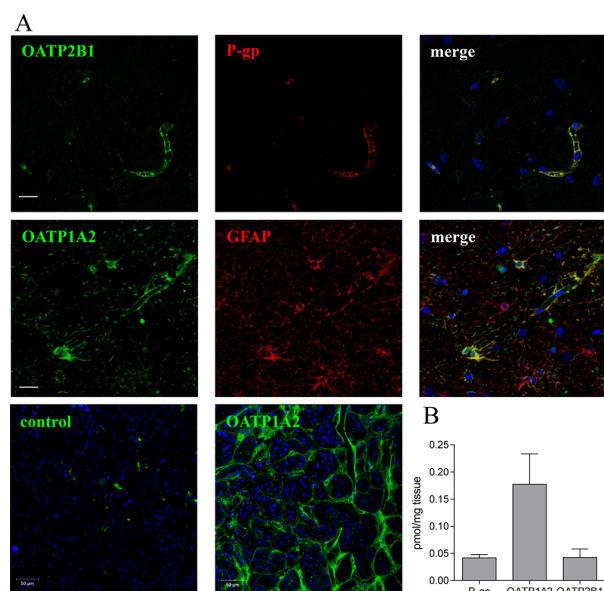


**Figure 1.** (A) Immunofluorescent staining of OATP2B1 (upper panel) and OATP1A2 (middle and lower panel, both green fluorescence) in human brain (upper and middle panel) as well as anterior pituitary gland sections (lower panel). Costaining was performed using P-gp (upper panel) or glial fibrillary acidic protein (GFAP, middle panel, both red fluorescence) specific antibodies and the DAPI nuclei dye (bars: 20  $\mu\text{m}$  (brain sections) and 50  $\mu\text{m}$  (pituitary gland sections)). (B) LC-MS/MS-based protein detection of OATP1A2, OATP2B1, and P-gp in human brain (mean  $\pm$  SD).

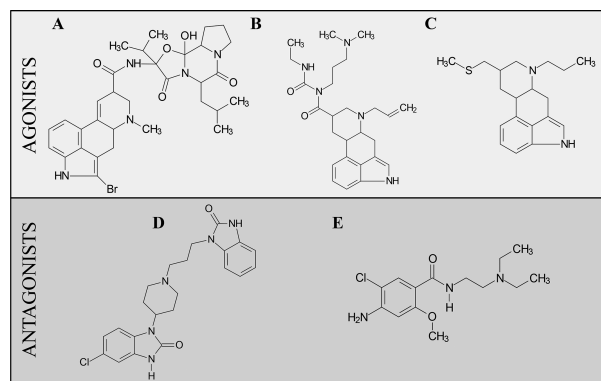


**Figure 2.** Molecular structure of the dopamine-receptor agonists bromocriptine (A), cabergoline (B), and pergolide (C) as well as the dopamine-receptor antagonists domperidone (D) and metoclopramide (E).

OATP1A2/OATP2B1, it was an aim of the study to establish a CCF method for OATP1A2 using MDCKII-OATP1A2 cells and its known substrate  $E_1S$ . Since CCF experiments are conducted under steady state conditions, the respective experimental settings were determined for the MDCKII-OATP1A2 cells (Figure 5A). For this cell line, a steady state of  $E_1S$  (1  $\mu\text{M}$ ) uptake was reached after 30 min. In the following CCF experiments, [ $^3\text{H}$ ]- $E_1S$  (0.3  $\mu\text{Ci}/\text{ml}$ ) was replaced by new [ $^3\text{H}$ ]- $E_1S$  (0.3  $\mu\text{Ci}/\text{ml}$ ) supplemented with the respective test compounds. As seen in Figure 5B,C, a new equilibrium was reached 7 min after the OATP1A2 substrates BSP and  $E_1S$  were added, respectively. The same experiments were

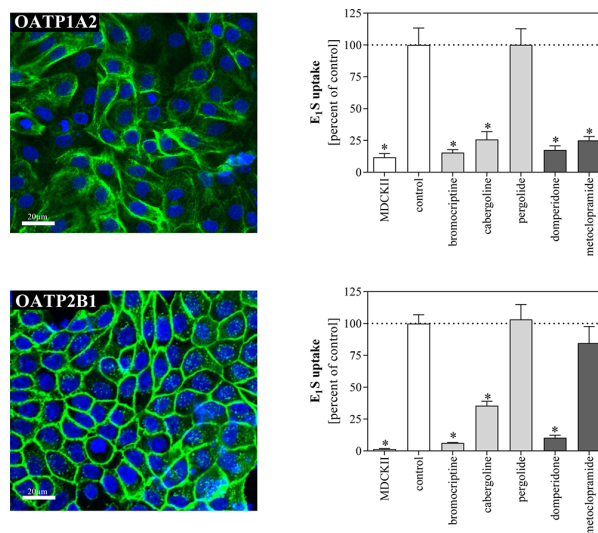


**Figure 3.** Left: Characterization of transporter expression in OATP1A2 and OATP2B1 transfected MDCKII cells (bars: 20  $\mu\text{m}$ ). Right: Interaction between dopamine-receptor agonists (bright gray) and antagonists (dark gray) and OATP-mediated transport.  $E_1S$  uptake (1  $\mu\text{mol}/\text{L}$ , 5 min) was studied in OATP1A2- and OATP2B1-overexpressing cells in the presence and absence of the respective compound (100  $\mu\text{mol}/\text{L}$ ). White bars present MDCKII- and solvent control. Data are represented in relation to the solvent control (\* $p < 0.05$ , one-way ANOVA, followed by Bonferroni's multiple comparisons test,  $n = 3$  independent experiments presented as mean  $\pm$  SD).

conducted in MDCKII-control cells, revealing no differences between control and BSP or  $E_1S$  treated cells. Subsequently, the DRA and DRAn were tested in CCF experiments for OATP1A2 and the previously established method for OATP2B1<sup>35</sup> with the recommended concentration of  $10 \times \text{IC}_{50}$ <sup>40</sup> for the test compounds. As shown in Figure 6A,B, bromocriptine and cabergoline significantly reduced the intracellular  $E_1S$  amount ( $p \leq 0.05$ ). Therefore, we assume that they are not only inhibitors but also substrates of OATP1A2 and OATP2B1. In addition, domperidone was identified as a possible substrate of OATP1A2 and OATP2B1, since it is competing with the transporter-mediated  $E_1S$  uptake ( $p \leq 0.05$ ), while metoclopramide was found to be a substrate only of OATP1A2.

**Verification of CCF Experiments by Direct Uptake Studies.** In order to validate the CCF results, cellular accumulation of domperidone was directly measured using tritium-labeled domperidone as tracer. In OATP1A2- and OATP2B1-transfected cells, significantly higher amounts of domperidone accumulated compared to MDCKII-control cells. Furthermore, this OATP-specific accumulation was sensitive to the known OATP1A2/OATP2B1 inhibitor naringin<sup>41,42</sup> (Figure 7A,B).

## DISCUSSION

In this study, we showed an interaction of frequently administered DRA and DRAn with OATP1A2 and OATP2B1. By the use of indirect and direct uptake experiments, we identified bromocriptine, cabergoline, and domperidone as substrates of both OATP1A2 and 2B1, whereas metoclopramide was a substrate only of OATP1A2. In addition, we verified the expression of both transporters in the

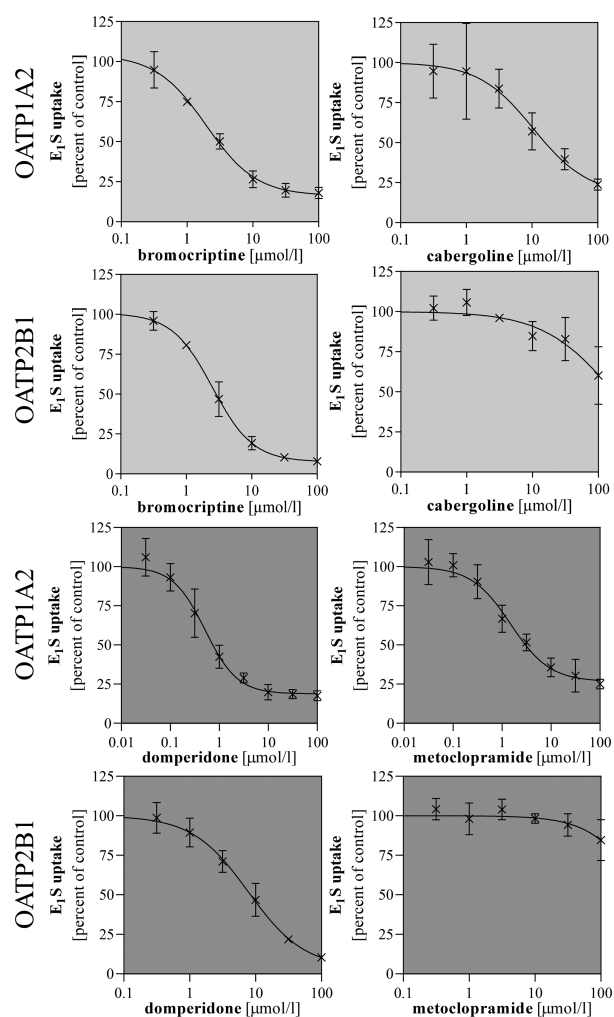


**Figure 4.** Determination of half-maximal inhibitory concentrations ( $IC_{50}$  values) for the dopamine-receptor agonists bromocriptine and cabergoline (bright gray) and the antagonists domperidone and metoclopramide (dark gray) using OATP-overexpressing MDCKII cells.  $IC_{50}$  values for OATP1A2 and OATP2B1 were determined for  $E_1S$  uptake ( $1 \mu\text{mol/L}$ , 5 min). Single data points are given as mean  $\pm$  SD from at least three independent experiments.

**Table 1.** Influence of DRA and DRAN on the OATP1A2 and OATP2B1-Mediated Uptake of  $E_1S^a$

	OATP1A2		OATP2B1	
	$IC_{50}$ [ $\mu\text{mol/L}$ ] (CI)			
bromocriptine	2.2 (1.8 to 2.8)	2.5 (2.1 to 3.1)		
cabergoline	10.5 (4.0 to 32.8)	>100		
domperidone	0.5 (0.4 to 0.7)	7.8 (5.2 to 10.6)		
metoclopramide	1.5 (1.0 to 2.4)	>100		

<sup>a</sup>Transport experiments performed in MDCKII-OATP1A2 and -OATP2B1 cells were used to estimate the inhibitory potency and calculate the respective  $IC_{50}$  value.

blood–brain barrier and demonstrated the localization of OATP1A2 in the pituitary gland.

To study an interaction between DRA/DRAN (bromocriptine, cabergoline, pergolide, domperidone, and metoclopramide) and both transporters, stably OATP-overexpressing

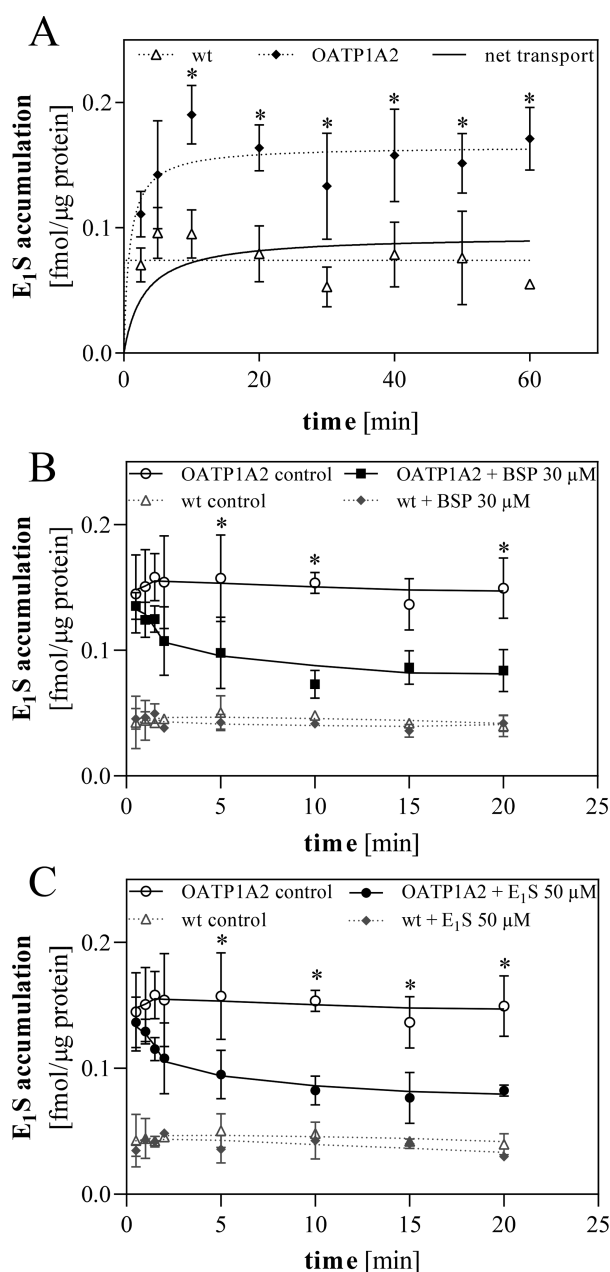


**Figure 5.** Establishment of CCF experiments to identify substrates of OATP1A2. In a time-dependent experiment, MDCKII-control and MDCKII-OATP1A2 cells were treated with radiolabeled estrone 3-sulfate ( $0.25 \mu\text{Ci/ml}$ ) to determine the steady state (A). In (B,C), the MDCKII-control and MDCKII-OATP1A2 cells were treated with [ $^3\text{H}$ ]- $E_1S$  ( $0.25 \mu\text{Ci/ml}$ ) for 30 min (steady state) before the supernatant was exchanged with new radiolabeled  $E_1S$  supplemented with the known OATP1A2 substrates BSP ( $30 \mu\text{M}$ , B) or  $E_1S$  ( $50 \mu\text{M}$ , C) to determine the equilibrium of competitive counterflow. Data are presented as mean  $\pm$  SD of  $n = 3$  independent experiments (\* $p < 0.05$ , one-way ANOVA, followed by Bonferroni's multiple comparisons test. For (B,C), \* indicates statistical significance between the two OATP1A2 curves).

MDCKII cells were used. Initially, an influence of these drugs on the transporter-mediated intracellular accumulation of the OATP1A2/OATP2B1 probe substrate  $E_1S$  was tested.

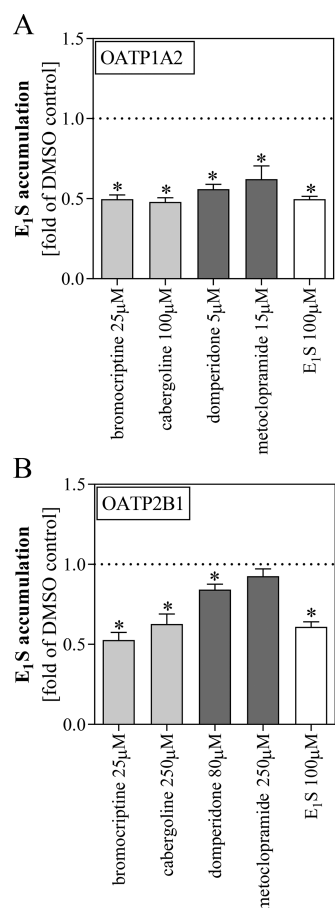


**Figure 6.** Competitive counterflow experiments with dopamine-receptor agonists (DRA) and dopamine-receptor antagonists (DRAN). MDCKII-OATP1A2 (A) and MDCKII-OATP2B1 (B) cells were treated with radiolabeled  $E_1S$  ( $0.25 \mu\text{Ci/ml}$ ) until steady state. Then, the supernatant was replaced by new  $[^3\text{H}]-E_1S$  supplemented with the DRA (bright gray) and DRAN (dark gray) with a concentration of  $10 \times \text{IC}_{50}$ . After 7 min, an intracellular amount of radioactivity was determined using liquid scintillation counting. DMSO was the solvent control;  $E_1S$  (white) served as a system control. Data are given as the mean  $\pm$  SD of  $n = 3$  independent experiments.  $*p \leq 0.05$ , one-way ANOVA corrected for multiple comparisons (Dunnett's test).

Bromocriptine was found to be an inhibitor of both OATP1A2 and OATP2B1 ( $\text{IC}_{50}$  values for OATP1A2 and OATP2B1 are 2.2 and 2.5  $\mu\text{M}$ , respectively), whereas cabergoline was only a poor inhibitor of OATP2B1 compared to its influence on OATP1A2 ( $\text{IC}_{50}$  values:  $>100$  vs 10.5  $\mu\text{M}$ ). Finally, no interaction with the transporters was observed for pergolide. All three compounds belong to the group of the ergolines. Interestingly, their interaction potential with the herein tested OATPs is different. While bromocriptine and cabergoline showed an interaction, pergolide did not. When comparing their chemical structures as shown in Figure 2, it is noticeable that the greatest difference lies in the modification at position 8. Bromocriptine and cabergoline exhibit a bulky modification containing amides, whereas pergolide has a methylthiomethyl group at this particular position.

A transporter-specific interaction potential was also observed for the DRAN. While metoclopramide only inhibited

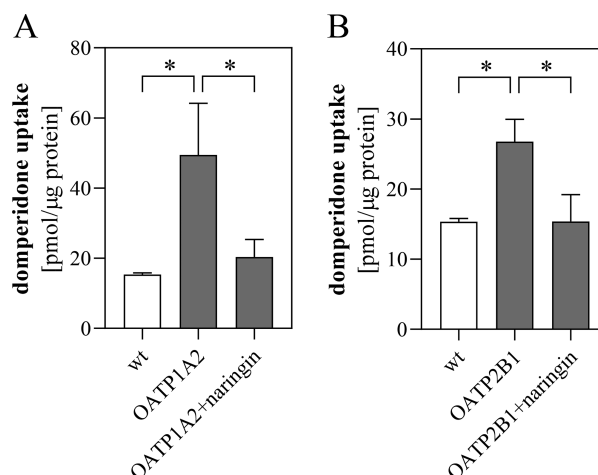


**Figure 7.** Direct uptake studies with domperidone in MDCKII-OATP1A2 (A) and -OATP2B1 (B) cells. Transporter-overexpressing as well as MDCKII-control cells were incubated with 0.1  $\mu\text{mol/L}$  domperidone supplemented with its tritium-labeled form for 5 min. Domperidone concentrations were normalized to the respective protein concentration. Intracellular radioactivity of domperidone was measured by scintillation counting. Data are given as mean  $\pm$  SD of  $n = 3$  independent experiments.  $*p \leq 0.05$ , one-way ANOVA followed by Dunnett's multiple comparisons test.

OATP1A2 but not OATP2B1 function ( $\text{IC}_{50}$  values:  $>100$  vs 1.5  $\mu\text{M}$ ), domperidone was a potent inhibitor of both OATPs ( $\text{IC}_{50}$  values: 0.5  $\mu\text{M}$  (OATP1A2); 7.8  $\mu\text{M}$  (OATP2B1)).

To test whether DRA/DRAN inhibiting OATP2B1 and OATP1A2 are also substrates of these transporters, the CCF method was applied. Harper and Wright established this method to distinguish between transported and nontransported compounds of the organic cation transporter 2 (OCT2).<sup>40</sup> Furthermore, the method was applied to organic anion transporters (OATs), as shown by a recent study identifying dantrolene as a substrate of OAT2 and OAT3.<sup>43</sup> We recently established CCF for OATP2B1, demonstrating that this method is also applicable to the OATP transporter family.<sup>35</sup> In the present study, the method was adapted for OATP1A2, for the first time. The time to reach steady state conditions between uptake and efflux of the high affinity OATP1A2/OATP2B1 substrate  $E_1S$  was determined to be 30 min for both transporters. The time to reach an equilibrium after the test compound was added was 4.6 times longer for OATP1A2 (7 min) compared to OATP2B1 (90 s).<sup>35</sup> To test the method, the known substrate BSP was identified as the OATP1A2 and OATP2B1 substrate by CCF, which is in line with literature results<sup>35,44</sup> and indicates the validity of the method for both transporters.

The following CCF experiments identified bromocriptine, cabergoline, and domperidone as new OATP1A2/OATP2B1 substrates, while metoclopramide was transported only by OATP1A2. Domperidone results were verified by direct uptake measurement using the tritium-labeled compound as a tracer, thereby confirming our recent findings for OATP2B1.<sup>35</sup> Moreover, the transporter-mediated domperidone uptake was sensitive to the OATP1A2/OATP2B1 inhibitor naringin.<sup>42</sup> The CCF method is a screening method to identify transporter substrates without the need of direct measurement. However, a limitation of the method is that it cannot be used to determine kinetic parameters of the transport.

The identification of bromocriptine as a new substrate of OATP1A2 and OATP2B1 was in line with a previous study demonstrating bromocriptine to be transported by OATP1B1.<sup>45</sup> While OATP1B1 shows a liver-specific expression profile and is therefore a candidate gene for systemic drug–drug interactions, OATP1A2 and OATP2B1 are expressed in different tissues including the BBB,<sup>14</sup> indicating a possible function in drug uptake to the brain. The brain expression of both transporters was supported by our LC–MS/MS results and immunofluorescence stainings. Interestingly, the abundance of OATP1A2 protein in whole brain tissue lysate was higher compared to OATP2B1 and P-gp. While our LC–MS/MS data only point to the general expression of both transporters in the brain, the results of the confocal microscopy confirmed the localization of OATP2B1 and OATP1A2 in endothelial cells, whereas OATP1A2 was also found to be expressed in glia cells. This finding corroborates the data of Gao et al. showing OATP1A2 expression in neurons of the human cortex, cerebellum, and hippocampus, while OATP2B1 was only detected in endothelial cells of brain capillaries.<sup>14</sup>

Bromocriptine acts as an agonist on cerebral dopamine receptors and is used in the treatment of various diseases including Parkinson's disease and hyperprolactinemia. Interestingly, animal studies using rat and monkey indicate a very poor distribution of this ergot derivative into the brain, while high concentrations were detected in the liver.<sup>46</sup> Due to the differences in tissue distribution, one may assume direct transport to be involved. Indeed, hepatic accumulation may be explained by the expression of the respective homologues of OATP1B1 (e.g., Oatp1b2) in hepatocytes, facilitating hepatocellular accumulation. In contrast, the low concentrations in the brain indicate a poor blood-to-brain penetration. In this context, it seems noteworthy that Vautier et al. found bromocriptine to be a P-gp substrate in *in vivo* experiments.<sup>7</sup> This efflux transporter is highly expressed at the luminal membrane of endothelial cells in brain capillaries and may explain the poor CNS entry of bromocriptine. Our observation of an OATP1A2/OATP2B1-mediated uptake of bromocriptine into the endothelial cells would counteract the P-gp function. Consequently, a compound's transfer into the brain highly depends on both uptake (e.g., by an OATP) and efflux (e.g., P-gp) processes.

This is further illustrated by our findings regarding the dopamine-receptor antagonists domperidone and metoclopramide. Both substances were identified as OATP1A2 substrates, and domperidone was also shown to be transported by OATP2B1, but they exhibit a different ability to cross the BBB. While domperidone has almost no central effects, metoclopramide is likely to have such effects.<sup>47</sup> The best explanation for this different behavior is the interaction with P-gp. While domperidone is a substrate of the efflux transporter and is therefore directly expelled back to the bloodstream, metoclopramide is not or only weakly transported by P-gp.<sup>48,49</sup> Taken together, OATP1A2-mediated transport might be more important for metoclopramide uptake into the brain compared to domperidone. It is conceivable that OATP1A2 inhibition, for example, by other substrates,<sup>50</sup> or genetic loss of function variants of the transporter<sup>20</sup> might reduce extrapyramidal side effects of metoclopramide; however, so far, such studies are not available.

In addition, inhibition of OATP1A2 (and OATP2B1) by bromocriptine, domperidone, metoclopramide, or other drugs

may alter the uptake of endogenous compounds like the neurosteroid DHEAS.<sup>17</sup>

Interestingly, we detected OATP1A2 not only in the BBB and glia cells but also in the anterior pituitary gland. The dopamine receptors play an important role in the pituitary gland, as they are for example involved in controlling prolactin secretion.<sup>51,52</sup> Therefore, DRA like bromocriptine are used in the treatment of hyperprolactinemia.<sup>1–3</sup> The anterior pituitary gland is closely connected to the brain but is not part of it. Here, OATP1A2 was shown to be localized most likely in blood vessels. Although the capillaries of this gland are lined by a fenestrated endothelium, endothelial OATP1A2 expression might be relevant for local uptake of its substrates such as bromocriptine.

In conclusion, we applied the competitive counterflow method to OATP1A2 and OATP2B1 and identified the DRA(n) bromocriptine, cabergoline, and domperidone as substrates for these transporters. In addition, OATP1A2 but not OATP2B1 was interacting with metoclopramide. Both transporters are expressed in the blood–brain barrier and therefore interesting candidates for central drug uptake of these compounds.

## ■ AUTHOR INFORMATION

### Corresponding Author

**Markus Grube** – Center of Drug Absorption and Transport (C\_DAT), Department of Pharmacology and Clinical Pharmacology, University Medicine Greifswald, 17487 Greifswald, Germany

### Authors

**Anima M. Schäfer** – Biopharmacy, Department Pharmaceutical Sciences, University of Basel, 4056 Basel, Switzerland; [orcid.org/0000-0002-3715-8405](https://orcid.org/0000-0002-3715-8405)

**Henriette E. Meyer zu Schwabedissen** – Biopharmacy, Department Pharmaceutical Sciences, University of Basel, 4056 Basel, Switzerland; [orcid.org/0000-0003-0458-4579](https://orcid.org/0000-0003-0458-4579)

**Sandra Bien-Möller** – Center of Drug Absorption and Transport (C\_DAT), Department of Pharmacology and Clinical Pharmacology, University Medicine Greifswald, 17487 Greifswald, Germany

**Andrea Hubeny** – Center of Drug Absorption and Transport (C\_DAT), Department of Pharmacology and Clinical Pharmacology, University Medicine Greifswald, 17487 Greifswald, Germany

**Silke Vogelgesang** – Department of Pathology, University Medicine Greifswald, 17487 Greifswald, Germany

**Stefan Oswald** – Center of Drug Absorption and Transport (C\_DAT), Department of Pharmacology and Clinical Pharmacology, University Medicine Greifswald, 17487 Greifswald, Germany; Institute of Pharmacology and Toxicology, Rostock, University Medical Center, 18057 Rostock, Germany; [orcid.org/0000-0001-6269-4368](https://orcid.org/0000-0001-6269-4368)

Complete contact information is available at:

<https://pubs.acs.org/10.1021/acs.molpharmaceut.0c00159>

### Author Contributions

The manuscript was written through contributions of all authors. All authors have given approval to the final version of the manuscript.

### Funding

This work was funded by funds of Biopharmacy at the University of Basel.

## Notes

The authors declare no competing financial interest.

### ACKNOWLEDGMENTS

We thank Tina Sonnenberger for her excellent technical assistance.

### ABBREVIATIONS

BBB, blood–brain barrier; BSP, bromosulphthalein; CCF, competitive counterflow; DMEM, Dulbecco's modified Eagle's medium; DRA, dopamine-receptor agonists; DRAn, dopamine-receptor antagonists; E<sub>1</sub>S, estrone 3-sulfate; FCS, fetal calf serum; GFAP, glial fibrillary acidic protein; Hanks', Hanks' balanced salt solution; OATP, organic anion transporting polypeptide; PD, Parkinson's disease; P-gp, P-glycoprotein; PBS, phosphate buffered saline

### REFERENCES

- Melmed, S.; Casanueva, F. F.; Hoffman, A. R.; Kleinberg, D. L.; Montori, V. M.; Schlechte, J. A.; Wass, J. A. Diagnosis and treatment of hyperprolactinemia: an Endocrine Society clinical practice guideline. *J. Clin. Endocrinol. Metab.* **2011**, *96* (2), 273–288.
- Broder, M. S.; Chang, E.; Ludlam, W. H.; Neary, M. P.; Carmichael, J. D. Patterns of pharmacologic treatment in US patients with acromegaly. *Curr. Med. Res. Opin.* **2016**, *32* (5), 799–805.
- Lee, S. Y.; Kim, J. H.; Lee, J. H.; Kim, Y. H.; Cha, H. J.; Kim, S. W.; Paek, S. H.; Shin, C. S. The efficacy of medical treatment in patients with acromegaly in clinical practice. *Endocr. J.* **2018**, *65* (1), 33–41.
- Beaulieu, J. M.; Gainetdinov, R. R. The physiology, signaling, and pharmacology of dopamine receptors. *Pharmacol. Rev.* **2011**, *63* (1), 182–217.
- Abbott, N. J.; Patabendige, A. A.; Dolman, D. E.; Yusof, S. R.; Begley, D. J. Structure and function of the blood-brain barrier. *Neurobiol. Dis.* **2010**, *37* (1), 13–25.
- Vautier, S.; Milane, A.; Fernandez, C.; Buyse, M.; Chacun, H.; Farinotti, R. Interactions between antiparkinsonian drugs and ABCB1/P-glycoprotein at the blood-brain barrier in a rat brain endothelial cell model. *Neurosci. Lett.* **2008**, *442* (1), 19–23.
- Vautier, S.; Lacomblez, L.; Chacun, H.; Picard, V.; Gimenez, F.; Farinotti, R.; Fernandez, C. Interactions between the dopamine agonist, bromocriptine and the efflux protein, P-glycoprotein at the blood-brain barrier in the mouse. *Eur. J. Pharm. Sci.* **2006**, *27* (2–3), 167–74.
- Orlowski, S.; Valente, D.; Garrigos, M.; Ezan, E. Bromocriptine modulates P-glycoprotein function. *Biochem. Biophys. Res. Commun.* **1998**, *244* (2), 481–8.
- Athanasoulia, A. P.; Sievers, C.; Ising, M.; Brockhaus, A. C.; Yassouridis, A.; Stalla, G. K.; Uhr, M. Polymorphisms of the drug transporter gene ABCB1 predict side effects of treatment with cabergoline in patients with PRL adenomas. *Eur. J. Endocrinol.* **2012**, *167* (3), 327–35.
- Schinkel, A. H.; Wagenaar, E.; Mol, C. A.; van Deemter, L. P-glycoprotein in the blood-brain barrier of mice influences the brain penetration and pharmacological activity of many drugs. *J. Clin. Invest.* **1996**, *97* (11), 2517–24.
- Bernini, G. P.; Lucarini, A. R.; Franchi, F.; Salvetti, A. Humoral effects of metoclopramide and domperidone in normal subjects and in hypertensive patients. *J. Endocrinol. Invest.* **1988**, *11* (10), 711–6.
- Shitara, Y.; Maeda, K.; Ikejiri, K.; Yoshida, K.; Horie, T.; Sugiyama, Y. Clinical significance of organic anion transporting polypeptides (OATPs) in drug disposition: their roles in hepatic clearance and intestinal absorption. *Biopharm. Drug Dispos.* **2013**, *34* (1), 45–78.
- Kalliokoski, A.; Niemi, M. Impact of OATP transporters on pharmacokinetics. *Br. J. Pharmacol.* **2009**, *158* (3), 693–705.
- Gao, B.; Vavricka, S. R.; Meier, P. J.; Stieger, B. Differential cellular expression of organic anion transporting peptides OATP1A2 and OATP2B1 in the human retina and brain: implications for carrier-mediated transport of neuropeptides and neurosteroids in the CNS. *Pfluegers Arch.* **2015**, *467* (7), 1481–1493.
- Gao, B.; Hagenbuch, B.; Kullak-Ublick, G. A.; Benke, D.; Aguzzi, A.; Meier, P. J. Organic anion-transporting polypeptides mediate transport of opioid peptides across blood-brain barrier. *J. Pharmacol. Exp. Ther.* **2000**, *294* (1), 73–79.
- Bronger, H.; Konig, J.; Koppow, K.; Steiner, H. H.; Ahmadi, R.; Herold-Mende, C.; Keppler, D.; Nies, A. T. ABC drug efflux pumps and organic anion uptake transporters in human gliomas and the blood-tumor barrier. *Cancer Res.* **2005**, *65* (24), 11419–28.
- Grube, M.; Hagen, P.; Jedlitschky, G. Neurosteroid Transport in the Brain: Role of ABC and SLC Transporters. *Front. Pharmacol.* **2018**, *9*, 354.
- Cheng, Z.; Liu, H.; Yu, N.; Wang, F.; An, G.; Xu, Y.; Liu, Q.; Guan, C. B.; Ayrton, A. Hydrophilic anti-migraine triptans are substrates for OATP1A2, a transporter expressed at human blood-brain barrier. *Xenobiotica* **2012**, *42* (9), 880–90.
- Urquhart, B. L.; Kim, R. B. Blood-brain barrier transporters and response to CNS-active drugs. *Eur. J. Clin. Pharmacol.* **2009**, *65* (11), 1063–70.
- Lee, W.; Glaeser, H.; Smith, L. H.; Roberts, R. L.; Moeckel, G. W.; Gervasini, G.; Leake, B. F.; Kim, R. B. Polymorphisms in human organic anion-transporting polypeptide 1A2 (OATP1A2): implications for altered drug disposition and central nervous system drug entry. *J. Biol. Chem.* **2005**, *280* (10), 9610–7.
- Chan, T.; Zhu, L.; Madigan, M. C.; Wang, K.; Shen, W.; Gillies, M. C.; Zhou, F. Human organic anion transporting polypeptide 1A2 (OATP1A2) mediates cellular uptake of all-trans-retinol in human retinal pigmented epithelial cells. *Br. J. Pharmacol.* **2015**, *172* (9), 2343–53.
- Grube, M.; Kock, K.; Oswald, S.; Draber, K.; Meissner, K.; Eckel, L.; Bohm, M.; Felix, S. B.; Vogelgesang, S.; Jedlitschky, G.; Siegmund, W.; Warzok, R.; Kroemer, H. K. Organic anion transporting polypeptide 2B1 is a high-affinity transporter for atorvastatin and is expressed in the human heart. *Clin. Pharmacol. Ther.* **2006**, *80* (6), 607–620.
- Kobayashi, D.; Nozawa, T.; Imai, K.; Nezu, J.; Tsuji, A.; Tamai, I. Involvement of human organic anion transporting polypeptide OATP-B (SLC21A9) in pH-dependent transport across intestinal apical membrane. *J. Pharmacol. Exp. Ther.* **2003**, *306* (2), 703–8.
- Keiser, M.; Kaltheuner, L.; Wildberg, C.; Muller, J.; Grube, M.; Partecke, L. I.; Heidecke, C. D.; Oswald, S. The Organic Anion-Transporting Peptide 2B1 Is Localized in the Basolateral Membrane of the Human Jejunum and Caco-2 Monolayers. *J. Pharm. Sci.* **2017**, *106* (9), 2657–2663.
- Ferreira, C.; Hagen, P.; Stern, M.; Hussner, J.; Zimmermann, U.; Grube, M.; Meyer Zu Schwabedissen, H. E. The scaffold protein PDZK1 modulates expression and function of the organic anion transporting polypeptide 2B1. *Eur. J. Pharm. Sci.* **2018**, *120*, 181–190.
- Sakamoto, A.; Matsumaru, T.; Yamamura, N.; Uchida, Y.; Tachikawa, M.; Ohtsuki, S.; Terasaki, T. Quantitative expression of human drug transporter proteins in lung tissues: analysis of regional, gender, and interindividual differences by liquid chromatography-tandem mass spectrometry. *J. Pharm. Sci.* **2013**, *102* (9), 3395–406.
- Pizzagalli, F.; Varga, Z.; Huber, R. D.; Folkers, G.; Meier, P. J.; St-Pierre, M. V. Identification of steroid sulfate transport processes in the human mammary gland. *J. Clin. Endocrinol. Metab.* **2003**, *88* (8), 3902–12.
- Kim, M.; Deacon, P.; Tirona, R. G.; Kim, R. B.; Pin, C. L.; Meyer Zu Schwabedissen, H. E.; Wang, R.; Schwarz, U. I. Characterization of OATP1B3 and OATP2B1 transporter expression in the islet of the adult human pancreas. *Histochem. Cell Biol.* **2017**, *148*, 345.
- St-Pierre, M. V.; Hagenbuch, B.; Ugele, B.; Meier, P. J.; Stallmach, T. Characterization of an organic anion-transporting

polypeptide (OATP-B) in human placenta. *J. Clin. Endocrinol. Metab.* **2002**, *87* (4), 1856–63.

(30) Niessen, J.; Jedlitschky, G.; Grube, M.; Bien, S.; Schwertz, H.; Ohtsuki, S.; Kawakami, H.; Kamiie, J.; Oswald, S.; Starke, K.; Strobel, U.; Siegmund, W.; Roskopf, D.; Greinacher, A.; Terasaki, T.; Kroemer, H. K. Human platelets express organic anion-transporting peptide 2B1, an uptake transporter for atorvastatin. *Drug Metab. Dispos.* **2009**, *37* (5), 1129–37.

(31) Knauer, M. J.; Urquhart, B. L.; Meyer zu Schwabedissen, H. E.; Schwarz, U. I.; Lemke, C. J.; Leake, B. F.; Kim, R. B.; Tirona, R. G. Human skeletal muscle drug transporters determine local exposure and toxicity of statins. *Circ. Res.* **2010**, *106* (2), 297–306.

(32) Schiffer, R.; Neis, M.; Holler, D.; Rodriguez, F.; Geier, A.; Gartung, C.; Lammert, F.; Dreuw, A.; Zwadlo-Klarwasser, G.; Merk, H.; Jugert, F.; Baron, J. M. Active influx transport is mediated by members of the organic anion transporting polypeptide family in human epidermal keratinocytes. *J. Invest. Dermatol.* **2003**, *120* (2), 285–91.

(33) Meyer zu Schwabedissen, H. E.; Ferreira, C.; Schaefer, A. M.; Oufir, M.; Seibert, I.; Hamburger, M.; Tirona, R. G. Thyroid Hormones Are Transport Substrates and Transcriptional Regulators of Organic Anion Transporting Polypeptide 2B1. *Mol. Pharmacol.* **2018**, *94* (1), 700–712.

(34) Shirasaka, Y.; Mori, T.; Murata, Y.; Nakanishi, T.; Tamai, I. Substrate- and dose-dependent drug interactions with grapefruit juice caused by multiple binding sites on OATP2B1. *Pharm. Res.* **2014**, *31* (8), 2035–43.

(35) Schaefer, A. M.; Bock, T.; Meyer Zu Schwabedissen, H. E. Establishment and Validation of Competitive Counterflow as a Method To Detect Substrates of the Organic Anion Transporting Polypeptide 2B1. *Mol. Pharmaceutics* **2018**, *15*, 5501.

(36) Satoh, H.; Yamashita, F.; Tsujimoto, M.; Murakami, H.; Koyabu, N.; Ohtani, H.; Sawada, Y. Citrus juices inhibit the function of human organic anion-transporting polypeptide OATP-B. *Drug Metab. Dispos.* **2005**, *33* (4), 518–23.

(37) Hubeny, A.; Keiser, M.; Oswald, S.; Jedlitschky, G.; Kroemer, H. K.; Siegmund, W.; Grube, M. Expression of Organic Anion Transporting Polypeptide 1A2 in Red Blood Cells and Its Potential Impact on Antimalarial Therapy. *Drug Metab. Dispos.* **2016**, *44* (10), 1562–8.

(38) Drozdziak, M.; Busch, D.; Lapczuk, J.; Muller, J.; Ostrowski, M.; Kurzawski, M.; Oswald, S. Protein Abundance of Clinically Relevant Drug-Metabolizing Enzymes in the Human Liver and Intestine: A Comparative Analysis in Paired Tissue Specimens. *Clin. Pharmacol. Ther.* **2018**, *104* (3), 515–524.

(39) Groer, C.; Bruck, S.; Lai, Y.; Paulick, A.; Busemann, A.; Heidecke, C. D.; Siegmund, W.; Oswald, S. LC-MS/MS-based quantification of clinically relevant intestinal uptake and efflux transporter proteins. *J. Pharm. Biomed. Anal.* **2013**, *85*, 253–261.

(40) Harper, J. N.; Wright, S. H. Multiple mechanisms of ligand interaction with the human organic cation transporter, OCT2. *Am. J. Physiol. Renal Physiol.* **2013**, *304* (1), F56–67.

(41) Bailey, D. G.; Dresser, G. K.; Leake, B. F.; Kim, R. B. Naringin is a major and selective clinical inhibitor of organic anion-transporting polypeptide 1A2 (OATP1A2) in grapefruit juice. *Clin. Pharmacol. Ther.* **2007**, *81* (4), 495–502.

(42) Shirasaka, Y.; Shichiri, M.; Mori, T.; Nakanishi, T.; Tamai, I. Major active components in grapefruit, orange, and apple juices responsible for OATP2B1-mediated drug interactions. *J. Pharm. Sci.* **2013**, *102* (9), 3418–26.

(43) Burckhardt, B. C.; Henjakovic, M.; Hagos, Y.; Burckhardt, G. Counter-flow suggests transport of dantrolene and 5-OH dantrolene by the organic anion transporters 2 (OAT2) and 3 (OAT3). *Pfluegers Arch.* **2016**, *468* (11–12), 1909–1918.

(44) Kullak-Ublick, G. A.; Hagenbuch, B.; Stieger, B.; Schteingart, C. D.; Hofmann, A. F.; Wolkoff, A. W.; Meier, P. J. Molecular and functional characterization of an organic anion transporting polypeptide cloned from human liver. *Gastroenterology* **1995**, *109* (4), 1274–82.

(45) Lu, W. J.; Huang, K.; Lai, M. L.; Huang, J. D. Erythromycin alters the pharmacokinetics of bromocriptine by inhibition of organic anion transporting polypeptide C-mediated uptake. *Clin. Pharmacol. Ther.* **2006**, *80* (4), 421–2.

(46) Markey, S. P.; Colburn, R. W.; Kopin, I. J.; Aamodt, R. L. Distribution and excretion in the rat and monkey of [<sup>32</sup>Br] bromocriptine. *J. Pharmacol. Exp. Ther.* **1979**, *211* (1), 31–35.

(47) Tonini, M.; Cipollina, L.; Poluzzi, E.; Crema, F.; Corazza, G. R.; De Ponti, F. Review article: clinical implications of enteric and central D2 receptor blockade by antidopaminergic gastrointestinal prokinetics. *Aliment. Pharmacol. Ther.* **2004**, *19* (4), 379–90.

(48) Tournier, N.; Bauer, M.; Pichler, V.; Nics, L.; Klebermass, E. M.; Bamminger, K.; Matzneller, P.; Weber, M.; Karch, R.; Caille, F.; Auvity, S.; Marie, S.; Jager, W.; Wadsak, W.; Hacker, M.; Zeitlinger, M.; Langer, O. Impact of P-Glycoprotein Function on the Brain Kinetics of the Weak Substrate (11)C-Metoclopramide Assessed with PET Imaging in Humans. *J. Nucl. Med.* **2019**, *60* (7), 985–991.

(49) Tsujikawa, K.; Dan, Y.; Nogawa, K.; Sato, H.; Yamada, Y.; Murakami, H.; Ohtani, H.; Sawada, Y.; Iga, T. Potentiation of domperidone-induced catalepsy by a P-glycoprotein inhibitor, cyclosporin A. *Biopharm. Drug Dispos.* **2003**, *24* (3), 105–14.

(50) Kovacsics, D.; Patik, I.; Ozvegy-Laczka, C. The role of organic anion transporting polypeptides in drug absorption, distribution, excretion and drug-drug interactions. *Expert Opin. Drug Metab. Toxicol.* **2017**, *13* (4), 409–424.

(51) Caron, M. G.; Beaulieu, M.; Raymond, V.; Gagne, B.; Drouin, J.; Lefkowitz, R. J.; Labrie, F. Dopaminergic receptors in the anterior pituitary gland. Correlation of [<sup>3</sup>H]dihydroergocryptine binding with the dopaminergic control of prolactin release. *J. Biol. Chem.* **1978**, *253* (7), 2244–2253.

(52) Pivonello, R.; Waaijers, M.; Kros, J. M.; Pivonello, C.; de Angelis, C.; Cozzolino, A.; Colao, A.; Lamberts, S. W. J.; Hofland, L. J. Dopamine D2 receptor expression in the corticotroph cells of the human normal pituitary gland. *Endocrine* **2017**, *57* (2), 314–325.



## Chapter 3

### **Constituents of *Passiflora incarnata*, but Not of *Valeriana officinalis*, Interact with the Organic Anion Transporting Polypeptides (OATP)2B1 and OATP1A2**

Schäfer AM<sup>1</sup>, Gilgen PM<sup>1</sup>, Spirgi C<sup>1</sup>, Potterat O<sup>2</sup>, Meyer zu Schwabedissen HE<sup>1</sup>

#### *Laboratories of Origin:*

<sup>1</sup>Biopharmacy, Department of Pharmaceutical Sciences, University of Basel, 4056 Basel, Switzerland

<sup>2</sup>Pharmaceutical Biology, Department of Pharmaceutical Sciences, University of Basel, 4056 Basel, Switzerland

#### *Contribution of Anima Schäfer:*

Study design, acquisition, analysis and interpretation of data, drafting of manuscript

#### *Journal:*

Planta Medica (2021) 18



# Constituents of *Passiflora incarnata*, but Not of *Valeriana officinalis*, Interact with the Organic Anion Transporting Polypeptides (OATP)2B1 and OATP1A2

## Authors

Anima M. Schäfer<sup>1</sup> , Pierrine M. Gilgen<sup>1</sup>, Clara Spirgi<sup>1</sup>, Olivier Potterat<sup>2</sup> , Henriette E. Meyer zu Schwabedissen<sup>1</sup>

## Affiliations

- 1 Biopharmacy, Department Pharmaceutical Sciences, University of Basel, Basel, Switzerland
- 2 Pharmaceutical Biology, Department Pharmaceutical Sciences, University of Basel, Basel, Switzerland

## Key words

OATP2B1, OATP1A2, interaction, sulfated steroids, *Passiflora incarnata*, Passifloraceae, *Valeriana officinalis*, Caprifoliaceae

## received

July 8, 2020

## accepted after revision

November 6, 2020

## published online

## Bibliography

Planta Med 2021

DOI 10.1055/a-1305-3936

ISSN 0032-0943

© 2021. Thieme. All rights reserved.

Georg Thieme Verlag KG, Rüdigerstraße 14,  
70469 Stuttgart, Germany

## Correspondence

Prof. Dr. med. Henriette E. Meyer zu Schwabedissen  
Biopharmacy, Department of Pharmaceutical Sciences,  
University of Basel  
Klingelbergstrasse 50, 4056 Basel, Switzerland  
Phone: + 41 (0) 6 12 07 14 95, Fax: + 41 (0) 6 12 07 14 98  
h.meyertzuschwabedissen@unibas.ch



Supplementary material is available under  
<https://doi.org/10.1055/a-1305-3936>

## ABSTRACT

Herbal medication used in the treatment of sleep disorders and anxiety often contain extracts of *Valeriana officinalis* or *Passiflora incarnata*. Valerenic acid in *V. officinalis* and apigenin, orientin, and vitexin in *P. incarnata* are thought to contribute to their therapeutic effect. It was the aim of this study to test whether these constituents of herbal extracts are interacting with the uptake of estrone 3-sulfate, pregnenolone sulfate, and dehydroepiandrosterone sulfate mediated by the uptake transporters organic anion transporting polypeptide 2B1 (OATP2B1) or organic anion transporting polypeptide 1A2 (OATP1A2). Madin-Darby canine kidney cells overexpressing OATP2B1 or OATP1A2 were used to determine the influence of the constituents on the cellular accumulation of the sulfated steroids. Subsequently, competitive counterflow experiments were applied to test whether identified inhibitors are also substrates of the transporters. Valerenic acid only interacted with OATP2B1, whereas apigenin, orientin, and vitexin interacted with OATP2B1 and OATP1A2. Competitive counterflow revealed that orientin is a substrate of both transporters, while apigenin was transported by OATP1A2 and vitexin by OATP2B1. In a next step, commercially available *P. incarnata* preparations were assessed for their influence on the transporters, revealing inhibition of transporter-mediated estrone 3-sulfate uptake. HPLC-UV-MS analysis confirmed the presence of orientin and vitexin in these preparations, thereby suggesting that these constituents are involved in the interaction. Our data indicate that constituents of *P. incarnata* may alter the function of OATP2B1 and OATP1A2, which could affect the uptake of other compounds relying on uptake mediated by the transporters.

## Introduction

The family of OATPs is assumed to play an important role in the absorption, elimination, and distribution of exogenous and endogenous compounds in the human body, as they facilitate cellular entry. OATP2B1 is ubiquitously expressed with validated expression in the intestines, kidneys, and liver where it is assumed to contribute to drug absorption and elimination [1–3]. Numerous endogenous substrates have been identified including E<sub>1</sub>S, DHEAS, and thyroid hormones [4, 5]. Its exogenous substrate

drugs belong to different classes and include HMG-CoA reductase inhibitors (e.g., atorvastatin), dopamine receptor antagonists (e.g., domperidone), antihistamines (e.g., fexofenadine), and antidiabetics (e.g., glibenclamide) [6–9]. The transporter is also known to be expressed in organs that are known to exhibit barrier function such as the placenta or the blood-brain barrier. In the placenta, OATP2B1 is expressed at the fetal side of the syncytiotrophoblasts, and is assumed to be involved in the transfer of its substrates from the fetus to the mother [10]. At the blood-brain barrier, OATP2B1 is located on the luminal side of endothelial

## ABBREVIATIONS

BSP	bromosulphophthalein
CCF	competitive counterflow
CNS	central nervous system
DHEAS	dehydroepiandrosterone sulfate
E <sub>1</sub> S	estrone 3-sulfate
GABA	gamma-aminobutyric acid
HBSS	Hank's balanced salt solution
MDCK cells	Madin-Darby canine kidney cells
OATP	organic anion transporting polypeptide
PregS	pregnenolone sulfate

cells, suggesting that it is involved in the penetration of its substrates into the brain [11].

OATP1A2 is another member of the OATP family. This transporter is expressed in villous syncytiotrophoblasts, cytotrophoblasts, and in extravillous trophoblasts of the placenta and was previously reported to be involved in the transfer from the mother to the fetus [12]. However, this transporter exhibits its highest expression in the brain. In contrast to OATP2B1, the transporter is not only expressed in endothelial cells of the blood-brain barrier [13], but also in other cells of the CNS, namely, glial cells and neurons [11, 14]. Exogenous substrates of OATP1A2 are the opioid peptide deltorphin II and the HMG-CoA reductase inhibitor rosuvastatin [15, 16]. It has also been shown to transport sulfated steroids [17, 18]. Besides synthetic compounds, there are also herbal constituents that interact with OATP1A2 or OATP2B1. The flavanone naringin, for example, a constituent in grapefruit juice, was shown to be an inhibitor of both transporters [19, 20]. Furthermore, OATP2B1 and OATP1A2 are inhibited by honey flavonoids and catechins found in green tea [21, 22]. Finally, the most researched constituents of St. John's wort, hyperforin and hypericin, were recently identified as interacting with OATP2B1 [23]. Extracts of St. John's wort are assumed to exert their pharmacological effect in the CNS and are used to treat mild depressive symptoms. Passionflower is another herbal remedy that is assumed to act on the CNS, as passionflower extracts were shown to be anxiolytic [24]. The observed effect is possibly mediated by the GABA system, as extracts of *Passiflora actinia* and *Passiflora incarnata* have been reported to interact with the GABA<sub>A</sub> receptor and the benzodiazepine-binding site *in vitro* [25, 26]. However, Appel et al. confirmed an interaction with the GABA<sub>A</sub> receptor, and reported an interaction with the GABA binding site, but not with the benzodiazepine binding site [27]. The flavonoids orientin, apigenin, and its glycosylated form vitexin seem to play a role in the antidepressant, anxiolytic, and sedative effects of the plant [28, 29]. Notably, apigenin has previously been reported to inhibit OATP2B1- and OATP1A2-mediated uptake of the dye bromosulphophthalein (BSP), atorvastatin, and fexofenadine in transporter overexpressing cells [30].

*Valeriana officinalis* is a plant assumed to also act on the GABAergic system and is used in the treatment of sleep disorders [31]. In addition, the herbal extract was identified to have an anxiolytic effect, as shown in rats [32]. It is assumed that valerenic

acid is the driving force acting on the GABA system, allosterically modulating the GABA<sub>A</sub> binding site [33].

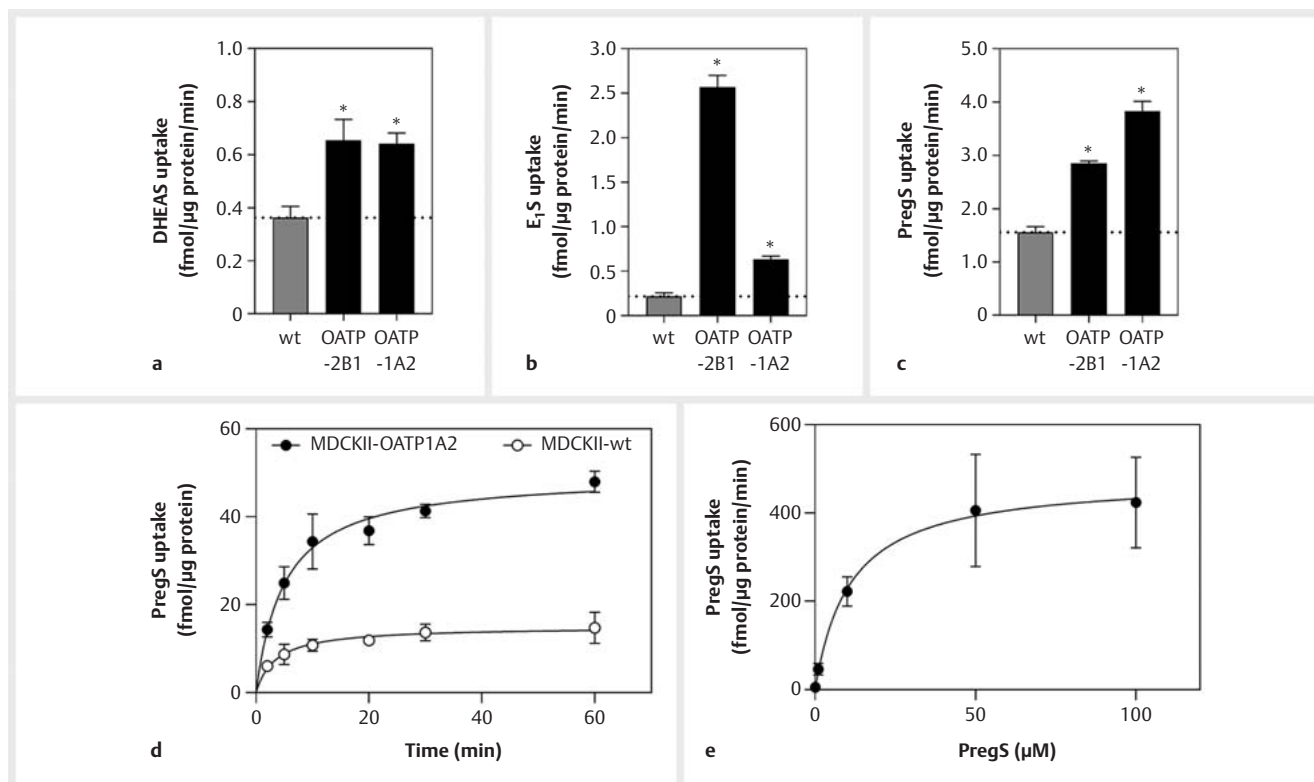
Since OATP2B1 and OATP1A2 are both known to transport endogenous sulfated steroid hormones, which are assumed to play a role in neurosteroid homeostasis [17], we wanted to test whether flavonoids found in *P. incarnata* and *V. officinalis* interact with this function. The impact of flavonoids on the OATP2B1- or OATP1A2-mediated transport of E<sub>1</sub>S, PregS, and DHEAS was assessed, followed by competitive counterflow (CCF) experiments. This indirect method provides a fast and cost saving way to test whether a compound is a substrate of OATPs, and is independent of issues associated with the direct measurement of transported substances such as availability of radioactive tracers or isolation of intracellular accumulated molecules. The applicability of this method to identify substrates of OATP2B1 and OATP1A2 was recently verified by our laboratory [7, 14]. Finally, the commercially available formulations of *P. incarnata* were tested for their interaction with OATP2B1 and OATP1A2 in transport experiments and for the presence of the flavonoids (apigenin, vitexin, and orientin) by HPLC-UV-MS analysis.

## Results

At first, we validated the OATP1A2- or OATP2B1-mediated transport of the conjugated steroids DHEAS, E<sub>1</sub>S, and PregS in MDCKII cells overexpressing the respective transport protein. As shown in ► **Fig. 1 a**, we observed an enhanced cellular amount of DHEAS in cells overexpressing OATP2B1 or OATP1A2, respectively, compared to wild-type cells ( $p \leq 0.05$ ). Similar results were obtained measuring the cellular amount of E<sub>1</sub>S ( $p \leq 0.05$ ) (► **Fig. 1 b**). PregS was confirmed as a substrate of OATP2B1 and was identified as a substrate of OATP1A2 (► **Fig. 1 c**). Testing the time-dependent uptake of PregS in MDCKII-OATP1A2 cells revealed a steady state after around 30 min (► **Fig. 1 d**). Determination of the kinetic parameters of PregS revealed an affinity ( $k_m$ ) and a maximum transport velocity ( $V_{max}$ ) of 10.98  $\mu\text{M}$  (CI 4.21 to 27.6  $\mu\text{M}$ ) and 0.48 pmol/ $\mu\text{g}$  protein/min (CI 0.39 to 0.61  $\mu\text{M}$ ), respectively (► **Fig. 1 e**).

In order to determine whether there is an interaction between apigenin, orientin, and vitexin (found in *P. incarnata*) and valerenic acid and valeric acid (found in *V. officinalis*) with the membrane transporters, MDCKII cells stably overexpressing OATP2B1 or OATP1A2 were tested for DHEAS, E<sub>1</sub>S, and PregS accumulation in the presence of the constituents. In ► **Fig. 2 a, c, e**, the influence of *P. incarnata* or *V. officinalis* constituents on the OATP2B1-mediated cellular accumulation of DHEAS, E<sub>1</sub>S, or PregS is shown. The *P. incarnata* constituent apigenin reduced accumulation of the three sulfated steroids in OATP2B1 overexpressing cells. Orientin decreased the cellular amount of DHEAS and PregS, but did not influence that of E<sub>1</sub>S. However, vitexin decreased the amount of E<sub>1</sub>S and PregS, but not that of DHEAS in OATP2B1 expressing cells. Finally, valerenic acid only inhibited PregS accumulation, and no interaction was found for valeric acid.

Testing the interaction of the constituents with OATP1A2 (► **Fig. 2 b, d, f**) we identified apigenin as an inhibitor of the accumulation of all three conjugated steroid hormones. No interaction with the transporter was observed for orientin. Vitexin only influ-



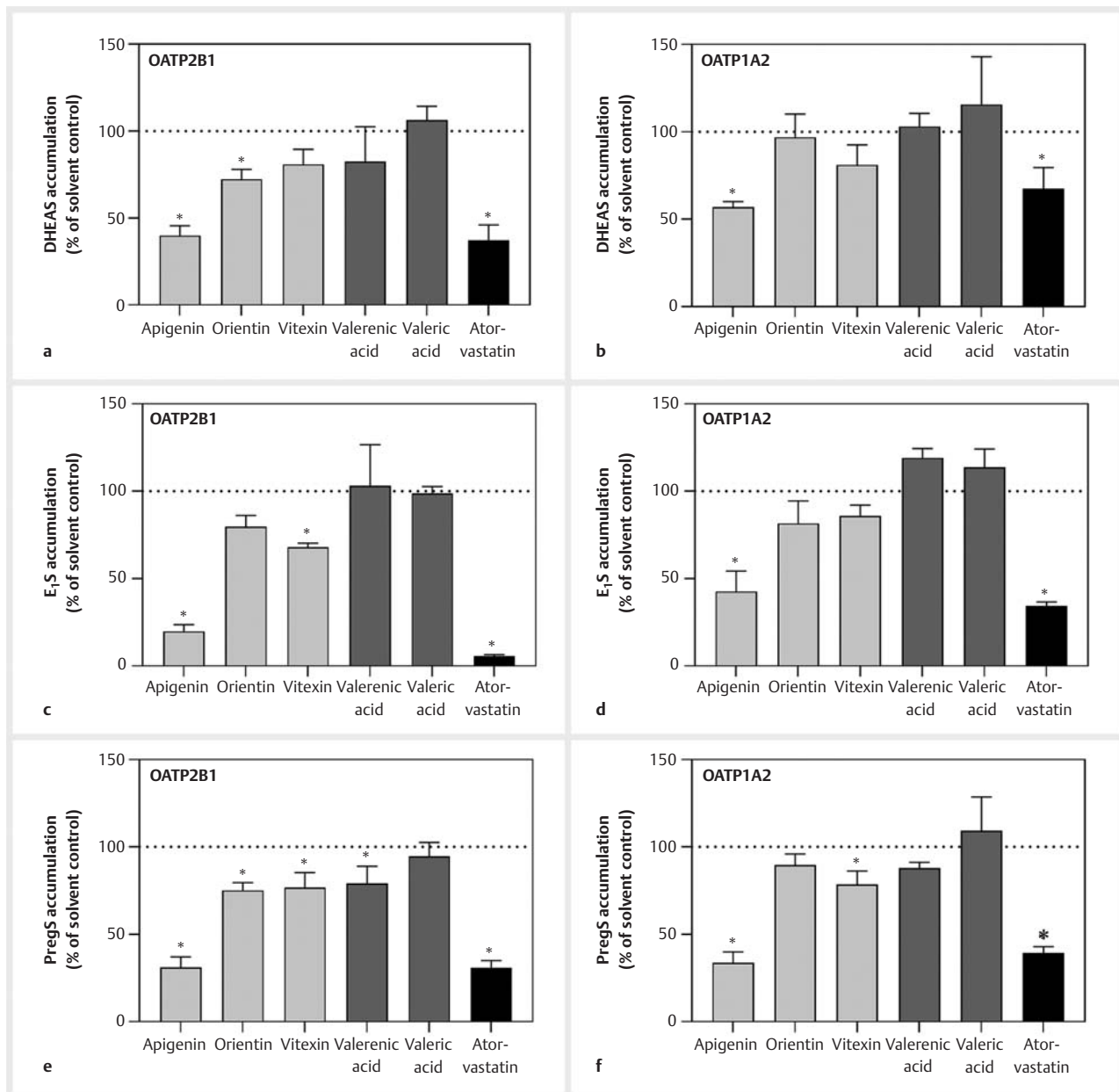
► **Fig. 1** Accumulation of sulfated steroids in OATP2B1 or OATP1A2 overexpressing cells. The cellular amount of dehydroepiandrosterone sulfate (DHEAS) (a), estrone-3 sulfate (E<sub>1</sub>S) (b), and pregnenolone sulfate (PregS) (c) was quantified after 5 min exposure in MDCKII cells stably expressing OATP2B1 or OATP1A2. The intracellular amount was normalized to protein content and time and compared to MDCKII wild type. Data were analyzed applying a one-way ANOVA corrected for multiple comparisons (Dunnett's test, \* $p \leq 0.05$ ) of  $n = 3$  experiments, each conducted in biological triplicate. Time-dependent uptake of PregS in MDCKII-OATP1A2 was compared to wild-type cells (d), and kinetics ( $V_{max}$ ) as well as affinity ( $K_m$ ) was calculated based on a concentration-dependent PregS uptake (e) ( $n = 3$  in biological triplicate, data are presented as mean  $\pm$  SD).

enced the OATP1A2-mediated uptake of PregS. No interaction with OATP1A2 was observed for valeric acid and valerenic acid in this experimental setup. Atorvastatin was used as a positive control as it is a known inhibitor of both transporters.

CCF experiments have recently been successfully applied to identify substrates of OATP2B1 and OATP1A2 [7, 14]. A drawing elaborating the difference between transport inhibition assays and CCF experiments is provided in ► **Fig. 3**. CCF experiments were performed in the steady state of the known substrate E<sub>1</sub>S and at a concentration of 10 times the observed inhibitory concentration ( $IC_{50}$ ) of the test compound [34]. The inhibitory potency was determined for the constituents, which were identified as inhibitors of the OATP-mediated accumulation of E<sub>1</sub>S. As shown in ► **Fig. 4a, c** the observed  $IC_{50}$  of apigenin was 6.0  $\mu$ M (CI 2.6 to 13.1  $\mu$ M) and 1.41  $\mu$ M (CI 0.31 to 6.48  $\mu$ M) for OATP2B1 and OATP1A2, respectively. The  $IC_{50}$  of vitexin tested in MDCKII-OATP2B1 cells was estimated to be 242  $\mu$ M (CI 182 to 324  $\mu$ M) (► **Fig. 4b**). Additionally, because it will be used in CCF experiments as a positive control [35] and it has not been described so far, the inhibitory potency of atorvastatin for OATP1A2-mediated E<sub>1</sub>S transport was determined (32.3  $\mu$ M, CI 18.2 to 57  $\mu$ M) (► **Fig. 4d**).

In the next step, the CCF method was applied to test whether the constituents are substrates of the transporters. However, due to solubility issues, the highest concentration we used was 250  $\mu$ M. As shown in ► **Fig. 5a, b**, the presence of orientin significantly decreased the steady state concentration of E<sub>1</sub>S testing cells expressing either OATP1A2 or OATP2B1, suggesting that orientin is not only an inhibitor but also a substrate of both transporters. For vitexin, this effect was only seen for OATP2B1, while apigenin only reduced the steady state concentration in OATP1A2 expressing cells. This implies that vitexin is an inhibitor and substrate of OATP2B1, while apigenin is a substrate and inhibitor of OATP1A2. Valerenic acid and valeric acid did not affect the steady state of E<sub>1</sub>S in the CCF, implying that they are no substrates of OATP1A2. However, valerenic acid seems to induce the accumulation of intracellular E<sub>1</sub>S, as it is statistically significantly higher compared to the control. Atorvastatin being a substrate of both OATPs [6, 35] was confirmed in the CCF experiments as it significantly decreased the steady state.

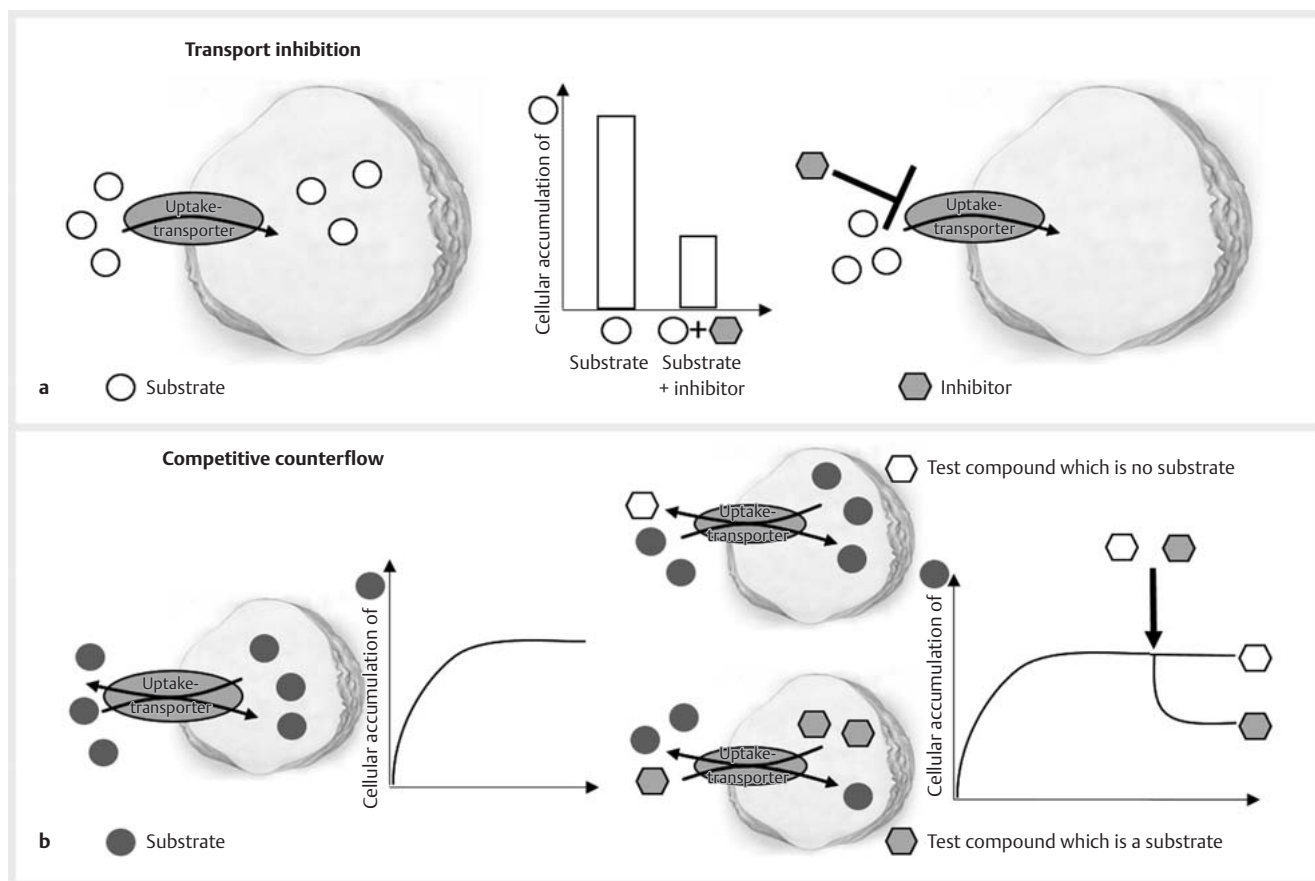
In a following step, two over-the-counter formulations [Arkocaps "Passionsblume" (German for passionflower) and Valverde "Beruhigung" (German for sedation)] containing *P. incarnata* were tested for interactions with the transporters. The formulations were used at a final concentration of 0.05 mg/mL of the extracts.



► **Fig. 2** Inhibition of herbal constituents on OATP-mediated steroid hormone transport. Intracellular accumulation of DHEAS (a, b), E<sub>1</sub>S (c, d), or PregS (e, f) was assessed in MDCKII-OATP2B1 (a, c, e) or MDCKII-OATP1A2 (b, d, f) cells and normalized to the solvent control. Apigenin, orientin, and vitexin (light grey) are constituents found in *P. incarnata*, and valerenic acid and valeric acid (dark grey) are present in *V. officinalis*. Atorvastatin (black) served as a positive control. Data are presented as mean ± SD of three independent experiments, each performed in biological triplicate. For statistical analysis, a one-way ANOVA with Dunnett's correction for multiple comparisons was applied; \*p ≤ 0.05.

As shown in ► **Fig. 6**, Valverde tablets had an influence on every steroid hormone transport of both transporters ( $p \leq 0.05$ ) (► **Fig. 6a–f**). However, the Arkocaps capsule extract influenced the E<sub>1</sub>S and PregS transport in OATP2B1 transfected cells (► **Fig. 6c, e**), whereas transport of DHEAS and PregS was inhibited in MDCKII-OATP1A2 cells (► **Fig. 6b, f**). No effect was observed on the accumulation of DHEAS in MDCKII-OATP2B1 cells (► **Fig. 6a**) or the E<sub>1</sub>S accumulation in MDCKII-OATP1A2 cells (► **Fig. 6d**).

Since apigenin, orientin, and vitexin showed interactions with one or both OATPs and since orientin and vitexin are assumed to be major constituents of *P. incarnata*, the formulations were analyzed for the presence of these molecules using HPLC-UV-MS analysis to see whether the observed OATP interaction could be attributed to the tested constituents. Arkocaps capsule extract (► **Fig. 7a**) and Valverde tablets (► **Fig. 7b**) clearly showed a similar chromatogram. However, based on the signal intensity (UV 254 nm), the content of the flavonoids in the Valverde tablets ap-



► **Fig. 3** Illustration of the principle and expected results of a transport inhibition assay and a CCF experiment. **a** Cellular, transporter-mediated uptake of a substrate is assessed in the absence (left side, solvent control) and presence of a molecule (right side). If the molecule is an inhibitor of the transporter, this would reduce the cellular accumulation, as depicted in the hypothetical figure in the middle. Importantly, the data do not resolve the question whether inhibition is competitive or not. **b** CCF experiments were performed in the steady state (left side). If a test compound added in the equilibrium decreases the equilibrium, and therefore the intracellular amount of the substrate, it interacts with the transporter and is identified as substrate. No change of the substrate in the steady state is observed if the test compound is not a substrate of the transporter.

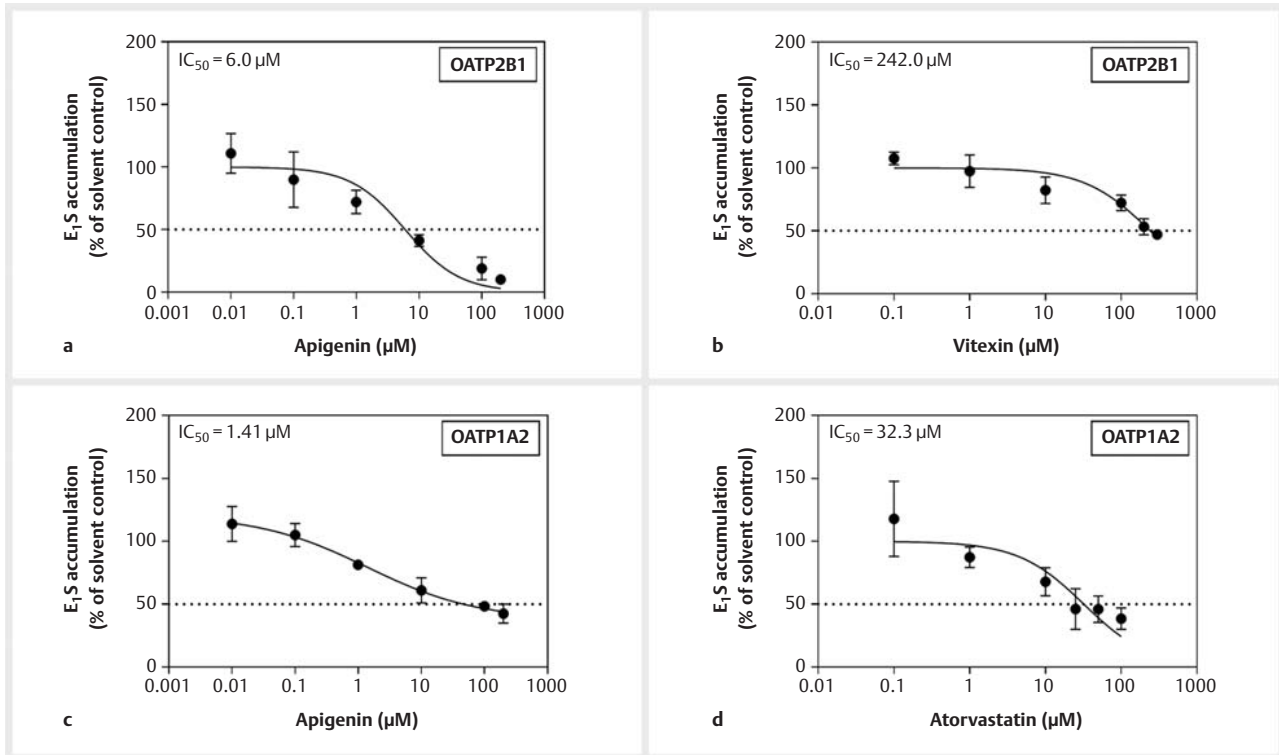
pears to be approximately 2 times higher. By comparison with commercial references and analysis of their mass spectra, we were able to unambiguously confirm the presence of orientin ( $t_R$  10.7 min) and vitexin ( $t_R$  12.6 min) in both preparations. In addition, two major peaks eluting at  $t_R$  10.3 and  $t_R$  12.8 min, respectively, were assigned to isoorientin and isovitexin, respectively, two further known flavonoids of *P. incarnata* (► **Fig. 7 d, e** and **Fig. 15–5S**, Supporting information). In contrast, apigenin was not detected in either of the tested formulations.

## Discussion

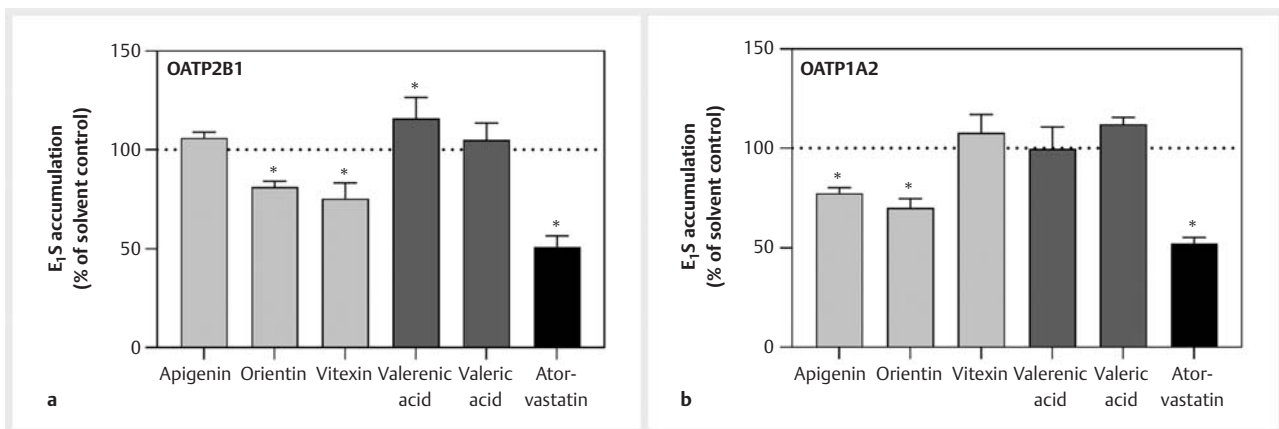
In this study, we report on the interaction of constituents of *P. incarnata*, an herbal remedy commonly used to treat sleep disorders and anxiety, and the OATP2B1- or OATP1A2-mediated transport of the sulfated steroids  $E_1S$ , DHEAS, and PregS. We not only confirmed uptake of  $E_1S$ , DHEAS, and PregS by OATP2B1 [4, 36], but also uptake of  $E_1S$  and DHEAS by OATP1A2 [35]. We also report that PregS is a substrate of OATP1A2, which exhibits an affinity ( $K_m$ ) of 10.98  $\mu M$  and a maximum transport ( $V_{max}$ ) of 0.48 pmol/ $\mu g$  protein/min, as determined in overexpressing cells.

Phytopharmaceuticals are multicomponent mixtures and, in general, it is assumed that the summary of their constituents is the basis of their pharmacological activity. However, in our study, we not only tested the mixture, but also a group of flavonoids (apigenin, orientin, and vitexin) for interaction with the uptake transporters. The herein selected flavonoids are thought to take part in the neuroprotective, anxiolytic, and tranquilizing effect of *Passiflora* species [26, 37]. Notably, in order to reach their site of action, the constituents would have to cross cellular barriers. In general, transport proteins mediating cellular entry are assumed to be one of the mechanisms modulating the crossing of cellular membranes. In this study, we assessed whether flavonoids and/or the herbal remedies interact with OATP2B1 and OATP1A2 using sulfated steroids as substrates or victims since their transport across the cellular membrane via OATP2B1 and OATP1A2 would be impeded. Apigenin influenced the OATP2B1- and OATP1A2-mediated uptake of DHEAS,  $E_1S$ , and PregS, thereby confirming findings by Mandery et al. [30].

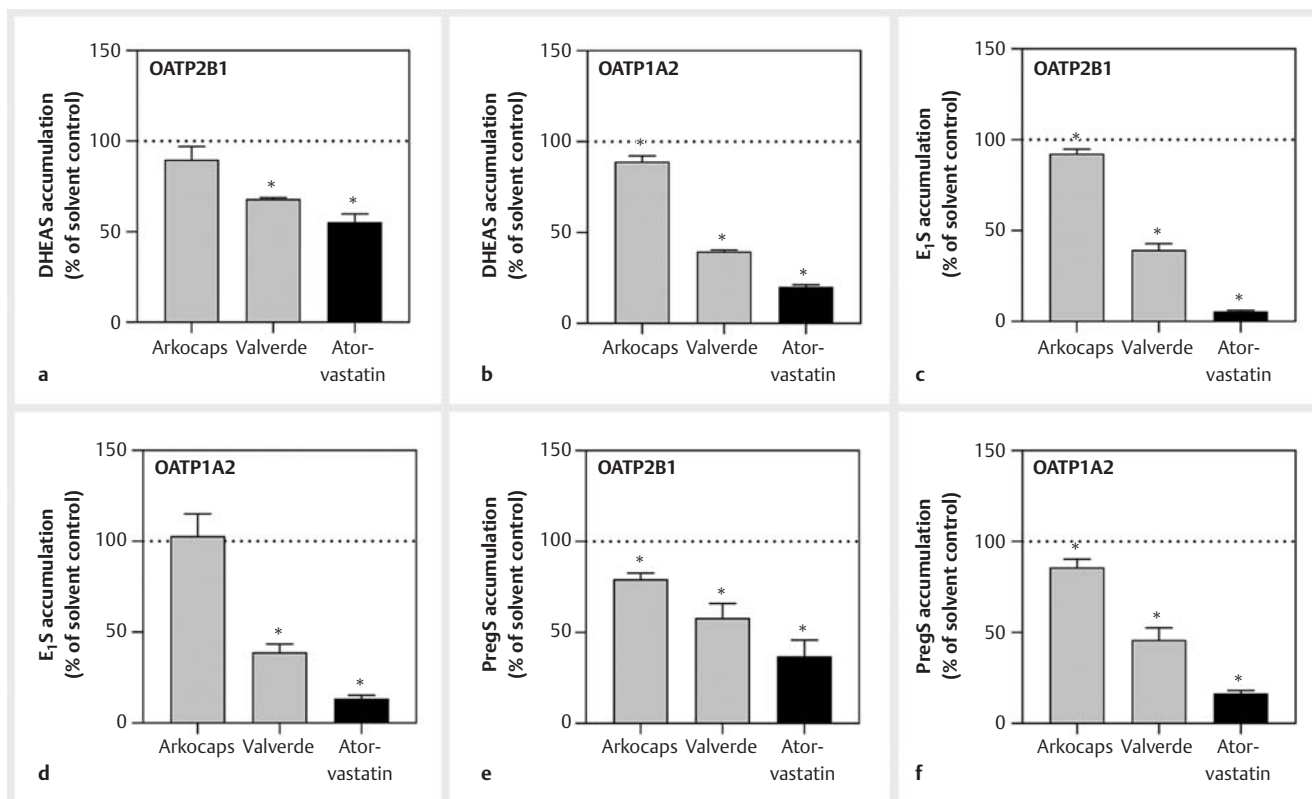
Moreover, apigenin was identified as a substrate of OATP1A2, but not of OATP2B1, applying CCF experiments. The glycosylated form of apigenin, namely, the vitexin, showed a lower inhibitory



▶ **Fig. 4** Estimation of potency of the OATP1A2 and OATP2B1 inhibitors. Inhibition of OATP2B1- or OATP1A2-mediated E<sub>1</sub>S uptake was assessed in transporter overexpressing MDCKII cells. Concentration dependency was assessed for apigenin and vitexin with OATP2B1 (a, b), and for apigenin and atorvastatin, with OATP1A2 (c, d). Results were a basis for the estimation of inhibitory potency (IC<sub>50</sub> value) fitting the data to a sigmoidal log (inhibitor)-normalized response curve (a, b, d) or to a log(inhibitor) vs. response curve (variable slope, four parameters, c) without weighing or constraining of the top or bottom. Data are shown as the mean ± SD of at least three independent experiments, each performed in biological triplicate.



▶ **Fig. 5** CCF experiments with the herbal constituents. MDCKII-OATP2B1 (a) and MDCKII-OATP1A2 (b) cells were exposed to [<sup>3</sup>H]-labelled E<sub>1</sub>S until steady state was reached. Subsequently, the supernatant was replaced by fresh [<sup>3</sup>H]-E<sub>1</sub>S supplemented with the test compounds (light grey = constituents of *P. incarnata*; dark grey = constituents of *V. officinalis*) or solvent control. Atorvastatin served as a positive control. Statistical analysis was conducted applying a one-way ANOVA with Dunnett's multiple comparisons test; \*p < 0.05. Data are presented as the mean ± SD of n = 3 experiments, each performed in biological triplicate.



► **Fig. 6** Interaction of commercially available *P. incarnata* formulations with OATP2B1 or OATP1A2. The extract obtained from the Arkocaps capsules or powdered Valverde tablets were solved in DMSO, and inhibition of OATP-mediated DHEAS (a,b), E<sub>1</sub>S (c,d), and PregS (e,f) accumulation was determined in transporter overexpressing MDCKII cells. One-way ANOVA corrected for multiple comparisons (Dunnett's test) was used to test for statistical significance, \*p < 0.05. Data are presented as the mean ± SD and experiments were performed 3 times in biological triplicate.

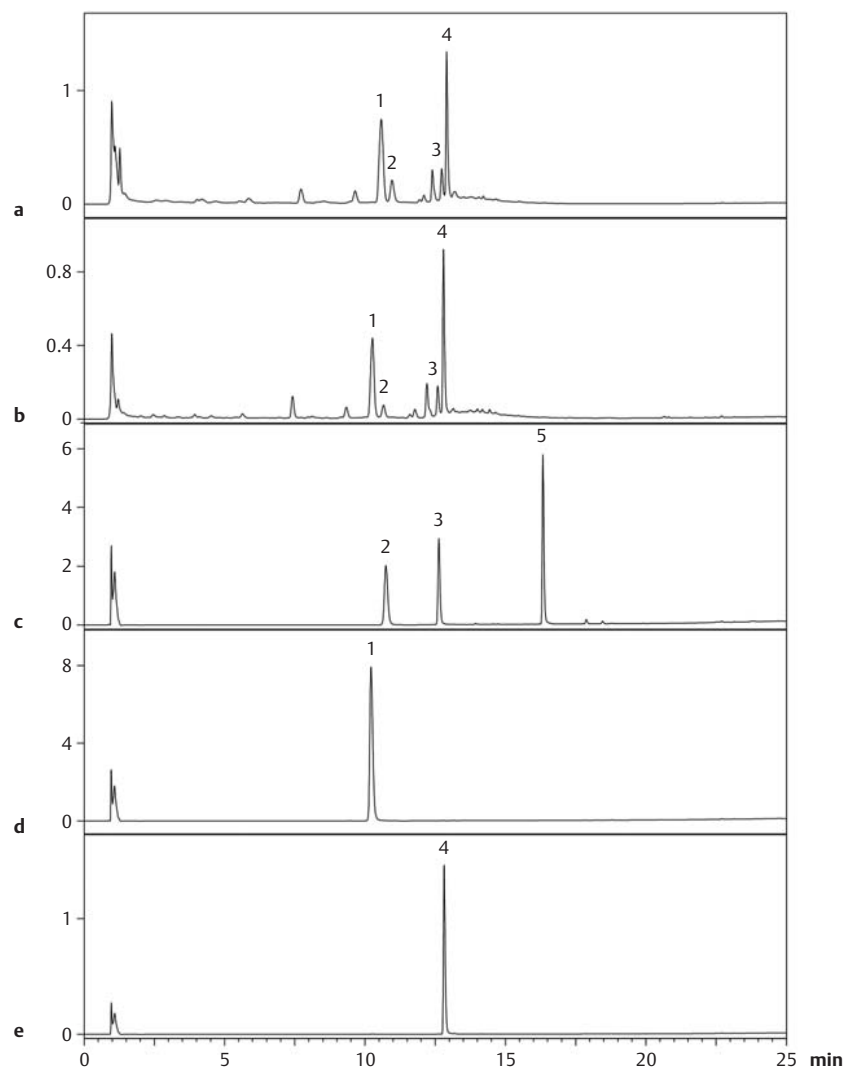
potency for OATP2B1 and OATP1A2. However, it was identified as a substrate of OATP2B1, but not of OATP1A2. Orientin, which is also a glycosylated flavonoid, was identified as a substrate of both OATPs, although it did not inhibit the transporter function at a concentration of 50 μM. Notably, glycosylated flavonoids (orientin and vitexin) were identified as OATP2B1 substrates while the non-glycosylated flavonoid apigenin was not. However, we did not find such an association for OATP1A2, since apigenin and orientin were identified as substrates but not vitexin.

In a next step, we tested the commercially available formulations Arkocaps Passionsblume and Valverde Beruhigung and observed an interaction with both transporters. The inhibitory potency of Valverde tablets was higher for both transporters compared to that of the extract from the Arkocaps capsules. This may be explained by the higher flavonoid content as detected by HPLC-UV-MS in the Valverde tablets. When analyzing the extracts for the presence of orientin and vitexin, two further flavonoids were observed, namely, isovitexin and isoorientin. Importantly, apigenin was not found in any of the herein tested formulations. Our findings are in line with those by Gadioli et al., who screened 34 species of *Passiflora* plants, reporting orientin and vitexin as the most abundant flavonoids [38]. In regard to the interaction of the formulations with OATP2B1 and OATP1A2, it may be speculated that vitexin and orientin have contributed to the inhibition.

Whether isoorientin or isovitexin are also inhibitors of the transporters is currently unknown.

Even if it is generally assumed that flavonoids show little bioavailability after oral application due to extensive metabolism in the intestines and liver, there are data showing the presence of flavonoids in the circulation, and even in the brain [39,40]. Whether the herein shown interaction of the flavonoids and the OATPs is of physiological relevance cannot be clarified. However, it can be speculated that if present at the blood-brain barrier, they may influence steroid homeostasis in the brain due to the localization of OATP2B1 and OATP1A2 at the blood-brain barrier. Indeed, steroid hormone homeostasis is pivotal for the CNS. An important function of both sulfated and desulfated steroid hormones is the modulation of neuronal excitability [41]. It is assumed that steroids are directly synthesized in neurons or glia cells [42]. However, the origin of the sulfated precursors within the brain remains to be determined. One mechanism that may contribute to the CNS entry of sulfated steroids is transporter-mediated uptake by OATP1A2 or OATP2B1, which both have been shown to be expressed in endothelial cells, as also discussed by Grube et al. [17].

Interaction with OATP2B1 may also be of relevance in the intestines, where the transporter functions as a facilitator of oral absorption [43]. Consequently, the inhibition of OATP2B1 by concomitantly administered *P. incarnata* extracts might influence the handling of other xenobiotics such as atorvastatin, a well-known



► **Fig. 7** HPLC-UV chromatograms of commercially available *P. incarnata* formulations and reference compounds. Arkocaps capsule extract (a), Valverde tablets (b), orientin, vitexin, and apigenin (c), isorientin (d), and isovitexin (e) were analyzed by HPLC-UV-MS. Detection was performed at 254 nm. The corresponding HPLC-MS traces are shown as Supporting Information (Figs. 1S–5S, Supporting Information). Peak numbers correspond to isorientin (1), orientin (2), vitexin (3), isovitexin (4), and apigenin (5).

substrate of OATP2B1, as also addressed in the work of Mandery et al. [30]. Glaeser et al. found OATP1A2 to be localized at the apical brush border membrane of human duodenal tissue sections [44], however, in mass spectrometric-based screenings of membrane transporters along the intestines, OATP1A2 was not detected [45]. Accordingly, the presence and thereby contribution of OATP1A2 to oral drug absorption is a matter of debate in the field.

The other constituents that were assessed for interaction with OATP2B1 and OATP1A2 were the sesquiterpenoid valerenic acid and the structurally unrelated alkanolic acid valeric acid, two constituents of *V. officinalis*. No interaction was observed for valeric acid and the OATP2B1- or OATP1A2-mediated uptake of steroid hormones. This might be explained by its simple chemical struc-

ture, a linear alkanolic acid which may passively diffuse through membranes. For valerenic acid, Neuhaus et al. suggested that it is not able to cross membranes passively but relies on active mechanisms. The transport proteins involved in the process are still unknown [46], however, the compound does not seem to interact with the herein tested transporters.

Overall, our study showed that OATP2B1 and OATP1A2 might mediate the uptake and influence the effect of the selected constituents of the tranquilizing herbal remedy *P. incarnata*. Furthermore, the extracts of *P. incarnata* might influence the steroid homeostasis or the pharmacokinetic of other substrates of the transporters, which needs to be taken into account when thinking about drug absorption in organs expressing OATP2B1 or OATP1A2.

## Material and Methods

### Substances

Apigenin, vitexin, orientin, isoorientin, and atorvastatin were obtained from Sigma-Aldrich. Isovitexin was purchased from Extrasynthèse. The commercially available formulation Arkocaps Passionsblume is made by Arkopharma, and Valverde Beruhigung was manufactured by Sidroga. Both commercial preparations solely consist of *Passiflorae herba*. The radioactively labelled [<sup>3</sup>H]-estrone 3-sulfate (E<sub>1</sub>S) and [<sup>3</sup>H]-pregnenolone sulfate (PregS) were obtained from Hartmann Analytic. [<sup>3</sup>H]-dehydroepiandrosterone sulfate (DHEAS) was purchased from Perkin Elmer.

### Cell culture

MDCKII cells (p7-p20; ATCC no. CRL-2936) were obtained from the ATCC and cultivated at 37 °C and 5% CO<sub>2</sub> in DMEM (Sigma-Aldrich) supplemented with 10% fetal calf serum (Bio Concept) and 1% glutamine 200 mM (Bio Concept). MDCKII cells stably expressing OATP2B1 (p3-p8) or OATP1A2 (p14-p20) were generated as described elsewhere [47] and were cultured under constant selection by the addition of hygromycin B (750 µg/mL; Carl Roth) or geneticin (500 µg/mL; Carl Roth), respectively.

### Transport experiments

MDCKII, MDCKII-OATP2B1, or MDCKII-OATP1A2 cells were seeded at a density of 50 000 cells/24 wells. One day after seeding, the cells were treated with 2 mM sodium butyrate for 24 h. After that, cells were washed once with prewarmed PBS followed by incubation with HBSS at 37 °C for 10 min. Intracellular uptake was determined by incubating the cells with 1 nM E<sub>1</sub>S, 1 nM DHEAS, or 1 nM PregS, each supplemented with 100 000 dpm/well of the respective tritiated tracer. After 5 min, the cells were washed twice with ice-cold PBS before 200 µL lysis buffer (SDS 0.2% in 5 mM EDTA) were added. After cell lysis at 37 °C for 30 min, the protein content was measured using the Pierce BCA Protein Assay Kit (Thermo Fisher Scientific) and the microplate reader Infinite M200 Pro (Tecan) according to the manufacturer's instructions. The amount of substrate was quantified, assessing the radiolabel by liquid scintillation counting using 2 mL scintillation fluid (Rotiszint eco Plus, Carl Roth) and Tri-Carb 4910TR (Perkin Elmer).

The time-dependent uptake of PregS in OATP1A2 was determined at 2, 5, 10, 20, 30, and 60 min using the same amount of PregS as mentioned above. Kinetic parameters of transport were calculated testing the cellular accumulation of increasing amounts of PregS (0.1, 1, 10, 50, 100 µM) in MDCKII-OATP1A2 cells.

Apigenin, vitexin, and orientin from *P. incarnata* and valeric acid and valeric acid from *V. officinalis* (50 µM each) were tested for inhibition of OATP2B1- and OATP1A2-mediated transport of the abovementioned substrates DHEAS, E<sub>1</sub>S, and PregS. Subsequently, increasing concentrations of the constituents were used (0.01, 0.1, 1, 10, 100, and 200 µM) to estimate the inhibitory potency. Arkocaps capsules were extracted with 70% ethanol by pressurized liquid extraction in a Dionex ASE 200 Accelerated Solvent Extractor. Three cycles of extraction were performed with the temperature set at 70 °C and the pressure at 120 bar. After

evaporation of ethanol, the extract was dissolved in DMSO. Valverde tablets, which contain an ethanolic extract, were milled before dissolving in DMSO. To ensure complete dissolution, mixtures were sonicated for 30 s. The final concentration used for transport experiments was 0.05 mg/mL.

### Competitive counterflow

CCF experiments were performed following previously established protocols [7, 14]. Briefly, MDCKII-OATP2B1 and MDCKII-OATP1A2 cells were seeded and treated with sodium butyrate as described above. After washing the cells with PBS and preincubation with HBSS, the buffer was removed and 150 µL radioactively labelled estrone-3 sulfate ([<sup>3</sup>H]-E<sub>1</sub>S, 100 000 dpm/well) in HBSS were added followed by incubation at 37 °C for 30 min to reach steady state. Afterwards, the [<sup>3</sup>H]-E<sub>1</sub>S solution was removed and 150 µL of test compound in HBSS containing [<sup>3</sup>H]-E<sub>1</sub>S (100 000 dpm/well) were added followed by incubation at 37 °C for 90 s and 7 min for OATP2B1 and OATP1A2, respectively [7, 14]. The cells were washed, lysed, and protein content was measured as described above. The remaining samples were analyzed by scintillation counting. For CCF experiments, the applied concentration of the test compounds corresponded to 10 × IC<sub>50</sub> as recommended by Harper and Wright [34].

### HPLC-UV-MS analysis of commercially available products containing *Passiflora incarnata*

First, 100 mg of milled Valverde tablets and 10 mg Arkocaps capsule extract were separately dissolved in 1 mL DMSO. The mixtures were filtrated through a syringe filter (Chromafil O-20/15 MS, pore-size 0.2 µm; Macherey-Nagel). Subsequently, the Valverde solution was diluted to 10 mg/mL. The reference compounds orientin, vitexin, apigenin, isoorientin, and isovitexin were dissolved in DMSO (0.3 mg/mL). HPLC-UV-MS analysis was performed on a chromatographic system consisting of a degasser, a quaternary pump (LC-20AD), a column oven (CTO-20AC), a PDA detector (SPD-M20A), and a triple quadrupole mass spectrometer (LCMS-8030; Shimadzu). The mobile phase consisted of water (A) and acetonitrile (B), both containing 0.1% formic acid. Separations were achieved on a Poroshell120 EC-C18 column (3.0 × 100 mm, 2.7 µm) with a gradient of 10–15% B in 10 min, then 15–70% B in 10 min before reaching 90% B in 3 min and going back to 10% in 8 min. The flow rate was 0.5 mL/min. Then, 10 µL (Arkocaps capsule extract), 2 µL (Valverde tablets), and 5 µL (reference compounds) were injected.

### Statistical analysis

The statistical analysis of the experimental data was performed using GraphPad Prism software 8.0 (GraphPad Software) and Microsoft Excel. The herein reported concentrations, where half-maximal inhibition was observed (IC<sub>50</sub> values), were estimated by nonlinear curve fitting using normalized values. For calculation of the kinetic parameters of PregS with OATP1A2, the net transport normalized to the protein content and time was used. To get the maximum enzyme velocity (V<sub>max</sub>) and the affinity (K<sub>m</sub>), nonlinear regression was performed and analyzed with Michaelis-Menten enzyme kinetics. The resulting data are shown as the mean ± standard deviation (SD). A p value ≤ 0.05 was considered

statistically significant. The statistical test used to analyze the data is described in the context of their reporting.

### Supporting information

HPLC-MS chromatographic traces of commercial formulations and reference substances are available as Supporting Information.

### Contributors' Statement

A.M. Schäfer and H.E. Meyer zu Schwabedissen participated in research design; A.M. Schäfer, P.M. Gilgen, C. Spirgi, O. Potterat, and H.E. Meyer zu Schwabedissen conducted experiments; A.M. Schäfer, P.M. Gilgen, C. Spirgi, O. Potterat, and H.E. Meyer zu Schwabedissen performed data analysis and interpretation; A.M. Schäfer, P.M. Gilgen, C. Spirgi, O. Potterat, and H.E. Meyer zu Schwabedissen wrote or contributed to the writing of the manuscript.

### Conflict of Interest

The authors declare that they have no conflict of interest.

### References

- [1] Kobayashi D, Nozawa T, Imai K, Nezu J, Tsuji A, Tamai I. Involvement of human organic anion transporting polypeptide OATP-B (SLC21A9) in pH-dependent transport across intestinal apical membrane. *J Pharmacol Exp Ther* 2003; 306: 703–708
- [2] Kullak-Ublick GA, Ismail MG, Stieger B, Landmann L, Huber R, Pizzagalli F, Fattinger K, Meier PJ, Hagenbuch B. Organic anion-transporting polypeptide B (OATP-B) and its functional comparison with three other OATPs of human liver. *Gastroenterology* 2001; 120: 525–533
- [3] Ferreira C, Hagen P, Stern M, Hussner J, Zimmermann U, Grube M, Meyer zu Schwabedissen HE. The scaffold protein PDZK1 modulates expression and function of the organic anion transporting polypeptide 2B1. *Eur J Pharm Sci* 2018; 120: 181–190
- [4] Pizzagalli F, Varga Z, Huber RD, Folkers G, Meier PJ, St-Pierre MV. Identification of steroid sulfate transport processes in the human mammary gland. *J Clin Endocrinol Metab* 2003; 88: 3902–3912
- [5] Meyer zu Schwabedissen HE, Ferreira C, Schaefer AM, Oufir M, Seibert I, Hamburger M, Tirona RG. Thyroid hormones are transport substrates and transcriptional regulators of organic anion transporting polypeptide 2B1. *Mol Pharmacol* 2018; 94: 700–712
- [6] Grube M, Kock K, Oswald S, Draber K, Meissner K, Eckel L, Bohm M, Felix SB, Vogelgesang S, Jedlitschky G, Siegmund W, Warzok R, Kroemer HK. Organic anion transporting polypeptide 2B1 is a high-affinity transporter for atorvastatin and is expressed in the human heart. *Clin Pharmacol Ther* 2006; 80: 607–620
- [7] Schaefer AM, Bock T, Meyer zu Schwabedissen HE. Establishment and validation of competitive counterflow as a method to detect substrates of the organic anion transporting polypeptide 2B1. *Mol Pharm* 2018; 15: 5501–5513
- [8] Shirasaka Y, Mori T, Murata Y, Nakanishi T, Tamai I. Substrate- and dose-dependent drug interactions with grapefruit juice caused by multiple binding sites on OATP2B1. *Pharm Res* 2014; 31: 2035–2043
- [9] Satoh H, Yamashita F, Tsujimoto M, Murakami H, Koyabu N, Ohtani H, Sawada Y. Citrus juices inhibit the function of human organic anion-transporting polypeptide OATP-B. *Drug Metab Dispos* 2005; 33: 518–523
- [10] Grube M, Reuther S, Meyer zu Schwabedissen H, Kock K, Draber K, Ritter CA, Fusch C, Jedlitschky G, Kroemer HK. Organic anion transporting polypeptide 2B1 and breast cancer resistance protein interact in the transepithelial transport of steroid sulfates in human placenta. *Drug Metab Dispos* 2007; 35: 30–35
- [11] Gao B, Vavricka SR, Meier PJ, Stieger B. Differential cellular expression of organic anion transporting peptides OATP1A2 and OATP2B1 in the human retina and brain: implications for carrier-mediated transport of neuropeptides and neurosteroids in the CNS. *Pflugers Arch* 2015; 467: 1481–1493
- [12] Loubiere LS, Vasilopoulou E, Bulmer JN, Taylor PM, Stieger B, Verrey F, McCabe CJ, Franklyn JA, Kilby MD, Chan SY. Expression of thyroid hormone transporters in the human placenta and changes associated with intrauterine growth restriction. *Placenta* 2010; 31: 295–304
- [13] Lee W, Glaeser H, Smith LH, Roberts RL, Moeckel GW, Gervasini G, Leake BF, Kim RB. Polymorphisms in human organic anion-transporting polypeptide 1A2 (OATP1A2): implications for altered drug disposition and central nervous system drug entry. *J Biol Chem* 2005; 280: 9610–9617
- [14] Schäfer AM, Meyer zu Schwabedissen HE, Bien-Moller S, Hubeny A, Vogelgesang S, Oswald S, Grube M. OATP1A2 and OATP2B1 are interacting with dopamine-receptor agonists and antagonists. *Mol Pharm* 2020; 17: 1987–1995
- [15] Gao B, Hagenbuch B, Kullak-Ublick GA, Benke D, Aguzzi A, Meier PJ. Organic anion-transporting polypeptides mediate transport of opioid peptides across blood-brain barrier. *J Pharmacol Exp Ther* 2000; 294: 73–79
- [16] Ho RH, Tirona RG, Leake BF, Glaeser H, Lee W, Lemke CJ, Wang Y, Kim RB. Drug and bile acid transporters in rosuvastatin hepatic uptake: function, expression, and pharmacogenetics. *Gastroenterology* 2006; 130: 1793–1806
- [17] Grube M, Hagen P, Jedlitschky G. Neurosteroid transport in the brain: Role of ABC and SLC transporters. *Front Pharmacol* 2018; 9: 354
- [18] Meyer zu Schwabedissen HE, Tirona RG, Yip CS, Ho RH, Kim RB. Interplay between the nuclear receptor pregnane X receptor and the uptake transporter organic anion transporter polypeptide 1A2 selectively enhances estrogen effects in breast cancer. *Cancer Res* 2008; 68: 9338–9347
- [19] Johnson EJ, Won CS, Kock K, Paine MF. Prioritizing pharmacokinetic drug interaction precipitants in natural products: application to OATP inhibitors in grapefruit juice. *Biopharm Drug Dispos* 2017; 38: 251–259
- [20] Bailey DG, Dresser GK, Leake BF, Kim RB. Naringin is a major and selective clinical inhibitor of organic anion-transporting polypeptide 1A2 (OATP1A2) in grapefruit juice. *Clin Pharmacol Ther* 2007; 81: 495–502
- [21] Navratilova L, Ramos Mandikova J, Pavek P, Mladenka P, Trejtnar F. Honey flavonoids inhibit hOATP2B1 and hOATP1A2 transporters and hOATP-mediated rosuvastatin cell uptake *in vitro*. *Xenobiotica* 2018; 48: 745–755
- [22] Roth M, Timmermann BN, Hagenbuch B. Interactions of green tea catechins with organic anion-transporting polypeptides. *Drug Metab Dispos* 2011; 39: 920–926
- [23] Schäfer AM, Potterat O, Seibert I, Fertig O, Meyer zu Schwabedissen HE. Hyperforin-induced activation of the pregnane X receptor is influenced by the organic anion-transporting polypeptide 2B1. *Mol Pharmacol* 2019; 95: 313–323
- [24] Akhondzadeh S, Naghavi HR, Vazirian M, Shayeganpour A, Rashidi H, Khani M. Passionflower in the treatment of generalized anxiety: a pilot double-blind randomized controlled trial with oxazepam. *J Clin Pharm Ther* 2001; 26: 363–367
- [25] Lolli LF, Sato CM, Romanini CV, Villas-Boas Lde B, Santos CA, de Oliveira RM. Possible involvement of GABA A-benzodiazepine receptor in the anxiolytic-like effect induced by *Passiflora actinia* extracts in mice. *J Ethnopharmacol* 2007; 111: 308–314
- [26] Grundmann O, Wang J, McGregor GP, Butterweck V. Anxiolytic activity of a phytochemically characterized *Passiflora incarnata* extract is mediated via the GABAergic system. *Planta Med* 2008; 74: 1769–1773

- [27] Appel K, Rose T, Fiebich B, Kammler T, Hoffmann C, Weiss G. Modulation of the gamma-aminobutyric acid (GABA) system by *Passiflora incarnata* L. *Phytother Res* 2011; 25: 838–843
- [28] Li R, Wang X, Qin T, Qu R, Ma S. Apigenin ameliorates chronic mild stress-induced depressive behavior by inhibiting interleukin-1beta production and NLRP3 inflammasome activation in the rat brain. *Behav Brain Res* 2016; 296: 318–325
- [29] Liu Y, Lan N, Ren J, Wu Y, Wang ST, Huang XF, Yu Y. Orientin improves depression-like behavior and BDNF in chronic stressed mice. *Mol Nutr Food Res* 2015; 59: 1130–1142
- [30] Mandery K, Bujok K, Schmidt I, Keiser M, Siegmund W, Balk B, König J, Fromm MF, Glaeser H. Influence of the flavonoids apigenin, kaempferol, and quercetin on the function of organic anion transporting polypeptides 1A2 and 2B1. *Biochem Pharmacol* 2010; 80: 1746–1753
- [31] Houghton PJ. The scientific basis for the reputed activity of Valerian. *J Pharm Pharmacol* 1999; 51: 505–512
- [32] Murphy K, Kubin ZJ, Shepherd JN, Ettinger RH. *Valeriana officinalis* root extracts have potent anxiolytic effects in laboratory rats. *Phytomedicine* 2010; 17: 674–678
- [33] Trauner G, Khom S, Baburin I, Benedek B, Hering S, Kopp B. Modulation of GABAA receptors by valerian extracts is related to the content of valerenic acid. *Planta Med* 2008; 74: 19–24
- [34] Harper JN, Wright SH. Multiple mechanisms of ligand interaction with the human organic cation transporter, OCT2. *Am J Physiol Renal Physiol* 2013; 304: F56–F67
- [35] Koenen A, Kock K, Keiser M, Siegmund W, Kroemer HK, Grube M. Steroid hormones specifically modify the activity of organic anion transporting polypeptides. *Eur J Pharm Sci* 2012; 47: 774–780
- [36] Grube M, Kock K, Karner S, Reuther S, Ritter CA, Jedlitschky G, Kroemer HK. Modification of OATP2B1-mediated transport by steroid hormones. *Mol Pharmacol* 2006; 70: 1735–1741
- [37] Gazola AC, Costa GM, Zucolotto SM, Castellanos L, Ramos FA, de Lima TCM, Schenkel EP. The sedative activity of flavonoids from *Passiflora quadrangularis* is mediated through the GABAergic pathway. *Biomed Pharmacother* 2018; 100: 388–393
- [38] Gadioli IL, da Cunha MSB, de Carvalho MVO, Costa AM, Pineli LLO. A systematic review on phenolic compounds in *Passiflora* plants: Exploring biodiversity for food, nutrition, and popular medicine. *Crit Rev Food Sci Nutr* 2018; 58: 785–807
- [39] van Praag H, Lucero MJ, Yeo GW, Stecker K, Heivand N, Zhao C, Yip E, Afanador M, Schroeter H, Hammerstone J, Gage FH. Plant-derived flavanol (–)epicatechin enhances angiogenesis and retention of spatial memory in mice. *J Neurosci* 2007; 27: 5869–5878
- [40] Angelino D, Berhow M, Ninfali P, Jeffery EH. Caecal absorption of vitexin-2-O-xyloside and its aglycone apigenin, in the rat. *Food Funct* 2013; 4: 1339–1345
- [41] Reddy DS. Neurosteroids: endogenous role in the human brain and therapeutic potentials. *Prog Brain Res* 2010; 186: 113–137
- [42] Giatti S, Diviccaro S, Serafini MM, Caruso D, Garcia-Segura LM, Viviani B, Melcangi RC. Sex differences in steroid levels and steroidogenesis in the nervous system: Physiopathological role. *Front Neuroendocrinol* 2020; 56: 100804
- [43] Koenen A, Kroemer HK, Grube M, Meyer zu Schwabedissen HE. Current understanding of hepatic and intestinal OATP-mediated drug-drug interactions. *Expert Rev Clin Pharmacol* 2011; 4: 729–742
- [44] Glaeser H, Bailey DG, Dresser GK, Gregor JC, Schwarz UI, McGrath JS, Jolicoeur E, Lee W, Leake BF, Tirona RG, Kim RB. Intestinal drug transporter expression and the impact of grapefruit juice in humans. *Clin Pharmacol Ther* 2007; 81: 362–370
- [45] Drozdik M, Groer C, Penski J, Lapczuk J, Ostrowski M, Lai Y, Prasad B, Unadkat JD, Siegmund W, Oswald S. Protein abundance of clinically relevant multidrug transporters along the entire length of the human intestine. *Mol Pharm* 2014; 11: 3547–3555
- [46] Neuhaus W, Trauner G, Gruber D, Oelzant S, Klepal W, Kopp B, Noe CR. Transport of a GABAA receptor modulator and its derivatives from *Valeriana officinalis* L. s. l. across an *in vitro* cell culture model of the blood-brain barrier. *Planta Med* 2008; 74: 1338–1344
- [47] Hubeny A, Keiser M, Oswald S, Jedlitschky G, Kroemer HK, Siegmund W, Grube M. Expression of organic anion transporting polypeptide 1A2 in red blood cells and its potential impact on antimalarial therapy. *Drug Metab Dispos* 2016; 44: 1562–1568



## Chapter 4

### **Hyperforin-Induced Activation of the Pregnane X Receptor Is Influenced by the Organic Anion-Transporting Polypeptide 2B1**

Schäfer AM<sup>1</sup>, Potterat O<sup>2</sup>, Seibert I<sup>1</sup>, Fertig O<sup>2</sup>, Meyer zu Schwabedissen HE<sup>1</sup>

#### *Laboratories of Origin:*

<sup>1</sup>Biopharmacy, Department of Pharmaceutical Sciences, University of Basel, 4056 Basel, Switzerland

<sup>2</sup>Pharmaceutical Biology, Department of Pharmaceutical Sciences, University of Basel, 4056 Basel, Switzerland

#### *Contribution of Anima Schäfer:*

Study design, acquisition, analysis and interpretation of data, drafting of manuscript

#### *Journal:*

Molecular Pharmacology (2019) 95, 313-323



# Hyperforin-Induced Activation of the Pregnane X Receptor Is Influenced by the Organic Anion-Transporting Polypeptide 2B1

Anima M. Schäfer, Olivier Potterat, Isabell Seibert, Orlando Fertig, and Henriette E. Meyer zu Schwabedissen

Laboratories of origin: Biopharmacy (A.M.S., I.S., H.E.M.z.S.) and Pharmaceutical Biology (O.P., O.F.), Department Pharmaceutical Sciences, University of Basel, Basel, Switzerland

Received August 21, 2018; accepted December 17, 2018

## ABSTRACT

The herbal remedy St. John's wort (SJW) is used in the treatment of mild depressive symptoms and is known for its drug-drug interaction potential when enhanced expression of CYP3A4 modifies clearance of concomitantly applied substrate drugs. Hyperforin is one constituent of SJW that alters CYP3A4 expression by activation of the nuclear receptor pregnane X receptor (PXR). However, little is known about the transmembrane transport of hyperforin. One membrane protein that modulates cellular entry of drugs is the organic anion-transporting polypeptide (OATP) 2B1. It was the aim of this study to test whether hyperforin interacts with this transport protein. Transport inhibition studies and competitive counterflow experiments suggested that hyperforin is a substrate of OATP2B1. This notion was validated by showing that the presence of OATP2B1 enhanced the hyperforin-induced PXR

activation in cell-based luciferase assays. Moreover, in Caco-2 cells transcellular transport of the known OATP2B1 substrate atorvastatin was changed in the presence of hyperforin, resulting in an increased efflux ratio. Eleven commercially available SJW formulations were assessed for their influence on OATP2B1-mediated transport of estrone 3-sulfate and for their impact on CYP3A4 promoter transactivation. The correlation between effect size and the hyperforin content as determined by high-performance liquid chromatography with ultraviolet detection suggested that hyperforin is the major determinant. Our results indicate an interaction between hyperforin and OATP2B1, which is not only known to contribute to hepatocellular uptake but also to intestinal absorption of its substrates. These findings extend the complexity of mechanisms that should be considered when evaluating the interaction potential of SJW preparations.

## Introduction

St. John's wort is an herbal extract of *Hypericum perforatum* and is commonly taken to treat depressive symptoms. The extract is a complex mixture of structurally diverse constituents, including flavonol glycosides, phloroglucinols, proanthocyanidins, naphthodianthrones, and phenylpropanoids (Nahrstedt and Butterweck, 1997). The naphthodianthrones pseudohypericin and hypericin were originally assumed to be the active components of *Hypericum* extracts (Suzuki et al., 1984). Accordingly, hypericin became the constituent on which therapeutically used extracts are standardized. However, even though the antidepressive activity is still not fully understood, more recent studies suggest that it is most probably linked to the phloroglucinol hyperforin. (Mennini and Gobbi, 2004).

Beside its antidepressant activity, St. John's wort is known for its pronounced influence on expression and activity of genes involved in drug metabolism (Soleymani et al., 2017). Indeed, hyperforin enhances expression and activity of

CYP3A4, thereby modifying the first-pass metabolism and clearance of concomitantly applied substrates (Wang et al., 2013). Similar results were shown for the efflux transporter P-glycoprotein (P-gp, ABCB1, MDR1), when treatment with St. John's wort extracts increased intestinal ABCB1 expression, explaining the reduced bioavailability of ABCB1 substrates (Dürr et al., 2000). The underlying mechanism is the activation of the pregnane X receptor (PXR) (Kliwer et al., 2002). PXR is a nuclear receptor functioning as ligand-activated transcription factor of a gene network comprising various proteins involved in drug metabolism, including CYP3A4 (Lehmann et al., 1998), the efflux transporter P-gp (Geick et al., 2001), the multidrug-resistance protein 3 (ABCC3, MRP3) (Aleksunes and Klaassen, 2012), the organic anion-transporting polypeptide (OATP) 1A2 (Meyer zu Schwabedissen et al., 2008), the UDP-glucuronosyltransferase 1a5 (Ugt1a5), and the sulfotransferase 2a2 (Sult2a2) (Aleksunes and Klaassen, 2012). Accordingly, PXR activation in general results in enhanced metabolic activity and increased metabolic clearance. Hyperforin, even if very potent, is not the only activator of PXR, since multiple drugs in clinical use function as activating ligands (Meyer zu Schwabedissen and Kim, 2009). Accordingly, PXR is also called a xenosensor as it senses drug exposure and modulates metabolic activity in response. There are multiple examples

This work was conducted without support by external funding agencies. None of the authors has a conflict of interest to declare.  
<https://doi.org/10.1124/mol.118.114066>.

 This article has supplemental material available at [molpharm.aspetjournals.org](http://molpharm.aspetjournals.org).

**ABBREVIATIONS:** BSP, bromosulfophthalein; CCF, competitive counterflow; E<sub>1</sub>S, estrone 3-sulfate; HPLC, high-performance liquid chromatography; MDCKII cells, Madin-Darby canine kidney epithelial cells; MRP, multidrug resistance-associated protein; OATP, organic anion-transporting polypeptide; PBS, phosphate-buffered saline; PXR, pregnane X receptor; SJW, St. John's wort.

in the literature in which PXR activation is the basis of observed drug-drug interactions, e.g., simultaneous administration of indinavir and St. John's wort reduces exposure of the protease inhibitor (Piscitelli et al., 2000). Additionally, Ruschitzka et al. (2000) reported heart transplant rejections in patients concomitantly treated with cyclosporine and St. John's wort. The authors report reduced oral bioavailability and increased hepatic clearance of the victim drug. Importantly, to interact with PXR and to activate transcription of the targeted genes, hyperforin has to enter the cell. So far, little is known about the transmembrane transport and cellular uptake of this molecule.

Recent findings by our group suggest that hyperforin is a substrate of OATP2B1, as was observed by testing whether the method of competitive counterflow (CCF) can be applied to identify substrates of this uptake transporter (Schäfer et al., 2018). OATP2B1 is a member of the organic anion-transporting polypeptide family, and facilitates the sodium-independent uptake of its substrates. Since its first description (Tamai et al., 2000) multiple endogenous and exogenous substrates of the transporter have been identified (Roth et al., 2012). OATP2B1 exhibits two substrate binding sites that can be distinguished in experimental setting by their contribution to the cellular uptake of estrone 3-sulfate ( $E_1S$ ); one accepts  $E_1S$  at low concentration (binding site A), whereas the other (binding site B) mainly drives uptake at high concentrations of the sulfated steroid (Shirasaka et al., 2012). Another characteristic of OATP2B1 is its ubiquitous expression, with high amounts of the transporter in brain, heart, kidney, lung, mammary gland, placenta, platelets, skeletal muscle and skin (St-Pierre et al., 2002; Pizzagalli et al., 2003; Schiffer et al., 2003; Bronger et al., 2005; Grube et al., 2006; Niessen et al., 2009; Knauer et al., 2010; Sakamoto et al., 2013; Ferreira et al., 2018). Considering the abovementioned impact of PXR on hepatic clearance and oral bioavailability, it seems noteworthy that OATP2B1 is expressed in the sinusoidal membrane of hepatocytes (Kullak-Ublick et al., 2001) and in the intestine (Kobayashi et al., 2003; Keiser et al., 2017), thereby contributing to hepatic clearance and intestinal absorption, respectively. Even if several drug transporters are part of the PXR-regulated gene network, OATP2B1 is not (Knauer et al., 2013; Meyer zu Schwabedissen et al., 2018). However, our preliminary findings (Schäfer et al., 2018) suggest that drug-drug interactions involving hyperforin may not be limited to targets of PXR but may also involve OATP2B1-mediated uptake. It was the aim of the present study to further evaluate this notion.

## Materials and Methods

**Cell Culture.** All cell lines were maintained at 37°C in a humidified atmosphere with 5% CO<sub>2</sub>. The cell lines Madin-Darby canine kidney epithelial cells (MDCKII; ATCC no. CRL-2936), HeLa (ATCC no. CCL2), HepG2 (ATCC no. HB-8065), and Caco-2 (ATCC no. HTB37) were originally obtained from the American Type Culture Collection (ATCC, Wesel, Germany) and were cultured in Dulbecco's modified Eagle's medium (DMEM; Sigma-Aldrich, Buchs, Switzerland) supplemented with 10% fetal calf serum (Sigma-Aldrich) and 1% stable glutamine (BioConcept, Basel, Switzerland). For Caco-2 cells the medium was supplemented with 1% penicillin/streptomycin (BioConcept, Basel, Switzerland). MDCKII-OATP2B1 cells have been established and characterized as described elsewhere (Grube et al., 2006) and were kept under continuous selection with 750 µg/ml hygromycin B (Carl Roth, Karlsruhe, Germany).

**Transport Experiments.** MDCKII-OATP2B1 cells were seeded in 24-well plates at a density of 50,000 cells/well (Eppendorf, Hamburg, Germany). After 1 day in culture, cells were treated with sodium butyrate (2 mM) and cultured for an additional day. Uptake experiments were started by washing the cells with prewarmed phosphate-buffered saline (PBS) followed by a 10-minute equilibration with Hanks' balanced salt solution (H8264, with sodium bicarbonate, without phenol red, pH 7.4; Sigma-Aldrich). To test the inhibitory potency of hyperforin (as hyperforin dicyclohexylammonium salt; Sigma-Aldrich) and hypericin (Tocris, Bio-Techne AG, Zug, Switzerland) cells were exposed to either estrone 3-sulfate (0.005 or 50 µM; Sigma-Aldrich) or 0.1 µM bromosulphophthalein (BSP; Sigma-Aldrich), supplemented with 50,000 dpm/well of [<sup>3</sup>H]- $E_1S$  (3 nM; Hartmann Analytic, Braunschweig, Germany), or [<sup>3</sup>H]-BSP (9 nM; Hartmann Analytic) in the presence of different concentrations of the respective compound. After 5 minutes of exposure the cells were washed with ice-cold PBS, lysed in 200 µl of 0.2% SDS-5 mM EDTA, and the cellular content of  $E_1S$  or BSP was quantified determining the amount of tracer by liquid scintillation counting using the Rotiszint eco Plus (Carl Roth) and the Tri-Carb 2900TR counter (TopLab, Basel, Switzerland). An aliquot was used to assess the amount of protein in each well using the Pierce BCA Protein Assay Kit (Thermo Fisher Scientific, Reinach, Switzerland) and the microplate reader Infinite 200 Pro (Tecan, Männedorf, Switzerland). CCF experiments were performed as previously described by our group (Schäfer et al., 2018). MDCKII-OATP2B1 and MDCKII cells were seeded, treated, and prepared for transport experiments as described above. Since CCF experiments are conducted in the steady state, cells were preincubated with [<sup>3</sup>H]- $E_1S$  (100,000 dpm/well) for 30 minutes. For a time-dependent CCF experiment in MDCKII-OATP2B1 cells, the supernatant was exchanged to either [<sup>3</sup>H]- $E_1S$  alone or supplemented with hyperforin (5 µM) or hypericin (100 µM). Cellular accumulation of [<sup>3</sup>H]- $E_1S$  was measured as described above after 10, 20, 30, 45, 60, 90, 120, and 180 seconds. Since the system was equilibrated again after 90 seconds, this was defined as the time point when intracellular accumulation of [<sup>3</sup>H]- $E_1S$  was measured in CCF experiments. MDCKII-OATP2B1 and MDCKII cells were treated with [<sup>3</sup>H]- $E_1S$  until steady state before medium was changed to the same concentration of [<sup>3</sup>H]- $E_1S$  supplemented with hyperforin, hypericin, atorvastatin (2.5 µM; Sigma-Aldrich) as positive, and penicillin G (250 µM; Sigma-Aldrich) as negative control. For inhibition studies, 2.5 µM atorvastatin supplemented with 50,000 dpm/well [<sup>3</sup>H]-atorvastatin (7.5 nM; PerkinElmer, Waltham, MA) was used. Cellular accumulation after 5 minutes of exposure was assessed in presence of different concentrations of hyperforin (0.1, 1, 5 µM) or hypericin (10, 50, 100 µM).

**Cell-Based Reporter Gene Assays.** The previously reported CYP3A4-XREM-pGL3 plasmid was used to test the influence of OATP2B1 on PXR-mediated transactivation. Briefly, HepG2 and HeLa cells were seeded in 24-well plates at a density of 50,000 cells/well. The cells were then transfected with 250 ng of CYP3A4-XREM-pGL3 (Tirona et al., 2003), 25 ng of pRL-TK, 250 ng of PXR-pEF6 (Meyer zu Schwabedissen et al., 2008), 250 ng of RXR $\alpha$ -pEF6, 250 ng of OATP2B1-pEF6, or 250 ng of pEF6-V5/HIS as control (Thermo Fisher Scientific), using 2.25 µl/µg of DNA jetPRIME (Polyplus distributed by Chemie Brunschwig, Basel, Switzerland). After 4 hours, the medium was changed, and the cells were kept in culture until treatment started 24 hours after transfection. Hyperforin, hypericin, bromosulphophthalein, and rifampicin were used at a final concentration of 0.1, 1, 10, and 10 µM, respectively. The formulations were tested at a 1/100 dilution of one tablet or capsule dissolved in 200 ml. To avoid phototoxicity the experiment was performed in the dark. Finally, the cells were lysed after 24 hours of exposure and luciferase activity was determined using the Dual-Luciferase Assay System (Promega, Dübendorf, Switzerland) and the plate reader Infinite M200 Pro (Tecan) as recommended by the manufacturer. The observed activity of the firefly luciferase was normalized to that of the *Renilla*.

**Transwell Transport of Hyperforin and Hypericin.** Experiments were performed as previously described (Meyer zu Schwabedissen et al., 2018). Briefly, Caco-2 cells were seeded at a density of  $3 \times 10^5$  cells/well onto polycarbonate membranes with 0.4- $\mu\text{m}$  pore size inserted in 12-well plates (Chemie Brunschwig, Basel, Switzerland) and cultivated for 14 days with medium change every second day. Measuring the trans-epithelial electrical resistance value of at least 200  $\Omega/\text{cm}$  1 day before the experiment confirmed the integrity of the monolayer. Furthermore, integrity was tested after the experiment by addition of 1 mg/ml Lucifer yellow (Sigma-Aldrich) to the apical side and measurement of absorbance in the basolateral compartment after 1 hour by spectrofluorometry. On the day of the experiment, cells were washed once with prewarmed PBS before incubation with Krebs-Henseleit buffer (118 mM NaCl, 25 mM NaHCO<sub>3</sub>, 1.2 mM KH<sub>2</sub>PO<sub>4</sub>, 2.5 mM CaCl<sub>2</sub>, 1.2 mM MgSO<sub>4</sub>, 11 mM glucose, 4.7 mM KCl) for 20 minutes at 37°C. The buffer was adjusted to a pH of 5.5 in the apical compartment and to a pH of 7.4 in the basolateral compartment. [<sup>3</sup>H]-Atorvastatin (100,000 dpm/well) was added either to the apical or to the basolateral side to determine apical to basal (a–b) or basal to apical (b–a) permeability. Hyperforin (0.1  $\mu\text{M}$ ) was added to either the apical or the basal compartment. Amount of atorvastatin was assessed in 100- $\mu\text{l}$  aliquots by scintillation counting as described above. The amount of transported [<sup>3</sup>H]-atorvastatin per time was calculated as permeability coefficient ( $P_{app}$ ) as previously described (Hubatsch et al., 2007).  $P_{app}$  of the apical (a)-to-basal (b) or of the b-to-a direction was used to calculate the uptake and efflux ratio, respectively, with the following equations:

$$\text{uptake ratio } P_{a-b} = \frac{P_{app}(a \text{ to } b)}{P_{app}(b \text{ to } a)} \quad \text{efflux ratio } P_{b-a} = \frac{P_{app}(b \text{ to } a)}{P_{app}(a \text{ to } b)}$$

**Transport Studies with 11 Swiss Formulations Containing St. John's Wort.** Before transport experiments, pills were milled using the mixer mill MM 400 (Retsch GmbH, Haan, Germany) or capsules were opened to release the content. The concentration for inhibition experiments was estimated by calculating the expected concentration in the intestine when the pill or capsule would be ingested with 200 ml water. Two days before the experiment MDCKII-OATP2B1 cells were seeded as described above. After washing the cells with PBS and a 10-minute preincubation in Hanks' balanced salt solution buffer, influence was tested by treating the cells with 0.005  $\mu\text{M}$  E<sub>1</sub>S supplemented with radiolabeled E<sub>1</sub>S (50,000 dpm/well) and the respective formulation diluted 1:100 and 1:1000. After 5 minutes, cells were washed with ice-cold PBS and lysed in 200  $\mu\text{l}$  of 0.2% SDS-5 mM EDTA. Protein amount and intracellular accumulation of [<sup>3</sup>H]-E<sub>1</sub>S was measured as described in detail above.

**Western Blot Analysis.** HepG2 and HeLa cells were seeded at a density of  $1.8 \times 10^6$  cells/10-cm culture dish (Eppendorf). After reaching confluence, cells were harvested in 5 mM Tris-HCl (pH 7.4) supplemented with the protease inhibitor cocktail (Sigma-Aldrich). After several cycles of freezing and thawing, protein content in the cell lysate was quantified using the Pierce BCA Protein Assay Kit (Thermo Fisher Scientific). Proteins were separated by SDS-PAGE (Mini-PROTEAN System) followed by blotting onto a nitrocellulose membrane with the Mini Trans-blot Cell (Bio-Rad Laboratories AG, Cressier, Switzerland). Fetal calf serum (5%)–Tris-buffered saline–0.04% Tween 20 (TBS-T) was used to block unspecific binding before the primary antibody anti-HNF4 $\alpha$  (ab41898; Abcam, Lucerna Chem AG, Luzern, Switzerland, diluted 1:1000) or anti-OATP2B1 [(Grube et al., 2005) diluted 1:5000] was added and incubated at 4°C overnight. Actin (sc-1616, diluted 1:1000; Santa Cruz Biotechnology, Heidelberg, Germany) served as control. HRP-labeled secondary antibodies and the ECL Western blotting substrate (Pierce/Thermo Fisher Scientific) were used to detect binding of the primary antibody. The Chemidoc XRS System (Bio-Rad Laboratories AG) was used for visualization and digitization of chemiluminescence.

**Determination of Hyperforin and Hypericin Content in 11 Swiss Formulations with High-Performance Liquid Chromatography.** One-hundred milligrams of the powdered samples was dissolved in 1 ml of DMSO and centrifuged at 13,000 rpm for 5 minutes before filtration through a disposable syringe filter (Micropur PTFE,

pore-size: 0.45- $\mu\text{m}$ , Altmann Analytik, Munich, Germany). Dissolution of the solid residue of Deprivita, Hyperiplant, Rebalance, Sandoz Hypericum, and Vogel Hyperiforce using the same procedure confirmed >80% and >90% dissolution of hypericin and hyperforin, respectively. Hypericin was TOCRIS brand and had >98% purity according to manufacturer. A calibration curve was prepared with a hypericin dilution ranging from 1 to 0.002 mg/ml. The hypericin calibration curve was also used for the simultaneous quantification of pseudohypericin since both compounds have the same chromophore. The identity of pseudohypericin was confirmed by chromatographic comparison with a reference sample purchased from Sigma-Aldrich. The content of hypericin was calculated as the sum of the content of hypericin and pseudohypericin. Hyperforin was purchased from Sigma-Aldrich as dicyclohexylammonium salt. According to the manufacturer, purity was 98% as a mixture of hyperforin and adhyperforin. Considering that both compounds have the same chromophore and taking into account their respective molecular weights, the commercial sample was determined by high-performance liquid chromatography with UV detection (HPLC-UV) to contain 83.6% hyperforin and 16.4% adhyperforin. Two calibration curves were therefore prepared for hyperforin (0.9–0.007 mg/ml) and adhyperforin (0.18–0.0014 mg/ml) and the content of hyperforin was calculated as the sum of both phloroglucinols. Since hyperforin is highly sensitive to light and oxygen all preparatory steps for measuring hyperforin content were performed under exclusion of light. Prior to grinding and solving of the samples, the respective tubes were pre-filled with nitrogen to avoid oxidation. HPLC analyses were performed on an Alliance 2690 chromatographic system coupled to a PDA996 detector (Waters, Milford, MA). The mobile phase consisted of water (A) and acetonitrile (B) both containing 0.1% trifluoroacetic acid (hyperforin analysis) or 0.5% trifluoroacetic acid (hypericin analysis). Separation of hyperforin was achieved using a 115 Zorbax Eclipse XDB-C8 Narrow-Bore column (2.1  $\times$  150 mm, 3.5  $\mu\text{m}$ ; Agilent, Santa Clara, CA) with a gradient of 50%–100% B in 20 minutes, then 100% B for 15 minutes at a flow rate of 0.4 ml/minute. Hypericin was analyzed on an Ascentis Express C18 column (3  $\times$  100 mm, 2.7  $\mu\text{m}$ ; Supelco, Bellefonte, PA) with a gradient of 45%–100% in 15 minutes, then 100% B for 5 minutes at a flow rate of 0.6 ml/minute. The injection volume was 10  $\mu\text{l}$  for the calibrators and the formulation samples. Detection was at 272 nm (hyperforin) or 588 nm (hypericin). Separations were performed at 30°C. Data are reported as mean  $\pm$  S.D. of three independent analyses.

**Statistical Analysis.** Microsoft Excel (Microsoft, Redmond, USA) and GraphPad Prism software 6.0 (GraphPad Software, La Jolla, CA) was used to analyze the data sets reported herein. Tests used for statistical analysis are described in the context of data presentation. A *P*-value below 0.05 was considered statistically significant.

## Results

**Interaction of Hyperforin and Hypericin with OATP2B1-Mediated Uptake.** To validate the interaction of hyperforin and hypericin with OATP2B1, their impact on the cellular accumulation of the known substrates estrone 3-sulfate (Pizzagalli et al., 2003) and bromosulfophthalein (Kullak-Ublick et al., 2001) was determined in MDCKII-OATP2B1 cells. As shown in Fig. 1 the estrone 3-sulfate inhibition studies accounted for the previously reported two binding sites (Shirasaka et al., 2012) testing the influence of hyperforin and hypericin on estrone 3-sulfate accumulation at low (Fig. 1, A and D; representing binding site A) and at high concentrations (Fig. 1, B and E, representing binding site B). For hyperforin, we observed concentration-dependent inhibition for both binding sites recognizing E<sub>1</sub>S. The inhibition data were the basis for an estimation of the respective IC<sub>50</sub> values, which revealed the highest potency for binding site

A-mediated transport of  $E_1S$ , with an  $IC_{50}$  value of  $0.32 \mu M$  (CI  $0.24$ – $0.42 \mu M$ , Fig. 1A), whereas for binding site B the  $IC_{50}$  value was  $5.55 \mu M$  (CI  $2.10$ – $14.73 \mu M$ , Fig. 1B). Inhibition of OATP2B1-mediated cellular accumulation of BSP resulted in an estimated  $IC_{50}$  value for hyperforin of  $0.82 \mu M$  (CI  $0.53$ – $1.26 \mu M$ , Fig. 1C). Similar results were obtained for hypericin, even if this compound exhibited much lower  $IC_{50}$  values for binding site A ( $20.79 \mu M$ ; CI  $13.90$ – $31.10 \mu M$ , Fig. 1D), binding site B  $256.2 \mu M$  (CI  $119.4$ – $550.0 \mu M$ , Fig. 1E), and for BSP ( $108.7 \mu M$  (CI  $76.39$ – $154.8 \mu M$ , Fig. 1F). To test whether hyperforin and hypericin are also substrates of OATP2B1 we applied the method of competitive counterflow. The basis of the experimental procedure used to identify substrates competing for substrate recognition is depicted in Fig. 1G. Briefly, interaction with the transporter is assessed in the steady state. Reduction of the intracellular estrone 3-sulfate amount in the equilibrium would be attributable to competitive inhibition, showing that the test compound is a substrate of the facilitating mechanism, whereas inhibitors would not influence the cellular equilibrium (Harper and Wright, 2013). As shown in Fig. 1H, presence of the known OATP2B1 substrate atorvastatin, as well as hyperforin ( $5 \mu M$ ) or hypericin ( $100 \mu M$ ), reduced the amount of  $E_1S$  in the steady state ( $P < 0.05$ ), thereby suggesting that both constituents of St. John's wort are not only inhibitors but also substrates of OATP2B1. Penicillin G served as nonsubstrate control (Schäfer et al., 2018). In the CCF experiments in MDCKII cells, no influence on the cellular amount of  $E_1S$  was observed for any of the compounds tested herein (Supplemental Fig. 1). Assessing the time-dependency of reaching the second equilibrium for hyperforin (Supplemental Fig. 2A) and hypericin (Supplemental Fig. 2B) revealed that it is reached after 90 seconds of exposure, which is comparable to that previously reported (Schäfer et al., 2018).

**Influence of OATP2B1 on Hyperforin-Mediated Transactivation of CYP3A4.** Hyperforin is a well known ligand and activator of the human pregnane X receptor, which thereby influences transcription of CYP3A4 (Moore et al., 2000). To verify that hyperforin is a substrate of OATP2B1, we deployed cell-based reporter gene assays to assess the transactivation of a synthetic CYP3A4-XREM-pGL3 reporter gene construct. As shown in Fig. 2A, HepG2-cells transfected with PXR- and OATP2B1-pEF6 exhibited higher luciferase activation ( $P < 0.05$ ) than cells not heterologously expressing the transporter. Testing the influence of  $10 \mu M$  BSP on hyperforin-induced ( $0.1 \mu M$ ) PXR-mediated transactivation of CYP3A4 in OATP2B1-overexpressing cells showed that presence of this competitive inhibitor of the transporter reduced luciferase activity statistically significantly. Importantly, BSP did not influence the luciferase activity (Fig. 2B).

**Impact of Hyperforin and Hypericin on Transcellular Fluxes in Caco-2 Cells.** Expression of OATP2B1 is assumed to contribute to intestinal absorption of orally applied drugs. Transcellular flux experiments using the intestinal model cell line Caco-2 cells are often applied in the preclinical phase to not only predict bioavailability but also to determine whether there is an active transport component influencing the transcellular path of a new molecular entity. OATP2B1 is expressed in Caco-2 cells and is part of the network of transporters influencing the transcellular flux (Meyer zu Schwabedissen et al., 2018). To determine whether hyperforin influences transcellular fluxes, and thereby oral

bioavailability, experiments were performed using the known OATP2B1 substrate drug atorvastatin (Grube et al., 2006). At first, interaction of hyperforin with OATP2B1-mediated atorvastatin uptake was tested (Fig. 3A), revealing a decreased amount of intracellular atorvastatin with increasing concentrations ( $P < 0.05$ ). As controls, BSP and  $E_1S$  were included in the transport inhibition study. Estimation of the inhibitory potency, even though a limited number of data points was used as a basis, suggested an  $IC_{50}$  value for hyperforin of  $0.23 \mu M$  (CI  $0.11$ – $0.48 \mu M$ ). As shown in Fig. 3B, hyperforin increased the efflux ratio observed for atorvastatin (mean efflux ratio  $\pm$  S.D.; hyperforin vs. DMSO;  $2.863 \pm 0.415$  vs.  $1.828 \pm 0.332$ ;  $P = 0.028$ ). The observed effect can mainly be attributed to changes in the flux from apical (a) to basal (b), as there was a trend toward lower movement in this direction [mean  $P_{app}$  (a–b)  $\pm$  S.D. (cm/s); hyperforin vs. DMSO;  $1.33 \times 10^{-6} \pm 3.161 \times 10^{-7}$  vs.  $1.83 \times 10^{-6} \pm 2.621 \times 10^{-7}$ ;  $P = 0.103$ , Fig. 3C]. No trend for a change was observed for the atorvastatin flux in b to a direction [mean  $P_{app}$  (b–a)  $\pm$  S.D. (cm/s); hyperforin vs. DMSO  $3.81 \times 10^{-6} \pm 1.153 \times 10^{-6}$  vs.  $3.36 \times 10^{-6} \pm 8.502 \times 10^{-7}$ ;  $P = 0.615$ , Fig. 3D]. Taken together these data suggest that hyperforin interacts with intestinal absorption of atorvastatin, which is in part mediated by OATP2B1.

**Effect of St. John's Wort Formulations on OATP2B1-Mediated Transport.** St. John's wort is widely used as medication to treat mild to moderate depression. In Switzerland there are currently 11 solid formulations marketed. These formulations contain different amounts of hypericin and hyperforin as reported by the manufacturer and summarized in Table 1. In a screening experiment, we tested for interaction of the formulations with OATP2B1-mediated  $E_1S$  uptake in MDCKII-OATP2B1 cells. This screening was conducted using two concentrations of the respective formulation, representing a 1/100 or 1/1000 dilution of one tablet or capsule dissolved in 200 ml of liquid. As shown in Fig. 4A, none of the 1/1000 dilutions lowered the cellular accumulation of  $E_1S$  compared with solvent control ( $P > 0.05$ ). However, for the formulations Arkocaps, Deprivita, Hänseler Menopause, Hyperiplant, Jarsin, Sandoz Hypericum, and Solevita, we observed reduced OATP2B1-mediated uptake of estrone 3-sulfate for the 1/100 dilution ( $P < 0.05$ ). Rebalance, Remotiv, Vogel Hyperimed, and Vogel Hyperiforce did not affect OATP2B1-mediated  $E_1S$  uptake in our experiments.

Subsequently, we assessed the influence of the respective formulation on the PXR-mediated transactivation of CYP3A4 either in HepG2 (Fig. 4B), or HeLa (Fig. 4C). Notably, in accordance with our transport inhibition experiments, Rebalance, Remotiv, Vogel Hyperimed, and Vogel Hyperiforce did not affect luciferase activation in either cell-based reporter gene assay ( $P > 0.05$ ). Interestingly, treatment of HepG2 cells resulted in an up to 125-fold induction in presence of a 1/100 dilution of the formulations, whereas a maximum of about 7-fold induction was observed in HeLa cells. This might be explained by the endogenous expression of HNF4 $\alpha$ , which is permissive for the transactivation of CYP3A4 by PXR (Tirona et al., 2003). The lack of HNF4 $\alpha$  expression in HeLa cells was verified by Western blot analysis (Fig. 4D; mean HNF4 $\alpha$  expression normalized to actin  $\pm$  S.D.; HepG2 vs. HeLa;  $17.88 \pm 3.43$  vs.  $0.26 \pm 0.02$ ;  $P < 0.05$ ,  $n = 3$ , unpaired  $t$  test with Welch's correction), whereas no difference in expression of OATP2B1 was observed (Fig. 4E; mean OATP2B1 expression

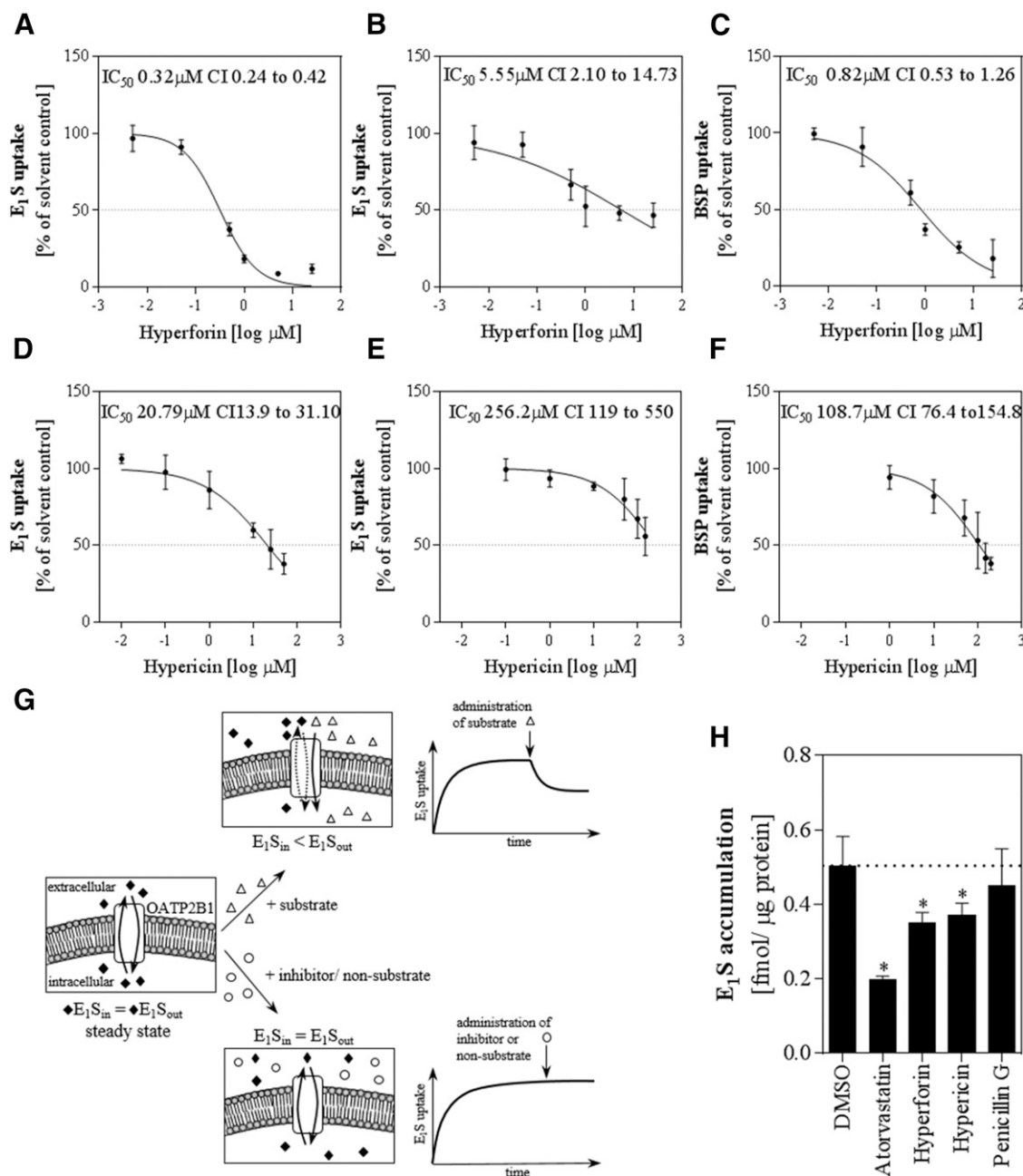


**Fig. 1.** Interaction of hyperforin and hypericin with OATP2B1. Inhibition of OATP2B1-mediated transport by hyperforin and hypericin was tested in MDCKII-OATP2B1 cells. The influence on cellular accumulation of estrone 3-sulfate was determined at low (0.005  $\mu$ M; A and D) or high (50  $\mu$ M; B and E) concentration to account for binding site A or B, respectively, or of bromosulphthalein (C and F). The  $IC_{50}$  values were calculated fitting the data to a sigmoidal log(inhibitor)-normalized response curve, without constraining of top or bottom, or weighting. (G) Schematic of the molecular basis of competitive-counterflow experiments, in which substrates are reduced by the amount of another substrate in the steady state. Tested was the influence of hyperforin or hypericin on the cellular equilibrium of  $E_1S$  in MDCKII-OATP2B1 cells compared with DMSO control (H). Atorvastatin and penicillin G were used as positive and negative controls, respectively. Data are presented as mean  $\pm$  S.D. of  $n = 3$  independent experiments, each performed in biologic triplicates. \* $P \leq 0.05$ , one-way analysis of variance with Dunnett's multiple comparisons test.

normalized to actin  $\pm$  S.D.; HepG2 vs. HeLa;  $1.52 \pm 1.28$  vs.  $1.41 \pm 0.72$ ;  $P > 0.05$ ,  $n = 3$ , unpaired  $t$  test with Welch's correction).

**Quantification of Hyperforin and Hypericin Content in the St. John's Wort Formulations.** As mentioned before, most manufacturers merely provide information on the content of hypericin in their formulation owing to the primal assumption that this component determines biologic activity of the extract. We quantified the amount of hyperforin

(as the sum of hyperforin and adhyperforin) and hypericin (as the sum of hypericin and pseudohypericin) in each formulation by HPLC. As summarized in Table 1 and depicted in Supplemental Figs. 3 and 4, all formulations contained hypericin, but hyperforin was detected in all medications but Vogel Hyperimed and Vogel Hyperiforce and to a low extent in Rebalance and Remotiv. Importantly, these four medications neither interacted with OATP2B1-mediated  $E_1S$  accumulation nor did they transactivate CYP3A4 in the cell-based

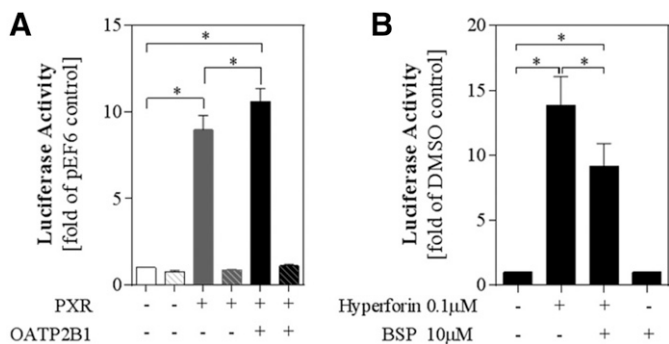


**Fig. 2.** Influence of OATP2B1 on hyperforin-induced PXR-mediated transactivation of CYP3A4. Luciferase activation was determined in HepG2 cells transfected with PXR-pEF6 in presence or absence of heterologously expressed OATP2B1 and treated with 0.1 μM hyperforin or DMSO (striped bars) (A). The influence of bromosulfophthalein on hyperforin-induced PXR activation was assessed in HepG2 cells transiently transfected with PXR-pEF6 and OATP2B1-pEF6 (B). Firefly luciferase activity was normalized to that of *Renilla*. Data are presented as mean ± S.D. of  $n = 3$  independent experiments each performed in biologic triplicates. \* $P$ -value ≤ 0.05, two-way analysis of variance with Tukey's multiple comparisons test.

reporter gene assays reported herein, suggesting that hyperforin is the key determinant of the observed effects. To test this notion, we analyzed whether the relationship between hyperforin content and the observed luciferase activation assessed in transfected HepG2 (Fig. 5A) or HeLa cells (Fig. 5B) revealed a

direct correlation. The association as determined by Pearson correlation was most pronounced when Hyperplant, the formulation containing the highest amount of hyperforin, was excluded. An indirect and statistically significant correlation was observed for the percentage of  $E_1S$  uptake and hyperforin content in MDCKII-OATP2B1 cells (Fig. 5C). Importantly, no correlation was observed for hypericin and the experimental results (Fig. 5, D–F).

## Discussion

In this study we report that the constituents of St. John's wort—hyperforin and to a lower extent hypericin—are inhibitors of the ubiquitously expressed membrane transporter OATP2B1. Furthermore, CCF experiments suggested that the compounds are not only inhibitors but also substrates of OATP2B1. This was further supported by findings in reporter gene assays, in which OATP2B1 enhanced hyperforin-induced transactivation of CYP3A4, which was reduced in the presence of the competitive inhibitor bromosulfophthalein.

Hyperforin is known especially as a major determinant of drug-drug interactions observed during coadministration of St. John's wort, with the expected result of a pronounced increase in CYP3A4 activity (Willson and Kliewer, 2002). However, the influence of concomitant use of St. John's wort is not limited to CYP3A4-substrates as the underlying mechanism; it is the binding and activation of PXR that finally

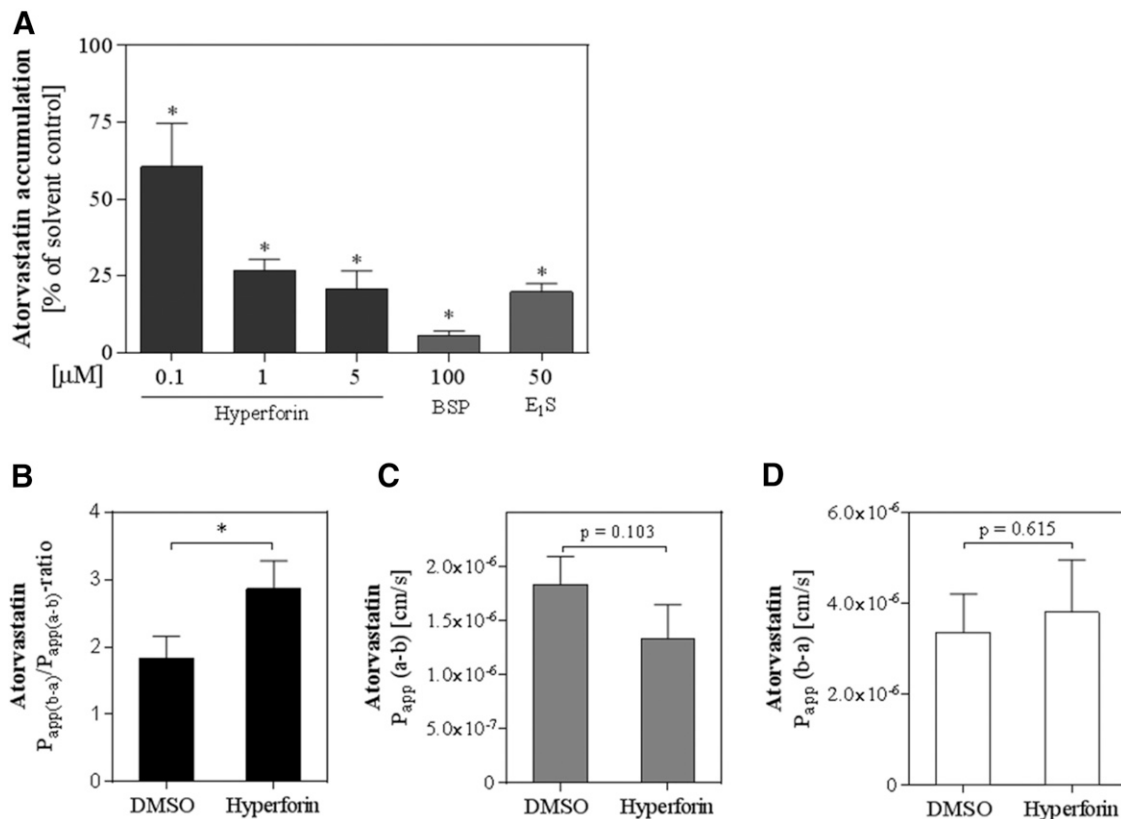


**Fig. 3.** Interaction of hyperforin with OATP2B1-mediated transport of atorvastatin. The inhibitory effect of hyperforin on atorvastatin transport was determined in MDCKII-OATP2B1 cells, bromosulfophthalein, and estrone 3-sulfate served as control (A). The influence on transcellular fluxes was assessed on permeable supports using cultured Caco-2 cells. The unidirectional  $P_{app}$ -coefficients in (C) apical (a)-to-basal (b), or (D) b-to-a directions for atorvastatin were used to calculate (B) the efflux ratio [ $P_{app}(b-a)/P_{app}(a-b)$ ]. Data are presented as mean ± S.D. of  $n = 3$  independent experiments each performed in biologic triplicates, \* $P$  ≤ 0.05 one-way analysis of variance with Dunnett's multiple comparisons test (A) or Student's  $t$  test (B, C, D).

TABLE 1

Content of hypericin and hyperforin determined by HPLC-UV

Percentage of hypericin or hyperforin content given in the compendium was converted to content per 100 mg extract. For quantification by HPLC, a standard curve was used to calculate the concentration of hypericin or hyperforin, respectively. Data from quantification are from three independent experiments.

Formulation (Tradename)	Hypericin <sup>a</sup> (Declared Content)	Hypericin <sup>a</sup> (Quantified by HPLC)		Hyperforin <sup>b</sup> (Declared Content)	Hyperforin <sup>b</sup> (Quantified by HPLC)	
	mg/100 mg	mg/100 mg	± S.D.	mg/100 mg	mg/100 mg	± S.D.
ARKOCAPS <sup>c</sup>	0.3	0.09	± 0.04	—	0.24	± 0.01
DEPRIVITA <sup>d</sup>	0.1–0.3	0.18	± 0.01	—	1.04	± 0.05
HAENSELER MENOPAUSE <sup>e</sup>	0.1–0.3	0.10	± 0.01	—	0.34	± 0.01
HYPERIPLANT <sup>f</sup>	0.1–0.3	0.15	± 0.02	36	1.62	± 0.03
JARSIN <sup>g</sup>	0.1–0.3	0.20	± 0.02	—	0.70	± 0.02
REBALANCE <sup>h</sup>	0.1–0.3	0.08	± 0.01	<0.2	0.02	± 0.01
REMOTIV <sup>h</sup>	0.1–0.3	0.09	± 0.01	<0.2	0.02	± 0.01
SANDOZ HYPERICUM <sup>i</sup>	0.1–0.3	0.21	± 0.02	—	0.85	± 0.04
SOLEVITA <sup>d</sup>	0.1–0.3	0.16	± 0.03	—	1.02	± 0.07
VOGEL HYPERIMED <sup>j</sup>	0.5–0.8	0.08	± 0.01	—	—	—
VOGEL HYPERIFORCE <sup>j</sup>	0.2–2.1	0.08	± 0.01	—	—	—

<sup>a</sup>The content of hypericin corresponds to the sum of the content of hypericin and pseudohypericin.

<sup>b</sup>The content of hyperforin corresponds to the sum of the content of hyperforin and adhyperforin.

<sup>c</sup>Arko Diffusion SA, Les Avacias, Switzerland.

<sup>d</sup>Permamed AG, Therwil, Switzerland.

<sup>e</sup>Hänseler AG, Herisau, Switzerland.

<sup>f</sup>Schwabe Pharma AG, Küssnacht, Switzerland.

<sup>g</sup>Vifor SA, Bern, Switzerland.

<sup>h</sup>Zeller AG, Romanshorn, Switzerland.

<sup>i</sup>Sandoz Pharmaceuticals AG, Holzkirchen, Germany.

<sup>j</sup>Bioforce AG, Roggwil, Switzerland.

results in induced expression of multiple target genes, most of them with functions in drug elimination (Tolson and Wang, 2010). Indeed, one compound exemplifying this is the cardiac glycoside digoxin (Johns et al., 1999). This drug is commonly used in clinics and is not a CYP3A4 substrate (Lacarelle et al., 1991), but findings by Greiner et al. (1999) clearly showed that concomitant oral intake of digoxin and rifampin decreased drug disposition and exposure owing to induction of P-glycoprotein (P-gp, ABCB1, MDR1) expression. Importantly, rifampin is another well known activating ligand of PXR and can be applied to analyze the influence of PXR activation on drug metabolism (Chen and Raymond, 2006). Accordingly, the reduction in oral bioavailability of digoxin can be explained by enhanced expression of ABCB1 (Greiner et al., 1999). This transporter is responsible for active extrusion of substrates from enterocytes back into the intestinal lumen (Shapiro and Ling, 1995). Considering our findings on inhibition of OATP2B1-mediated transport by hyperforin and hypericin, the interaction of St. John's wort is extended to a further class of compounds, namely OATP2B1 substrates, whose mechanism of interaction would most probably be the competitive inhibition of cellular uptake.

OATP2B1 is assumed to play a role in intestinal absorption of orally administered drugs (Shitara et al., 2013). Testing the influence of hyperforin on transcellular transport of atorvastatin revealed an enhanced efflux ratio for atorvastatin. The experimental setup of Caco-2 cells cultured on permeable supports is commonly utilized for predictions of bioavailability and the contribution of transporters to intestinal absorption (Hubatsch et al., 2007). Indeed, when an efflux ratio, which is calculated relating the net flux in b-to-a direction with that in a-to-b direction, is above 1.5, it is assumed to indicate that active transporter-mediated processes are involved in the transcellular transport of a compound (Hubatsch et al., 2007). From the results of our study, one is certainly tempted to attribute the observed effect of an enhanced efflux ratio to the inhibition of OATP2B1 only. However, what was assessed

were net fluxes, and even though it has been reported as an OATP2B1 substrate (Grube et al., 2006), atorvastatin is not a specific substrate of this transporter. Indeed, atorvastatin is also a substrate of the efflux transporters multidrug resistance-associated protein (MRP)1 (ABCC1), MRP4 (ABCC4), MRP5 (ABCC5) (Knauer et al., 2010), and ABCB1 (Wu et al., 2000). Especially for ABCB1, some data suggest that hyperforin may influence transport activity directly (Hennessy et al., 2002). Our data suggest that, when present, hyperforin acutely interacts with oral absorption of OATP2B1 substrates, enhancing the complexity of drug-hyperforin interactions that should be considered when evaluating the interaction potential of St. John's wort preparations.

In addition to its involvement in intestinal drug absorption, OATP2B1 is assumed to contribute to the hepatocellular uptake. Recent findings by Lutz et al. (2018) suggest that there is at least some induction of OATP-mediated transport, as observed for concomitant treatment with rosuvastatin and pravastatin and increasing doses of rifampin. Even if OATP2B1 (OATP-B) may contribute to the hepatocellular uptake of these statins (Knauer et al., 2010; Shirasaka et al., 2010), OATP2B1 is not regulated in primary human hepatocytes treated with the PXR-inducer (Jigorel et al., 2006). Although there was no direct regulation by PXR, we recently reported interaction of the transporter with PDZ domain containing 1 (PDZK1), which influences OATP2B1 membrane localization (Ferreira et al., 2018). PDZK1 is transcriptionally controlled by multiple nuclear receptors (Ferreira et al., 2018; Prestin et al., 2017). Accordingly, whether long-term exposure to hyperforin influences localization of OATP2B1 remains to be determined, as we only tested the acute influence. Our findings suggest that the intracellular abundance of hyperforin, and thereby PXR-mediated transactivation of CYP3A4, is influenced by OATP2B1. Considering this finding, one might speculate that changes in OATP2B1 activity could influence the extent of PXR activation. Multiple mechanisms affect the activity of a transporter, and one possibility is the

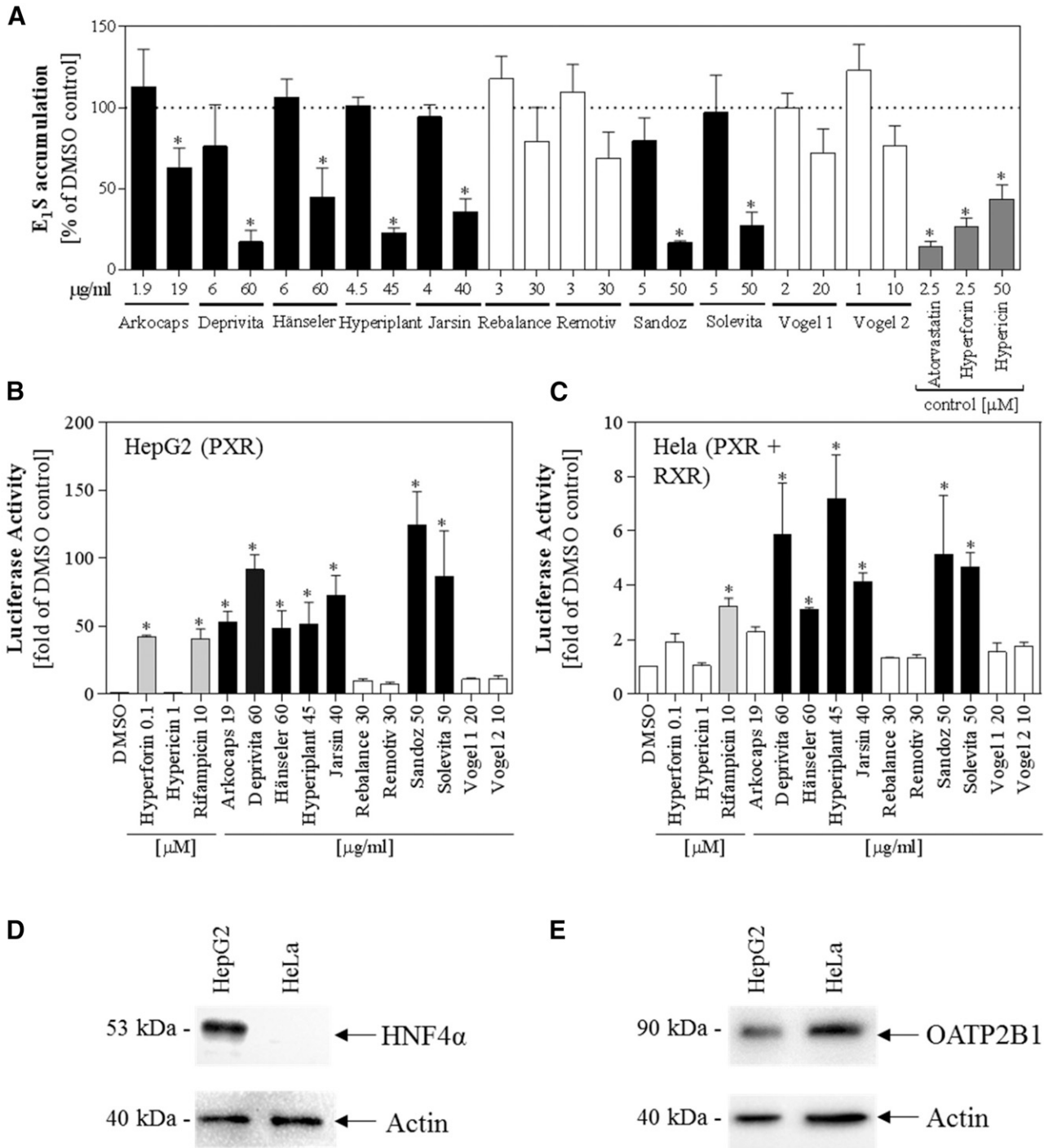


**Fig. 4.** Influence of commercially available St. John's wort preparations on OATP2B1 function and transactivation of CYP3A4. Transport inhibition studies assessing binding site A were conducted in MDCKII-OATP2B1 cells. Formulations were tested in two concentrations representing a 1/100 or 1/1000 dilution of the respective formulation dissolved in 200 ml liquid (A). The influence of each formulation (1/100 dilution) on CYP3A4 activation was determined in cell-based reporter gene assays using (B) HepG2 or (C) HeLa cells as cellular models. Firefly luciferase was normalized to that of *Renilla* in each sample. Expression of HNF4 $\alpha$  and OATP2B1 in HepG2 and HeLa cells was detected by Western blot analysis; actin served as control (D, E). Data are presented as mean  $\pm$  S.D. of  $n = 3$  independent experiments. \* $P$ -value  $\leq 0.05$  one-way analysis of variance followed by Dunnett's multiple comparisons test; Vogel 1, Hyperimex; Vogel 2, Hyperiforce.

change in expression by transcriptional modifiers. Another would be modifications in genetic information with influence on transport activity. We recently reported that OATP2B1 is transcriptionally modulated by thyroid hormones (Meyer zu Schwabedissen et al., 2018), thereby associating thyroid hormone status to OATP2B1 transport function, and Nozawa

et al. (2002) identified genetic polymorphisms that changed the maximal transport velocity ( $V_{max}$ ) of OATP2B1.

Testing extracts from all oral formulations of St. John's wort currently marketed in Switzerland for their influence on OATP2B1 transport activity, and the influence of OATP2B1 on their transactivating activity, revealed a clear association

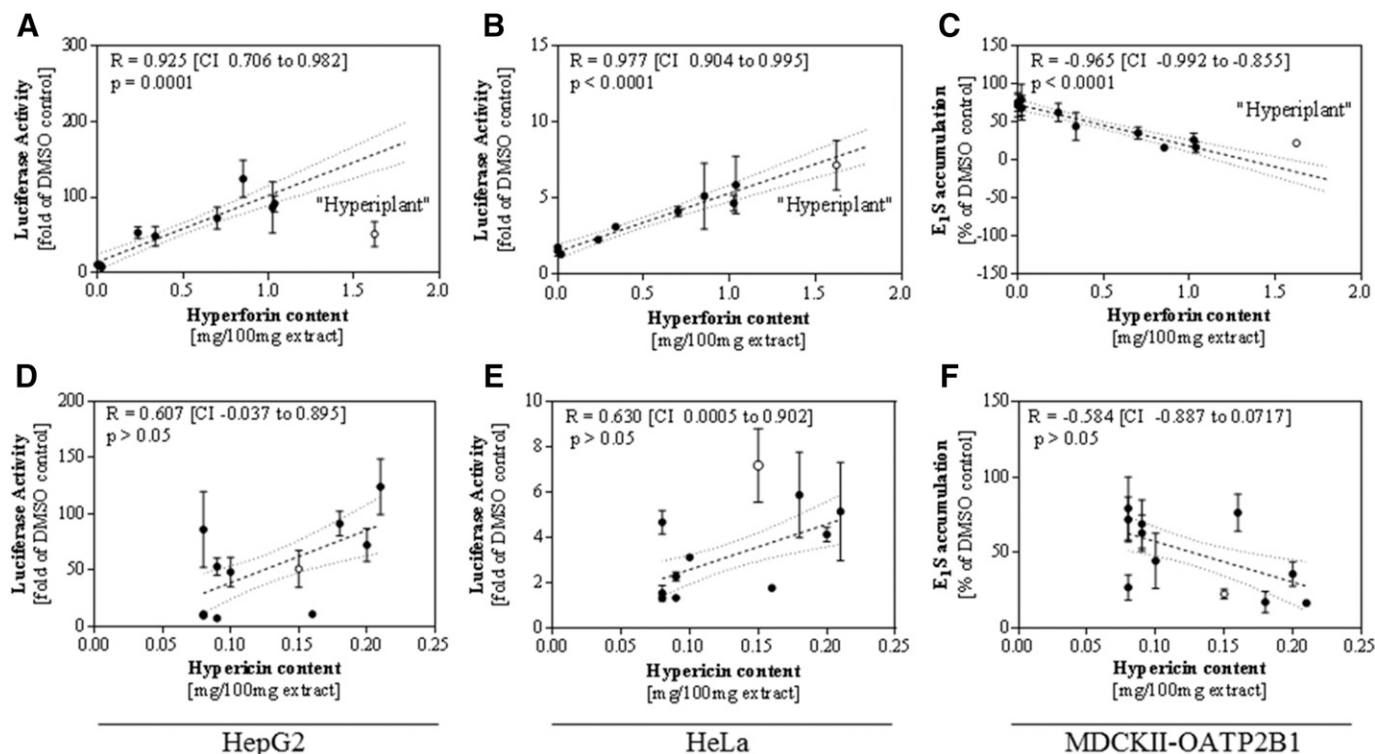


**Fig. 5.** Association of hyperforin or hypericin content with the observed effects in cell-based reporter gene assays, or transport inhibition studies. Luciferase activity was determined in transiently transfected HepG2 (A, D) or HeLa cells (B, E). Inhibition studies were conducted in MDCKII stably expressing OATP2B1 (C, F). Association of the observed effect with hyperforin or hypericin content was analyzed by linear regression (indicated by dotted line, shown with confidence interval), correlation was determined by calculating the Pearson coefficient. Data are presented as mean  $\pm$  S.D. with results of  $n = 3$  independent experiments performed in biologic triplicates. R, Pearson coefficient; open symbol indicated "Hyperiplant", which was neither included in the linear regression nor the calculation of the Pearson coefficient.

between hyperforin content and the observed effect for most formulations. Importantly, no such association was observed for hypericin content and PXR-mediated transactivation, thus confirming that hypericin is no activator of PXR (Moore et al., 2000; Wentworth et al., 2000). Furthermore, there is no clear association of hypericin content and OATP2B1 inhibition, which is in line with the much lower inhibitory potency observed for hypericin compared with hyperforin. This indicates that hyperforin is the component of St. John's wort extracts involved in interaction with OATP2B1-mediated uptake.

The formulations were tested in cell-based reporter gene assays using HepG2 or HeLa cells as cellular models. In the liver cell model we observed a huge induction of luciferase activity of about 50- to 100-fold, whereas the increase in activity was only about 5- to 7-fold in HeLa cells, with some formulations not affecting transactivation. On the one hand, the difference in extent of activation might certainly be explained by endogenous expression of HNF4 $\alpha$  in HepG2 cells, which is not present in HeLa cells as confirmed by Western blot analysis in this study and previously reported by Knauer et al. (2013). Importantly, HNF4 $\alpha$  is permissive for the transcriptional regulation by PXR (Ma et al., 2008). On the other hand, the fact that we observed induction in HeLa cells and a clear association of the extent of activation with the hyperforin content suggests that hyperforin is the driving component, but also that there is at least some HNF4 $\alpha$ -independent PXR activation.

As mentioned before, the hyperforin content was directly correlated with the observed luciferase activation. However,

this association was most pronounced when Hyperiplant was excluded from the correlation. In other words, the observed effect of Hyperiplant on OATP2B1-mediated transport or CYP3A4 activation was lower than expected considering the hyperforin content. In this context, it seems noteworthy that hyperforin is phototoxic (Onoue et al., 2011), inducing acute cell lysis. Even though our experiments were conducted under light protection, we cannot exclude the presence of some toxicity that could have modified the experimental outcome.

Taken together we report that hyperforin is a potent inhibitor of OATP2B1-mediated cellular uptake and we suggest that it is also a substrate. Inhibition of the transporter may influence the contribution of OATP2B1 to pharmacokinetics of its substrate drugs. Moreover, OATP2B1 activity influences intracellular accumulation of hyperforin and thereby its binding to the xenosensor. With this study, we added to the complexity of potential mechanisms that should be included in the evaluation of potential drug-drug interactions associated with the dispensing of St. John's wort.

#### Acknowledgments

The study reported herein will be part of the thesis of A.M.S.

#### Authorship Contributions

*Participated in research design:* Schäfer, Potterat, Meyer zu Schwabedissen.

*Conducted experiments:* Schäfer, Potterat, Seibert, Fertig, Meyer zu Schwabedissen.

*Contributed new reagents or analytic tools:* Potterat, Meyer zu Schwabedissen.

*Performed data analysis:* Schäfer, Potterat, Meyer zu Schwabedissen.

*Wrote or contributed to the writing of the manuscript:* Schäfer, Potterat, Seibert, Fertig, Meyer zu Schwabedissen.

## References

- Aleksunes LM and Klaassen CD (2012) Coordinated regulation of hepatic phase I and II drug-metabolizing genes and transporters using AhR-, CAR-, PXR-, PPAR $\alpha$ -, and Nr1f2-null mice. *Drug Metab Dispos* **40**:1366–1379.
- Bronger H, König J, Koppow K, Steiner HH, Ahmadi R, Herold-Mende C, Keppler D, and Nies AT (2005) ABC drug efflux pumps and organic anion uptake transporters in human gliomas and the blood-tumor barrier. *Cancer Res* **65**: 11419–11428.
- Chen J and Raymond K (2006) Roles of rifampicin in drug-drug interactions: underlying molecular mechanisms involving the nuclear pregnane X receptor. *Ann Clin Microbiol Antimicrob* **5**:3.
- Dürr D, Stieger B, Kullak-Ublick GA, Rentsch KM, Steinert HC, Meier PJ, and Fattinger K (2000) St John's wort induces intestinal P-glycoprotein/MDR1 and intestinal and hepatic CYP3A4. *Clin Pharmacol Ther* **68**:598–604.
- Ferreira C, Hagen P, Stern M, Hussner J, Zimmermann U, Grube M, and Meyer Zu Schwabedissen HE (2018) The scaffold protein PDZK1 modulates expression and function of the organic anion transporting polypeptide 2B1. *Eur J Pharm Sci* **120**: 181–190.
- Ferreira C, Prestin K, Hussner J, Zimmermann U, and Meyer Zu Schwabedissen HE (2018) PDZ domain containing protein 1 (PDZK1), a modulator of membrane proteins, is regulated by the nuclear receptor THR $\beta$ . *Mol Cell Endocrinol* **461**: 215–225.
- Geick A, Eichelbaum M, and Burk O (2001) Nuclear receptor response elements mediate induction of intestinal MDR1 by rifampin. *J Biol Chem* **276**: 14581–14587.
- Greiner B, Eichelbaum M, Fritz P, Kreichgauer HP, von Richter O, Zundler J, and Kroemer HK (1999) The role of intestinal P-glycoprotein in the interaction of digoxin and rifampin. *J Clin Invest* **104**:147–153.
- Grube M, Köck K, Oswald S, Draber K, Meissner K, Eckel L, Böhm M, Felix SB, Vogelgesang S, Jedlitschky G, et al. (2006) Organic anion transporting polypeptide 2B1 is a high-affinity transporter for atorvastatin and is expressed in the human heart. *Clin Pharmacol Ther* **80**:607–620.
- Grube M, Meyer Zu Schwabedissen H, Draber K, Präger D, Mörizt KU, Linnemann K, Fusch C, Jedlitschky G, and Kroemer HK (2005) Expression, localization, and function of the carnitine transporter octn2 (slc22a5) in human placenta. *Drug Metab Dispos* **33**:31–37.
- Harper JN and Wright SH (2013) Multiple mechanisms of ligand interaction with the human organic cation transporter, OCT2. *Am J Physiol Renal Physiol* **304**: F56–F67.
- Hennessy M, Kelleher D, Spiers JP, Barry M, Kavanagh P, Back D, Mulcahy F, and Feely J (2002) St John's wort increases expression of P-glycoprotein: implications for drug interactions. *Br J Clin Pharmacol* **53**:75–82.
- Hubatsch I, Ragnarsson EG, and Artursson P (2007) Determination of drug permeability and prediction of drug absorption in Caco-2 monolayers. *Nat Protoc* **2**: 2111–2119.
- Jigorel E, Le Vee M, Boursier-Neyret C, Parmentier Y, and Fardel O (2006) Differential regulation of sinusoidal and canalicular hepatic drug transporter expression by xenobiotics activating drug-sensing receptors in primary human hepatocytes. *Drug Metab Dispos* **34**:1756–1763.
- John A, Brockmüller J, Bauer S, Maurer A, Langheinrich M, and Roots I (1999) Pharmacokinetic interaction of digoxin with an herbal extract from St John's wort (Hypericum perforatum). *Clin Pharmacol Ther* **66**:338–345.
- Keiser M, Kalthauer L, Wildberg C, Müller J, Grube M, Partecke LI, Heidecke CD, and Oswald S (2017) The organic anion-transporting peptide 2B1 is localized in the basolateral membrane of the human jejunum and Caco-2 monolayers. *J Pharm Sci* **106**:2657–2663.
- Kliwer SA, Goodwin B, and Willson TM (2002) The nuclear pregnane X receptor: a key regulator of xenobiotic metabolism. *Endocr Rev* **23**:687–702.
- Knauer MJ, Girdwood AJ, Kim RB, and Tirona RG (2013) Transport function and transcriptional regulation of a liver-enriched human organic anion transporting polypeptide 2B1 transcriptional start site variant. *Mol Pharmacol* **83**:1218–1228.
- Knauer MJ, Urquhart BL, Meyer zu Schwabedissen HE, Schwarz UI, Lemke CJ, Leake BF, Kim RB, and Tirona RG (2010) Human skeletal muscle drug transporters determine local exposure and toxicity of statins. *Circ Res* **106**: 297–306.
- Kobayashi D, Nozawa T, Imai K, Nezu J, Tsuji A, and Tamai I (2003) Involvement of human organic anion transporting polypeptide OATP-B (SLC21A9) in pH-dependent transport across intestinal apical membrane. *J Pharmacol Exp Ther* **306**:703–708.
- Kullak-Ublick GA, Ismail MG, Stieger B, Landmann L, Huber R, Pizzagalli F, Fattinger K, Meier PJ, and Hagenbuch B (2001) Organic anion-transporting polypeptide B (OATP-B) and its functional comparison with three other OATPs of human liver. *Gastroenterology* **120**:525–533.
- Lacarelle B, Rahmani R, de Sousa G, Durand A, Placidi M, and Cano JP (1991) Metabolism of digoxin, digoxigenin digitoxosides and digoxigenin in human hepatocytes and liver microsomes. *Fundam Clin Pharmacol* **5**: 567–582.
- Lehmann JM, McKee DD, Watson MA, Willson TM, Moore JT, and Kliwer SA (1998) The human orphan nuclear receptor PXR is activated by compounds that regulate CYP3A4 gene expression and cause drug interactions. *J Clin Invest* **102**: 1016–1023.
- Lutz JD, Kirby BJ, Wang L, Song Q, Ling J, Massetto B, Worth A, Kearney BP, and Mathias A (2018) Cytochrome P450 3A induction predicts P-glycoprotein induction; part 1: establishing induction relationships using ascending dose rifampin. *Clin Pharmacol Ther* **104**:1182–1190.
- Ma X, Cheung C, Krausz KW, Shah YM, Wang T, Idle JR, and Gonzalez FJ (2008) A double transgenic mouse model expressing human pregnane X receptor and cytochrome P450 3A4. *Drug Metab Dispos* **36**:2506–2512.
- Mennini T and Gobbi M (2004) The antidepressant mechanism of Hypericum perforatum. *Life Sci* **75**:1021–1027.
- Meyer Zu Schwabedissen HE, Ferreira C, Schaefer AM, Oufir M, Seibert I, Hamburger M, and Tirona RG (2018) Thyroid hormones are transport substrates and transcriptional regulators of organic anion transporting polypeptide 2B1. *Mol Pharmacol* **94**:700–712.
- Meyer zu Schwabedissen HE and Kim RB (2009) Hepatic OATP1B transporters and nuclear receptors PXR and CAR: interplay, regulation of drug disposition genes, and single nucleotide polymorphisms. *Mol Pharm* **6**:1644–1661.
- Meyer zu Schwabedissen HE, Tirona RG, Yip CS, Ho RH, and Kim RB (2008) Interplay between the nuclear receptor pregnane X receptor and the uptake transporter organic anion transporter polypeptide 1A2 selectively enhances estrogen effects in breast cancer. *Cancer Res* **68**:9338–9347.
- Moore LB, Goodwin B, Jones SA, Wisely GB, Serabjit-Singh CJ, Willson TM, Collins JL, and Kliwer SA (2000) St. John's wort induces hepatic drug metabolism through activation of the pregnane X receptor. *Proc Natl Acad Sci USA* **97**: 7500–7502.
- Nahrstedt A and Butterweck V (1997) Biologically active and other chemical constituents of the herb of Hypericum perforatum L. *Pharmacopsychiatry* **30** (Suppl 2): 129–134.
- Niessen J, Jedlitschky G, Grube M, Bien S, Schwertz H, Ohtsuki S, Kawakami H, Kamiie J, Oswald S, Starke K, et al. (2009) Human platelets express organic anion-transporting peptide 2B1, an uptake transporter for atorvastatin. *Drug Metab Dispos* **37**:1129–1137.
- Nozawa T, Nakajima M, Tamai I, Noda K, Nezu J, Sai Y, Tsuji A, and Yokoi T (2002) Genetic polymorphisms of human organic anion transporters OATP-C (SLC21A6) and OATP-B (SLC21A9): allele frequencies in the Japanese population and functional analysis. *J Pharmacol Exp Ther* **302**:804–813.
- Onoue S, Seto Y, Ochi M, Inoue R, Ito H, Hatano T, and Yamada S (2011) In vitro photochemical and phototoxicological characterization of major constituents in St. John's wort (Hypericum perforatum) extracts. *Phytochemistry* **72**:1814–1820.
- Piscitelli SC, Burstein AH, Chaitt D, Alfaro RM, and Falloon J (2000) Indinavir concentrations and St John's wort. *Lancet* **355**:547–548.
- Pizzagalli F, Varga Z, Huber RD, Folkers G, Meier PJ, and St-Pierre MV (2003) Identification of steroid sulfate transport processes in the human mammary gland. *J Clin Endocrinol Metab* **88**:3902–3912.
- Prestin K, Hussner J, Ferreira C, Seibert I, Breitung V, Zimmermann U, and Meyer Zu Schwabedissen HE (2017) Regulation of PDZ domain-containing 1 (PDZK1) expression by hepatocyte nuclear factor-1 $\alpha$  (HNF1 $\alpha$ ) in human kidney. *Am J Physiol Renal Physiol* **313**:F973–F983.
- Roth M, Obaidat A, and Hagenbuch B (2012) OATPs, OATs and OCTs: the organic anion and cation transporters of the SLCO and SLC22A gene superfamilies. *Br J Pharmacol* **165**:1260–1287.
- Ruschitzka F, Meier PJ, Turina M, Lüscher TF, and Noll G (2000) Acute heart transplant rejection due to Saint John's wort. *Lancet* **355**:548–549.
- Sakamoto A, Matsumaru T, Yamamura N, Uchida Y, Tachikawa M, Ohtsuki S, and Terasaki T (2013) Quantitative expression of human drug transporter proteins in lung tissues: analysis of regional, gender, and interindividual differences by liquid chromatography-tandem mass spectrometry. *J Pharm Sci* **102**:3395–3406.
- Schäfer AM, Bock T, and Meyer Zu Schwabedissen HE (2018) Establishment and validation of competitive counterflow as a method to detect substrates of the organic anion transporting polypeptide 2B1. *Mol Pharm* **15**:5501–5513.
- Schiffer R, Neis M, Höller D, Rodriguez F, Geier A, Gartung C, Lammert F, Dreuw A, Zwadlo-Klarwasser G, Merk H, et al. (2003) Active influx transport is mediated by members of the organic anion transporting polypeptide family in human epidermal keratinocytes. *J Invest Dermatol* **120**:285–291.
- Shapiro AB and Ling V (1995) Reconstitution of drug transport by purified P-glycoprotein. *J Biol Chem* **270**:16167–16175.
- Shirasaka Y, Mori T, Shichiri M, Nakanishi T, and Tamai I (2012) Functional pleiotropy of organic anion transporting polypeptide OATP2B1 due to multiple binding sites. *Drug Metab Pharmacokin* **27**:360–364.
- Shirasaka Y, Suzuki K, Nakanishi T, and Tamai I (2010) Intestinal absorption of HMG-CoA reductase inhibitor pravastatin mediated by organic anion transporting polypeptide. *Pharm Res* **27**:2141–2149.
- Shitara Y, Maeda K, Ikejiri K, Yoshida K, Horie T, and Sugiyama Y (2013) Clinical significance of organic anion transporting polypeptides (OATPs) in drug disposition: their roles in hepatic clearance and intestinal absorption. *Biopharm Drug Dispos* **34**:45–78.
- Soleymani S, Bahramsoltani R, Rahimi R, and Abdollahi M (2017) Clinical risks of St John's wort (Hypericum perforatum) co-administration. *Expert Opin Drug Metab Toxicol* **13**:1047–1062.
- St-Pierre MV, Hagenbuch B, Ugele B, Meier PJ, and Stallmach T (2002) Characterization of an organic anion-transporting polypeptide (OATP-B) in human placenta. *J Clin Endocrinol Metab* **87**:1856–1863.
- Suzuki O, Katsumata Y, Oya M, Bladt S, and Wagner H (1984) Inhibition of monoamine oxidase by hypericin. *Planta Med* **50**:272–274.
- Tamai I, Nezu J, Uchino H, Sai Y, Oku A, Shimane M, and Tsuji A (2000) Molecular identification and characterization of novel members of the human organic anion transporter (OATP) family. *Biochem Biophys Res Commun* **273**:251–260.
- Tirona RG, Lee W, Leake BF, Lan LB, Cline CB, Lamba V, Parviz F, Duncan SA, Inoue Y, Gonzalez FJ, et al. (2003) The orphan nuclear receptor HNF4 $\alpha$  determines PXR- and CAR-mediated xenobiotic induction of CYP3A4. *Nat Med* **9**: 220–224.
- Tolson AH and Wang H (2010) Regulation of drug-metabolizing enzymes by xenobiotic receptors: PXR and CAR. *Adv Drug Deliv Rev* **62**:1238–1249.

- Wang Z, Lin YS, Dickmann LJ, Poulton EJ, Eaton DL, Lampe JW, Shen DD, Davis CL, Shuhart MC, and Thummel KE (2013) Enhancement of hepatic 4-hydroxylation of 25-hydroxyvitamin D3 through CYP3A4 induction in vitro and in vivo: implications for drug-induced osteomalacia. *J Bone Miner Res* **28**: 1101–1116.
- Wentworth JM, Agostini M, Love J, Schwabe JW, and Chatterjee VK (2000) St John's wort, a herbal antidepressant, activates the steroid X receptor. *J Endocrinol* **166**: R11–R16.
- Willson TM and Kliewer SA (2002) PXR, CAR and drug metabolism. *Nat Rev Drug Discov* **1**:259–266.
- Wu X, Whitfield LR, and Stewart BH (2000) Atorvastatin transport in the Caco-2 cell model: contributions of P-glycoprotein and the proton-monocarboxylic acid co-transporter. *Pharm Res* **17**:209–215.

---

**Address correspondence to:** Dr. Henriette E. Meyer zu Schwabedissen, Biopharmacy, Department of Pharmaceutical Sciences, University of Basel, Klingelbergstrasse 50, 4056 Basel, Switzerland. E-mail: h.meyerschwabedissen@unibas.ch

---



## Conclusion and Outlook

With the results of the underlying work, I conclude that the indirect method of competitive counterflow (CCF) is applicable to identify substrates of OATP2B1 and OATP1A2. The applicability of the CCF was validated with known substrates and the conducted screening revealed new substrates either of synthetic or natural origin. The method was established for both transporters using estrone 3-sulfate (E<sub>1</sub>S) as model substrate. However, the experimental procedure had to be adapted. Although both transporters reached the steady state after 30 minutes, the time to reach the equilibrium in presence of a test compound was much longer for OATP1A2. Indeed, after addition of the test compound OATP2B1 transport was equilibrated after 90 seconds, while cells overexpressing OATP1A2 reached this state only after 7 minutes. Whether this discrepancy reflects the known differences in affinity and capacity of the tested transporters to E<sub>1</sub>S remains to be further validated. However, the currently available data suggest that this phenomenon is linked to the affinity  $K_m$  OATP2B1 vs. OATP1A2, 1.56  $\mu$ M vs. 16.1  $\mu$ M and transport capacity  $V_{max}$  OATP2B1 vs. OATP1A2, 1.15 nmol/mg protein/min vs. 0.156 nmol/mg protein/min [25, 117]. Nevertheless, this assumption is rather speculative and has to be validated comparing the time to reach equilibrium for other OATPs. Notably, many OATPs recognize E<sub>1</sub>S as substrate including the kidney-specific OATP4C1 [118] or OATP3A1 and OATP4A1 [49]. For these OATPs, there is little information on their substrate spectrum, especially from the chemical space of drugs. It remains to be tested whether the CCF method could be applied to search for substrates of these transporters. For such an approach the CCF appears to be a cost and time saving alternative. As mentioned before, the strength of the CCF experiments is the possibility to screen for substrates. However, obtaining transport kinetics requires subsequent characterization using the methods described earlier [85], especially as the results of CCF experiments do not capture these parameters. Specifically, results of a CCF experiment provide the percentage of the intracellular amount of the primary substrate in the equilibrium of cells treated with the solvent control. Furthermore, the data are

obtained in presence of 10 x the estimated  $IC_{50}$  of the competitive substrate as this concentration is expected to occupy around 90% of the available binding sites [88]. Neither the  $IC_{50}$  nor the  $K_m$  or  $V_{max}$  are predictive for the observed percentage change in cellular probe substrate accumulation. For illustration, I provide the examples for the drugs glibenclamide, atorvastatin, and fexofenadine. For glibenclamide the  $IC_{50}$  was 0.57  $\mu M$ , the reported  $K_m$  and  $V_{max}$  are  $6.26 \pm 3.15 \mu M$  and  $112 \pm 52.2 \text{ pmol/mg protein/min}$ , respectively [119] while there was an about 51% change in equilibrium in the CCF experiment. For atorvastatin the estimated  $IC_{50}$  was 0.26  $\mu M$ , with reported  $K_m$  and  $V_{max}$  values of  $0.2 \pm 0.1 \mu M$  and  $30.5 \pm 2.9 \text{ pmol/mg protein/min}$  [51] and in CCF we observed a reduction of around 70%. Finally, the estimated  $IC_{50}$  for fexofenadine was 524.50  $\mu M$  and its  $K_m$  and  $V_{max}$  were reported to be  $0.140 \pm 0.062 \mu M$  and  $0.183 \pm 0.060 \text{ fmol/min/oocyte}$ , respectively [120]. The change in equilibrium in CCF was 55%. For OATP1A2 a larger compound screen needs to be performed in order to find whether there is a similar disconnection between percent reduction in equilibrium and  $K_m$  or  $V_{max}$ .

Even if there are multiple substrates identified for OATP2B1, there is still a limited understanding of its contribution to pharmacokinetics *in vivo*. One factor that may underlie this limitation is that most of the currently identified and clinically tested molecules (glibenclamide, montelukast, rosuvastatin) are also substrates of the hepatically expressed OATP1B transporters [35, 121, 122]. The colocalization of OATP2B1 and OATP1B-transporters in the sinusoidal membrane of hepatocytes and the substrate overlap with OATP1B transporters may confound the ability to show the influence of OATP2B1 on the process of hepatic clearance. Interestingly, using data from proteomic analyses by LC-MS/MS, McFeely *et al.* determined the relative abundance of the transporter in comparison to other transporters in the liver and intestine. Due to the high expression, they conclude that OATP2B1 could play an important role in those organs [123]. However, when Drozdik and coworkers compared the absolute

protein contents in the liver, they observed a lower amount of OATP2B1 compared to the OATP1B transporters [124].

For the role in intestinal absorption, the data on coadministration with fruit juices are convincing but have been subject of debates in the field, which was fueled by their inconsistency. While Mougey *et al.* observed an influence of OATP2B1 genetic variants on the plasma concentration of montelukast, Tapaninen *et al.* were unable to confirm these findings [125, 126]. Furthermore, Vaidyanathan *et al.* identified aliskiren as a substrate of OATP2B1 which served as explanation for observed changes in aliskiren pharmacokinetics after co-ingestion with citrus juices [63, 127]. However, a more recent study couldn't confirm aliskiren as a substrate of OATP2B1 [128]. Lastly, the debate was stimulated by the finding that OATP2B1 is localized in the basolateral membrane of enterocytes [62]. Notably, in contrast to the well studied and better understood OATP1B transporters, OATP2B1 is ubiquitously expressed. Changes in OATP2B1 function may therefore impact not only intestinal absorption and hepatic/renal elimination, but also the distribution of the test compound. In this scenario, where OATP2B1 influences uptake in other compartments, one may speculate that inhibition could influence the apparent volume of distribution (Vd). One extravascular compartment where OATP2B1 has been shown to be expressed is the skeletal muscle [57]. It remains to be determined, whether changes in OATP2B1 activity (due to genetic variants or drug-drug interaction) influences substrate distribution and therefore the Vd. In clinical studies this would be the pharmacokinetic parameter that could be monitored as a surrogate for altered extravascular drug distribution. At this point it seems noteworthy, that the functional consequences of the genetic variants of OATP2B1 (in contrast to those reported for OATP1B1 [19]) are rather limited and that the minor allele frequency of genetic variants with functional consequences is extremely low in most populations [123]. Even if currently available data suggest a contribution of OATP2B1 in the ADME processes of distribution, elimination, and absorption, it may not be sensitive to quantify its relevance through inference from

pharmacokinetic parameters. One possibility to tackle this issue could eventually be to determine changes in the pharmacodynamic effect of a selected substrate drug.

One region where proper function of uptake and efflux transporters is assumed to play a pivotal role is the blood-brain barrier (BBB). Here, there is data reporting the expression of OATP2B1 and OATP1A2 suggesting their contribution to compound permeation into the brain [22-24]. Furthermore, OATP1A2 is suggested to contribute to neuronal processes since expression was found in neuronal cells [24]. Using mass spectrometric analysis I was able to confirm the presence of both transporters in cellular structures of the BBB. Importantly, OATP2B1 was shown to be expressed in the vascular endothelium and OATP1A2 was also found in glial cells. Quantification of the transporter confirmed the restricted and broad central nervous system expression of OATP2B1 and OATP1A2, respectively.

Currently available data suggest that OATP2B1 and OATP1A2 transport sulfated steroid hormones such as dehydroepiandrosterone sulfate (DHEAS) and pregnenolone sulfate (PregS). In the context of the central nervous system, it seems noteworthy that both DHEAS and PregS are considered to be neurosteroids and important regulators of processes in the brain [80]. However, whether they are synthesized within the brain or depend on the supply from the systemic circulation involving the permeation of the BBB is currently not fully understood [31]. Despite that, it may be hypothesized that OATP1A2 and/or OATP2B1 are involved if they are taken up from the circulation. It may further be speculated that administration of substances functioning as (competitive) inhibitors of these transporters influences their homeostasis and potentially their function. Besides the neurosteroids, there are substrates of OATP2B1 and OATP1A2 that have to penetrate the BBB to exert their pharmacological effect. Applying CCF we identified the dopamine receptor agonists bromocriptine and cabergoline as substrates of both transporters. Furthermore, dopamine receptor antagonists were screened identifying domperidone as a substrate of OATP1A2 and OATP2B1, and metoclopramide as a substrate of

OATP1A2. It remains to be determined whether changes in activity of the transporters influence their brain entry, and therefore the outcome of patients treated with them.

In the context of the central nervous system and the potential involvement of transporter mediated entry, I have investigated constituents of *Passiflora incarnata* and *Valeriana officinalis* for interaction with OATP2B1 and OATP1A2. Therapeutically, both extracts find their indication in pathologies of the brain as anxiolytic or sedative agents. Constituents of *Valeriana officinalis* only weakly interacted with the transporters. However, constituents of *Passiflora incarnata* act as substrates of OATP2B1 and/or OATP1A2. It remains to be determined whether and to what extent these constituents are available in the systemic circulation and therefore are reaching the BBB. In general, it is assumed that the investigated flavonoids exhibit only limited bioavailability [114, 115]. Nevertheless, considering the contribution of OATP2B1 to intestinal drug absorption, interaction with the transporter needs to be considered especially when the herbal remedy is given orally with another OATP2B1 substrate drug or inhibitor.

Another herbal constituent I identified in CCF experiments as substrate of OATP2B1 is hyperforin. For this component of St. John's wort, I was able to compile a data set supporting the idea that OATP2B1 not only acts as a cellular entry mechanism, but also influences its effect as a modulator of drug metabolism. Briefly, in a cell based reporter gene assay assessing the transactivation of a synthetic CYP3A4-reporter gene construct presence of OATP2B1 significantly increased the transactivation. Moreover, using the Caco-2 transwell system, hyperforin was shown to influence the transcellular flux of the known OATP2B1 substrate atorvastatin. Taken together, our *in vitro* data suggest that St. John's wort formulations containing hyperforin could influence the pharmacokinetics of OATP2B1 substrates. Furthermore, the activity of OATP2B1 could influence the intracellular amount of hyperforin and therefore its impact on the PXR-regulated genes in drug metabolism. This finding would

add another class of compounds that must be considered when assessing the interaction potential of St. John's wort - namely OATP2B1 substrates. I think this should be further studied in *in vivo* experiments. In this regard, animal studies using the currently available knockout mouse models could be the first step [73, 129]. The study design would be similar to that reported by Medwid *et al.* investigating the influence of OATP2B1 on intestinal drug absorption [73]. Briefly, the known OATP2B1 substrate fexofenadine was orally administered to knockout and wildtype mice and the influence of the transporter on fexofenadine  $AUC_{(0-last)}$  and  $C_{max}$  was compared. Importantly, a decrease of fexofenadine  $AUC_{(0-last)}$  and  $C_{max}$  was seen in animals lacking the transporter. Subsequently, fexofenadine was co-administered with grapefruit juice which revealed a decreased  $AUC_{(0-last)}$  and  $C_{max}$  in wildtype animals whereas no effect was observed in knockout mice [73]. Adapting this experimental strategy for my purposes would include the co-administration of a known OATP2B1 substrate and a St. John's wort formulation containing hyperforin. However, it may also be possible to test for OATP2B1-mediated differences in hyperforin "efficacy" by comparing knockout and wildtype animals. In order to test for the influence of OATP2B1 on the activation of the drug metabolism, long term studies would be needed [130]. The induction of PXR target genes including the rodent orthologues of ABCB1 and CYP3A4 in wildtype animals could be compared to animals in which the transporter was knocked-out.

A prerequisite for these studies would be to validate that hyperforin is also a substrate of the mouse OATP2B1 transporter orthologue, and that hyperforin is also an activating ligand of mouse PXR. Notably, this nuclear receptor is known to exhibit species-specific differences in terms of activating ligands [131]. Pronounced differences were found for the probe-ligand rifampicin, which is recommended as clinical inducer by most agencies<sup>5</sup>. While rifampicin is

---

<sup>5</sup> US Food and Drug Administration. Guidance for industry: drug interaction studies—study design, data analysis, implications for dosing, and labeling recommendations. 2012; European Medicines Agency. Guideline on the Investigation of Drug Interactions, 2012, last access on February 18, 2021; last access on February 18, 2021

known to greatly induce the human PXR target genes there is minimal induction of genes in rodents due to species-selected ligand transactivation [132]. On the contrary, pregnenolone-16 $\alpha$ -carbonitrile activates rodent PXR and greatly induces the rodent CYP3A enzymes but shows only little activation of human PXR [132]. So far, there is only little data available investigating the interaction between the mouse PXR and hyperforin [133]. In this regard, Bray *et al.* report an increased catalytic activity of CYP3A in mice treated with St. John's wort compared to control. Whether this observation is based on mouse PXR transactivation was not addressed by the authors [134]. In a comparative study published by the Nuclear Receptor Resource, the effect of hyperforin on human and mouse PXR was investigated performing Luciferase reporter assays. Dose response relationships obtained from the luciferase activity revealed activation of the mouse PXR, albeit less active compared to the human [135].

In terms of hyperforin as substrate of the rodent PXR, one has to consider that there may also be species specificity. Unfortunately, there is only limited and contradictory data available reporting on the rodent variants. Medwid *et al.* identified the exogenous compounds bromosulphophthalein, fexofenadine and rosuvastatin as well as the endogenous DHEAS and E<sub>1</sub>S as substrates of the mouse OATP2B1. However, no significant difference between control cells and cells transfected with the mouse OATP2B1 were found by Sugiura *et al.* when performing *in vitro* uptake studies with E<sub>1</sub>S [136]. Consequently, further studies investigating characteristics of the rodent transporter and the rodent nuclear receptor are needed to determine to what extent the data obtained herein can be translated from *in vitro* to *in vivo* experiments.

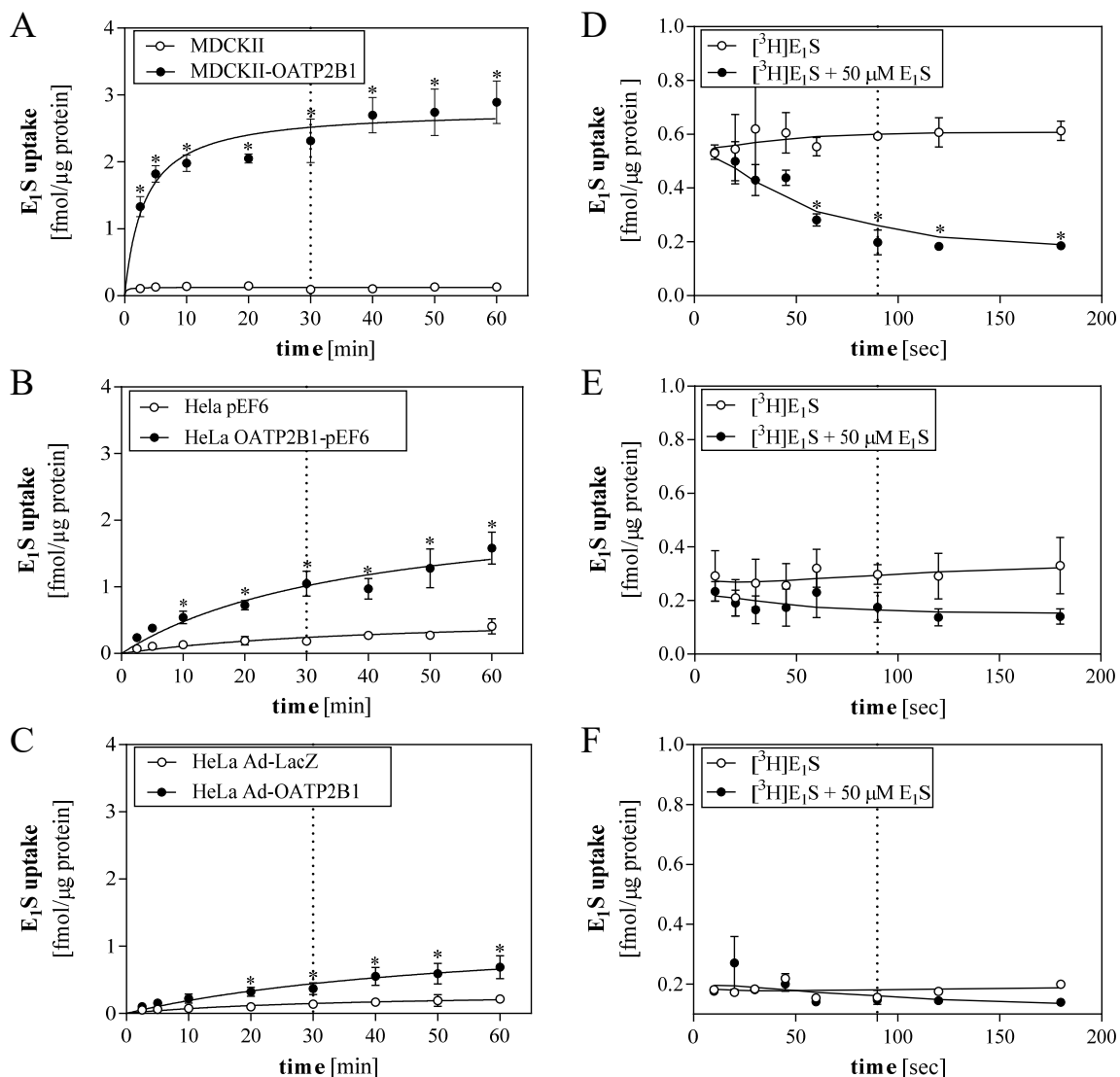
In summary, the competitive counterflow experiment can be used as a cost and time saving screening tool to identify substrates of OATP2B1 and OATP1A2 and might be a useful method in the challenging goal of finding transporter specific substrates. Using this method, I was able to identify centrally active drugs of synthetic and herbal origin as substrates. With the confirmation of OATP2B1 and OATP1A2 in the blood-brain barrier, the possibility is raised

that these uptake transporters enable brain entry of their substrates. Furthermore, OATP2B1 might also play a role in the intestinal absorption of the drugs. In this context, another herbal constituent was identified as OATP2B1 substrate namely hyperforin, a constituent of St. John's wort. Hyperforin is widely known to intracellularly activate PXR to induce target genes and therefore to cause drug-herb interactions. With the identification of hyperforin as OATP2B1 substrate the list of possible candidates that are influenced by hyperforin might be extended to OATP2B1 substrates. Furthermore, the activity of OATP2B1 could influence the intracellular amount of hyperforin and therefore its induction of PXR target genes. Importantly, these conclusions are based on *in vitro* experiments and whether these investigations are of clinical relevance remains to be determined. Nevertheless, my findings unraveled novel determinants contributing to cellular compound uptake, which might influence ADME processes and effects of drugs.

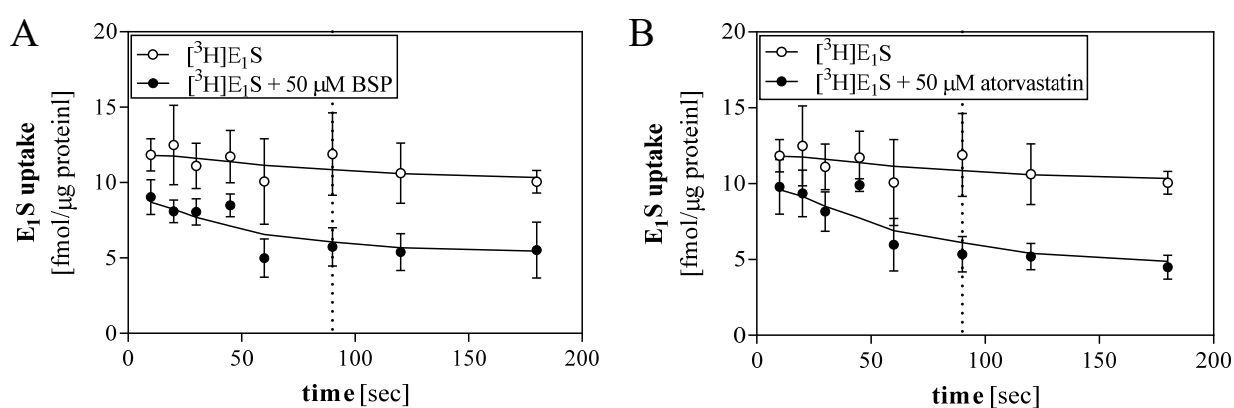
Supporting information to the manuscript “Establishment and validation of competitive counterflow as a method to detect substrates of the organic anion transporting polypeptide 2B1”

*Anima M. Schäfer, Thomas Bock, Henriette E. Meyer zu Schwabedissen*

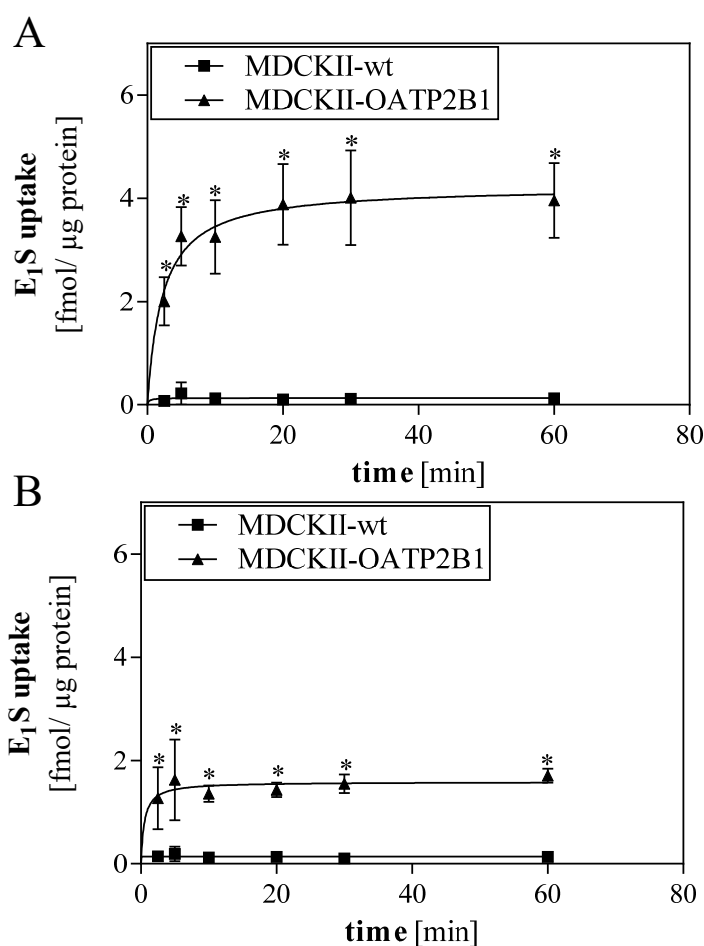
This supporting information is providing data about the establishment of experimental conditions for competitive counterflow, the time dependent uptake of estrone 3-sulfate at pH 5.5 and pH 7.4, a summary of the data underlying Figure 2 of the manuscript, and transport experiments performed in native MDCKII cells.



**Supporting Information Figure 1. Time-dependent cellular accumulation of estrone 3-sulfate applying different systems for cellular overexpression.** For experiments MDCKII-OATP2B1 (A, D) a vTF-7 based (B, E) and an adenoviral (C, F) expression system in HeLa cells were used to determine time dependent uptake of 6 nM radiolabeled estrone 3-sulfate (A, B, C). After the steady state was reached the equilibrium of competitive counterflow was determined by removing the supernatant and then adding the same amount of radiolabeled  $E_1S$  plus 50  $\mu$ M unlabeled  $E_1S$  (D, E, F). Data are presented as mean  $\pm$  SD,  $n=3$  independent experiments followed by nonlinear curve fitting with Savitsky-Golay smoothing.  $*p \leq 0.05$ , two-way ANOVA with Sidak's multiple comparisons test.



**Supporting Information Figure 2. Time of reaching equilibrium in CCF experiments using BSP and atorvastatin.** MDCKII-OATP2B1 cells were exposed to 6 nM [<sup>3</sup>H]-E<sub>1</sub>S for 30 min to reach steady state. Then the supernatant was replaced by 6 nM [<sup>3</sup>H]-E<sub>1</sub>S plus 50 μM BSP (A) or 50 μM atorvastatin (B). Data are presented as mean ± SD, n=3 independent experiments followed by nonlinear curve fitting with Savitsky-Golay smoothing.

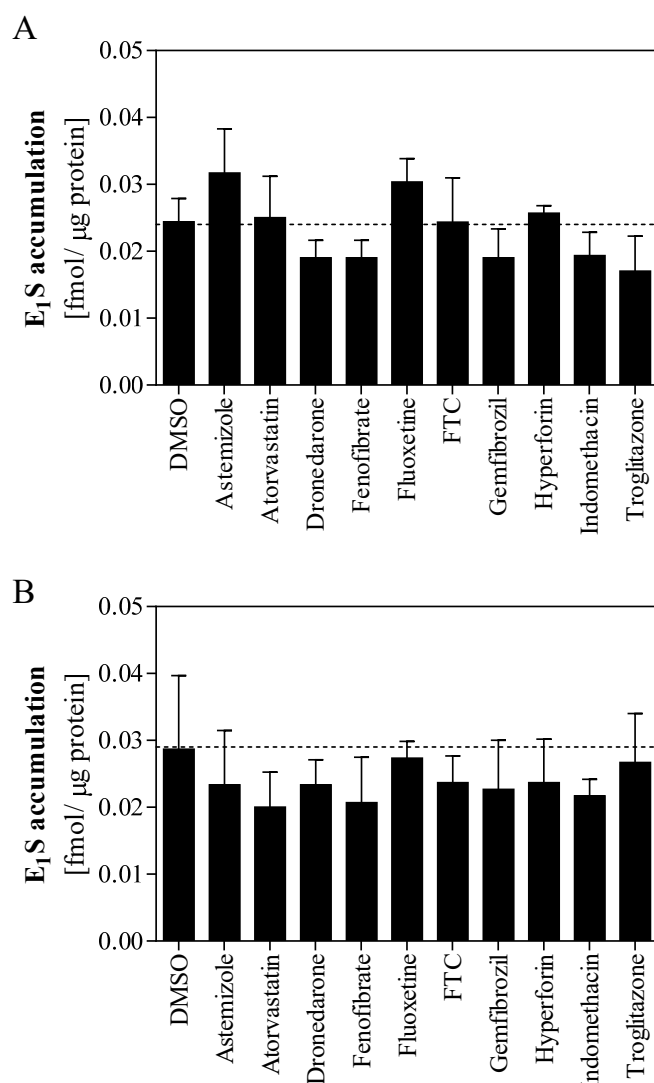


**Supporting Information Figure 3. Time dependent uptake of estrone 3-sulfate at pH 5.5 (A) and pH 7.4 (B) determined in MDCKII-wt and MDCKII-OATP2B1 cells.** Data are presented as mean  $\pm$  SD,  $n=3$  in biological triplicates,  $*p \leq 0.05$  two-way ANOVA with Sidak's multiple comparisons test.

**Supporting Information Table 1: Summary of data obtained assessing various molecules for their influence on the cellular amount of estrone-3 sulfate applying competitive counterflow experiments in MDCKII-OATP2B1 cells.** Each compound was tested against its solvent (DMSO, ethanol, or H<sub>2</sub>O). n=3 independent experiments each performed in biological triplicates. \* $p \leq 0.05$ , one-way ANOVA with Dunnett's multiple comparisons test.

	E <sub>1</sub> S-content [% of solvent control] mean ± SD		E <sub>1</sub> S-content [% of solvent control] mean ± SD
Astemizole	48.01 ± 7.26 *	Loxiglumide	44.87 ± 6.93 *
Atorvastatin	32.93 ± 7.03 *	Metoprolol	92.60 ± 11.85
Bromosulphothalein <sup>h</sup>	37.67 ± 4.71 *	Naringin	38.00 ± 8.36 *
Cerivastatin†	50.45 ± 9.02 *	Paclitaxel	87.10 ± 15.74
Cyclosporine A <sup>e</sup>	57.36 ± 11.34 *	Penicillin G <sup>h</sup>	92.78 ± 11.94
Domperidone	72.72 ± 8.95 *	Probenecid	77.75 ± 8.79
Dronedarone†	79.15 ± 7.77	Proglumide <sup>h</sup>	89.96 ± 10.12
Enalapril	127.7 ± 17.85 *	Sunitinib†	73.96 ± 9.62 *
Erythromycin <sup>e</sup>	95.05 ± 8.90	Talinolol†	70.90 ± 10.92 *
Etoposide†	44.10 ± 5.38 *	Teniposide	61.13 ± 6.67 *
Fenofibrate†	80.10 ± 12.09	Thyroxine	66.75 ± 9.99 *
Fexofenadine†	54.98 ± 11.81 *	Tolbutamide	104.2 ± 13.04
Fluoxetine	128.1 ± 23.06 *	Triiodothyronine	23.64 ± 3.52 *
Fumitremorgin C	147.6 ± 14.64 *	Troglitazone	87.26 ± 17.08
Gemfibrozil†	85.59 ± 12.09	Valproate	103.9 ± 18.77
Glibenclamide	49.51 ± 8.37 *	Valsartan	93.91 ± 13.47
Hyperforin	67.61 ± 15.22 *	Venlafaxin <sup>h</sup>	113.0 ± 9.12
Indomethacin	80.74 ± 9.76	Verapamil	110.0 ± 18.34
Irbesartan	44.38 ± 12.61 *	<i>Solvent controls</i>	
Itraconazole†	74.94 ± 14.93 *	DMSO control	102.1 ± 5.76
Ketoconazole	52.67 ± 9.31 *	ethanol control	100.0 ± 3.34
Lorglumide	48.41 ± 7.35 *	H <sub>2</sub> O control	100.0 ± 5.33

† concentration used in the experiment was below the recommended 10-fold IC<sub>50</sub>. <sup>h</sup> solvent was H<sub>2</sub>O; <sup>e</sup> solvent was ethanol



**Supporting Information Figure 4. Cellular accumulation of estrone 3-sulfate (E<sub>1</sub>S) was determined in MDCKII-wt cells.** (A) In a transport inhibition study MDCKII cells were incubated with E<sub>1</sub>S in presence of compounds identified as inhibitors and substrates (astemizole, atorvastatin, hyperforin) of OATP2B1, molecules that did not interact with OATP2B1 in the competitive counterflow but were identified as inhibitors in the primary assessment (dronedarone, fenofibrate, gemfibrozil, indomethacin, troglitazone) and a selection of compounds which were significantly increasing E<sub>1</sub>S accumulation in CCF experiments (fluoxetine, funitremorgin C). (B) Competitive counterflow experiments were performed in MDCKII-wt cells using the same compounds. None of the molecules significantly influences the cellular accumulation of E<sub>1</sub>S in native MDCKII cells. DMSO served as solvent control. Data are presented as mean ± SD; n = 3, performed in biological duplicates and for statistical analysis one-way ANOVA corrected for multiple comparisons (Dunnett's test) was used. FTC, funitremorgin C

## Supplementary material

### **Constituents of *Passiflora incarnata*, but Not of *Valeriana officinalis*, Interact with the Organic Anion Transporting Polypeptides (OATP)2B1 and OATP1A2**

**Anima M. Schäfer<sup>1</sup>, Pierrine M. Gilgen<sup>1</sup>, Clara Spirgi<sup>1</sup>, Olivier Potterat<sup>2</sup>,  
Henriette E. Meyer zu Schwabedissen<sup>1</sup>**

#### **Affiliations**

<sup>1</sup>Biopharmacy, Department Pharmaceutical Sciences, University of Basel, Switzerland

<sup>2</sup>Pharmaceutical Biology, Department Pharmaceutical Sciences, University of Basel,  
Switzerland

#### **Correspondence**

***Prof. Dr. med. Henriette E. Meyer zu Schwabedissen***

Biopharmacy

Department of Pharmaceutical Sciences

University of Basel

Klingelbergstrasse 50

4056 Basel

Switzerland

Phone: +41 (0)61-20 71495

Fax: +41 (0)61 20 71498

[h.meyerschwabedissen@unibas.ch](mailto:h.meyerschwabedissen@unibas.ch)

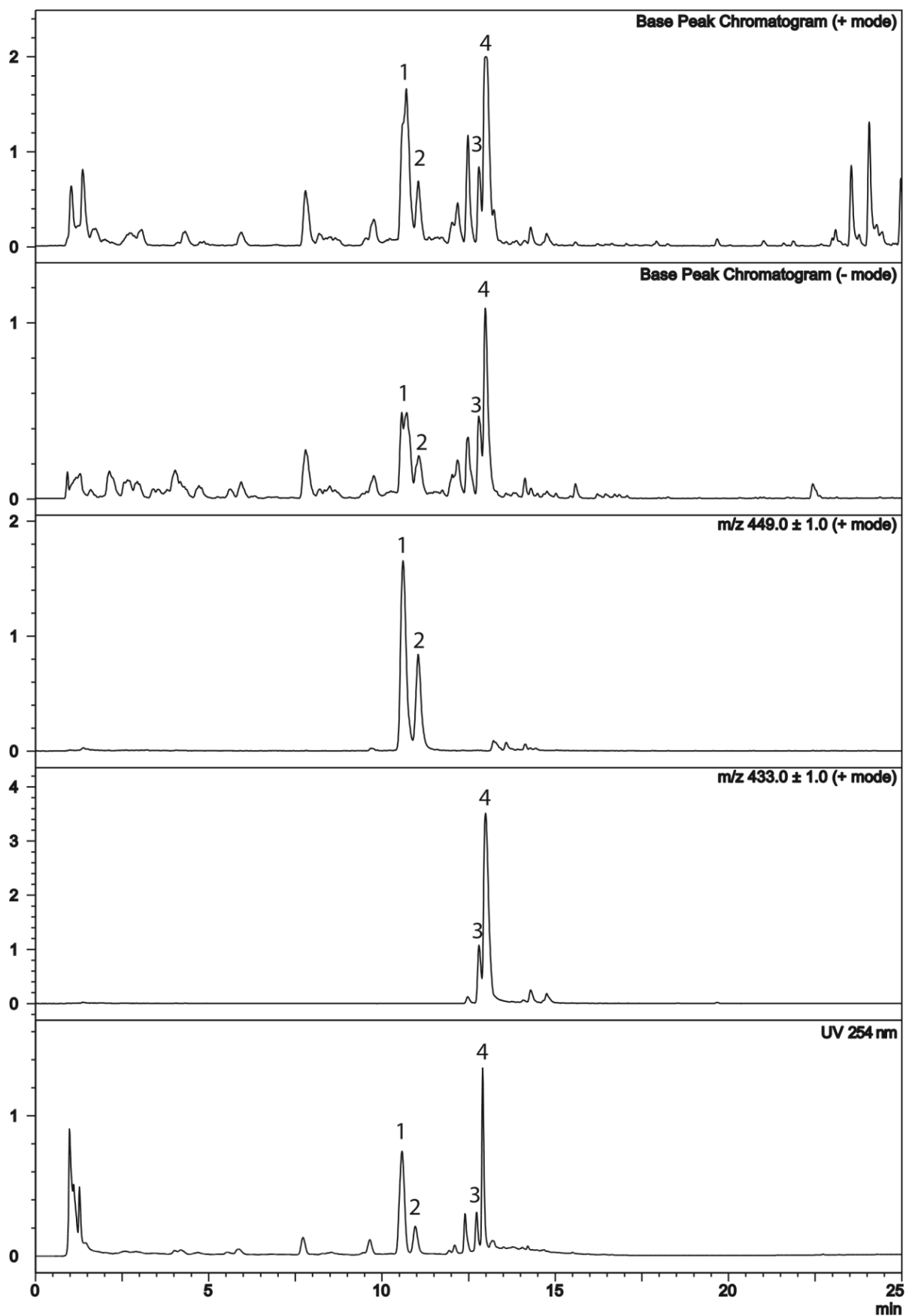


**Fig. 1S** HPLC-UV-MS analysis of Arkocaps capsule extract. Numbers refer to isoorientin (1), orientin (2), vitexin (3), and isovitexin (4).

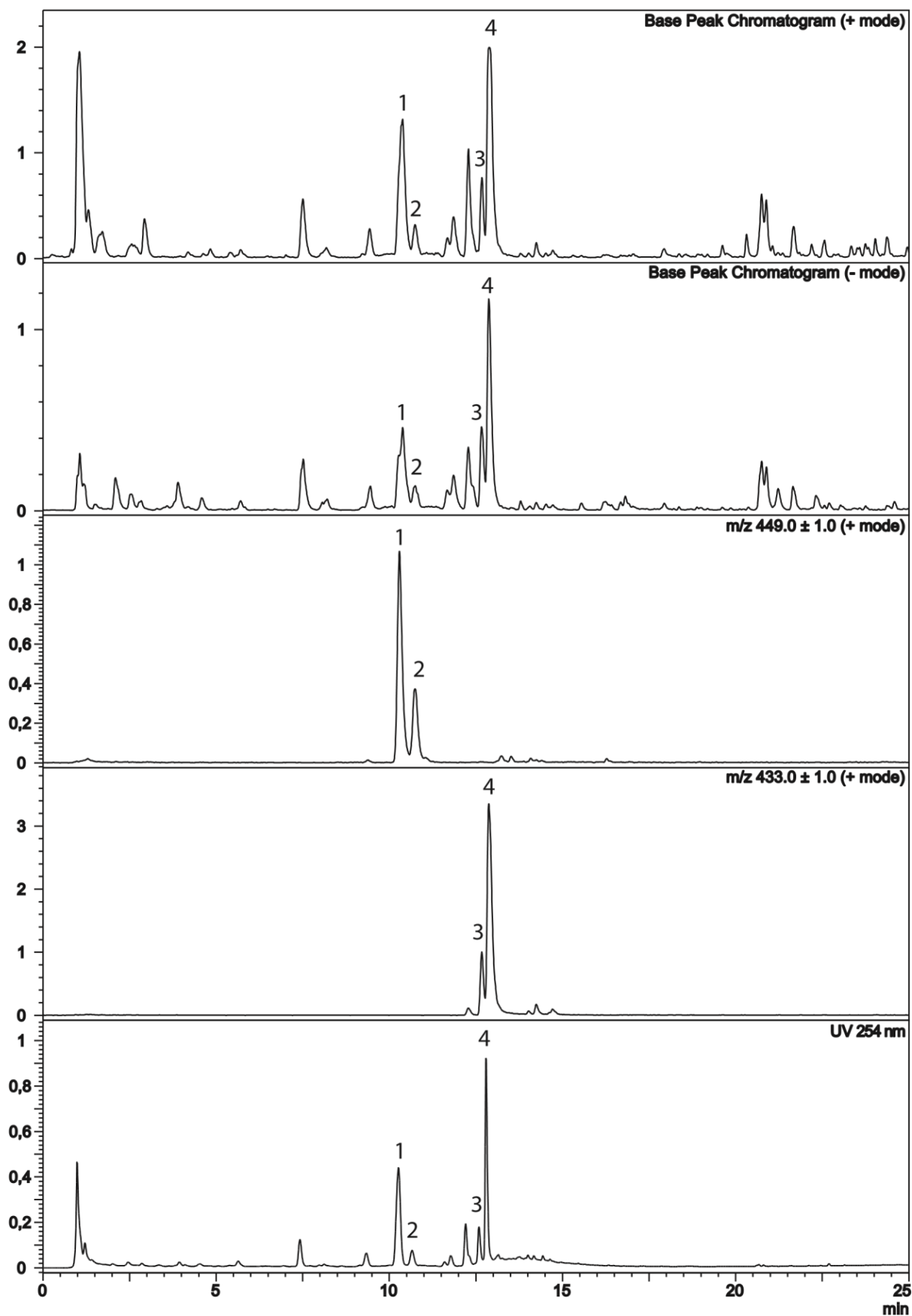


**Fig. 2S** HPLC-UV-MS analysis of Valverde tablets. Numbers refer to isoorientin (1), orientin (2), vitexin (3), and isovitexin (4).

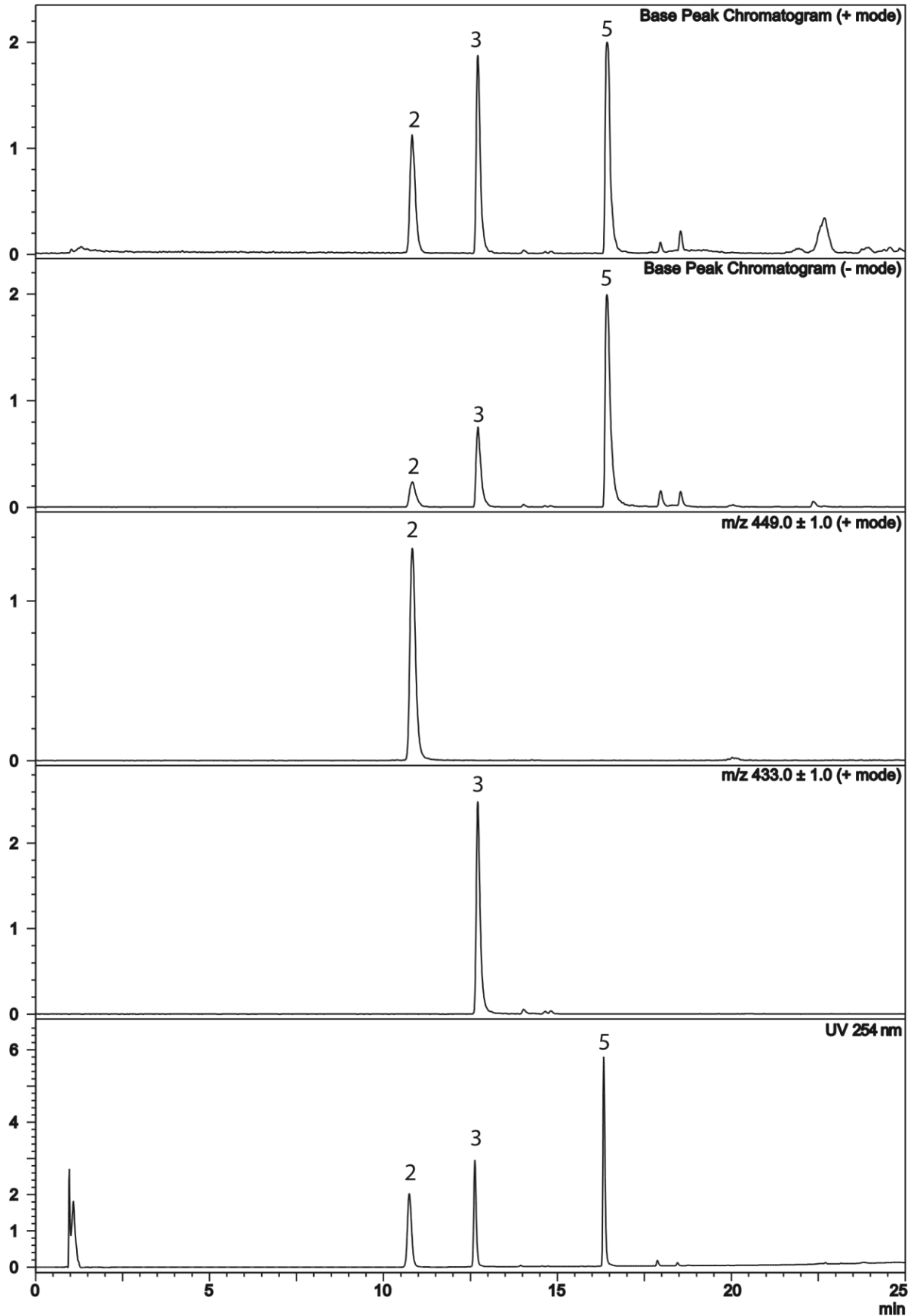


**Fig. 3S** HPLC-UV-MS analysis of the references orientin (2), vitexin (3), and apigenin (5).

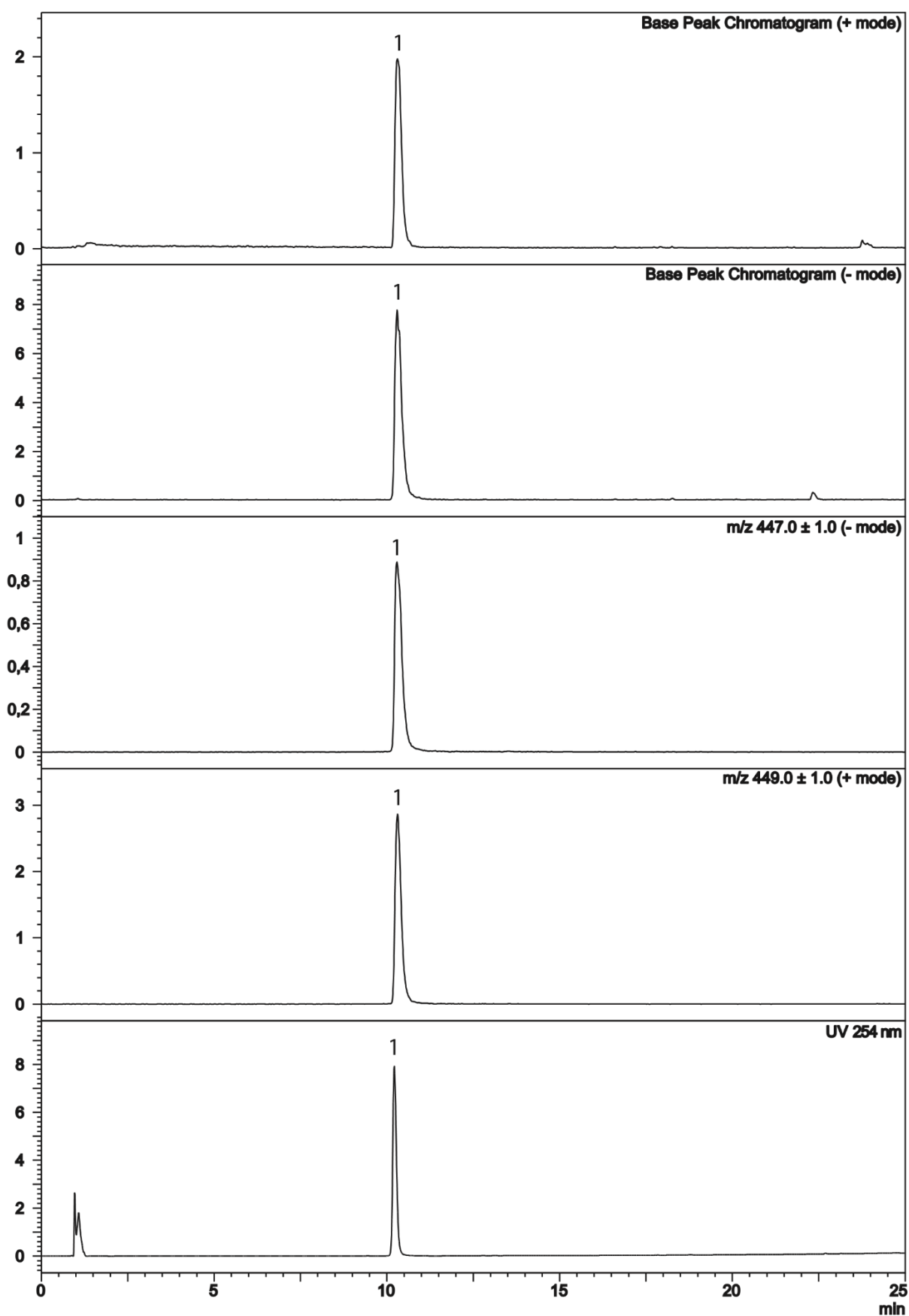
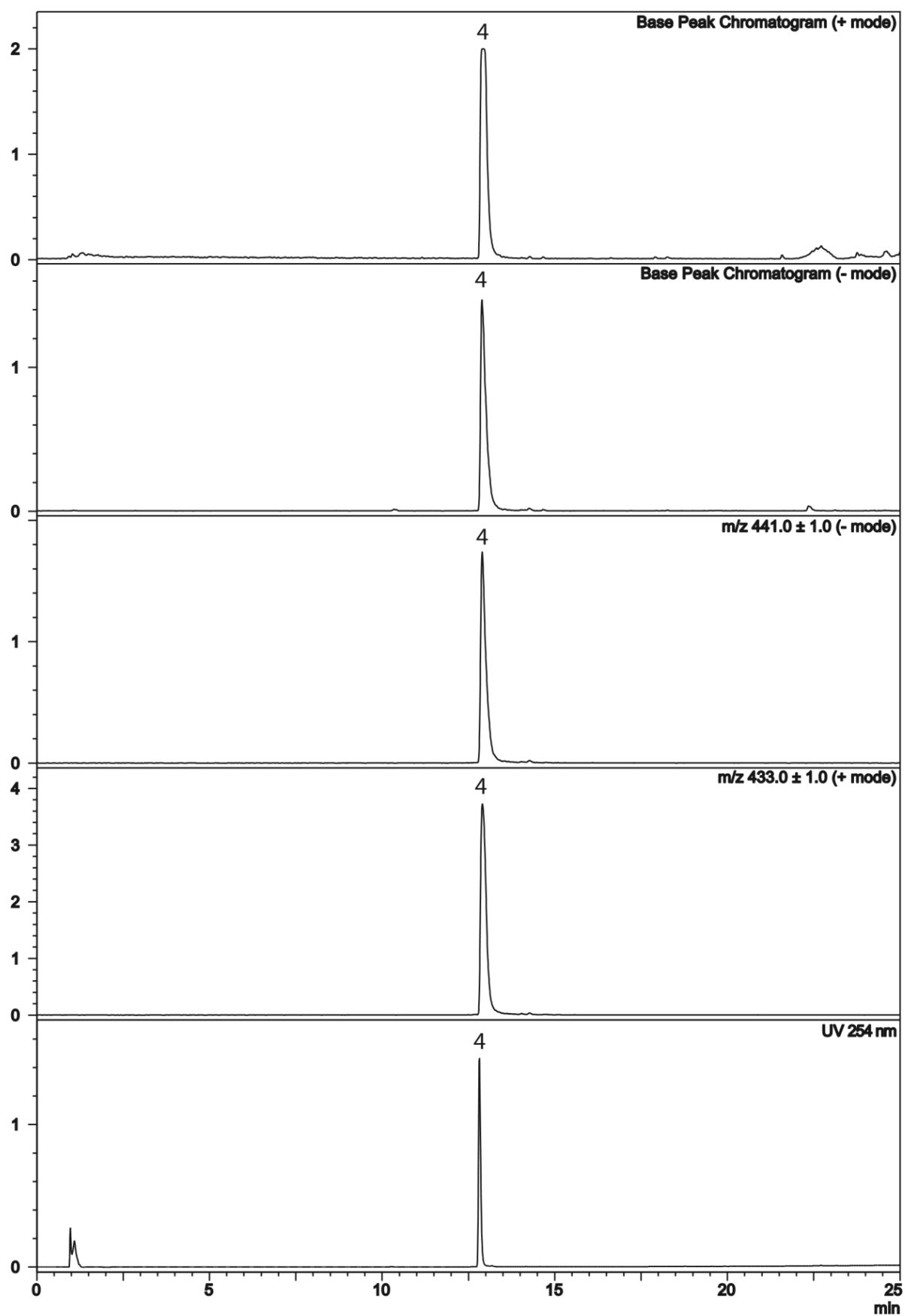


Fig. 4S HPLC-UV-MS analysis of the reference isoorientin (1).

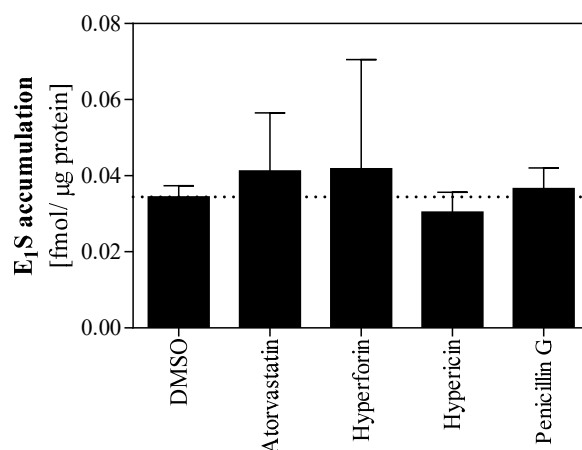


**Fig. 5S** HPLC-UV-MS analysis of the reference isovitexin (4).

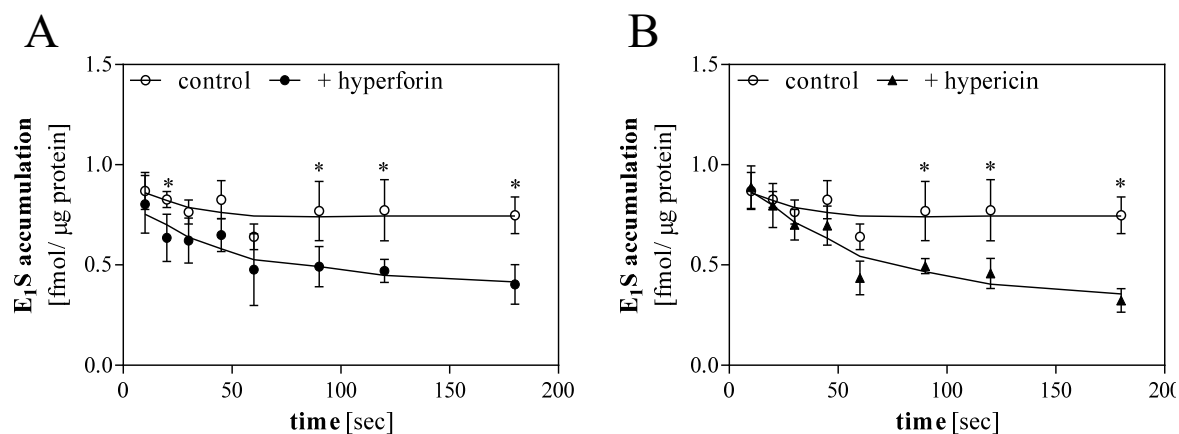
**Hyperforin induced activation of the Pregnane X Receptor is influenced by the Organic Anion Transporting Polypeptide 2B1 (OATP2B1)**

Anima M. Schäfer, Olivier Potterat, Isabell Seibert, Orlando Fertig, Henriette E. Meyer zu Schwabedissen

*- Supplemental Data -*

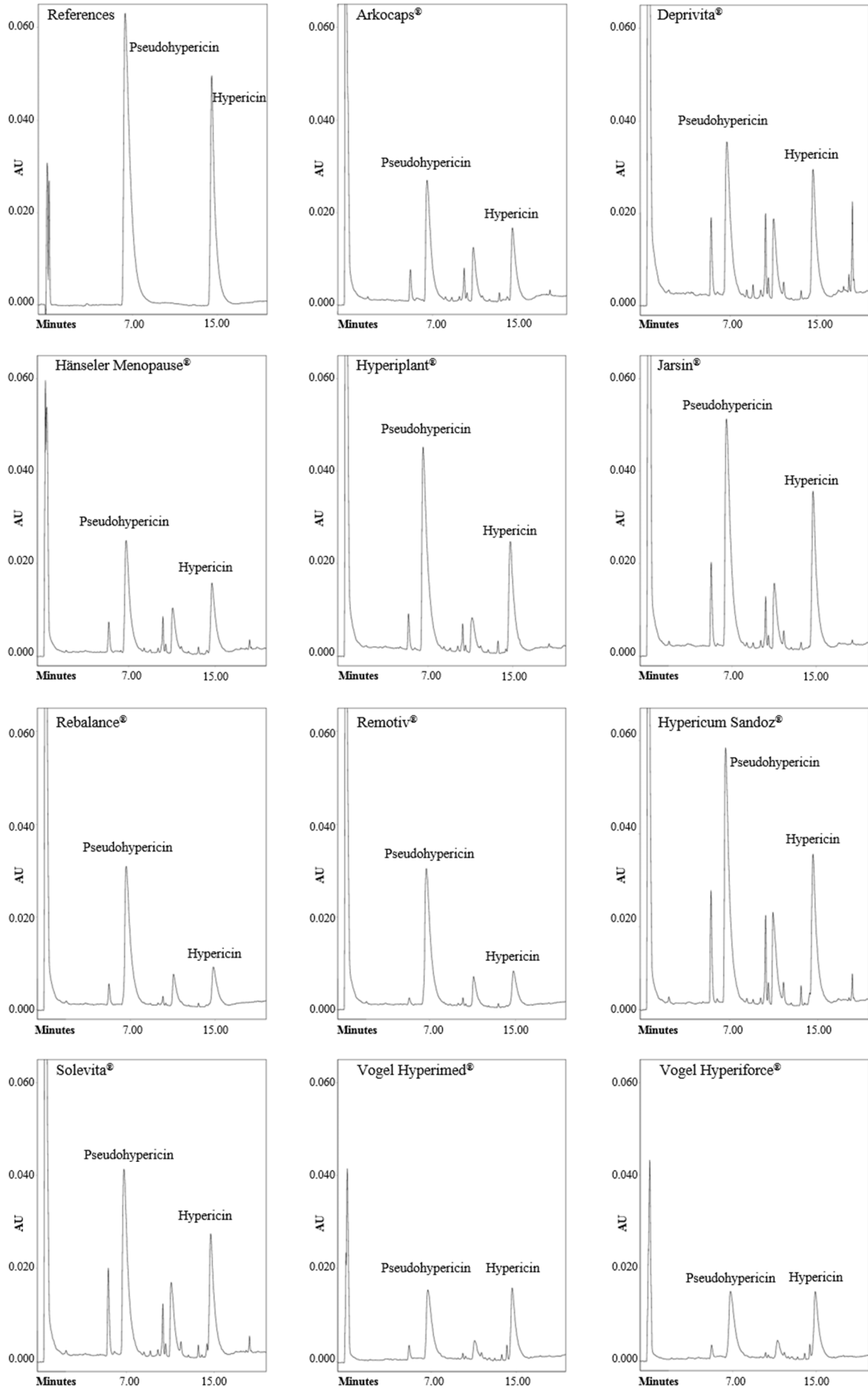


**Supplemental Figure 1. Counterflow experiments performed in MDCKII cells.** Cells were exposed to [<sup>3</sup>H]-E<sub>1</sub>S for 30 min. After reaching the steady state the supernatant was replaced by [<sup>3</sup>H]-E<sub>1</sub>S supplemented with DMSO or the respective test compound. Atorvastatin was used as positive control, penicillin G served as negative control, DMSO was the solvent control. Data are presented as mean ± SD of n=3 independent experiments each performed in biological triplicates. For statistical analysis one-way ANOVA was used corrected for multiple comparisons (Dunnett's test).



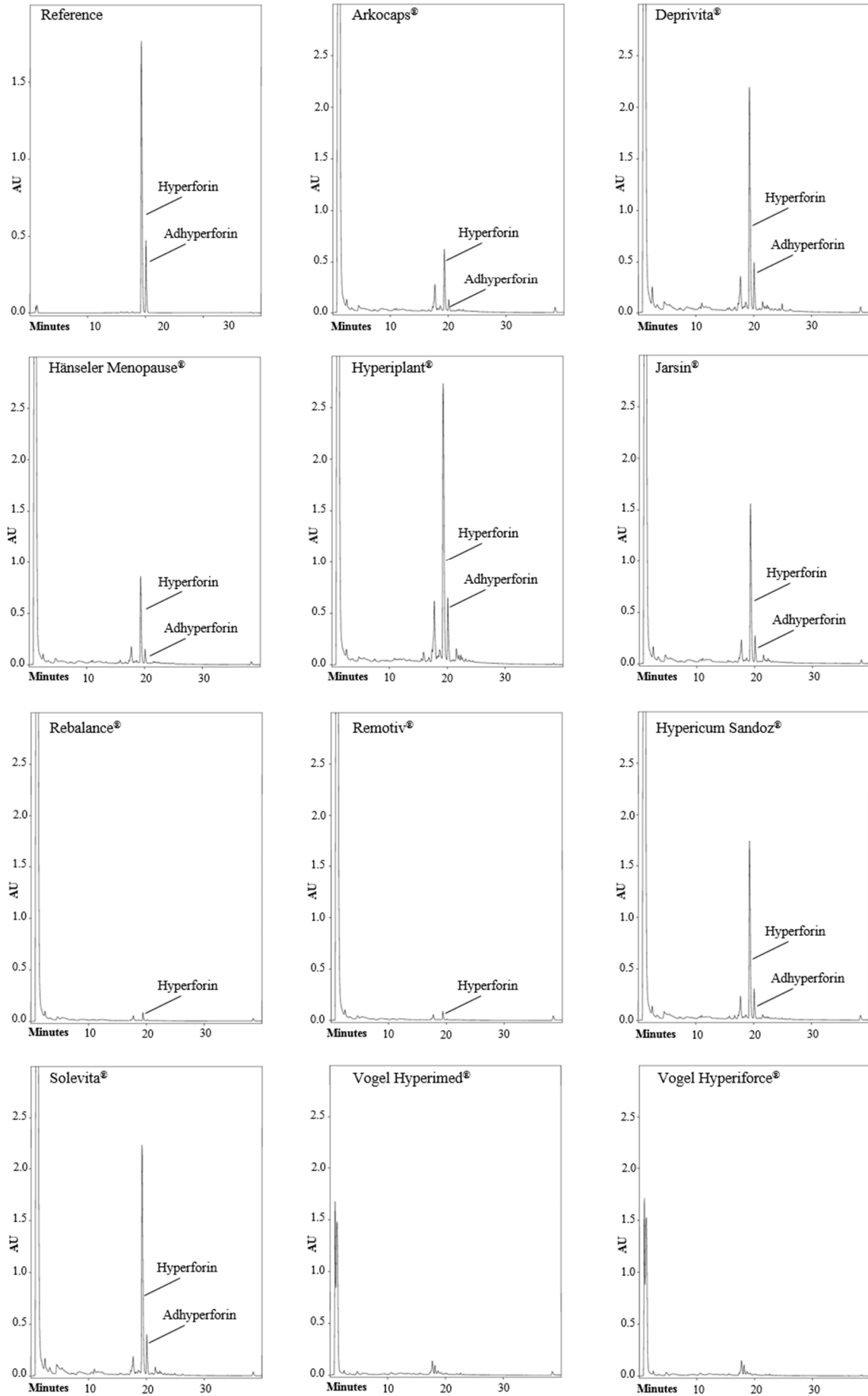
**Supplemental Figure 2. Competitive counterflow experiment with hyperforin (A) or hypericin (B).** MDCKII-OATP2B1 cells were treated with [ $^3$ H]- $E_1S$  for 30 min to reach steady state. Then the supernatant was removed and cells were exposed to either the same amount of [ $^3$ H]- $E_1S$  (control) or the same amount of [ $^3$ H]- $E_1S$  supplemented with either hyperforin (0.5  $\mu$ M, A) or hypericin (100  $\mu$ M, B). Cellular accumulation of the radiolabel was quantified at the respective time points by liquid scintillation counting. Data are presented as mean  $\pm$  SD, of  $n=3$  independent experiments performed in biological duplicates followed by nonlinear curve fitting with Savitsky-Golay smoothing. \* $p \leq 0.05$ , two-way ANOVA with Sidak's multiple comparisons test.

## Molecular Pharmacology - MOL # 114066 - Supplemental Data



**Supplemental Figure 3. Chromatograms of a mixture of the references hypericin (TOCRIS) and pseudohypericin (Sigma-Aldrich), and of the 11 in Switzerland marketed St. John's wort formulations.** Detection was at 588 nm. Experiments were performed n=3 with three independent experiments, one representative chromatogram is shown.

## Molecular Pharmacology - MOL # 114066 - Supplemental Data



**Supplemental Figure 4. Chromatograms of the reference hyperforin (Sigma-Aldrich) and of the 11 in Switzerland marketed St. John's wort formulations.** Detection was at 272 nm. Experiments were performed n=3 with three independent experiments, one representative chromatogram is shown.



## Appendix

**Table 1.** Summary of clinical studies to investigate drug-drug or drug-food interactions with known OATP1A2 substrates.

OATP1A2 substrate and competitor	Participants and study approach/ type	Outcome of the study	Ref
Fexofenadine (2x60mg) and Grapefruit juice (2 concentrations) or orange juice or apple juice	10 healthy volunteers single-dose, balanced, randomized, 5-way crossover study	Grapefruit (high concentration), orange, apple juices decreased fexofenadine AUC <sub>(0-8h)</sub> to 30% and C <sub>max</sub> to 40% Grapefruit juice (low concentration) to 80% No difference of fexofenadine t <sub>max</sub> and t <sub>1/2</sub> between treatments Grapefruit (high conc), orange, apple juices reduced urinary fexofenadine excretion to 30% Grapefruit juice (low conc) to 79%	[137]
Fexofenadine (120mg) and Grapefruit juice (300mL vs. 1200mL)	12 healthy volunteers single-dose, randomized 4-way crossover study	300mL: decrease of fexofenadine AUC <sub>(0-8h)</sub> to 58%, C <sub>max</sub> to 53% 1200mL: decrease of fexofenadine AUC <sub>(0-8h)</sub> to 36% and C <sub>max</sub> to 33%	[42]
Fexofenadine (120mg) and Grapefruit juice (300mL) (-4h vs. -2h vs. simultaneous (0h) administration)	12 healthy subjects single-dose, randomized, open, crossover	-4h: no effect -2h: decrease of fexofenadine AUC <sub>(0-8h)</sub> to 38% 0h: decrease of fexofenadine AUC to 52%	[29]
Fexofenadine (120mg) and Grapefruit juice (300ml) or naringin solution	12 healthy subjects single-dose, randomized, open, crossover	Grapefruit juice decreased fexofenadine AUC <sub>(0-8h)</sub> to 55% and C <sub>max</sub> to 58%; naringin solution decreased fexofenadine AUC <sub>(0-8h)</sub> to 75% No difference of fexofenadine t <sub>max</sub> and t <sub>1/2</sub> between treatments	[39]
Fexofenadine (120mg) and Grapefruit juice (300ml) or mediate/low concentrated naringin solutions	12 healthy subjects single-dose, randomized, open, crossover	Grapefruit juice decreased fexofenadine AUC <sub>(0-8h)</sub> to 57% and C <sub>max</sub> to 61%; No effect on fexofenadine AUC <sub>(0-8h)</sub> and C <sub>max</sub> with mediate/low concentrated naringin solutions	[39]
Nadolol (30mg) after green tea consumption (700ml/day) for 14 days	10 healthy volunteers single-dose, randomized, crossover, 2-phases	Green tea decreased nadolol AUC <sub>(0-48)</sub> to 85% and C <sub>max</sub> to 85.3% Reduction of urine nadolol	[34]

		excretion by 81.6% Reduced nadolol-induced effect on systolic blood pressure	
Aliskiren (300mg) and Grapefruit juice (300mL)	28 healthy subjects single-dose, open-label, 2-way crossover	Grapefruit juice decreased AUC <sub>(0-96)</sub> by 37% and C <sub>max</sub> by 61%	[138]
Nadolol (30mg) and low dose (LD) of green tea extract or high dose (HD) of green tea extract (both 300mL)	30 healthy volunteers three-phase, randomized, crossover	Green tea (LD) decreased nadolol AUC <sub>(0-8h)</sub> to 69%, HD to 53% and C <sub>max</sub> to 59% (LD) and 50% (HD) No changes for blood pressure and pulse rate	[139]
Fexofenadine (120mg) and folic acid (5mg) and D3 (0.5µg)	10 healthy volunteers prospective single arm, single center	No change in fexofenadine or folic acid absorption due to vitamin D3	[48]

**Table 2.** Summary of OATP1A2 polymorphisms and their *in vitro* or *in vivo* observations.

rs number	Nucleotide/ amino acid exchange	Consequence	global minor allele frequency (%)	Ref
rs11568563 rs45502302 NA rs11568557	c.516A>C p.172E>D c.404A>T p.135N>Y  c.559G>A p.187A>Y c.2003C>G p.668T>S	reduced capacity for uptake of E <sub>1</sub> S and delta-opioid receptor agonists  substrate dependent change in transport activity	1.9 EA, 2.0 ME 1.3 AA  4.4 AA, 1.0 ME	[25]
rs10841795 rs11568563 rs11568564 NA	c.38T>C p.13I>T  c.516A>C p.172E>D  c.502C>T p.168R>C c.833A>- p.278N>del	induced uptake of E <sub>1</sub> S and MTX  reduced transport capacity of E <sub>1</sub> S and MTX  hypofunctional  non-functional	2.5 AA, 16.3 EA, 5.0 ME  1.9 EA, 2.0 ME  0.6 EA  0.6 AA	[26]
rs3764043	intronic c.-423G>A aka c.-361G>A	significantly lower imatinib clearance than patients with GA or AA, but no clinical response	2.0 EA, 14 Asian	[45]

rs10841795	c.38T>C p.13I>T	slightly higher CSF darunavir penetration compared to AA	2.5 AA, 16.3 EA, 5.0 ME	[46]
rs4762699  rs2857468	intronic c.-62-16425A>T  intronic c.-62-4294T>A	highly association with risk of life-threatening febrile neutropenia in breast cancer patients treated with docetaxel and doxorubicin	NA  88 EA, 70 AA, 100 Asian	[47]
NA	-189_-188InsA	-A or AA showed reduced total clearance of rocuronium compared to wild type	NA	[48]
NA	E184K, D185N, T259P, D288N	impaired E <sub>1</sub> S, imatinib and MTX transport	NA	[140]

AA, African American; CSF, cerebrospinal fluid; EA, European American; E<sub>1</sub>S, estrone 3-sulfate; ME, Mexican American; MTX, methotrexate; NA, not currently available



## Bibliography

1. Juliano, R.L. and V. Ling, *A surface glycoprotein modulating drug permeability in Chinese hamster ovary cell mutants*. Biochim Biophys Acta, 1976. **455**(1): p. 152-62.
2. Hodges, L.M., et al., *Very important pharmacogene summary: ABCB1 (MDR1, P-glycoprotein)*. Pharmacogenet Genomics, 2011. **21**(3): p. 152-61.
3. Robey, R.W., et al., *Revisiting the role of ABC transporters in multidrug-resistant cancer*. Nat Rev Cancer, 2018. **18**(7): p. 452-464.
4. Keppler, D., J. König, and M. Buchler, *The canalicular multidrug resistance protein, cMRP/MRP2, a novel conjugate export pump expressed in the apical membrane of hepatocytes*. Adv Enzyme Regul, 1997. **37**: p. 321-33.
5. König, J., et al., *Characterization of the human multidrug resistance protein isoform MRP3 localized to the basolateral hepatocyte membrane*. Hepatology, 1999. **29**(4): p. 1156-63.
6. Fromm, M.F., et al., *The effect of rifampin treatment on intestinal expression of human MRP transporters*. Am J Pathol, 2000. **157**(5): p. 1575-80.
7. Schaub, T.P., et al., *Expression of the MRP2 gene-encoded conjugate export pump in human kidney proximal tubules and in renal cell carcinoma*. J Am Soc Nephrol, 1999. **10**(6): p. 1159-69.
8. St-Pierre, M.V., et al., *Expression of members of the multidrug resistance protein family in human term placenta*. Am J Physiol Regul Integr Comp Physiol, 2000. **279**(4): p. R1495-503.
9. Mao, Q. and J.D. Unadkat, *Role of the breast cancer resistance protein (BCRP/ABCG2) in drug transport--an update*. AAPS J, 2015. **17**(1): p. 65-82.
10. Roth, M., A. Obaidat, and B. Hagenbuch, *OATPs, OATs and OCTs: the organic anion and cation transporters of the SLCO and SLC22A gene superfamilies*. Br J Pharmacol, 2012. **165**(5): p. 1260-87.
11. Li, L., et al., *Identification of glutathione as a driving force and leukotriene C4 as a substrate for oatp1, the hepatic sinusoidal organic solute transporter*. J Biol Chem, 1998. **273**(26): p. 16184-91.
12. Li, L., P.J. Meier, and N. Ballatori, *Oatp2 mediates bidirectional organic solute transport: a role for intracellular glutathione*. Mol Pharmacol, 2000. **58**(2): p. 335-40.
13. Satlin, L.M., V. Amin, and A.W. Wolkoff, *Organic anion transporting polypeptide mediates organic anion/HCO<sub>3</sub><sup>-</sup> exchange*. J Biol Chem, 1997. **272**(42): p. 26340-5.
14. Leuthold, S., et al., *Mechanisms of pH-gradient driven transport mediated by organic anion polypeptide transporters*. Am J Physiol Cell Physiol, 2009. **296**(3): p. C570-82.
15. Hagenbuch, B., *Cellular entry of thyroid hormones by organic anion transporting polypeptides*. Best Pract Res Clin Endocrinol Metab, 2007. **21**(2): p. 209-21.
16. König, J., et al., *Localization and genomic organization of a new hepatocellular organic anion transporting polypeptide*. J Biol Chem, 2000. **275**(30): p. 23161-8.
17. König, J., et al., *A novel human organic anion transporting polypeptide localized to the basolateral hepatocyte membrane*. Am J Physiol Gastrointest Liver Physiol, 2000. **278**(1): p. G156-64.
18. Alam, K., et al., *Regulation of Organic Anion Transporting Polypeptides (OATP) 1B1- and OATP1B3-Mediated Transport: An Updated Review in the Context of OATP-Mediated Drug-Drug Interactions*. Int J Mol Sci, 2018. **19**(3).
19. Kalliokoski, A. and M. Niemi, *Impact of OATP transporters on pharmacokinetics*. Br J Pharmacol, 2009. **158**(3): p. 693-705.
20. Shitara, Y., *Clinical importance of OATP1B1 and OATP1B3 in drug-drug interactions*. Drug Metab Pharmacokinet, 2011. **26**(3): p. 220-7.
21. Kullak-Ublick, G.A., et al., *Molecular and functional characterization of an organic anion transporting polypeptide cloned from human liver*. Gastroenterology, 1995. **109**(4): p. 1274-82.
22. Gao, B., et al., *Organic anion-transporting polypeptides mediate transport of opioid peptides across blood-brain barrier*. J Pharmacol Exp Ther, 2000. **294**(1): p. 73-9.
23. Bronger, H., et al., *ABCC drug efflux pumps and organic anion uptake transporters in human gliomas and the blood-tumor barrier*. Cancer Res, 2005. **65**(24): p. 11419-28.

24. Gao, B., et al., *Differential cellular expression of organic anion transporting peptides OATP1A2 and OATP2B1 in the human retina and brain: implications for carrier-mediated transport of neuropeptides and neurosteroids in the CNS*. *Pflugers Arch*, 2015. **467**(7): p. 1481-1493.
25. Lee, W., et al., *Polymorphisms in human organic anion-transporting polypeptide 1A2 (OATP1A2): implications for altered drug disposition and central nervous system drug entry*. *J Biol Chem*, 2005. **280**(10): p. 9610-7.
26. Badagnani, I., et al., *Interaction of methotrexate with organic-anion transporting polypeptide 1A2 and its genetic variants*. *J Pharmacol Exp Ther*, 2006. **318**(2): p. 521-9.
27. Loubiere, L.S., et al., *Expression of thyroid hormone transporters in the human placenta and changes associated with intrauterine growth restriction*. *Placenta*, 2010. **31**(4): p. 295-304.
28. Wang, H., et al., *Alteration in placental expression of bile acids transporters OATP1A2, OATP1B1, OATP1B3 in intrahepatic cholestasis of pregnancy*. *Arch Gynecol Obstet*, 2012. **285**(6): p. 1535-40.
29. Glaeser, H., et al., *Intestinal drug transporter expression and the impact of grapefruit juice in humans*. *Clin Pharmacol Ther*, 2007. **81**(3): p. 362-70.
30. Drozdzik, M., et al., *Protein abundance of clinically relevant multidrug transporters along the entire length of the human intestine*. *Mol Pharm*, 2014. **11**(10): p. 3547-55.
31. Grube, M., P. Hagen, and G. Jedlitschky, *Neurosteroid Transport in the Brain: Role of ABC and SLC Transporters*. *Front Pharmacol*, 2018. **9**: p. 354.
32. Fujiwara, K., et al., *Identification of thyroid hormone transporters in humans: different molecules are involved in a tissue-specific manner*. *Endocrinology*, 2001. **142**(5): p. 2005-12.
33. Cvetkovic, M., et al., *OATP and P-glycoprotein transporters mediate the cellular uptake and excretion of fexofenadine*. *Drug Metab Dispos*, 1999. **27**(8): p. 866-71.
34. Misaka, S., et al., *Green tea ingestion greatly reduces plasma concentrations of nadolol in healthy subjects*. *Clin Pharmacol Ther*, 2014. **95**(4): p. 432-8.
35. Ho, R.H., et al., *Drug and bile acid transporters in rosuvastatin hepatic uptake: function, expression, and pharmacogenetics*. *Gastroenterology*, 2006. **130**(6): p. 1793-806.
36. Cheng, Z., et al., *Hydrophilic anti-migraine triptans are substrates for OATP1A2, a transporter expressed at human blood-brain barrier*. *Xenobiotica*, 2012. **42**(9): p. 880-90.
37. Urquhart, B.L. and R.B. Kim, *Blood-brain barrier transporters and response to CNS-active drugs*. *Eur J Clin Pharmacol*, 2009. **65**(11): p. 1063-70.
38. Hu, S., et al., *Interaction of imatinib with human organic ion carriers*. *Clin Cancer Res*, 2008. **14**(10): p. 3141-8.
39. Bailey, D.G., et al., *Naringin is a major and selective clinical inhibitor of organic anion-transporting polypeptide 1A2 (OATP1A2) in grapefruit juice*. *Clin Pharmacol Ther*, 2007. **81**(4): p. 495-502.
40. Navratilova, L., et al., *Honey flavonoids inhibit hOATP2B1 and hOATP1A2 transporters and hOATP-mediated rosuvastatin cell uptake in vitro*. *Xenobiotica*, 2018. **48**(7): p. 745-755.
41. Roth, M., B.N. Timmermann, and B. Hagenbuch, *Interactions of green tea catechins with organic anion-transporting polypeptides*. *Drug Metab Dispos*, 2011. **39**(5): p. 920-6.
42. Dresser, G.K., R.B. Kim, and D.G. Bailey, *Effect of grapefruit juice volume on the reduction of fexofenadine bioavailability: possible role of organic anion transporting polypeptides*. *Clin Pharmacol Ther*, 2005. **77**(3): p. 170-7.
43. Li, J., et al., *Quantitative and Mechanistic Understanding of AZD1775 Penetration across Human Blood-Brain Barrier in Glioblastoma Patients Using an IVIVE-PBPK Modeling Approach*. *Clin Cancer Res*, 2017. **23**(24): p. 7454-7466.
44. Zhou, Y., et al., *Genetic polymorphisms and function of the organic anion-transporting polypeptide 1A2 and its clinical relevance in drug disposition*. *Pharmacology*, 2015. **95**(3-4): p. 201-8.
45. Yamakawa, Y., et al., *Pharmacokinetic impact of SLC01A2 polymorphisms on imatinib disposition in patients with chronic myeloid leukemia*. *Clin Pharmacol Ther*, 2011. **90**(1): p. 157-63.
46. Calcagno, A., et al., *Determinants of darunavir cerebrospinal fluid concentrations: impact of once-daily dosing and pharmacogenetics*. *AIDS*, 2012. **26**(12): p. 1529-33.

47. Callens, C., et al., *High-throughput pharmacogenetics identifies SLCO1A2 polymorphisms as candidates to elucidate the risk of febrile neutropenia in the breast cancer RAPP-01 trial.* Breast Cancer Res Treat, 2015. **153**(2): p. 383-9.
48. Costa, A.C.C., et al., *The SLCO1A2 -189\_-188InsA polymorphism reduces clearance of rocuronium in patients submitted to elective surgeries.* Eur J Clin Pharmacol, 2017. **73**(8): p. 957-963.
49. Tamai, I., et al., *Molecular identification and characterization of novel members of the human organic anion transporter (OATP) family.* Biochem Biophys Res Commun, 2000. **273**(1): p. 251-60.
50. Hussner, J., et al., *Expression of OATP2B1 as determinant of drug effects in the microcompartment of the coronary artery.* Vascul Pharmacol, 2015. **72**: p. 25-34.
51. Grube, M., et al., *Organic anion transporting polypeptide 2B1 is a high-affinity transporter for atorvastatin and is expressed in the human heart.* Clin Pharmacol Ther, 2006. **80**(6): p. 607-20.
52. Sakamoto, A., et al., *Quantitative expression of human drug transporter proteins in lung tissues: analysis of regional, gender, and interindividual differences by liquid chromatography-tandem mass spectrometry.* J Pharm Sci, 2013. **102**(9): p. 3395-406.
53. Pizzagalli, F., et al., *Identification of steroid sulfate transport processes in the human mammary gland.* J Clin Endocrinol Metab, 2003. **88**(8): p. 3902-12.
54. Kim, M., et al., *Characterization of OATP1B3 and OATP2B1 transporter expression in the islet of the adult human pancreas.* Histochem Cell Biol, 2017. **148**(4): p. 345-357.
55. St-Pierre, M.V., et al., *Characterization of an organic anion-transporting polypeptide (OATP-B) in human placenta.* J Clin Endocrinol Metab, 2002. **87**(4): p. 1856-63.
56. Niessen, J., et al., *Human platelets express organic anion-transporting peptide 2B1, an uptake transporter for atorvastatin.* Drug Metab Dispos, 2009. **37**(5): p. 1129-37.
57. Knauer, M.J., et al., *Human skeletal muscle drug transporters determine local exposure and toxicity of statins.* Circ Res, 2010. **106**(2): p. 297-306.
58. Schiffer, R., et al., *Active influx transport is mediated by members of the organic anion transporting polypeptide family in human epidermal keratinocytes.* J Invest Dermatol, 2003. **120**(2): p. 285-91.
59. Kullak-Ublick, G.A., et al., *Organic anion-transporting polypeptide B (OATP-B) and its functional comparison with three other OATPs of human liver.* Gastroenterology, 2001. **120**(2): p. 525-33.
60. Ferreira, C., et al., *The scaffold protein PDZK1 modulates expression and function of the organic anion transporting polypeptide 2B1.* Eur J Pharm Sci, 2018. **120**: p. 181-190.
61. Kobayashi, D., et al., *Involvement of human organic anion transporting polypeptide OATP-B (SLC21A9) in pH-dependent transport across intestinal apical membrane.* J Pharmacol Exp Ther, 2003. **306**(2): p. 703-8.
62. Keiser, M., et al., *The Organic Anion-Transporting Peptide 2B1 Is Localized in the Basolateral Membrane of the Human Jejunum and Caco-2 Monolayers.* J Pharm Sci, 2017. **106**(9): p. 2657-2663.
63. Tapaninen, T., P.J. Neuvonen, and M. Niemi, *Orange and apple juice greatly reduce the plasma concentrations of the OATP2B1 substrate aliskiren.* Br J Clin Pharmacol, 2011. **71**(5): p. 718-26.
64. Ieiri, I., et al., *Microdosing clinical study: pharmacokinetic, pharmacogenomic (SLCO2B1), and interaction (grapefruit juice) profiles of celiprolol following the oral microdose and therapeutic dose.* J Clin Pharmacol, 2012. **52**(7): p. 1078-89.
65. Imanaga, J., et al., *The effects of the SLCO2B1 c.1457C > T polymorphism and apple juice on the pharmacokinetics of fexofenadine and midazolam in humans.* Pharmacogenet Genomics, 2011. **21**(2): p. 84-93.
66. Kashiwara, Y., et al., *Small-Dosing Clinical Study: Pharmacokinetic, Pharmacogenomic (SLCO2B1 and ABCG2), and Interaction (Atorvastatin and Grapefruit Juice) Profiles of 5 Probes for OATP2B1 and BCRP.* J Pharm Sci, 2017. **106**(9): p. 2688-2694.
67. Mougey, E.B., et al., *Effect of citrus juice and SLCO2B1 genotype on the pharmacokinetics of montelukast.* J Clin Pharmacol, 2011. **51**(5): p. 751-60.

68. Kim, T.E., et al., *The Effect of Genetic Polymorphisms in SLCO2B1 on the Lipid-Lowering Efficacy of Rosuvastatin in Healthy Adults with Elevated Low-Density Lipoprotein*. Basic Clin Pharmacol Toxicol, 2017. **121**(3): p. 195-201.
69. Johnson, M., et al., *Inhibition of Intestinal OATP2B1 by the Calcium Receptor Antagonist Ronacaleret Results in a Significant Drug-Drug Interaction by Causing a 2-Fold Decrease in Exposure of Rosuvastatin*. Drug Metab Dispos, 2017. **45**(1): p. 27-34.
70. Lee, S.W., et al., *Oral absorption of voriconazole is affected by SLCO2B1 c.\*396T>C genetic polymorphism in CYP2C19 poor metabolizers*. Pharmacogenomics J, 2020. **20**(6): p. 792-800.
71. Johnson, E.J., et al., *Prioritizing pharmacokinetic drug interaction precipitants in natural products: application to OATP inhibitors in grapefruit juice*. Biopharm Drug Dispos, 2017. **38**(3): p. 251-259.
72. Shirasaka, Y., et al., *Major active components in grapefruit, orange, and apple juices responsible for OATP2B1-mediated drug interactions*. J Pharm Sci, 2013. **102**(9): p. 3418-26.
73. Medwid, S., et al., *Fexofenadine and Rosuvastatin Pharmacokinetics in Mice with Targeted Disruption of Organic Anion Transporting Polypeptide 2B1*. Drug Metab Dispos, 2019. **47**(8): p. 832-842.
74. Mandery, K., et al., *Influence of the flavonoids apigenin, kaempferol, and quercetin on the function of organic anion transporting polypeptides 1A2 and 2B1*. Biochem Pharmacol, 2010. **80**(11): p. 1746-53.
75. Meyer Zu Schwabedissen, H.E., et al., *Thyroid Hormones Are Transport Substrates and Transcriptional Regulators of Organic Anion Transporting Polypeptide 2B1*. Mol Pharmacol, 2018. **94**(1): p. 700-712.
76. Bednarczyk, D. and C. Boisselle, *Organic anion transporting polypeptide (OATP)-mediated transport of coproporphyrins I and III*. Xenobiotica, 2016. **46**(5): p. 457-66.
77. Yoshikado, T., et al., *PBPK Modeling of Coproporphyrin I as an Endogenous Biomarker for Drug Interactions Involving Inhibition of Hepatic OATP1B1 and OATP1B3*. CPT Pharmacometrics Syst Pharmacol, 2018. **7**(11): p. 739-747.
78. Shen, H., et al., *Comparative Evaluation of Plasma Bile Acids, Dehydroepiandrosterone Sulfate, Hexadecanedioate, and Tetradecanedioate with Coproporphyrins I and III as Markers of OATP Inhibition in Healthy Subjects*. Drug Metab Dispos, 2017. **45**(8): p. 908-919.
79. Grube, M., et al., *Modification of OATP2B1-mediated transport by steroid hormones*. Mol Pharmacol, 2006. **70**(5): p. 1735-41.
80. Reddy, D.S., *Neurosteroids: endogenous role in the human brain and therapeutic potentials*. Prog Brain Res, 2010. **186**: p. 113-37.
81. Harteneck, C., *Pregnenolone sulfate: from steroid metabolite to TRP channel ligand*. Molecules, 2013. **18**(10): p. 12012-28.
82. Baulieu, E.E., *Neurosteroids: of the nervous system, by the nervous system, for the nervous system*. Recent Prog Horm Res, 1997. **52**: p. 1-32.
83. Maninger, N., et al., *Neurobiological and neuropsychiatric effects of dehydroepiandrosterone (DHEA) and DHEA sulfate (DHEAS)*. Front Neuroendocrinol, 2009. **30**(1): p. 65-91.
84. Hagenbuch, B. and B. Stieger, *The SLCO (former SLC21) superfamily of transporters*. Mol Aspects Med, 2013. **34**(2-3): p. 396-412.
85. International Transporter, C., et al., *Membrane transporters in drug development*. Nat Rev Drug Discov, 2010. **9**(3): p. 215-36.
86. Rosenberg, T. and W. Wilbrandt, *Uphill transport induced by counterflow*. J Gen Physiol, 1957. **41**(2): p. 289-96.
87. Stein, W.H., *The movement of molecules across cell membranes*. Academic Press: New York, 1967.
88. Harper, J.N. and S.H. Wright, *Multiple mechanisms of ligand interaction with the human organic cation transporter, OCT2*. Am J Physiol Renal Physiol, 2013. **304**(1): p. F56-67.
89. Burckhardt, B.C., et al., *Counter-flow suggests transport of dantrolene and 5-OH dantrolene by the organic anion transporters 2 (OAT2) and 3 (OAT3)*. Pflugers Arch, 2016. **468**(11-12): p. 1909-1918.
90. Czygan, F., *Kulturgeschichte und Mystik des Johanniskrauts*. Pharm. Unserer Zeit, 2003. **3**: p. 184-190.

91. Schrader, E., *Equivalence of St John's wort extract (Ze 117) and fluoxetine: a randomized, controlled study in mild-moderate depression*. *Int Clin Psychopharmacol*, 2000. **15**(2): p. 61-8.
92. Shelton, R.C., et al., *Effectiveness of St John's wort in major depression: a randomized controlled trial*. *JAMA*, 2001. **285**(15): p. 1978-86.
93. Woelk, H., *Comparison of St John's wort and imipramine for treating depression: randomised controlled trial*. *BMJ*, 2000. **321**(7260): p. 536-9.
94. Nahrstedt, A. and V. Butterweck, *Lessons learned from herbal medicinal products: the example of St. John's Wort (perpendicular)*. *J Nat Prod*, 2010. **73**(5): p. 1015-21.
95. Chatterjee, S.S., et al., *Hyperforin as a possible antidepressant component of hypericum extracts*. *Life Sci*, 1998. **63**(6): p. 499-510.
96. Butterweck, V., *Mechanism of action of St John's wort in depression : what is known?* *CNS Drugs*, 2003. **17**(8): p. 539-62.
97. Keksel, N., et al., *St John's wort extract influences membrane fluidity and composition of phosphatidylcholine and phosphatidylethanolamine in rat C6 glioblastoma cells*. *Phytomedicine*, 2019. **54**: p. 66-76.
98. Piscitelli, S.C., et al., *Indinavir concentrations and St John's wort*. *Lancet*, 2000. **355**(9203): p. 547-8.
99. Ruschitzka, F., et al., *Acute heart transplant rejection due to Saint John's wort*. *Lancet*, 2000. **355**(9203): p. 548-9.
100. Wang, Z., et al., *Enhancement of hepatic 4-hydroxylation of 25-hydroxyvitamin D3 through CYP3A4 induction in vitro and in vivo: implications for drug-induced osteomalacia*. *J Bone Miner Res*, 2013. **28**(5): p. 1101-16.
101. Durr, D., et al., *St John's Wort induces intestinal P-glycoprotein/MDR1 and intestinal and hepatic CYP3A4*. *Clin Pharmacol Ther*, 2000. **68**(6): p. 598-604.
102. Rao, Z.Z., et al., *miR-148a-mediated estrogen-induced cholestasis in intrahepatic cholestasis of pregnancy: Role of PXR/MRP3*. *PLoS One*, 2017. **12**(6): p. e0178702.
103. Miroddi, M., et al., *Passiflora incarnata L.: ethnopharmacology, clinical application, safety and evaluation of clinical trials*. *J Ethnopharmacol*, 2013. **150**(3): p. 791-804.
104. Grundmann, O., et al., *Anxiolytic activity of a phytochemically characterized Passiflora incarnata extract is mediated via the GABAergic system*. *Planta Med*, 2008. **74**(15): p. 1769-73.
105. Jawna-Zboinska, K., et al., *Passiflora incarnata L. Improves Spatial Memory, Reduces Stress, and Affects Neurotransmission in Rats*. *Phytother Res*, 2016. **30**(5): p. 781-9.
106. Soulimani, R., et al., *Behavioural effects of Passiflora incarnata L. and its indole alkaloid and flavonoid derivatives and maltol in the mouse*. *J Ethnopharmacol*, 1997. **57**(1): p. 11-20.
107. Akhondzadeh, S., et al., *Passionflower in the treatment of generalized anxiety: a pilot double-blind randomized controlled trial with oxazepam*. *J Clin Pharm Ther*, 2001. **26**(5): p. 363-7.
108. Appel, K., et al., *Modulation of the gamma-aminobutyric acid (GABA) system by Passiflora incarnata L.* *Phytother Res*, 2011. **25**(6): p. 838-43.
109. Gadioli, I.L., et al., *A systematic review on phenolic compounds in Passiflora plants: Exploring biodiversity for food, nutrition, and popular medicine*. *Crit Rev Food Sci Nutr*, 2018. **58**(5): p. 785-807.
110. Hu, M., F. Li, and W. Wang, *Vitexin protects dopaminergic neurons in MPTP-induced Parkinson's disease through PI3K/Akt signaling pathway*. *Drug Des Devel Ther*, 2018. **12**: p. 565-573.
111. Abbasi, E., et al., *Neuroprotective effects of vitexin, a flavonoid, on pentylenetetrazole-induced seizure in rats*. *Chem Biol Drug Des*, 2012. **80**(2): p. 274-8.
112. Gazola, A.C., et al., *Involvement of GABAergic pathway in the sedative activity of apigenin, the main flavonoid from Passiflora quadrangularis pericarp*. *Revista Brasileira De Farmacognosia-Brazilian Journal of Pharmacognosy*, 2015. **25**(2): p. 158-163.
113. Zanolli, P., R. Avallone, and M. Baraldi, *Behavioral characterisation of the flavonoids apigenin and chrysin*. *Fitoterapia*, 2000. **71 Suppl 1**: p. S117-23.
114. Cassidy, A. and A.M. Minihiene, *The role of metabolism (and the microbiome) in defining the clinical efficacy of dietary flavonoids*. *Am J Clin Nutr*, 2017. **105**(1): p. 10-22.
115. Murota, K., Y. Nakamura, and M. Uehara, *Flavonoid metabolism: the interaction of metabolites and gut microbiota*. *Biosci Biotechnol Biochem*, 2018. **82**(4): p. 600-610.

116. Suganuma, M., et al., *Wide distribution of [3H](-)-epigallocatechin gallate, a cancer preventive tea polyphenol, in mouse tissue*. *Carcinogenesis*, 1998. **19**(10): p. 1771-6.
117. Sai, Y., et al., *Predominant contribution of organic anion transporting polypeptide OATP-B (OATP2B1) to apical uptake of estrone-3-sulfate by human intestinal Caco-2 cells*. *Drug Metab Dispos*, 2006. **34**(8): p. 1423-31.
118. Yamaguchi, H., et al., *Transport of estrone 3-sulfate mediated by organic anion transporter OATP4C1: estrone 3-sulfate binds to the different recognition site for digoxin in OATP4C1*. *Drug Metab Pharmacokinet*, 2010. **25**(3): p. 314-7.
119. Satoh, H., et al., *Citrus juices inhibit the function of human organic anion-transporting polypeptide OATP-B*. *Drug Metab Dispos*, 2005. **33**(4): p. 518-23.
120. Shirasaka, Y., et al., *Substrate- and dose-dependent drug interactions with grapefruit juice caused by multiple binding sites on OATP2B1*. *Pharm Res*, 2014. **31**(8): p. 2035-43.
121. Chen, Y., et al., *Interaction of Sulfonylureas with Liver Uptake Transporters OATP1B1 and OATP1B3*. *Basic Clin Pharmacol Toxicol*, 2018. **123**(2): p. 147-154.
122. Varma, M.V., et al., *Transporter-Mediated Hepatic Uptake Plays an Important Role in the Pharmacokinetics and Drug-Drug Interactions of Montelukast*. *Clin Pharmacol Ther*, 2017. **101**(3): p. 406-415.
123. McFeely, S.J., et al., *Organic anion transporting polypeptide 2B1 - More than a glass-full of drug interactions*. *Pharmacol Ther*, 2019. **196**: p. 204-215.
124. Drozdzik, M., et al., *Protein Abundance of Clinically Relevant Drug Transporters in the Human Liver and Intestine: A Comparative Analysis in Paired Tissue Specimens*. *Clin Pharmacol Ther*, 2019. **105**(5): p. 1204-1212.
125. Mougey, E.B., et al., *Absorption of montelukast is transporter mediated: a common variant of OATP2B1 is associated with reduced plasma concentrations and poor response*. *Pharmacogenet Genomics*, 2009. **19**(2): p. 129-38.
126. Tapaninen, T., et al., *SLCO2B1 c.935G>A single nucleotide polymorphism has no effect on the pharmacokinetics of montelukast and aliskiren*. *Pharmacogenet Genomics*, 2013. **23**(1): p. 19-24.
127. Vaidyanathan, S., et al., *Pharmacokinetics of the oral direct renin inhibitor aliskiren in combination with digoxin, atorvastatin, and ketoconazole in healthy subjects: the role of P-glycoprotein in the disposition of aliskiren*. *J Clin Pharmacol*, 2008. **48**(11): p. 1323-38.
128. Bednarczyk, D. and M.V. Sanghvi, *Organic anion transporting polypeptide 2B1 (OATP2B1), an expanded substrate profile, does it align with OATP2B1's hypothesized function?* *Xenobiotica*, 2020. **50**(9): p. 1128-1137.
129. Chen, M., et al., *Role of Oatp2b1 in Drug Absorption and Drug-Drug Interactions*. *Drug Metab Dispos*, 2020. **48**(5): p. 419-425.
130. Yang, J.F., et al., *The time-dependent effects of St John's wort on cytochrome P450, uridine diphosphate-glucuronosyltransferase, glutathione S-transferase, and NAD(P)H-quinone oxidoreductase in mice*. *J Food Drug Anal*, 2018. **26**(1): p. 422-431.
131. LeCluyse, E.L., *Pregnane X receptor: molecular basis for species differences in CYP3A induction by xenobiotics*. *Chem Biol Interact*, 2001. **134**(3): p. 283-9.
132. Graham, M.J. and B.G. Lake, *Induction of drug metabolism: species differences and toxicological relevance*. *Toxicology*, 2008. **254**(3): p. 184-91.
133. Chang, T.K., *Activation of pregnane X receptor (PXR) and constitutive androstane receptor (CAR) by herbal medicines*. *AAPS J*, 2009. **11**(3): p. 590-601.
134. Bray, B.J., et al., *St. John's wort extract induces CYP3A and CYP2E1 in the Swiss Webster mouse*. *Toxicol Sci*, 2002. **66**(1): p. 27-33.
135. Vanden Heuvel, J.P., *Species Differences in Pregnane X Receptor Activation: Examination of common laboratory animal species*. *Nuclear Receptor Resource*, INDIGO Biosciences, Inc, 2016.
136. Sugiura, T., et al., *PDZK1 regulates organic anion transporting polypeptide Oatp1a in mouse small intestine*. *Drug Metab Pharmacokinet*, 2010. **25**(6): p. 588-98.
137. Dresser, G.K., et al., *Fruit juices inhibit organic anion transporting polypeptide-mediated drug uptake to decrease the oral availability of fexofenadine*. *Clin Pharmacol Ther*, 2002. **71**(1): p. 11-20.

138. Rebello, S., et al., *Intestinal OATP1A2 inhibition as a potential mechanism for the effect of grapefruit juice on aliskiren pharmacokinetics in healthy subjects*. Eur J Clin Pharmacol, 2012. **68**(5): p. 697-708.
139. Abe, O., et al., *Role of (-)-epigallocatechin gallate in the pharmacokinetic interaction between nadolol and green tea in healthy volunteers*. Eur J Clin Pharmacol, 2018. **74**(6): p. 775-783.
140. Zhou, F., et al., *Functional analysis of novel polymorphisms in the human SLC01A2 gene that encodes the transporter OATP1A2*. AAPS J, 2013. **15**(4): p. 1099-108.